



University of Kentucky  
UKnowledge

---

University of Kentucky Doctoral Dissertations

Graduate School

---

2010

# IMMOBILIZATION OF MERCURY AND ARSENIC THROUGH COVALENT THIOLATE BONDING FOR THE PURPOSE OF ENVIRONMENTAL REMEDIATION

Lisa Y. Blue

*University of Kentucky*, [lisayblue@gmail.com](mailto:lisayblue@gmail.com)

[Right click to open a feedback form in a new tab to let us know how this document benefits you.](#)

---

## Recommended Citation

Blue, Lisa Y., "IMMOBILIZATION OF MERCURY AND ARSENIC THROUGH COVALENT THIOLATE BONDING FOR THE PURPOSE OF ENVIRONMENTAL REMEDIATION" (2010). *University of Kentucky Doctoral Dissertations*. 785.

[https://uknowledge.uky.edu/gradschool\\_diss/785](https://uknowledge.uky.edu/gradschool_diss/785)

This Dissertation is brought to you for free and open access by the Graduate School at UKnowledge. It has been accepted for inclusion in University of Kentucky Doctoral Dissertations by an authorized administrator of UKnowledge. For more information, please contact [UKnowledge@lsv.uky.edu](mailto:UKnowledge@lsv.uky.edu).

ABSTRACT OF DISSERTATION

Lisa Y. Blue

The Graduate School  
University of Kentucky

2010

IMMOBILIZATION OF MERCURY AND ARSENIC THROUGH  
COVALENT THIOLATE BONDING FOR THE PURPOSE OF  
ENVIRONMENTAL REMEDIATION

---

ABSTRACT OF DISSERTATION

---

A dissertation submitted in partial fulfillment of the  
requirements for the degree of Doctor of Philosophy in the  
College of Arts and Sciences  
at the University of Kentucky

By  
Lisa Y. Blue

Lexington, Kentucky

Director: Dr. David A. Atwood, Professor of Chemistry

Lexington, Kentucky

2010

Copyright © Lisa Y. Blue 2010

## ABSTRACT OF DISSERTATION

### IMMOBILIZATION OF MERCURY AND ARSENIC THROUGH COVALENT THIOLATE BONDING FOR THE PURPOSE OF ENVIRONMENTAL REMEDIATION

Mercury and arsenic are widespread contaminants in aqueous environments throughout the world. The elements arise from multiple sources including mercury from coal-fired power plants and wells placed in natural geological deposits of arsenic-containing minerals. Both elements have significant negative health impacts on humans as they are cumulative toxins that bind to the sulfhydryl groups in proteins, disrupting many biological functions. There are currently no effective, economical techniques for removing either mercury or arsenic from aqueous sources. This thesis will demonstrate a superior removal method for both elements by formation of covalent bonds with the sulfur atoms in N,N'-Bis(2-mercaptoethyl)isophthalamide (commonly called "B9"). That B9 can precipitate both elements from water is unusual since aqueous mercury exists primarily as a metal(II) dication while aqueous arsenic exists as As(III) and As(V) oxyanions.

**KEYWORDS:** Arsenic, Covalent Bonding, Mercury, Remediation, Sulfur

Lisa Y Blue

November 30, 2009

IMMOBILIZATION OF MERCURY AND ARSENIC THROUGH  
COVALENT THIOLATE BONDING FOR THE PURPOSE OF  
ENVIRONMENTAL REMEDIATION

By

Lisa Y. Blue

Dr. David Atwood  
Director of Dissertation

Dr. Mark Meier  
Director of Graduate Studies

November 30, 2009



DISSERTATION

Lisa Y. Blue

The Graduate School  
University of Kentucky

2010

IMMOBILIZATION OF MERCURY AND ARSENIC THROUGH  
COVALENT THIOLATE BONDING FOR THE PURPOSE OF  
ENVIRONMENTAL REMEDIATION

---

DISSERTATION

---

A dissertation submitted in partial fulfillment of the  
requirements for the degree of Doctor of Philosophy in the  
College of Arts and Sciences  
at the University of Kentucky

By

Lisa Y. Blue

Lexington, Kentucky

Director: Dr. David A. Atwood, Professor of Chemistry

Lexington, Kentucky

2010

Copyright © Lisa Y. Blue 2010



*This work is dedicated to my boys:  
Spencer and Benjamin, I hope to one day inspire you as much as you've inspired me.  
Jesse, thanks for being my rock.*

*Education is not the filling of a pail, but the lighting of a fire.*

—William Butler Yeats

## ACKNOWLEDGEMENTS

David, I must start my acknowledgements by thanking you for encouraging me to pursue every project and opportunity that has ever piqued my interest and for hanging in there with me while I followed a rather non-linear path to a Ph.D. under your guidance. I've always appreciated your indefatigable optimism and the freedoms allowed to me while in your group. You've taught me an incredible amount of self-reliance in research.

Gail, first of all, I must thank you for the quote underneath the signature line of your emails. Those few words have bothered me and goaded me into action more than I would have thought possible, especially on the tough days, when I hear that quote resounding in my head and find the courage to keep moving. Thank you, too, for serving as the reality check I needed, even when I was not necessarily receptive to said reality check. Thanks for creating a wonderful learning environment in the lab and for allowing me to participate so fully in the ERTL mission. Thanks, too, for the bracing insight into my future aspirations and potential career paths. You have inspired me for a lifetime.

The main thrust of my research efforts were supported by the fine folks at ERTL, especially Tricia Coakley, John May, James Ward and Katy Ward. These four were in the trenches with me almost from the beginning and I am in their debt for the endless constructive critiques of experimental methods, results, and written research products, for training on various instruments and techniques, for their friendship, and for their constant encouragement. These four quickly became personally invested in my success as a doctoral candidate and it was always a pleasure to share my triumphs with them.

I must also thank each of you charged with the duty of serving on my doctoral committee for your support during this process. Chris, I still swear that all I ever knew about soil chemistry I learned from you. Thanks for such a solid grounding in soil chemistry which I continue to build upon today. Who knew I could get so much mileage out of a single course? Dr. Bramwell, I appreciate your support, your professionalism and your kind words of encouragement before my qualifying exam when it was delayed. Dr. Lovell, thanks for coming in so late in the game to see me to the finish line.

In the Atwood lab, I'd like to thank all of my predecessors for laying the groundwork for the research described in this dissertation. I'd like to thank my contemporaries in the group, especially Eduardo Santillán-Jiménez and Christopher

Preece for the excellent discussions of inorganic chemistry, uranium, zinc, arsenic, mercury, and all things graduate school. I was also fortunate enough to work with many wonderfully talented undergraduate researchers including Railey White and Kristen Bird, with whom I worked most extensively, and several others including J. David Clem, Shaun Masters, Kyle Slone, Laura Fletcher, Chrissy Minton, Crystal Holcomb, Jared Daugherty and Kateland Beals. This group was affectionately known as the “Blue Crew” and the semester that I had nine of them in the lab was one of the most amazing and productive times I can recall. Thanks for the fun, Blue Crew! You are sorely missed.

I must extend thanks to all of my collaborators on various projects throughout my research career at the University of Kentucky. On the arsenic in poultry litter amended soils project, E. Glynn Beck of the Kentucky Geological Survey in western Kentucky and Greg Henson from the McLean County Extension office were a great help for coordination of the field work, the selection of fields, sample collection, sample transportation to the lab, and enlightened discussions concerning the project. It was a pleasure working on the thimerosal in vaccines project with Dr. Laura Hewiston of the Magee Women’s Research Institute in Pittsburgh and Dr. Andy Wakefield from the Thoughtful House for Children based in Austin, Texas. I appreciate the use of Dr. Boyd Haley’s instrument for analysis of the project’s samples as well. I’m very appreciative for Abhijit Mukerjee and Alan Fryar testing my arsenic remediation columns in West Bengal. I also appreciate the hospitality of Evan Granite when visiting him at the Pittsburgh DOE NETL laboratory to discuss his research on gas phase mercury capture and the possibility of testing our compounds in his lab-scale simulated coal-fired power plant set-up. I can’t neglect the value imparted by the bi-monthly dissertation defenses (aka “business meetings”) with Robert (Cal) Calmes, Rudy Schmidt, and various others at Merloc, LLC., in Lexington, Kentucky. I’m already a timid flier, but after basically conducting a defense at 50,000 feet with turbulence during one trip, I feel that I’ve been left with nerves of steel for the final defense—thanks, guys! Last, but not least, I have deep gratitude for the funding that supported all of this exciting research including my RCTF fellowship, the Dissertation Year Fellowship, the ERTL scholarship, and funding from Merloc, LLC, Magee-Women’s Research Institute, the University of Kentucky

Graduate College, the University of Kentucky Chemistry Department, and Merloc LLC, of Lexington, Kentucky, who provided the funding for this research.

I feel that I've saved the best for last: I must thank my husband Jesse and my sons, Spencer and Benjamin, for keeping my life both grounded and balanced. It's been a long road for all of us.

While some are fortunate enough to graduate Magna Cum Laude or Summa Cum Laude, I am happy enough to join the ranks of the vast majority that graduate "Thank the Laude." The Man loves a good joke; I fully believe that the key to living a full and enjoyable life lies in learning to laugh with Him.

## TABLE OF CONTENTS

ACKNOWLEDGEMENTS .....	iii
LIST OF TABLES .....	ix
LIST OF SCHEMES .....	x
LIST OF FIGURES .....	xi
LIST OF ABBREVIATIONS AND SYMBOLS .....	xii
CHAPTER ONE: INTRODUCTION.....	1
Problematic Metal(loid)s in the Environment.....	1
Mercury.....	2
Classical Mercury Applications through Modern Day Uses .....	2
Anthropogenic Mercury Emissions and Prevention .....	6
Future Mercury Emissions Projections.....	13
Environmental Mercury Chemistry .....	14
Mercury Toxicity .....	23
Mercury Remediation .....	28
Arsenic .....	29
Arsenic Geology, Applications and Anthropogenic Inputs to the Environment.....	29
Arsenic Speciation, Environmental Chemistry, and Toxicity .....	39
Arsenic and Human Health.....	46
Arsenic Remediation.....	48
Preferential Sulfur Binding: A Template for Permanent Remediation.....	48
Mercury and Arsenic Binding Affinities .....	48
Use of B9 to Explore Preferential Binding.....	50
Goals of the Current Work.....	50
Extension of Ligand Utility .....	51
Explore Ligand Stability with the Thiophilic Species Mercury and Arsenic in Aqueous Media.....	52
Develop a More Robust, Permanent and Inexpensive Means of Remediation .....	53

CHAPTER TWO: REMEDIATION OF Hg(II) USING A B9 COLUMN .....	54
Introduction.....	54
Key Deployment Targets for Improved Remediation Technology .....	54
Competing Mercury Remediation Technology .....	55
B9: Intelligent Ligand Design to Exploit Preferential Mercury-Sulfur	
Binding .....	63
Goals of the Current Work.....	63
Experimental.....	64
B9 Synthesis and Characterization .....	64
B9 Supported by Activated Carbon .....	65
B9 Supported by White Quartz Sand.....	66
Characterization and Stability of B9-Hg.....	66
Analytical Procedures .....	67
Results and Discussion .....	68
B9 Filtration Columns.....	68
B9-Hg Characterization and Stability.....	73
Conclusions.....	83
CHAPTER THREE: REMEDIATION OF As(III) USING A SIMPLE B9 COLUMN ..	84
Introduction.....	84
Competing Groundwater Arsenic Remediation Technology.....	84
Goals of the Current Work.....	86
Experimental.....	88
Batch Testing of Column Packing Materials .....	88
Column Testing Using Standard Arsenic Solutions .....	89
Field Column Construction.....	90
Sampling Area and Procedures .....	91
Characterization and Stability of B9-As(III) .....	94
Analytical Procedures .....	94
Results and Discussion .....	95
Batch Testing of Column Packing Materials .....	95
Column Testing Using Standard Arsenic Solutions .....	102
Field Study Column .....	103
Stability of B9-As(III) Products and Potential for Regeneration.....	106
Conclusions.....	107
CHAPTER FOUR: CONCLUSIONS.....	109
General Conclusions .....	109
Covalent Thiolate Bonding to Problematic Species .....	112

CHAPTER FIVE: DIRECTIONS FOR FURTHER RESEARCH.....	115
Introduction.....	115
Application to Related Species.....	115
Methylmercury.....	115
Aqueous Selenium.....	115
Elemental Mercury Liquid.....	118
Gas Phase Elemental Mercury Flask-to-Flask Study.....	121
Gas Phase Elemental Mercury Filter Frit Studies.....	123
Feasibility of Application in Coal Fired Power Plants.....	129
Questions to Consider.....	129
The Prototype Gas Phase Flow Reactor.....	129
Plans for the All-Steel Gas Phase Flow Reactor.....	134
Conclusions.....	135
APPENDIX.....	137
Analytical Procedures for the Determination of Hg by ICP in Liquid and Gas Phase Elemental Mercury Experiments.....	137
Procedure for Coating Glass Beads with B9.....	137
REFERENCES.....	139
VITA.....	163

## LIST OF TABLES

Table 2.1: Results for the Sand-Only Filtration Column with 20 ppm Hg.....	70
Table 2.2: Results for 20 ppm Hg passed through a B9 Supported by Sand Remediation Column.....	71
Table 2.3: Results for Low pH and Reductive Leaching Study of B9-Hg .....	75
Table 2.4: Results for High pH and Oxidative Leaching Study of B9-Hg.....	77
Table 3.1: Column Dimensions and Treatment Results for the ZVI Only As(V) Study Columns .....	90
Table 3.2: Dimensions for the B9 ZVI Field Study Column.....	91
Table 3.3: Results for B9 and AC Batch Tests.....	97
Table 3.4: Results of the Field Study Column Test for Samples with Detectable Pre-Treatment Arsenic.....	105
Table 3.5: Arsenic Leached from the B9-As Products over Time.....	106
Table 5.1: Selenium Concentrations for the B9 Batch Remediation Experiment .....	117
Table 5.2: Liquid Phase Hg Capture under Vacuum at Elevated Temperatures .....	120
Table 5.3: Hg Content of B9 from Gas Phase Flask-to-Flask Hg Capture.....	122
Table 5.4: Hg Capture by Various Particle Sizes of B9 Suspended on a Filter Frit at Ambient Temperatures.....	125
Table 5.5: Hg Capture Capacity by 125 – 250 $\mu\text{m}$ Filter Frit B9 at Ambient Frit Temperature at Varying Time Lengths.....	126
Table 5.6: Gas Phase Hg Capture at Elevated Frit Temperatures.....	128



## LIST OF SCHEMES

Scheme 1.1: Relevant Equilibrium Expressions for Hg-S Species in Solution.....	19
Scheme 1.2: Interaction of Copper, Chromium, and Arsenic with Wood Components....	38
Scheme 2.1: Mechanism of Mercury Capture Using Metal Oxide Catalysts.....	59
Scheme 2.2: Synthesis of B9 .....	65

## LIST OF FIGURES

Figure 1.1: Arsine Species .....	40
Figure 1.2: Arsenic Species Commonly Found in Soils, Sediments and Water.....	42
Figure 1.3: Arsenic Species Common to Marine Animals and Terrestrial Fungi .....	43
Figure 1.4: Basic Sketch of the Challenger Mechanism.....	46
Figure 2.1: Hg Concentration vs. Flow Rate for the B9 Supported in Sand Remediation Column .....	72
Figure 2.2: Proposed Structure of the B9-Hg(II) Product.....	73
Figure 2.3: Low pH B9-Hg Leaching Results .....	75
Figure 2.4: All High pH B9-Hg Leaching Results .....	77
Figure 2.5: B9-Hg Leaching Results at pH 9.....	78
Figure 2.6: B9-Hg Leaching Results at pH 11.....	79
Figure 2.7: B9-Hg Leaching Results at pH 13.....	79
Figure 3.1: Map of West Bengal Showing the Arsenic-Affected Areas and Sampling Areas.....	93
Figure 3.2: Proposed Structures of the B9-As(III) Insoluble Products.....	98
Figure 3.3: Speciation of Arsenite under pH 0 – 14 Conditions .....	100
Figure 3.4: Speciation of Arsenate under pH 0 – 14 Conditions .....	102
Figure 3.5: Arsenic Leached from the B9-As Products versus Time .....	107
Figure 5.1: Comparison of Arsenic and Selenium Oxyanion Structures.....	116
Figure 5.2: Comparison of Potential B9-As(III) and B9-Se(IV) Precipitates Formed ....	118
Figure 5.3: Prototype Gas Phase Flow Reactor Schematic.....	131
Figure 5.4: Real-Time Results for the Prototype Gas Phase Flow Reactor.....	134

## LIST OF ABBREVIATIONS AND SYMBOLS

General:	
Å	angstrom, $10^{-10}$ meters
AC	activated carbon
ACI	activated carbon injection
AMD	acid mine drainage
BDL	below detection limit
CAFO	concentrated animal feed operation
CCA	chromated copper arsenate
CCB	coal combustion byproduct
C-GA-AA	combustion gold amalgamation atomic absorption
cm	centimeter
CV	curve verifier
CVAA	cold vapor atomic absorption
dec	decomposed
DI	18 MΩ (mega-ohm) deionized water
DIP	direct insertion probe
DMA	direct mercury analyzer
DMHg	dimethylmercury
DOC	dissolved organic carbon
DOM	dissolved organic matter
DSMA	disodium methylarsonate
EA	elemental analysis
ECO	electro-catalytic oxidation
EI MS	electron impact mass spectra
ESP	electrostatic precipitator
EtOH	ethanol
FDA	United States Food and Drug Administration
FF	fabric filters
FGD	flue gas desulfurization
FTIR	Fourier transform infrared spectroscopy
g	grams
GFAAS	graphite furnace atomic absorption spectroscopy
GTAA	graphite tube atomic absorption spectroscopy
Hg-p	particle-associated mercury
hr	hours
Hz	Hertz, $s^{-1}$
IC	ion chromatography
ICP OES	inductively coupled plasma optical emission spectroscopy
IR	infrared spectroscopy
kJ	kilojoules
kg	kilogram
LCS	laboratory control sample

## LIST OF ABBREVIATIONS AND SYMBOLS, CONTINUED

General, continued:

μg	microgram
MΩ	mega ohm
MB	method blank
MMA	monomethylarsonic acid
MSMA	monosodium methylarsonate
MeHg	monomethylmercury
min	minute
mg	milligram
mmol	millimole
mL	milliliter
mo	month
mp	melting point
MS	mass spectrometry
nm	nanometer
NMR	nuclear magnetic resonance
PM	permanganate
ppb	parts per billion
ppm	parts per million
ppth	parts per thousand
pptr	parts per trillion
PT	permeation tube
PTV	permeation tube vessel
RO	reverse osmosis
RSD	relative standard deviation
s	seconds
SCR	selective catalytic reduction
SOM	soil organic matter
SRB	sulfate reducing bacteria
t	time
T	temperature
TDS	total dissolved solids
THF	tetrahydrofuran, C <sub>4</sub> H <sub>8</sub> O
UV	ultraviolet
w	weak
wk	week
yr	year
ZVI	zero-valent iron

## LIST OF ABBREVIATIONS AND SYMBOLS, CONTINUED

For infrared (IR) spectra:

br	broad
$\text{cm}^{-1}$	wavenumbers
FT IR	Fourier Transform Infrared Spectra
s	strong
sh	shoulder
$\nu$	vibrational frequency ( $\text{cm}^{-1}$ )
vs	very strong
w	weak

For nuclear magnetic resonance (NMR) spectra:

$\delta$	chemical shift, in parts per million
d	doublet
J	coupling constant
m	multiplet
q	quartet
s	singlet
t	triplet

## **CHAPTER ONE: INTRODUCTION**

### **PROBLEMATIC METAL(LOID)S IN THE ENVIRONMENT**

Metals, metalloids, and compounds of these elements are natural components of every ecosystem<sup>1</sup>. However, certain metal(loid)s are known to cause detrimental health effects due to their toxicity when present in certain chemical forms. Two such elements are mercury and arsenic, the chemistry of which will be explored in depth. These elements are of great concern because of the widespread distribution of their compounds in the environment and for the ability of mercury in particular to bioaccumulate along food chains. While the fundamental chemical properties of these elements differ starkly from one another, they have a tendency to react in a similar fashion when brought in contact with certain classes of compounds, making them amenable to a common method of remediation.

The natural occurrence and distribution of mercury and arsenic in the lithosphere, hydrosphere, and atmosphere will be discussed. As anthropogenic activities are a major source of both elements, human use, production, and environmental input will be identified before the natural cycling of mercury and arsenic is explored. The abiotic and biotic transformations of the common mercury and arsenic compounds will be reviewed before discussing their chemistry and ensuing toxicity effects within the biosphere, especially as they pertain to humans.

The ultimate goal is to permanently sequester the toxic mercury and arsenic compounds from the environment before they have a chance to poison both humans and animals. Many remediation technologies are currently employed to achieve this goal but each method has inherent strengths and weaknesses. Rather than continue pursuing such methods as adsorption, ion exchange, precipitation/coagulation, filtration and membrane separation techniques, each with their shortcomings that have no obvious, simple, or inexpensive solutions, we propose that a superior removal method exists that exploits the similar reactions of both elements with sulfur. The history of this remediation method with other problematic metals in the environment will be reviewed, gaps in the current body of knowledge identified, and the utility of this method extended to treat the problems at hand.

## MERCURY

**Classical Mercury Applications through Modern Day Uses.** Mercury is a comparatively rare element with a crustal abundance of only 0.5 parts-per-million (ppm).<sup>2-4</sup> Owing to its chalcophilic nature, as the earth's crust was cooling under a reducing atmosphere, mercury separated primarily into the sulfide phase.<sup>5</sup> For this reason, cinnabar ( $\alpha$ -HgS), a red crystalline mineral that is found along lines of former volcanic activity, constitutes the only significant mercury ore.<sup>5,6</sup> The separation of mercury from cinnabar can be accomplished by simply heating the mineral in a wood fire and collecting the elemental mercury that pools in the ashes.<sup>5</sup> Modern techniques for separating mercury from cinnabar generally include crushing, concentration by flotation, then heating the ore with or without the addition of scrap iron or quicklime and addition of a heated oxygen stream.<sup>5</sup> The mercury is condensed from the resulting stream of mercury vapor. The mercury is purified by blowing hot air through the hot, crude liquid metal to oxidize trace metal impurities which are easily removed from the surface of the liquid.<sup>5</sup> Further purification is accomplished by distillation of the metal under reduced pressure.<sup>5</sup>

The varied and unique properties of elemental mercury and its compounds have led to many applications since ancient times. When ground, cinnabar is a brilliant red pigment known as "vermillion" and the use of this pigment has been documented in Chinese bureaucratic texts dating back 3000 years.<sup>3,6,7</sup> Mercuric sulfide and mercuric oxide have both been used to color paints and mercuric sulfide is still used as a red colorant in modern tattoo dyes.<sup>8</sup>

Though Egyptians used mercury compounds to treat skin infections,<sup>6</sup> mercury has also been found in Egyptian tombs though it is unclear whether it was there for its preservative properties or to protect against evil spirits.<sup>3</sup> It is interesting to note that even in modern times, American *botanicas* continue to sell elemental mercury under various monikers due to the perceived medicinal and religious properties the metal has taken on in Latin American, Caribbean, and Asian cultures.<sup>8-10</sup> In fact, use of mercury in the religions of Voodoo, Santeria, and Espiritismo has been documented and numerous Chinese herbal remedies have been found to contain as much as 1.2 mg of mercury per dose.<sup>8</sup> Even certain homeopathic remedies commercially available in large chain stores in

the United States continue to add mercury as *mercurius solubilis* for the treatment of minor maladies such as pain and swelling due to ear infections.

Perhaps the most famous use of mercury was for the manufacture of hats. Beginning in the seventeenth century, mercury nitrate was added to the dilute nitric acid solution used to roughen the surface of the animal hides used to make felt.<sup>5</sup> As the felt hats dried, evaporating mercury and exposure to the mercury-laden dust was infamous for causing “hatters shakes” and may be responsible for the term “mad as a hatter.”<sup>5</sup>

Alchemists also used mercury extensively, most notably for the amalgamation and extraction of fine metals such as silver and gold.<sup>3,4</sup> This process must have been truly awe-inspiring in ancient times as the amalgamated ore was slowly heated, driving off the invisible elemental mercury vapor and leaving pure gold as the final product.<sup>3</sup> This property was also exploited by the Spanish who were famous for shipping large quantities of mercury in 76-lb flasks from Almaden, Spain, to the Americas during the sixteenth century for the extraction of silver and gold.<sup>3,5</sup> Almaden, which is Arabic for “the metal,” has been one of the world’s principle sites for mining mercury since Roman times and continues to function as such to this day.<sup>3,6</sup> Despite the inherent risks to the process, precious metal extraction through mercury amalgamation, whether through the *patio* process or barrel amalgamation, is still a viable process applied to gold found in secondary deposits and river sediments of the Amazon basin and elsewhere.<sup>3,6,11,12</sup> The property of amalgamation was also exploited by the French nearly 150 years ago when they introduced the first dental amalgam of mercury and silver, a product that is used to this day despite concerns about possible side effects from the nearly 50% mercury composition.<sup>1,6,8,10</sup>

Inorganic mercury and mercury salts have found numerous medical applications since ancient times. For instance, a tablespoon of elemental mercury was often prescribed as a laxative treatment during the eighteenth century.<sup>10</sup> Surprisingly, while the vapor from elemental mercury is quite toxic, ingestion of the element is not considered a significant hazard.<sup>10</sup> Paracelsus was one of the first advocates of mercury treatments, but soon realized its toxic nature hence the famous quote, “Dose makes the poison” for which he is remembered.<sup>6</sup>



Calomel, mercurous chloride ( $\text{Hg}_2\text{Cl}_2$ ), is one of the oldest known pharmaceuticals and was once used extensively for its antiseptic properties.<sup>1,3,5</sup> Though originally prescribed for the treatment of syphilis, the diuretic properties of calomel and other medicinal mercury compounds were confirmed by 1919 and were later prescribed by physicians specifically for this purpose.<sup>3,13</sup> By the twentieth century calomel was such a popular cure-all that it was even added to infants' teething powder, laxatives, and worming medications.<sup>3,10</sup> However, contamination of calomel with the more soluble mercuric chloride ( $\text{HgCl}_2$ ), a poison made popular during the Middle Ages, made it a dangerous as an ingestible remedy.<sup>5</sup> Regardless of the toxicity, even mercuric chloride was used as a topical antiseptic and disinfectant.<sup>8</sup> To this day, inorganic mercury salts including ammoniated mercuric chloride and mercuric iodide are still found as the active ingredients in popular Third World skin-lightening creams.<sup>8,10</sup>

Even after the dangerous effects of calomel became apparent, alternative mercury treatments *still containing mercury* were developed as replacements. In the late 1880s, diethylmercury replaced calomel for the treatment of syphilis<sup>3,10</sup> and mersalyl was traded for use as a diuretic.<sup>14</sup> Despite the ban of mercury-containing products in the United States, topical antiseptics, disinfectants, and preservatives containing mercury still enjoy worldwide popularity. Tincture of mercurochrome (dibromohydroxymercurifluorescein) and merthiolate (thimerosal or ethylmercury thiosalicylate) are still used as topical antiseptics; thimerosal and phenylmercuric nitrate continue to be used as preservatives in vaccines, prescriptions, and over-the-counter medications.<sup>3,8,10,15</sup>

A related organomercurial salt, phenylmercuric acetate, has been exploited for its fungicidal properties that prevent discoloration due to mildew growth when added to both indoor and outdoor latex paints.<sup>3,8,10</sup> However, the use of organomercurials in paint was banned in 1991 when it became evident that mercury vapors were released as the paints degraded.<sup>8</sup> Phenylmercuric acetate has also found use in inks, adhesives, caulking compounds, and as an industrial catalyst for the synthesis of polyurethanes.<sup>8</sup> Phenylmercury even enjoyed a brief stint as an anti-fungal cloth diaper rinse until it was implicated as a protagonist of acrodynia, or "pink disease," a malady named for the characteristic pink coloration of the child's hands and soles.<sup>3,7,10,16</sup> Owing to their

common antifungal action, phenyl-, ethyl-, and even methyl-mercury salts were applied as agricultural seed dressings for a time.<sup>1-3, 10</sup>

In the late 1950s, reports of predatory birds in Sweden that were exhibiting aberrant neurological signs prompted an investigation of possible pollutants.<sup>2, 3, 10</sup> Analysis of feather samples revealed high mercury levels in the affected birds; the source of the toxin was small mammals implicated in the consumption of freshly planted mercury-treated seed grain.<sup>6, 10</sup> This suspicion was confirmed by the analysis of predatory bird feathers from museum specimens that chronicled a sharp increase in mercury levels concurrent with the introduction of mercurial fungicides in Sweden.<sup>10</sup>

Unfortunately, Swedish birds would not constitute the only fatalities due to mercurial fungicidal poisoning before their use was finally discontinued.<sup>1, 5, 10</sup> Human poisonings occurred in Iraq in 1956 and again in 1960 due to the ingestion of flour and wheat seed treated with ethylmercury-*p*-toluene. Similar incidents played out during the growing seasons of 1963, 1964, and 1965 in Guatemala and in Pakistan in 1969 due to methylmercury dicyandiamide treated seed wheat.<sup>17</sup> Except for the 1960 Iraqi poisoning when 1,000 people were affected, only a few hundred people fell victim to eating the treated grain in each area.<sup>17</sup>

When the Iraqi wheat crop failed in 1970, the largest commercial order for seed grain ever made was placed with a Mexican supplier. The seeds were treated with methylmercury, a red warning dye, and labeled with warnings (in Spanish) according to standard practice.<sup>6</sup> In light of the prevailing famine, many farmers were guilty of washing off the dye and then using it for preparing bread for their own consumption, resulting in hundreds of cases of mercury poisoning since the methylmercury had not been removed by the washing process.<sup>6, 10, 18</sup> It is likely that the farmers washed the grain and then fed it to their livestock to test for adverse affects before electing to consume it themselves. Unfortunately, the effects of methylmercury poisoning lie dormant for days to months before symptoms appear, and lulled the rural farmers into believing the washed grain was safe to eat.<sup>17</sup>

In all, over, 6,530 cases of methylmercury poisoning resulting in 459 deaths were seen in hospitals from 1971-1972 although as many as 40,000 people may have been affected.<sup>6, 17</sup> This scenario was repeated in Ghana with ethylmercury, resulting in 144

poisonings with 20 fatalities and again in China through the consumption of mercury-treated rice.<sup>3</sup> As the result of these mass poisonings, the use of mercurial antifungal seed dressings was finally discontinued in the late 1970s.<sup>10</sup>

**Anthropogenic Mercury Emissions and Prevention.** With growing concern over the use of mercury, many processes that once utilized this element are being phased out in favor of alternative products whenever possible. Presently the total anthropogenic release of mercury to the environment has been estimated between 2,000 and 6,000 metric tons annually; sources range in scale from substantial industrial effluent discharges down to the smallest broken fever thermometer.<sup>3, 8, 19-21</sup> A useful inventory of global mercury discharges from nine different source categories was compiled for the year 2000 by Pacyna, et al.<sup>21</sup> The inventory can broadly be separated into two categories: those which utilize the unique properties of mercury for industrial purposes and those that discharge mercury as an unintended byproduct of combustion. Industries that release mercury as a byproduct include the mercury mining industry as well as the manufacture of gold, caustic soda, batteries, measuring and control instruments, and electrical equipment. Mercury released via combustive processes includes the combustion of fossil fuels, metal smelting, cement production, waste incineration and human crematoria.

Primary mercury production itself ranked eighth as a source of global anthropogenic mercury emissions with an estimated 23.1 tons of mercury released in 2000.<sup>21</sup> World production of mercury reached a peak at 10,000 tons in 1973 but declined to 6,500 tons by 1980 while many mercury mines have either decreased production or closed at present.<sup>20, 22</sup> Records indicate the Phoenicians and Carthaginians first commercialized mercury production from the Almaden mines in 2,700 B.C. for use in amalgamating and concentrating precious metals but the technique was not widely used until the Romans began using the process in 50 A.D.<sup>12, 22</sup> Industrial-scale silver and gold production has its roots in the Spanish-American silver mines which operated from 1570-1820.<sup>11, 23</sup> Mercury amalgamation of precious metals was first used in the *patio* process where powdered ore of the precious metal is spread over large, paved surfaces and mixed with salt brine, copper and iron pyrites, and elemental mercury. The mixture is blended with hoes and rakes then allowed to react for days to weeks before removing the amalgam and roasting it in the open air to recover the gold or silver while the mercury is

volatized to the atmosphere.<sup>11, 22</sup> The patio process was quickly supplanted by “barrel amalgamation,” or Born process, that itself gave way to the cyanide amalgamation process introduced in 1900. Regardless of the shift in technology, an estimated 196,000 tons of mercury were discharged to the environment in South and Central America during the period of 1570-1900 when the *patio* process was in common use.<sup>23</sup>

The amalgamation process for recovering fine particles of gold and silver from secondary or low-grade ores and stream bed sediments has enjoyed popular use during every modern gold rush. Use of this technique was widespread during the California gold rush starting in 1850 but was significantly curtailed with the Sawyer Decision in 1884.<sup>24</sup> During the same time frame, gold rushes in South Dakota, Nevada, Australia and later in Canada also favored amalgamation for concentrating precious metals, but with the advent of cyanidization, the use of mercury as a significant mining technology virtually vanished.<sup>22</sup> However, the price of gold rose by a factor of 8 – 10 in the 1970s while many nations were coping with crippling socioeconomic difficulties, triggering yet another gold rush in South America, China, Southeast Asia and parts of Africa.<sup>12, 22</sup> Unfortunately, the inexpensive, reliable and portable nature of amalgamation process made it an attractive option, leading to its widespread use once again with techniques almost identical to those of the past.<sup>22</sup>

Large scale gold production using mercury technology ranked second in emissions with an estimated release of 248.0 tons of mercury to the environment in 2000.<sup>21</sup> Untold amounts of mercury in the abandoned mine wastes still act as a source of mercury discharge to the environment though no estimates on the magnitude of this release has been considered anywhere in the literature.<sup>23</sup> The barrel amalgamation process releases mercury directly to rivers during the sifting of amalgamated ores to separate the heavier fractions from the lighter ones and also during the open-air roasting process to volatize the mercury, leaving the gold behind.<sup>12, 22</sup> As an example of the effects, the Madeira River Basin in Brazil is one major site of the current gold mining operations and contributes  $32 \text{ ton}\cdot\text{yr}^{-1}$  of mercury release to the environment alone.<sup>25</sup> This has caused the Madeira River mercury levels to rise to  $13.8 \pm 2.5 \text{ ng}\cdot\text{L}^{-1}$  dissolved mercury, meaning the Madeira transports an astounding  $23 \text{ ton}\cdot\text{yr}^{-1}$  of mercury directly to the Amazon River into which it flows.<sup>25</sup> Total inputs of mercury into the Amazon due to

mining are estimated at  $90 - 120 \text{ ton}\cdot\text{yr}^{-1}$ .<sup>23</sup> These dynamics are repeated in several other tropical and Asian mining areas all around the world. Furthermore, it would seem that the only way to curtail mercury emissions from precious metal mining is to again abandon the inexpensive amalgamation technique in favor of cyanidization or other techniques for concentrating traces of gold.

The next largest source of mercury release due to direct industrial use of the element is caustic soda and chlorine production using the chlor-alkali process. Although the use of the continuous mercury cell to produce sodium hydroxide and chlorine has declined sharply due to the introduction of diaphragm cells, this process was still responsible for 65.1 tons of mercury release in 2000, representing the sixth highest source of anthropogenic mercury release.<sup>5, 19, 21, 26</sup> In 2003, the global consumption of mercury to support the chlor-alkali process was 800 tons.<sup>21</sup> Mercury is released as a byproduct in the hydrogen stream and from the end box and cell room ventilation air.<sup>21</sup> At a rate of 0.25-0.50 lb of Hg released per ton of sodium hydroxide produced, the chlor-alkali industry was once the major source of mercury release to the aquatic environment.<sup>2</sup> Presently, the complete loss of mercury to the environment is prevented through the use of mist eliminators, scrubbers, cooling of the gas stream, and mercury adsorption onto activated carbon (AC) and molecular sieves with efficiencies upwards of up to 90% mercury removal.<sup>21</sup>

The general category of “other sources” was the seventh largest contributor of mercury emissions in 2000 with an estimated 44.6 tons released with batteries, measuring devices, control instruments, electrical devices and electrical lighting comprising the bulk of this category.<sup>21</sup> Even though the use of mercury-containing batteries has declined in many regions, this industry was the main consumer of mercury in 2000, with a usage rate of  $1000 \text{ ton}\cdot\text{yr}^{-1}$ .<sup>21</sup> Due to its uniform thermal expansion over a wide range of temperatures, elemental mercury once found use as a component of many gauges including sphygmomanometers, barometers, thermometers, and natural gas regulators but this use has been curtailed as well.<sup>4, 5, 9</sup> However, there are a few remaining applications such as AC rectifiers, automobile switches, mercury arc street lamps, compact fluorescent lamps, and control devices such as thermostats that still rely heavily upon mercury usage.<sup>1, 5, 9, 26</sup> In fact, the environmental benefits of using the mercury-containing compact

fluorescent bulbs (CFLs) with their 75% reduction in energy use and 10-fold increase in lifetime has guaranteed a resurgence of mercury-containing devices at a time when most other types are being removed from the home.<sup>27</sup> While the older devices such as fever thermometers contained approximately 500 mg of elemental mercury, fluorescent light tubes and CFLs contain 0.7 - 115 mg and 3-5 mg mercury respectively.<sup>27</sup> Although information concerning mercury release from primary battery production was not available, emissions of mercury related to the production of electrical apparatus and instruments were considered relatively small due to the use of effective gaskets and seals.

Combustive processes that release mercury as a consequence of operation include the burning of fossil fuels for power generation, waste incineration, human crematoria, metal smelting, and cement production. The combustion of fossil fuels for power generation ranked highest of all sources in mercury emissions, accounting for an estimated 1422.4 tons of mercury released globally in 2000, or almost 2/3 of the 2189.9 total estimated anthropogenic global mercury emissions tallied by Pacyna et al. for that year.<sup>21, 28</sup> Mercury is found as cinnabar (HgS), bound to pyrite (FeS<sub>2</sub>) and bound to coal maceral (organic matter) with contamination rates ranging as widely as 70 - 33,000  $\mu\text{g}\cdot\text{kg}^{-1}$  depending on the coal's origins.<sup>2, 29-31</sup> More typical ranges of mercury content in coal are 0.01 – 1.5  $\text{mg}\cdot\text{kg}^{-1}$  with most U.S. coal averaging 1  $\text{mg}\cdot\text{kg}^{-1}$  of mercury.<sup>2, 21</sup> Oil and natural gas burned for power generation contribute less to mercury emissions. Mercury contamination of oil ranges from 0.01 – 0.5  $\text{mg}\cdot\text{kg}^{-1}$ . The mercury present in natural gas is typically removed during processing.<sup>21, 32</sup>

In the simplest terms, the amount of mercury released due to combustion of fossil fuels depends on the mercury content of the fuel, the amount of fuel combusted, and on the presence and efficiency of pollution control equipment.<sup>33</sup> However, factors that directly impact mercury chemistry in the exhaust gases such as flue gas temperature and the presence of other pollutants including unburned carbon, sulfur oxides (SO<sub>x</sub>), nitrogen oxides (NO<sub>x</sub>) and HCl gases, also play a major role in determining the total mercury released.<sup>30, 33, 34</sup>

All forms of mercury are initially released as Hg(0) during combustion ( $T > 800 - 1,400^\circ\text{C}$ ) and react with other flue gas constituents to form gas phase Hg(II) species including HgO and HgCl<sub>2</sub> as post-combustion temperatures cool to below  $400^\circ\text{C}$ .<sup>29, 30, 33,</sup>

<sup>35,36</sup> Minimal amounts of calomel ( $\text{Hg}_2\text{Cl}_2$ ) are also believed to form; however it disproportionates readily to  $\text{Hg}(0)_{(g)}$  and  $\text{HgCl}_{2(g)}$ .<sup>30,36,37</sup> Mercury chlorination appears to be the dominant mercury transformation and burning a high-chlorine coal will shift the disposition of mercury species by oxidizing even more  $\text{Hg}(0)$  to water-soluble  $\text{Hg}(\text{II})$ .<sup>29,30,33,38</sup> Mercury sorption onto particulates has been found to favor the formation of the Hg-particulate or “Hg-p” species  $\text{HgCl}_2$ ,  $\text{HgO}$ ,  $\text{HgSO}_4$ , and  $\text{HgS}$  due to the presence of reactive chemical species and oxidation catalysts on the surfaces of fly ash particles.<sup>30,33,36</sup> Although the interactions between mercury and fly ash surfaces are not clearly understood, it has been well-established that fly ash particles avidly capture mercury.<sup>30,36</sup> Total mercury concentrations in the flue gases range from 5 – 10  $\mu\text{g}\cdot\text{m}^{-3}$  and the relative distributions between  $\text{Hg}(0)$ ,  $\text{Hg}(\text{II})$ , and Hg-p vary widely.<sup>30,33</sup>

Reduction of mercury pollution from coal-fired power plants starts at the coal mine with the selection of low-sulfur, high-chlorine coals regardless of the coal grade or rank. Low-sulfur coals are chosen with the express purpose of reducing sulfur dioxide emissions but have the added benefit of eliminating the chalcophilic mercury contamination. Furthermore, opting for a high-chlorine coal favors the chlorination of  $\text{Hg}(0)$  to  $\text{HgCl}_2$  which is more easily removed from the flue gas stream as described later.<sup>29</sup> To increase the energy density and increase power plant efficiency, coal cleaning, or “beneficiation” to reduce mineral matter and the pyritic sulfur content has the added benefit of reducing both sulfur dioxide and mercury emissions.<sup>21</sup>

The efficacy of any mercury reduction measure depends on the mercury species generated in the stack gases. Particulate control devices offer another line of defense against mercury emissions from coal-fired power plants.<sup>39</sup> De-dusting equipment such as electrostatic precipitators (ESPs) and fabric filters (FF) will remove much of the Hg-p species,<sup>30,33,36,38</sup> accounting for a 30% decrease in overall emissions with FF showing greater mercury capture than ESP on average.<sup>21,39</sup> Furthermore, combustion conditions can be manipulated to generate a larger concentration of the particulate carbon, or fly ash content in the flue gas to favor the production of a larger fraction of Hg-p that can be captured.<sup>33,36</sup> Alkaline fly ash, however, removes chlorine responsible for Hg oxidation, reducing the fraction of Hg that can be captured.<sup>29</sup> Though very expensive and not widely used, activated carbon injection (ACI) and carbon filter beds installed specifically for the

reduction of mercury have shown promise in reducing mercury pollution by as much 90% by causing Hg adsorption and subsequent oxidation on the activated carbon (AC) surface.<sup>21, 29, 30, 33, 36-38</sup> Higher capture efficiencies have been reported for carbons impregnated with iodine or sulfur; lower captures result from high SO<sub>2</sub> concentrations in the flue gas due to competition of SO<sub>2</sub> with Hg for active sites on the AC.<sup>29, 39</sup> Sodium sulfide and sodium hydrogen sulfide injection has also been explored as a means to control mercury emissions through the formation of solid HgS that can be captured by particulate control devices.<sup>33, 36, 39</sup> The effects on the saleable coal combustion byproducts (CCBs), including the quality of the manipulated fly ash for the manufacture of pozzolanic cement, must also be considered as high carbon content may decrease the value of these products.<sup>29, 39</sup>

Several pollution mitigation technologies aimed at the reduction of sulfur and nitrogen gases exert the co-benefit of reducing mercury emissions.<sup>2, 39</sup> Flue gas desulfurization (FGD), whether exacted through wet scrubber systems or spray dry systems, can remove 30 - 50% or 35 - 85%, respectively, of mercury as Hg(II) but virtually none of the elemental mercury which is insoluble in water.<sup>21, 29, 30, 32, 33, 38-40</sup> Evidence has shown that a portion of the captured Hg(II) may also be reduced and re-emitted as Hg(0) from the scrubber solution under normal operating conditions.<sup>29, 39</sup> Furthermore, acidic conditions (pH < 3) with [Cl<sup>-</sup>] < 0.1 M or free SO<sub>2</sub> may cause the reduction of captured Hg(II) to Hg(I) which disproportionates to Hg(0) and Hg(II), further reducing the overall capture efficiency.<sup>33, 36</sup> For this reason, adding reagents to the scrubber solution to prevent reemission represents a prime opportunity for mercury remediation that no one has taken opportunity of at present.<sup>29, 34</sup> Selective catalytic reduction (SCR) used to mitigate NO<sub>x</sub> emissions also exhibit the co-benefit of decreasing mercury emissions by enhancing the Hg(0) oxidation to Hg(II) though the magnitude of this effect has proven to be both coal- and catalyst-specific.<sup>29, 36, 39</sup> Though still in the early stages of testing, the Electrocatalytic Oxidation (ECO) multi-pollutant control method has shown promise in reducing several problematic species. The ECO uses a dielectric barrier discharge to convert elemental mercury to HgO that is collected in an ammonia scrubber and ESP along with the co-contaminants SO<sub>2</sub>, NO<sub>x</sub>, and fine particulate matter.<sup>29, 36</sup>



Regardless of the mitigation technologies employed, mercury releases to the environment are imminent in coal-fired power plants. None of these pollution control devices is effective for Hg(0) which is ultimately released into the atmosphere.<sup>38</sup> Typical coal-fired power plants release 20-50 % of mercury as Hg(0), 50-80% as Hg(II) and < 5% as Hg-p.<sup>32, 33, 36</sup> Hg(II) and Hg-p are more apt to be deposited local to the emission site than Hg(0) with its low water-solubility, high vapor pressure, and propensity for long-range transport.<sup>29, 30, 33, 36, 39, 40</sup> Furthermore, all of these technologies convert the mercury to a more concentrated solid or liquid form, which is either disposed of in a landfill or adventitiously incorporated into CCBs such as cement or wallboard.<sup>29, 41</sup> The land application of ash residues from coal combustion serves as a large contributor to trace metal contaminants in soils.<sup>28</sup> From 50 – 90% of the captured mercury is associated with fly ash and scrubber sludge.<sup>36</sup> Further research is warranted as mercury captured in these CCBs or disposed fly ash and scrubber sludge has the potential to be re-emitted through volatilization, leaching, and microbe-mediated mobilization, a potential problem that will only be exacerbated as we strive to increase the fraction of soluble mercury and its capture in these residues.<sup>29, 39</sup>

Although the variable composition of municipal waste, hazardous waste, medical and pathological wastes, and sewage sludge belie an inherent difficulty in estimating mercury emissions, waste incineration considered together with human crematoria represent the fifth largest source of mercury release with a minimum of 66.4 tons of mercury emissions in 2000.<sup>21</sup> Human crematoria release Hg to the environment through the decomposition of dental amalgams from the corpses during combustion.<sup>42</sup> Municipal sewage sludge may have trace metal contamination great enough to preclude its application to land.<sup>28</sup> Municipal waste can contain up to  $5 \mu\text{g}\cdot\text{g}^{-1}$  mercury, primarily as Hg(0) and HgO, originating from batteries, electric switches, lighting components, paint residues and thermometers.<sup>26, 31-33, 37</sup> Selective removal of batteries, the largest source of mercury in municipal wastes, can reduce this amount to  $< 1 \mu\text{g}\cdot\text{g}^{-1}$ .<sup>33</sup> The dominant form of mercury released from waste incinerator stacks is Hg(II) at an estimated 75 - 85% with Hg(0) comprising only 10 - 20% of emissions and total mercury concentrations average  $100 - 1,000 \mu\text{g}\cdot\text{m}^{-3}$ .<sup>32, 33</sup> This shift to a higher fraction of Hg(II) over Hg(0) is in direct contrast to the ratios seen in coal-fired power plants and is attributable to the higher

fraction of HCl in stack gases due to chlorinated plastics and other chlorinated wastes shifting the equilibrium from Hg(0) to HgCl<sub>2</sub>.<sup>31, 33, 43</sup> The prevention of mercury pollution from these sources is accomplished through the combined use of ESPs with FGD.<sup>21</sup>

With 2000 global emissions estimated at 148.6 tons of mercury for the smelting of the non-ferrous metals copper, lead and zinc, this industry contributed the third largest source of mercury emissions tallied during this inventory.<sup>2, 21</sup> The amount of mercury released in the roasting, smelting, and refining process depends on the mercury content of the ore or scrap utilized, the method used to produce the non-ferrous metals, and the type and efficiency of emission control devices.<sup>21, 28</sup> Of the two main methods of metal production, high temperature roasting and thermal smelting tends to contribute more to atmospheric mercury emissions while electrolytic extraction of non-ferrous metals lends itself to disperse mercury contamination to aquatic systems.<sup>21</sup> Mercury pollution is mitigated through the use of ESPs and FGD in thermal smelters.<sup>21</sup>

Pig iron and steel production contributed the eighth largest amount of anthropogenic mercury to the environment with 31.3 tons in 2000.<sup>21</sup> The electric arc process is used for special alloy steels and for melting large amounts of scrap and contributes ten-fold the amount of mercury compared to the basic oxygen and older open hearth processes.<sup>21</sup> By far, the smelting of metallurgical coke surpassed all other iron and steel-making processes for the greatest emission of mercury to the environment.<sup>21</sup>

Cement production accounted for 140.4 tons of mercury emitted in 2000 and ranked as the fourth largest emitter of mercury pollution.<sup>21</sup> Mercury originates from the fuel used in the fuel-firing kiln systems and as also released from the clinker-cooling and clinker-handling systems used in the cement industry.<sup>21</sup> This pollution is controlled primarily through the use of ESPs.

**Future Mercury Emissions Projections.** On a global scale, the highest mercury emissions were seen during an intense period of worldwide economic growth and increasing population in the late 1970's that translated into the appearance of many new power plants to meet energy demands, few of which were equipped with pollution control devices in developing countries.<sup>21</sup> This trend caused global mercury emissions to peak at 3560 tons<sup>28</sup> in 1980, a benchmark which is supported by ice core mercury deposition data.<sup>24</sup> Throughout the 1980's, developed countries implemented more efficient FGDs

and ESPs and increased the use of natural gas instead of coal for energy production, bringing total mercury releases down to 1881 tons by 1990.<sup>21</sup> By the mid-1990's, however, major industrial development in Asia, Africa, and South America and increasing population superseded mercury emission reductions in developed countries and an overall increase to 2235 tons in global mercury inputs resulted in 1995.<sup>21</sup> Implementation of pollution control technology in the developing nations resulted in the net decrease in mercury to 2190 tons in 2000.<sup>21</sup>

Attempts to regulate mercury emissions globally have been complemented by like-minded efforts in the United States, beginning with the Clean Air Act of 1970 and followed later by the Clean Air Amendment in 1990.<sup>24</sup> More recently, the Clean Air Mercury Rule (CAMR) implemented in March 2005 used a “cap and trade” approach to reduce emissions by 20% (of 1999 levels at 48.5 ton·yr<sup>-1</sup>) to 38 tons in five years and 70% (15 tons) by 2018 but was subsequently vacated in 2008 along with the Clean Air Act.<sup>21, 38, 39</sup> The first phase of this cap and trade system was based on mercury emission reductions exacted as a co-benefit of other pollution control measures deemed necessary under the 1990 Clean Air Act while the second phase required the implementation of mercury-specific mitigation measures, a goal that has proven both elusive and expensive.<sup>38</sup>

Regardless of the laws created, mercury emissions are most likely to continue rising in the near future. In the first study of its kind, Streets and Zhang, predicted mercury emissions will continue to rise in three of the four scenarios used to forecast global mercury emissions for the year 2050.<sup>44</sup> The change in emissions ranges from -4% to +96% and are dependent primarily upon rapid expansion of coal-fired electricity generation in Asia.<sup>44</sup> Currently, Streets claims that only 18% of global mercury emissions are due to coal-fired power plants, but this fraction could rise as high as 50% in the future, a reason he feels “Coal-fired power plants...are the key target for Hg emission control.”<sup>44</sup>

**Environmental Mercury Chemistry.** To discuss the environmental chemistry of mercury, one must consider both the natural and anthropogenic sources of mercury and the resultant speciation of the metal before proceeding to discuss how mercury behaves on global, regional, and local level as it cycles through the environment. A survey of 270

years of ice-core records from a North American glacier revealed 52% of deposited mercury was from anthropogenic sources, 6% due to volcanic events, and 42% from background, or pre-industrial (before 1840) sources on the regional and global scale.<sup>24</sup> Citing the well-documented increase in anthropogenic mercury emissions to the environment, in a 1988 paper Nriagu accurately assessed the situation when stating that “...mankind has become the most important element in the global biogeochemical cycling of the trace metals,” a vision shared by many others.<sup>28, 45</sup> For instance, it is highly probable that most of the 300,000 tons of mercury released to the biosphere during the last 500 years of gold and silver mining may still participate in the global mercury cycle through leaching of abandoned mine tailings and remobilization from other contaminated areas.<sup>22</sup> Emissions from natural sources are difficult to assess, as demonstrated by annual estimates from as low as 1,700 tons to as high as 6,000 tons with a range of 2,000 - 3,000 tons of mercury most commonly quoted due to erosion, volcanic eruptions, and degassing from the earth’s crust, upper mantle, and bodies of water.<sup>2-4, 8, 19-21, 46-48</sup> Claims attributing the ultimate source of mercury emissions range from a roughly 50/50 assignation between natural and anthropogenic sources to the belief held by Pirrone, Morel, and others that mercury emissions probably result in equal thirds from natural sources, industrial sources, and *recycled* anthropogenic mercury.<sup>4, 26, 48-50</sup> Given the proclivity of mercury to undergo successive volatilization, condensation and re-emission, this estimate seems reasonable if not highly probable.

The environmental mercury cycle must be considered on global, regional, and local scales with the global cycle, involving the atmospheric transport of elemental mercury, and local cycles involving the methylation of inorganic mercury, bearing the brunt of responsibility for the overall environmental transport and distribution of the element.<sup>4, 51</sup> The current tropospheric mercury burden has been estimated at 6,000 tons, representing an increase by a factor of 2 – 5 over pre-industrialized estimates.<sup>11, 46, 50-52</sup> Hg(0) vapor is the main species emitted from natural sources although Hg-p, volatile organomercurials and inorganic mercury compounds cannot be ruled out.<sup>4, 50</sup> Background levels of atmospheric mercury are typically 90-95% Hg(0) and only 3-5% Hg(II) with the remainder of mercury existing as particulate Hg-p and methylated forms.<sup>33, 48-50</sup> With its high vapor pressure, the residence time of the relatively stable, monatomic Hg(0) gas in

the atmosphere is on the order of 0.5 - 2 yrs and accounts for the widespread distribution of mercury to even remote locations in the global environment far from mercury sources.<sup>4, 6, 11, 24, 30, 33, 36, 46, 48, 52</sup>

Different models have been proposed to explain the global mercury cycle but the process is still not well understood as several key transformations have proven difficult to explain.<sup>11, 33, 48</sup> Elemental and divalent mercury can sorb to particulate matter, or aerosols and undergo dry deposition (through gravitational settling and brownian motion) or wet deposition with the former dominating for Hg(0).<sup>4, 33, 36, 46, 48, 50</sup> Though elemental mercury is only sparingly soluble in water, wet deposition can occur following Hg(0) oxidation by OH<sup>•</sup>, O<sub>3</sub>, H<sub>2</sub>O<sub>2</sub>, NO<sub>3</sub><sup>•</sup>, Cl<sub>2</sub>, HSO<sub>3</sub><sup>-</sup>, or HOCl/OCl<sup>-</sup> in the gas phase or in atmospheric moisture to form soluble forms of highly reactive Hg(II) that are easily removed by rainfall.<sup>4, 6, 10, 11, 26, 33, 36, 46, 48, 53, 54</sup> This process can be complicated by atmospheric mercury reductants including SO<sub>2</sub>, SO<sub>3</sub><sup>-</sup>, CO, OH<sub>2</sub><sup>•</sup> and in particular by the photoreduction of Hg(OH)<sub>2</sub>.<sup>33, 46, 48</sup> Regardless of the exact mechanisms involved, elemental mercury is transported through the atmosphere over long distances from its sources and eventually deposited onto soil, plants, and into bodies of water.<sup>33, 48, 55</sup>

Soils, especially those high in clay and organic matter, serve as a “net sink” for environmental mercury even though some volatilization of atmospherically deposited mercury from soils does occur.<sup>4, 50, 56</sup> In aerated soils, mercury may be found as Hg(OH)<sub>2</sub>, HgCl<sub>2</sub>, HgOH<sup>+</sup>, HgS and Hg(0) while reducing conditions favor the formation of HgSH<sup>+</sup>, HgOHSH and HgClSH with only trace amounts of CH<sub>3</sub>Hg<sup>+</sup> and (CH<sub>3</sub>)<sub>2</sub>Hg present in the terrestrial environment.<sup>56</sup> Dimethylmercury and elemental mercury [formed by abiotic reduction of Hg(II)] are relatively water insoluble, volatile, and tend to evaporate from soils as a result.<sup>48, 50, 56, 57</sup> The other common terrestrial forms of mercury tend to sorb strongly to soil organic matter (SOM), clay, amorphous FeS and the amorphous oxides, hydroxides, and oxyhydroxides of iron, manganese and aluminum.<sup>2, 50, 56</sup> Mercury sorbs strongest to SOM followed by the oxides and clay minerals.<sup>56</sup> Ultimately, soils may serve as a significant mercury source to surface waters through the actions of erosion and transport with storm runoff.<sup>48, 56</sup>

Mercury is naturally transported to oceans and lakes via watershed runoff and through direct deposition of atmospheric mercury with the latter process being the most

significant as it pertains to oceanic mercury.<sup>2, 45, 52, 56, 58, 59</sup> Surface waters throughout the world generally contain less than  $0.1 \mu\text{g}\cdot\text{L}^{-1}$  Hg with exceptions occurring near mercury-rich mineral deposits and industrial waste effluent streams.<sup>2</sup> The total mercury burden in all of the earth's water is estimated at 10,800 tons.<sup>46</sup> Depending on the redox potential, the pH of the water, and the nature of stabilizing ligands present, mercury species present in natural waters will include elemental Hg(0), the mercuric Hg(II) ion and methylated mercury as monomethylmercury (MeHg) and dimethylmercury (DMHg).<sup>2, 45</sup> Dissolved Hg(0) constitutes a substantial fraction of oceanic mercury (ranging from 5-30% of total Hg) and natural waters are usually supersaturated with  $\text{Hg}(0)_{(\text{aq})}$  compared to the air above, leading to a net de-gassing of Hg(0) to the atmosphere.<sup>45, 48, 52, 59</sup> However, the presence of sufficient chloride and appropriate particulate surfaces are known to catalyze the oxidation of Hg(0) to Hg(II), the species by which all forms of mercury in natural waters are intricately linked.<sup>45, 48</sup>

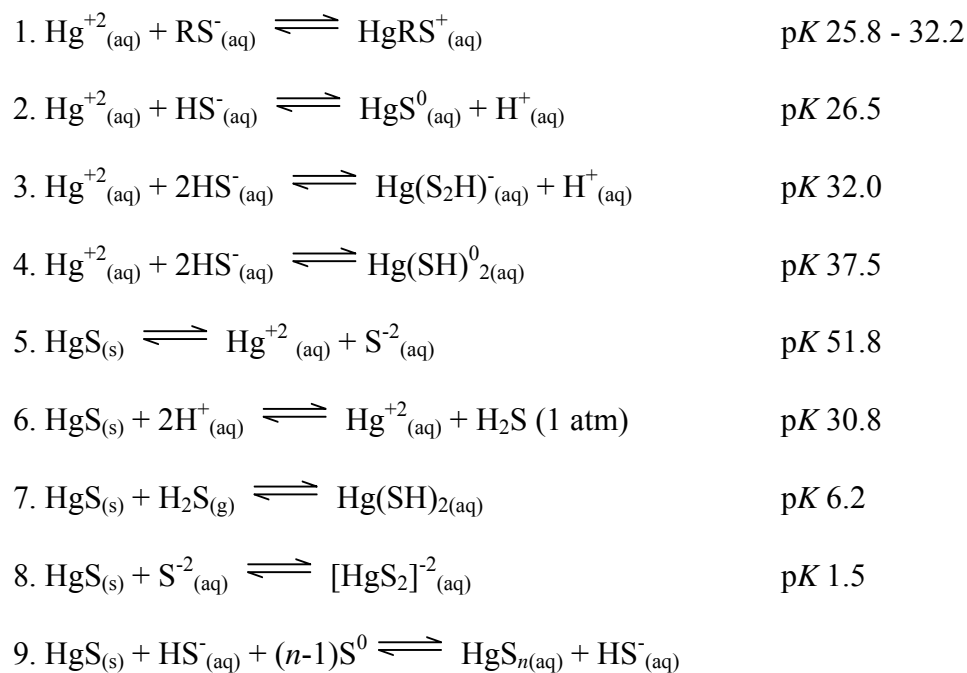
Hg(II) can be found in a variety of inorganic and organic complexes, the identity of which dictates the availability of the ion for transport, transformation, and bioavailability. Speciation of Hg(II) in natural waters is dominated by the formation of organic complexes that gradually are replaced by a progression of mercury-chloride complexes ( $\text{HgCl}^+$ ,  $\text{HgCl}_2$ ,  $\text{HgCl}_3^-$ , and  $\text{HgCl}_4^{2-}$ ) as one moves towards the higher chloride concentrations typical of estuarine and ocean water.<sup>2, 45, 48, 56, 60</sup> Although the extent of their importance is sometimes debated, mercury hydroxide complexes in natural waters, including  $\text{Hg}(\text{OH})^+$ ,  $\text{Hg}(\text{OH})_2$ ,  $\text{Hg}(\text{OH})_3^-$ , and  $\text{HgClOH}$  may also play a significant role, especially when controlling the sorption of mercury to inorganic surfaces.<sup>2, 48, 60, 61</sup> Unlike soils, the scavenging of mercury species by metal oxyhydroxides does not supersede the importance of mercury scavenging by organic matter with as much as 95% of Hg(II) in natural waters bound to dissolved organic matter (DOM).<sup>2, 48, 51, 62</sup> For this reason, lacustrine, estuarine and marine sediments serve as major mercury sinks as mercury is captured by DOM particulates in the water column and settle to the bottom as Hg-p.<sup>11, 45, 59, 63</sup>

DOM refers to the complex mixture of organic compounds resulting from the decay of plant and animal matter. While roughly 20% of DOM is readily identifiable as carbohydrates, carboxylic acids, amino acids and other compounds, the other 80 % is

composed of “humic” substances that are categorized based on their acidity and hydrophobicity.<sup>60</sup> In general, trace metals are bound to the more acidic sites in organic matter including carboxylic acids, phenols, ammonium, alcohols, and thiol groups.<sup>2, 60</sup> Mercury, with its highly polarizable outer shell electrons, has a remarkable affinity for other large, highly polarized ligands and bind only weakly to Lewis bases such as –COOH and other oxygen-containing functional groups in the DOM.<sup>56, 60</sup> For this reason, mercury is often found in complexes with thiols and other sulfur-containing functional groups.<sup>56, 60</sup>

Sulfur is a minor constituent comprising only 0.5% to 2.0% by weight of DOM and can be present in the reduced form (sulfides, thiols, polysulfides) or oxidized form (sulfonate, sulfate).<sup>60</sup> Only the reduced sulfur species, which are commonly found in the hydrophobic humic acid and fulvic acid fractions of DOM, are responsible for Hg binding with stability constants ranging from  $10^{25.8}$  –  $10^{32.2}$  as depicted by reaction (1) in Scheme 1.1.<sup>45, 60, 61, 64</sup> Strong bonds to multiple sulfur groups and additional weak coordination with the abundant oxygen functional groups in DOM are not uncommon and account in part for the variable nature of the binding constants.<sup>60</sup> For this reason, DOM sulfur often competes with inorganic sulfur for binding to mercury, especially in anaerobic environments.<sup>45, 56, 60</sup> The total sulfur content in natural environmental systems is usually 5-50 pM.<sup>60</sup>

The formation of highly insoluble  $\text{HgS}_{(s)}$ , either as red cinnabar or the black mineral metacinnabar, is the oft-cited process for removal of Hg(II) from the water column and incorporation into sediments.<sup>2, 45, 48, 60, 64</sup> The insolubility of HgS is reduced in natural waters through formation of complex species including  $\text{Hg}(\text{SH})_2$  in acid solution and  $\text{HgS}_2^{-2}$  in alkaline solution.<sup>5</sup> Specifically in Scheme 1.1, reactions 2 – 4 compare competing mercury-sulfur reactions in natural waters while reactions 5 – 9 give specific examples of competing complex formation directly responsible for cinnabar dissolution.<sup>2, 5, 48, 60, 64</sup> Cinnabar solubility is further enhanced through mercury-polysulfide complex formation with the zero-valent sulfur in sulfanes ( $\text{H}_2\text{S}_n$ ), hydropolysulfides ( $\text{HS}_n^{-1}$ ), and polysulfides ( $\text{S}_n^{-2}$ ) as depicted in reaction (9).<sup>48, 64</sup> The sum of these competing processes results in less Hg(II) sequestered in sediments and more reactive aqueous Hg(II) available in the water column.<sup>64</sup>



**Scheme 1.1:** Relevant Equilibrium Expressions for Hg-S Species in Solution.<sup>2, 5, 48, 55, 60, 64</sup>

Hg(II) not captured by sediments has the potential to either be reduced to Hg(0) or to become methylated through chemical and biological processes to MeHg or DMHg.<sup>45, 52, 60, 65</sup> Thermodynamically Hg(II) may be reduced to Hg(0) in aquatic systems; kinetically the conversion of Hg(II) to Hg(0) is a very slow reaction unless mediated by microbial populations or by the humic fraction of DOM.<sup>11, 45, 52, 60</sup> Evidence has also been discussed that alludes to Hg(II) reduction facilitated by photochemical processes that may themselves be enhanced by the presence of DOM.<sup>45, 48, 60</sup> Only a small portion of available Hg(II) is eventually methylated, resulting in a MeHg fraction of only 1% - 10% of total Hg.<sup>45</sup> The areas of greatest methylation occur at the top of the suboxic zone in waters, where dissolved oxygen and sulfide are low, and under hypoxic/anoxic conditions typical of the sediments.<sup>45, 66</sup> Worth noting is the absence of the water insoluble DMHg in the shallow, coastal areas, it does tend to be the more prevalent form of methylated mercury in intermediate and deep ocean waters.<sup>2, 45, 67</sup> This may be due to degassing of



the volatile, uncharged DMHg to the atmosphere or degradation by photochemical, thermal, or biotic pathways to MeHg in shallower waters.<sup>45, 56, 58, 59, 66, 67</sup>

The methylation process itself can proceed through abiotic and biotic processes, each depending on environmental factors including temperature, pH, redox potential, the presence of organic and inorganic complexing agents, and the activity of microbial communities.<sup>58, 60, 68</sup> In general, MeHg production has been found to increase with decreasing pH and decreasing chloride concentrations irrespective of the methylation process.<sup>58, 62</sup> Abiotic, or chemical methylation has been confirmed in multiple studies yet the mechanism governing this process remains obscure.<sup>58</sup> Chemical methylation requires the donation of a methyl group as carbocationic  $\text{Me}^+$ , carbanionic  $\text{Me}^-$  or radical  $\text{Me}^\cdot$  from any number of potential donors. Small organic molecules including acetate, methyl iodide and dimethylsulfide, organometallic complexes such as methyllead, methyltin, or methylcobalamin, and larger molecules in DOM all represent suitable candidates for methyl transfer to mercury under low-chloride conditions.<sup>45, 58</sup> Furthermore, high molecular weight humic and fulvic acids can contribute to direct abiotic methylation in organic-rich waters through poorly understood dark and photochemical processes.<sup>45, 48, 60</sup>

Microorganisms have several mechanisms by which they can deal with toxic mercury species to prevent the disruption of normal biochemical processes and cell damage. The first line of defense involves binding the Hg directly to the cell surface via free protein sulfhydryl groups, a phenomenon demonstrated by plankton or by uptake of mercury by extracellular polysaccharide coatings.<sup>2, 51, 69</sup> Alternatively, the precipitation of Hg as oxides or sulfides with deposition to the cell surface is another viable option rather than allowing cell penetration.<sup>51, 70</sup> Once inside the cell, other cellular defense mechanisms include efflux pumps removing Hg(II) from the cell, enzymatic reduction of Hg(II) to Hg(0), chelation by enzymatic proteins such as metallothionein or cysteine, or biomethylation.<sup>51, 69-71</sup>

Certain bacteria are known to metabolically mediate the reduction of Hg(II) to Hg(0) when high levels of Hg(II) (> 50 pM) trigger induction of the *mer* operon.<sup>45, 48, 56, 69-71</sup> The *mer* operon is a plasmid-encoded metalloregulatory mechanism that codes for a series of enzymes to deal with excess Hg(II).<sup>5, 48, 69</sup> Inorganic mercury is dealt with by

MerT, a membrane protein that facilitates the transport of Hg(II) across the cell membrane and MerA reductase that reduces Hg(II) to Hg(0) with a net production of energy for growth and the release of the less toxic Hg(0) by diffusion from the cell.<sup>48, 69, 70, 72</sup> While not present in all *mer*-carrying microorganisms, certain *mer* operons code for MerB lyase, an additional mercury resistance mechanism that acts specifically on organomercury compounds to form free Hg(II) that can be acted upon by MerA reductase.<sup>48, 69, 70, 72</sup> During these transformations, mercury is shuttled between enzymes as a mercury-cysteine complex.<sup>70, 72</sup>

Biotic methylation is another defense mechanism against mercury poisoning that can be invoked by a variety of aerobic bacteria, anaerobic bacteria, fungi, and iron-reducing bacteria with sulfate-reducing bacteria (SRB) in anoxic sediments dominating this process in the environment.<sup>45, 48, 55, 56, 58, 59, 68, 73-75</sup> The greatest levels of MeHg production occur at the top of the suboxic zone of the water column, an area characterized by the low oxygen and sulfide content, thus implying more Hg(II) is inherently available for methylation due to a low abundance of ligands for complexation.<sup>45</sup> The oxic-anoxic transition zones typical of sediments supporting sulfate reduction and methanogenesis are a second zone of optimized Hg(II) methylation.<sup>45, 61</sup> Furthermore, low pH, higher sulfate, and higher DOC concentrations have all been found to significantly enhance mercury biomethylation.<sup>58, 59, 68, 75</sup>

Although the biomethylation of mercury has been studied more extensively than any other element due to the extensive poisonings by mercurial compounds, very little is known about the mechanism(s) of methylation.<sup>45, 58, 75</sup> Bacteria can assimilate neutrally charged lipophilic mercury species such as  $\text{HgCl}_{2(\text{aq})}$  and  $\text{HgS}^0_{(\text{aq})}$  through passive diffusion and by active uptake of both neutral and charged species.<sup>48, 60, 62, 64, 68</sup> However, it remains unclear why SRB are resistant to mercury.<sup>58</sup> In complete oxidizing strains of SRB, the acetyl-CoA pathway for acetate oxidation is associated with mercury biomethylation but the pathway(s) for incomplete oxidizing SRB strains remains unknown.<sup>68</sup> Intracellular methylcobalamin has been suggested as the catalyst for methyl group transfer from potential methyl donors including the amino acid serine, acetylcoenzyme A, methyltetrahydrofolate, *S*-adenosyl methionine (SAM).<sup>2, 5, 48, 58, 68, 74,</sup>

<sup>75</sup> The eventual distribution of MeHg is dependent upon where it is produced and where it is compartmentalized in the environment after production.<sup>62</sup>

Water soluble MeHg ( $\text{CH}_3\text{Hg}^+$ ) behaves like a substituted salt, resulting in chemistry that is very similar to Hg(II) in natural waters in that MeHg can be found complexed with chloride, hydroxide, and DOM, all of which will limit its uptake by biota.<sup>2, 45, 48, 56, 59, 60, 62, 66, 76</sup> MeHg shows affinity for the common ligands in water in the order:  $\text{RS}^- > \text{SH}^- > \text{OH}^- > \text{Cl}^-$ , but unlike Hg(II), MeHg is limited in its ability to bind to multiple ligands.<sup>2, 56, 76</sup> In oxic waters, MeHg-humic acid complexes dominate while less oxic waters favor the formation of MeHg-sulfide complexes.<sup>45</sup> Unlike all other forms of mercury, MeHg has the curious property of bioaccumulating within organisms on the order of 10,000 to 100,000 times water concentrations and subsequently biomagnifying in the aquatic food chain more than a million-fold.<sup>2, 4, 45, 51, 58, 75</sup>

MeHg is concentrated from water, sediment and food by unicellular organisms.<sup>45</sup> This transfer of MeHg from water to organic phases occurs mainly in the form of the neutral species  $\text{CH}_3\text{HgCl}$  and  $\text{CH}_3\text{HgOH}$  which are then bound to the soluble fraction of the organism.<sup>48, 51</sup> This is in contrast to  $\text{HgCl}_2$ , which binds chiefly to cell membranes that are eventually excreted by the larger organisms during digestion of their unicellular prey.<sup>48</sup> In fact, the transfer efficiency of between unicellular organisms and their predators is often four times greater for MeHg than Hg(II).<sup>48</sup> Slow rates of MeHg elimination relative to uptake through dietary sources leads to bioaccumulation with higher concentrations increasing with both age and size of the affected organism.<sup>2, 45, 51</sup>

The accumulation of mercury in fish is of great concern because the consumption of MeHg affected fish and shellfish has become the main source of mercury exposure to humans.<sup>12, 19, 38, 45, 48, 56, 60</sup> Bioaccumulation of MeHg in fish occurs from ingestion of mercury during feeding and to a much smaller extent directly from mercury-affected water passing across the gills of fish.<sup>19, 48, 55, 60, 62</sup> The intestinal wall of fish is effective at blocking  $\text{HgCl}_2$  but is permeable to MeHg which can accumulate in the muscle over time even though MeHg typically shows preferential solubility in fatty animal tissues.<sup>48, 51, 60,</sup>  
<sup>74</sup> Due to this selective permeability, nearly all of the mercury (>95%) found in fish is MeHg.<sup>58, 60</sup> MeHg has a demonstrated affinity for the thiol-containing amino acids cysteine and glutathione and is often found complexed to them in fish.<sup>2, 10, 56, 58</sup> MeHg

concentrations increase moving up through the trophic levels of the aquatic food web, causing piscivorous fish to show higher mercury concentrations followed by fish from lower trophic levels such as omnivorous, detritivorous, and herbivorous species.<sup>12, 45</sup>

In the 1950's, Japanese fishermen and their families were poisoned by methylmercury through the consumption of seafood from Minamata Bay as a staple in their diet.<sup>19, 55, 77</sup> Depending upon the information source quoted, between 111 and 10,000 people were affected with 41 - 101<sup>77</sup> people suffering death directly related to MeHg poisoning and MeHg considered a contributing factor in another 800 deaths.<sup>2, 5, 77</sup> The fish were found to contain abnormally high levels of MeHg as a result of Hg(II) salts from a local chemical manufacturing plant being discharged directly into the shallow bay.<sup>5, 77</sup> As a result of the large number of people affected, "Minamata Disease" is the most widely known incident of organic mercury poisoning and has prompted much of the published research on MeHg toxicity.<sup>1, 2</sup>

**Mercury Toxicity.** While bacteria have developed coping mechanisms to deal with mercury toxicity, unfortunately human beings have no such strategy. A recent and poignant reminder of this fact occurred in 1997 when Professor Karen Wetterhahn died after a single exposure consisting of only a few drops (~0.44 ml) of dimethylmercury (DMHg) spilled from the tip of a pipette, penetrating her latex gloves.<sup>1, 10, 78, 79</sup> Although extremely toxic, DMHg is sometimes used to prepare nuclear magnetic resonance standards and mass spectrometer mercury calibration standards.<sup>8, 79</sup> The effects of the exposure were delayed for several weeks, but Dr. Wetterhahn eventually suffered severe neurotoxic effects and died within a year of the exposure.<sup>1, 10, 78, 79</sup>

The toxicological effects of mercury exposure vary depending on the mercury species in question and the mode of exposure although detrimental changes in the nervous, renal system, reproductive, immune, and cardiovascular systems are all recurring themes.<sup>7, 10, 16, 80, 81</sup> Elemental mercury, with its appreciable vapor pressure, is itself toxic and can cause such effects as headaches, tremors, inflammation of the bladder and erethism (memory loss, emotional lability, depression, insomnia, and shyness).<sup>5, 6, 10, 16</sup> Exposure to mercury vapor occurs principally from small mercury spills in the home, vaporization from dental amalgams, and from occupational exposure.<sup>16</sup> Inhalation of elemental mercury is the main exposure route of concern as 80% of inhaled mercury is

absorbed through the alveolar membranes while absorption of ingested metallic mercury is low (< 0.01%), leaving this exposure route relatively non-toxic.<sup>7,9,10,16</sup> Once inhaled, the Hg(0)<sub>(g)</sub> diffuses rapidly to all tissues, easily crosses cell membranes, and readily crosses both the placenta and blood-brain barrier.<sup>10,16</sup> A portion of the inhaled mercury remains in the bloodstream while the rest is deposited inside red blood cells, the liver, and central nervous system.<sup>7</sup> Inside cells, the dissolved vapor can be oxidized by the catalase-hydrogen peroxide pathway to Hg(II), the species which causes the mercury toxicity since Hg(0) cannot itself interact with any other ligands in the body.<sup>8,10</sup> Short-term, high-mercury exposure effects may cause lung damage, nausea, vomiting, diarrhea, increased blood pressure and/or heart rate, skin rashes, fatigue, fever, chills, and eye irritations while chronic exposure can damage the neurologic system.<sup>7-10,16</sup> Mercury elimination by the body occurs principally through excretion of urine and bile.<sup>7</sup> The U.S. Occupational Safety Health Administration recommends  $50 \mu\text{g}\cdot\text{m}^{-3}$  as the time-weighted average (TWA) for  $8 \text{ hr}\cdot\text{day}^{-1}$ ,  $5 \text{ days}\cdot\text{wk}^{-1}$  exposure while the American Conference of Governmental and Industrial Hygienists (ACGIH) recommends a maximum of only  $25 \mu\text{g}\cdot\text{m}^{-3}$  for the same exposure period.<sup>8,9</sup>

At one time mercury salts were commonplace as the active ingredients in laxatives, teething powders, skin-lightening creams, ointments and as preservatives used in medicine. The toxicity of the mercury salts varies with their water solubility and their subsequent potential for gastrointestinal absorption in the following, decreasing order:  $\text{HgNO}_3 > \text{HgCl}_2 > \text{HgSO}_4 > \text{Hg}_2\text{Cl}_2 > \text{HgO}$ .<sup>7,16</sup> While both mercurous and mercuric chloride are believed to be the agents responsible for acrodynia (painful extremities), or “pink disease” in children, modern poisoning by pure inorganic mercury salts is rare.<sup>10,16</sup> For this reason, the following toxicity discussion will center on the Hg(II) species in general terms as it can originate from MeHg biotransformations that will be discussed next.<sup>8</sup>

The toxic dose for HgCl<sub>2</sub> may be as low as 0.5 g and owing to its corrosive nature, initial symptoms of poisoning include gastrointestinal pain, vomiting, profuse bloody diarrhea, burning in the chest and rapid discoloration of the mucus membranes from precipitation of mercury-protein complexes in the mucosal lining.<sup>7,10,16</sup> The combination of mercury with free sulfhydryl groups in proteins impairs enzymatic

activity, explaining some of the toxicity of mercury compounds.<sup>2, 69</sup> If the onset of symptoms is survived, symptoms progress to more systemic effects including mercurial stomatitis, loosening of the teeth, and renal damage from accumulation of the Hg(II) salts in the kidneys.<sup>7, 10</sup> Hg(II) is limited in its ability to cross the blood-brain and placental barriers.<sup>7, 10</sup> Chronic Hg(II) poisoning typically occurs in combination with Hg(0) exposure and is characterized by severe leg cramps, irritability, paraesthesia (sensation of “pins and needles” in the skin), pink extremities, and skin exfoliation.<sup>7, 10</sup>

The human body has no way of actively eliminating mercury, causing excretion rates to be slow and making cumulative exposure very important.<sup>9, 81</sup> Hg(II) is avidly accumulated by the liver where it is excreted in bile as a complex with reduced glutathione until most of the body burden moves to the kidneys where it is excreted in urine.<sup>7, 10</sup> For this reason, the United States Environmental Protection Agency (EPA) and the United States Food and Drug Administration (FDA) have set the limit for inorganic mercury in drinking water at 5 ppb.<sup>8</sup>

Organomercury compounds are far more dangerous than either elemental mercury or inorganic mercury compounds as exemplified by the mass poisonings from MeHg-tainted fish in Minamata Bay in the 1950's and seed grain in Iraq in the 1970's.<sup>5, 6, 81</sup> This is due to the ability of organomercurials to penetrate biomembranes where they can concentrate in the blood, leading to a more immediate and permanent effect on the brain and central nervous system.<sup>5</sup> This is most likely due to the binding of organomercury to the thiol (-SH) groups of proteins.<sup>5</sup> Due to the vast amount of research that has occurred since the mass poisonings in Minamata and Iraq, most organomercury health recommendations boil down to simple anecdotal evidence based on methylmercury research.

The consumption of fish that have bioaccumulated MeHg is the main source of mercury exposure in humans.<sup>7, 12, 38, 45, 48, 56, 60, 80</sup> Dietary methylmercury is easily absorbed by the gastrointestinal tract (90 - 95% absorption) where it enters the bloodstream and dissolves almost completely, especially if present as CH<sub>3</sub>HgCl, and travels throughout the entire body.<sup>1, 6, 7, 76, 81</sup> Methylmercury can cross the blood-brain and placental barriers, resulting in mercury accumulation in the brain and fetus with fetal blood mercury levels reaching five to seven times that of maternal mercury blood

concentrations.<sup>4, 6, 76, 81</sup> Demethylation of MeHg by microflora in the intestines and phagocytic cells occurs by an unknown mechanism, resulting in an accumulation of Hg(II) in the central nervous system.<sup>6</sup> MeHg levels lower than those associated with neurotoxicity have been shown to correlate with an increased progression of atherosclerosis, higher risk of cardiovascular disease, high blood pressure and increased risk for cardiac arrhythmias.<sup>6, 7, 81</sup> MeHg has also been found to denature DNA, causing chromosomal damage.<sup>76</sup>

Even though the underlying mechanism is still unknown, MeHg poisoning is characterized by a long latent period lasting several weeks to months between exposure and the onset of symptoms.<sup>6, 7, 19</sup> For this reason, the discussion of the differences between acute and chronic exposures is meaningless as a single dose can elicit the same syndrome as chronic exposure.<sup>10</sup> Post-ingestion, gastrointestinal effects of MeHg exposure can range from nausea, vomiting, and abdominal pain to diarrhea, colitis and discoloration of the gums with higher doses of MeHg.<sup>7</sup> The toxic effects of MeHg are exacted almost exclusively upon the central nervous system causing mild numbness in the extremities, visual field constriction, blindness, loss of balance, loss of hearing and in severe cases death.<sup>6, 10, 68</sup> MeHg causes cell lysis in the central nervous system though it is unclear if the cell membrane is a primary target or if rupture is just a consequence of inhibition of enzyme activity integral to maintenance of the membrane.<sup>60, 76</sup> In any event, only certain cells are affected. Granule cells in the cerebellum will suffer from MeHg toxicity while neighboring Purkinje cells remain unaffected. This may be due either to the presence of repair systems or higher levels of glutathione in the Purkinje cells that are not present in the granule cells.<sup>6</sup> Regardless, damage to the adult brain is typically isolated to the cerebellum and visual cortex.<sup>7</sup>

Children are more sensitive than adults to mercury exposure because the blood-brain barrier is less resistant to mercury and the nervous system is still developing.<sup>9</sup> Autopsy results from infants exposed to high prenatal levels of MeHg that died shortly after birth show widespread damage to all areas of the brain with neuronal cell division and migration significantly inhibited.<sup>6, 10</sup> This is in direct contrast to the mature brain which will exhibit only focal points of damage.<sup>10</sup> Less severe cases of prenatal MeHg exposure result in delayed development.<sup>10</sup> Furthermore, children exposed to MeHg in

utero have show and increased incidence of high blood pressure that correlates well with the levels of prenatal MeHg exposure.<sup>6</sup>

The human toxicity of mercury is attributed to the high affinity MeHg has for the sulfur-containing proteins and amino acids including metallothionein, glutathione, and cysteine.<sup>60,76</sup> For this reason, MeHg is found almost exclusively bound to thiols in the human body.<sup>81</sup> In fact, binding of MeHg to L-cysteine facilitates transport of MeHg across the endothelial cells of the central nervous system as the MeHg-L-cysteine complex resembles L-methionine and is transported using the same neutral amino acid carrier.<sup>6,10,16</sup> Once inside the brain, MeHg is converted to Hg(II) but it remains unclear whether Hg(II) or MeHg radical is the agent responsible for neuronal damage.<sup>6</sup> In comparison, ethylmercury converts to Hg(II) much more rapidly than MeHg but does not cause the same neuronal damage as MeHg.<sup>6</sup> In any event, Hg(II) inside the brain is virtually immobile as it does not cross the blood-brain barrier.<sup>10</sup>

Urinary excretion of MeHg is negligible.<sup>6</sup> MeHg is also difficult to eliminate through the liver as MeHg undergoes extensive enterohepatic cycling.<sup>51</sup> MeHg excreted into the bile as the MeHg-glutathione complex is degraded in the bile duct and gall bladder to the MeHg-L-cysteine complex which is promptly re-absorbed in the portal circulation and either returned to the liver or metabolized in the red blood cells to Hg(II) that follows the biological distribution previously discussed.<sup>6,7,10,51</sup> Nevertheless, small amounts of MeHg avoid reabsorption and fecal excretion remains the primary method of eliminating MeHg from the body.<sup>7,10</sup>

The hydrophilic nature of DMHg permits absorption through the skin while the volatility of the compound allows for toxic exposure through inhalation.<sup>79</sup> Only a few drops (~400 mg) of DMHg is considered a lethal dose as demonstrated by the case of Dr. Wetterhahn.<sup>79</sup> DMHg is either promptly exhaled or converted to MeHg metabolites that can bind to cellular proteins. DMHg exposure is characterized by latent periods lasting from days to years before the neurotoxic effects become evident; the reason for this is unknown.<sup>79</sup>

The body naturally attempts to negate the toxic effects of certain heavy metals using the metallothionein protein and the antioxidant glutathione.<sup>1,7,10</sup> Once these proteins reach saturation, mercury will bind with other thiol-containing proteins in the



body, causing damage. Speculation exists suggesting that the thiol-like properties of selenium can also function to immobilize mercury, especially as inert HgSe deposits in the central nervous system.<sup>6, 16, 51, 81</sup> Chelation treatments that mimic these natural antagonists against mercury poisoning have demonstrated varying results. Therapies have included the use of British Anti-Lewisite (BAL), selenite, and penicillamine, all of which have their own health risks.<sup>3, 16</sup> Penicillamine is able to break the mercury-protein complexes in the body to facilitate excretion.<sup>3</sup> Dimercaptopropane sulfonic acid, a less toxic derivative of BAL, has also been used.<sup>16</sup> Thiol-containing resins that capture MeHg secreted in bile before it can cycle back into the hepatic system have demonstrated success.<sup>3, 6</sup> Perhaps the most promising agent against MeHg is *N*-acetylcysteine, a compound administered orally that carries a low toxicity, is widely available, and increases the excretion of MeHg significantly.<sup>6</sup>

In summary, all forms of mercury display some amount of toxicity with the effects of the organomercurials wreaking more havoc upon ingestion than inorganic mercury. This is due to the ability of the organomercurials to cross the blood-brain and placental barriers where they accumulate as Hg(II) and irreparably damage cells. For this reason, both MeHg already present in the environment and Hg(II) compounds available for methylation should be key targets of future, aggressive remediation strategies.

**Mercury Remediation.** It is important to assess how much global mercury pollution is due to “manageable” sources in order to effectively evaluate mercury pollution reductions. From the present discussion, it would seem that the regulation of mercury emissions from coal-fired power plants should serve as a primary target with lesser contributors such as mining effluents and industrial sources serving as secondary targets. Considering the species evolved from these particular pollution sources, Hg(0)<sub>(g)</sub>, Hg(II) and MeHg become the predominant target species for innovative remediation strategies. However, the general unreactivity and inaccessibility of atmospheric Hg(0) precludes it as being an immediate target for remediation. While methylmercury is the species responsible for the majority of human health concerns, the extremely high risk associated with handling such research material serves as a severe deterrent to working with this species. As a key component in the mercury cycle and the main species that undergoes atmospheric deposition, the reactive Hg(II) species figures prominently as the

most straightforward target. This is especially true when one considers that Hg(II) serves as the primary means of cellular uptake and methylation of inorganic mercury.<sup>48, 68</sup> Furthermore, the similarities in chemical properties between Hg(II) and MeHg, which tends to react chemically more like a substituted Hg(II) salt than an organic compound, makes Hg(II) a useful analog for studying potential remediation tactics without the associated extreme risk to the researcher.

With respect to the coal-fired power plant industry specifically, remediation of Hg(II) species makes sense in light of current technologies already in use that push the equilibrium of Hg(0) to Hg(II) to effect greater capture by FGD systems. Adding a technology that would remove the Hg(II) formed would suppress the reduction back to volatile Hg(0) that could be emitted from the flue gases. Furthermore, as more complementary mercury technologies are employed, the potential for even higher levels of Hg entrained in saleable combustion products such as fly ash for cement and gypsum for wallboard, preventing the emission of Hg(0) by pre-cleaning these materials for Hg(II) will become even more important. In fact, the action of coal beneficiation on reducing metal and metalloid co-contaminant emissions from the combustion process may even be improved if a pre-treatment with a mercury remediation agent were employed.

## **ARSENIC**

**Arsenic Geology, Applications and Anthropogenic Inputs to the Environment.** Arsenic is a chalcophilic element as represented by the principal ores realgar,  $\text{As}_4\text{S}_4$ ; orpiment,  $\text{As}_2\text{S}_3$ ; arsenopyrite,  $\text{FeAsS}$ ; and tennantite,  $\text{Cu}_{12}\text{As}_4\text{S}_{13}$ .<sup>5, 82</sup> Arsenic is found to a lesser extent in the minerals arsenolite,  $\text{As}_2\text{O}_3$ ; olivenite,  $\text{Cu}_2\text{OHAsO}_4$ ; dimorphite,  $\text{As}_4\text{S}_3$ ; cobaltite,  $\text{CoAsS}$ ; enargite,  $\text{Cu}_3\text{AsS}_4$ ; and proustite,  $\text{Ag}_3\text{AsS}_3$ .<sup>5, 82</sup> Arsenic is the 51<sup>st</sup> most abundant element with an average concentration of 1.5 – 2.0 parts-per-million (ppm or  $\text{g}\cdot\text{ton}^{-1}$ ) mostly as inorganic forms in crustal rocks.<sup>5, 83</sup> <sup>84</sup> Arsenic in soils can range in concentration from 1 – 50  $\text{mg}\cdot\text{kg}^{-1}$  with significantly higher levels common to areas of intense mining activity.<sup>85, 86</sup> Arsenic minerals are widely distributed throughout the world.<sup>5</sup> Arsenic is mobilized in the environment via

weathering, biological activity, volcanism, and dissolution of soils and sediments rich in arsenic.<sup>87</sup>

In addition to natural sources, various anthropogenic processes including mining, smelting, combustion, the production and the use of pesticides, herbicides, and insecticides are responsible for arsenic releases to the environment.<sup>88-91</sup> Elemental arsenic is produced industrially by smelting  $\text{FeAs}_2$  (pyrite) or  $\text{FeAsS}$  (arsenopyrite) in the absence of air and collecting the sublimed element.<sup>5,92</sup> Arsenic is commonly found in sulfide-rich mineral deposits of zinc, lead, copper, gold and manganese-rich pyrite and serves as an important “pathfinder” element in gold mining exploration as it is often more widespread than traces of gold from the gold-bearing ores with which it resides.<sup>83, 87, 92-94</sup> Gold is typically mineralized with arsenopyrite; the oxidation and breakdown of these minerals by iron- and sulfur-oxidizing bacteria leads to the mobilization of gold and arsenic.<sup>92</sup> The large-scale smelting of copper and lead also serves as major source of arsenic since the flue dust produced is rife with  $\text{As}_2\text{O}_3$ .<sup>5, 88, 93, 95</sup> Arsenic contamination to the environment is also likely when using sulfuric acid to extract metals from floated pyrite as the highly acidic metal wastes from this process is often stored in tailings ponds.<sup>91, 94</sup> Simply storing mine tailings can contribute to arsenic contamination as the tailings undergo oxidation, releasing acid mine drainage (AMD) containing high concentrations of metal contaminants.<sup>91, 93, 95</sup> This becomes an especially important problem as the soil, surface water and groundwater all run the risk of becoming contaminated by AMD.<sup>95</sup> Arsenic leaching from mine tailings at problematic concentrations have been reported in Australia, Canada, Mexico, Thailand, the United Kingdom, and the United States.<sup>83</sup>

Similar to mercury, significant amounts of arsenic are associated with sulfur in coal deposits, with a world average of  $9.0 \pm 0.8$  ppm for bituminous coals although extremes up to  $1,500 \text{ mg}\cdot\text{kg}^{-1}$  have been reported.<sup>84, 93, 96, 97</sup> Coal combustion releases arsenic in the flue gases where it can either be captured by FGD systems or adsorbed to fly ash particles and captured by ESPs.<sup>87, 88, 96, 98</sup> Arsenic poisoning due to the burning of arsenic-rich coal in personal stoves (inherently without pollution control devices) has reach epidemic proportions in China.<sup>93</sup> Little data exists on the semivolatile arsenic species formed in the flue gas, but it is theorized that  $\text{As}_2\text{O}_3$  reacts with  $\text{CaO}$  in the

alkaline fly ash or the lime and limestone products present in wet FGDs to form calcium arsenate,  $\text{Ca}_3\text{As}_2\text{O}_8(\text{s})$ .<sup>97-100</sup> The oxidation of As(III) to As(V) is known to proceed slowly but the process can be accelerated at the high pH values typical of western US coals.<sup>100</sup> For this reason, arsenic in fly ash can range in concentrations from 2 – 440  $\text{mg}\cdot\text{kg}^{-1}$  with world averages near  $50 \pm 8$  ppm for bituminous coal ash and exists predominantly as As(V).<sup>86, 96, 100</sup> The majority of fly ash (80%) is disposed of in landfills or surface impoundments where the leaching of trace element contaminants is a topic of concern because the influence of metal oxides on speciation and mobility is unknown.<sup>86, 98, 100</sup> To get an idea of the magnitude of the problem, in 2000 the EPA estimated that 120 million tons of fly ash were generated in the United States.<sup>100</sup>

The earliest intentional uses of arsenic were varied and spanned across many disciplines. Arsenic was used by the Egyptians in 300 B.C. and in ancient China to silver the surfaces of mirrors and statues but experienced only limited use as a bronzing agent.<sup>93</sup> Arsenic served as a flux to improve the crystallization of glass.<sup>93</sup> Both the red realgar ( $\text{As}_2\text{S}_2$ ) mineral and yellow orpiment ( $\text{As}_2\text{S}_3$ ) were used as depilatories in the leather industry and as pigments in paints and cosmetics.<sup>93</sup> In its natural state, the yellow color and mica-like sparkle of orpiment resembles gold.<sup>93</sup> Alchemists tried unsuccessfully to extract gold from orpiment, earning the mineral the title “fool’s gold”.<sup>93</sup> Alchemists found greater success in using arsenic to blanch copper, brass, and lead to the whiteness of silver.<sup>93</sup> Arsenic was used in wall paint as Paris-, Scheele’s-, Vienna-, and Emerald-greens, King’s or Naples yellow, magenta, in watercolors and even to color confectionary treats.<sup>5, 93, 101</sup> Molding of wallpaper colored with Scheele’s green was responsible for the release of “Gosio gas” (trimethylarsine), a garlic-smelling gas responsible for several deaths.<sup>87, 101</sup> Ancient Roman and Chinese wars used arsenic as incendiary materials and arsenic sulfides as toxic “holy smoke” bombs in the earliest examples of chemical warfare.<sup>93</sup> In quite the opposite application, arsenic compounds were used in flame retardants for children’s bedding until it was discovered that urine or sweat coming in contact with the materials was enough to release poisonous arsine gas, killing the children in a manner that resembled sudden infant death syndrome (SIDS).<sup>93</sup>

Perhaps the most enduring and widespread uses of arsenic stem from the medical field beginning in the fifth century B.C.<sup>5</sup> “Arsenic” is derived from the Greek word

*arsenikon*, meaning “potent.”<sup>93</sup> Realgar has been used to remove fungal flesh, unwanted hair, warts, boils, rough nails, lice, and abscesses while clearing up chronic coughs and ulcerations of the nose and mouth though the ingestion of arsenic compounds for therapeutic purposes did not start until after the sixteenth century in Western medicine.<sup>84, 93</sup> In the east, arsenic was one of the ingredients of the metallic elixirs consumed by the ancient Chinese in their quest for immortality.<sup>93</sup> Even today, many traditional, herbal and patented Chinese medicinal products still contain high levels of arsenic and mercury for the treatment of psoriasis, asthma, tuberculosis, leukemia, and other diseases.<sup>93</sup> Arsenophagy, or the folkloric medicinal practice of eating arsenic, is found in other cultures including the Styrians of the Austrian Alps and the fakirs of Persia.<sup>83, 93</sup>

Paracelsus was perhaps the first physician to use realgar internally against cancer-like tumors.<sup>93</sup> This was followed by the introduction of *Fowler’s solution*, an alkaline solution of potassium arsenite developed by Thomas Fowler for the treatment of anemia, leukemia Hodgkin’s disease and psoriasis in 1670.<sup>88, 93, 102</sup> Arsenic compounds, including sodium arsenate, Donovan’s solution (arsenic iodide), and Valagin’s solution (arsenic trichloride), among others, were used to treat fever, asthma, tuberculosis, hypertension, heartburn, rheumatism, black death, chorea, neuralgia, epilepsy, arthritis, tetanus, angina, acne, leprosy, impetigo, diabetes, herpes, and malaria.<sup>84, 88, 93, 102</sup> In a systematic search for an effective chemotherapy against blood-borne bacterial illnesses, Paul Ehrlich synthesized hundreds of organoarsenic compounds. Preparation “606,” also known as arsphenamine, “salvarsan (“salvation by arsenic”),” or 3-amino-4-hydroxyphenylarsenic(I) and preparation “909” (nearsphenamine or neosalvarsan) were particularly effective against syphilis and trypanosomiasis.<sup>83, 88, 93, 102, 103</sup> Both salvarsan and neosalvarsan were used extensively from 1907 until the late 1940s.<sup>93, 102</sup> Atoxyl and melarsoprol were used to treat sleeping sickness.<sup>93</sup> At the end of life, arsenic solutions were also used for embalming from the time of the American Civil War until 1910.<sup>93</sup>

Animal husbandry was a major consumer of arsenic compounds for use in treating wounds, removing insects on cows, horses, and sheep, as a feed additive, and as a deworming agent for cats and dogs.<sup>93, 102</sup> In fact, the poultry and swine industries have used a number of organoarsenical compounds to control the incidence of coccidial intestinal

parasites which in turn promotes feed conversion efficiency, weight gain, and an overall acceleration in growth rate.<sup>83, 87, 93, 104-111</sup> The use of arsenicals to suppress bacterial and parasitic diseases began with the application of sodium arsenilate (atoxyl) when it was found to be effective against chicken spirochetosis in 1907.<sup>93, 110</sup> Currently roxarsone, or 3-nitro-4-hydroxybenzenearsonic acid, is the most popular of the United States Food and Drug Administration (FDA) approved organoarsenicals, finding application in 69.8% and 73.9% of starter and grower feed rations respectively in 2002.<sup>83, 106, 112</sup> In addition to roxarsone, *p*-arsanilic acid (4-aminophylarsonic acid) is often used as a feed additive.<sup>83, 87, 104, 105, 110, 112-114</sup>

These arsenic compounds pose no threat to the poultry to which they are applied. Rather, the bulk of the arsenic additives pass through the gut of the animal largely unchanged.<sup>87, 110, 112, 115</sup> Roxarsone and 3-amino-4-hydroxyphenylarsonic acid (3-HPAA), a metabolite reported by Moody (1964), Morrison (1969) and others is found in the fresh poultry litter which itself is comprised of the manure, spilled feed, shed feathers and the wood chips or peanut hulls used as bedding material for the broiler chickens.<sup>111, 113, 116-119</sup> Greater than 90% of poultry litter finds commercial usage as an inexpensive nitrogen fertilizer applied to nearby fields where it is prized for its high macronutrient content and ability to improve soil aeration.<sup>120-122</sup> Transportation costs dictate that litter disposal must be done in close proximity to the concentrated animal feed operations (CAFOs) resulting in a high volume of litter spread over a relatively small area. Assuming each bird receives the maximum recommended dosage of 45.4 g roxarsone per ton of feed over the typical 42-day dosing regimen, Muir estimates that each bird excretes roughly 150 mg of roxarsone over its lifetime.<sup>109, 111</sup> If 70% of the 8.88 billion birds raised for slaughter in 2006, or 6.22 billion birds, received roxarsone, it is calculated that  $9.33 \times 10^5$  kg of roxarsone or  $2.66 \times 10^5$  kg of arsenic was introduced to the environment through the disposal of poultry litter alone.<sup>123</sup>

Roxarsone derived from poultry litter is highly water soluble and extremely mobile in the environment<sup>118, 124</sup>. Rutherford, et al., found that 76% of total As in poultry litter could be released with just one water extraction while 13 extractions released 95% of total As<sup>108</sup>. In a complementary study, Garbarino, et al., found As from the water extraction of poultry litter was present as roxarsone (91%), dimethylarsinate (1.5%),

arsenate (1.1%), arsenite (0.8%), and unknown As compounds (5.6%)<sup>125</sup>. Similarly, Jackson, et al., found that water extraction of poultry litter liberated a range of arsenic species including roxarsone (37%), arsenate (34%), 3-HPAA (12%), dimethylarsonic acid (7%), monomethylarsonic acid (1%) and arsenite (1%)<sup>113</sup>. These observations not only support the prediction of water solubility enabling roxarsone mobility, but that roxarsone also tends to degrade quickly under ambient environmental conditions.

Degradation rates are most likely due to a combination of biotic and abiotic mechanisms, the exact nature of which is greatly debated. While many researchers have generally ascribed the degradation process to microbial activity, only the recent work of Cortinas (2006) and Stolz (2006, 2007) have sought to identify the exact mechanisms and species responsible.<sup>116, 125-127</sup> Cortinas, et al., found that under anaerobic conditions, roxarsone was degraded to 3-HPAA due to microbial and, to a lesser extent, abiotic reactions. The conversion rate observed was much higher in the presence of anaerobic microbes that presumably initiated the reaction through the facile reduction of the nitro group. Long-term incubations in the study demonstrated the complete conversion of roxarsone to inorganic arsenite and arsenate.<sup>116</sup>

Unlike Cortinas, Stolz et al. proposed two possible degradation pathways in a 2006 paper.<sup>126</sup> The first pathway calls for the initial cleavage of the As-C bond to release the arsenate anion into the environment while the second pathway invokes the reduction of the nitro group followed by its removal through deamination to launch the degradation sequence to inorganic As.<sup>126</sup> In a later paper, Stolz tested these hypotheses using *Clostridium* naturally present in the chicken cecum and poultry litter as the anaerobe of interest.<sup>127</sup> The ability of *Clostridium* to produce roxarsone breakdown products such as 3-HPAA and inorganic As was confirmed. Computational analysis involving the electronic structure of roxarsone also confirmed that any reductive pathway must begin with the reduction of the nitro group while direct cleavage of the As-C bond to release arsenate was highly unlikely. Instead, Stolz proposed that arsenate is released to the environment through ring cleavage, but ultimately, the mechanism by which the As side group is released from the phenolic ring remains unknown.<sup>126</sup>

While the specific mechanisms are not always clear, it appears that microbes are able to perform methylation, demethylation, oxidation and reduction reactions involving

all manner of As species present in the poultry litter. Furthermore, abiotic processes may also be at work. In 2003, Bednar, et al., suggested that in addition to biotic processes, photoinduced cleavage of arsenite from the phenyl ring in the degradation process was an important abiotic mechanism.<sup>104</sup> In the same study, Bednar also found that reaction rate increased with increasing pH, increasing nitrate concentration, and natural organic matter concentration.<sup>104</sup> These are all variables that are themselves affected by litter management practices including storage, composting, and exposure to sunlight and to precipitation.<sup>104, 125</sup> While the exact nature of the roxarsone degradation remains unclear, it seems generally well agreed upon that inorganic arsenic is the predominant end product after prolonged composting.<sup>104, 125, 126, 128</sup> This presents its own set of problems since both arsenite and arsenate are more toxic than methylated forms of As and can be highly mobile in the environment depending on the Eh and pH of the soil pore water and the prevailing mineralogy of the soil column itself.<sup>87, 115, 129</sup>

Unfortunately, arsenic has not always been used for benign purposes. In the Middle Ages, arsenic trioxide took on a more insidious role as it became popular for inflicting death by suicide and homicide due to the odorless, tasteless white powder being both cheap and effective in small doses.<sup>84, 93, 102</sup> Furthermore, chronic and acute poisoning tends to mimic the symptoms of natural diseases such as hemorrhagic gastroenteritis, cardiac arrhythmias and psychiatric disease with the effects being cumulative, further obscuring the true cause of death.<sup>93, 102</sup> Homicidal arsenic poisoning decreased sharply when James Marsh published his method for detecting low levels of arsenic in 1836.<sup>84, 93</sup> However, arsenic compounds have found renewed uses as warfare agents. For instance, World War I saw the introduction of Lewisite, 2-chlorovinylchloroarsine gas, a chemical blister agent that was responsible for inflicting difficult-to-heal skin lesions.<sup>93, 130</sup> The Japanese Imperial Forces used diphenylchloroarsine and diphenylcyanoarsine in toxic smoke or “Red” canisters during World War II as strong irritants.<sup>131, 132</sup> Sodium cacodylate (a salt of dimethylarsinic acid) and dimethylarsinic acid, also known as “Agent Blue” and “Agent Orange,” were a part of the rainbow herbicides used during the Vietnam War to defoliate and desiccate a wide range of plants.<sup>88, 93</sup>

Inorganic arsenic compounds have been used as herbicides, pesticides, and insecticides for more than 100 years in the United States.<sup>83, 104</sup> Copper arsenate was most



likely the first arsenical applied as an insecticide.<sup>93</sup> Supposedly an exasperated farmer threw out some Paris green, a pigment made of copper arsenate, on his fields only to return later and find all of the potato beetles dead.<sup>93</sup> Paris green was commercialized as an insecticide beginning in 1867 but was soon supplanted by London purple, a by-product of the aniline industry that resulted in a mixture of calcium arsenate, arsenite, and organic matter.<sup>93</sup> London purple was cheaper, easier to apply, adhered to the plants well and had a more conspicuous color. Calcium arsenate was manufactured directly for cotton pests beginning in 1906 and sodium arsenite was used as a weed killer and soil sterilant.<sup>87, 93, 133</sup> In general, arsenic insecticides became popular because they were an inexpensive by-product from the smelting industry.<sup>93</sup>

Unfortunately, Paris green and London purple were phytotoxic. This problem was solved with the introduction of lead arsenate,  $\text{PbHAsO}_4$ , in 1892.<sup>87, 88, 93, 134</sup> Large amounts of lead arsenate were used in the U. S. agricultural industry as demonstrated by the following statistics: 5.4 million kg in 1919, 13 million kg in 1929, and an average of 23 million kg between 1930 and 1940 with a peak use of 40 million kg in 1944 on 41 registered feed and food crops.<sup>93</sup> Calcium arsenate was similarly popular with uses averaging 23 million kg from 1930-1940 with a peak of 36 million kg in 1944 on 83 different feed and food crops.<sup>93</sup> Crop over-spraying was also a common practice at the time, especially as insects and diseases became arsenic-resistant, requiring the introduction of even larger amounts arsenic compounds to the environment to have the same effect.<sup>93, 134</sup>

During the 1970s and 1980s, a variety of organoarsenical compounds were created to replace their inorganic herbicidal counterparts.<sup>93</sup> These included monosodium methylarsonate (MSMA), disodium methylarsonate (DSMA), dimethylarsinic acid (cacodylic acid) and arsonic acid.<sup>87, 88, 93, 104, 135</sup> In the United States, 10-12 million acres were treated with 2.1 million kg of a MSMA/DSMA mixture annually while arsonic acid was applied to 2.1 million acres at a rate of 3.3 million kg per year.<sup>93</sup> In the 1990s, the rate of MSMA/DSMA application had dropped to just over 3,000 metric tons per year and dimethylarsinic acid was at ~35 metric tons per year.<sup>135</sup> While these compounds were thought to be relatively non-toxic, biodegradation in the environment liberated the more toxic inorganic forms.<sup>93</sup> For this reason and due to the improper disposal of industrial

wastes resulting from the production of the arsenical herbicides, arsenic contamination is ubiquitous in the United States.<sup>93, 136</sup>

The preservation of wooden structures against decay due to bacterial, fungal, and insect infestations using organic and inorganic additives has been a challenge for many centuries.<sup>137</sup> Until the twentieth century, creosote, an oily liquid produced from the high-temperature treatment of coal, was used to protect wood.<sup>133, 138</sup> Coal tar creosote lost favor as a wood preservative because it left the surface of the wood unpaintable and had oily, potentially carcinogenic residues associated with its use.<sup>137</sup> Creosote was replaced by a waterborne preservative known as “CCA,” or chromated copper arsenate, developed in the 1930’s as a cheaper and cleaner alternative.<sup>93, 138, 139</sup> A typical CCA treatment infuses up to 250 liters of a 2-3% CCA solution per cubic meter of wood under high pressure with final Cu, Cr, and As concentrations in the wood of 1,000-19,000 mg·kg<sup>-1</sup> resulting, depending upon the intended use of the wood product.<sup>137, 138, 140, 141</sup> By weight percent, CCA-C, the most common formulation used, contained 47.5% CrO<sub>3</sub>, 18.5% CuO and 34% As<sub>2</sub>O<sub>5</sub>.<sup>142</sup> In 1986, 10.6 million cubic meters of preservative-treated wood was produced and by 1990, CCA treated lumber accounted for greater than 98% of the treated lumber on the market.<sup>137, 141, 143</sup>

Each component of the CCA treatment performs a variety of functions. The copper acts as a fungicide while maintaining low mammalian toxicity. Arsenic is used as an insecticide and as a secondary fungicide for copper-resistant species. Chromium’s main function is to act as a “fixing agent” to bind the arsenic and copper to the wood, the mechanisms of which are still poorly understood.<sup>138, 141, 144</sup> Dahlgren, et al., have proposed that when the CCA solution first contacts the wood, initial reactions include ion exchange and adsorption between the copper, chromium, and wood constituents.<sup>145</sup> Later, precipitation of the CCA components is driven by the reduction of hexavalent chromium to trivalent chromium, during which the pH of the wood steadily increases as it is oxidized.<sup>146-148</sup> These “fixation” reactions can continue for weeks and even months before reaching completion.<sup>149, 150</sup> The intermediate and final products of this process proposed by Van den Broeck, et al., are shown in Scheme 1.2.<sup>148</sup> The copper, chromium, and arsenic form a variety of complexes and adsorption products with carbonyl, carboxyl, methoxyl, and phenolhydroxy functional groups in the wood tissues that should

theoretically keep the CCA components locked into the wood to provide long-lasting protection from decay.<sup>148, 151-154</sup>

Copper Chromium → Arsenic	$\text{CuCrO}_4 \rightarrow$	Stable $\text{CuCrO}_4$ -lignin complexes
	$\text{CrAsO}_4 \rightarrow$	Lignin- $\text{CrAsO}_4$ complexes
		Inorganic $\text{CrAsO}_4$ precipitates on cellulose
	$\text{Cr}_2(\text{OH})_4\text{CrO}_4 \rightarrow$	Inorganic precipitates on cellulose
	$\text{Cu}^{+2} \rightarrow$	Lignin- $\text{Cu}^{+2}$ complexes
		Physisorbed on wood constituents
		Cellulose- $\text{Cu}^{+2}$ complexes
$\text{HCrO}_4^{-1} \rightarrow$	Lignin- $\text{HCrO}_4^{-1}$ complexes	

**Scheme 1.2:** Interactions of Copper, Chromium, and Arsenic with Wood Components (adapted from Van Den Broeck, et al., 1997)<sup>148</sup>

Early tests claimed that the CCA components in lumber were virtually leach resistant, an important feature considering that the average twelve-foot-long two-by-six contains more than an ounce of arsenic, a dose large enough to poison 250 adults if ingested.<sup>138, 155</sup> In the 1980's, small amounts of the copper, chromium and arsenic were found to be easily dislodged and/or leached from pressure-treated lumber, prompting the United States Environmental Protection Agency (EPA) to begin requiring that pallets of CCA treated lumber be labeled with the following warning: "Exposure to inorganic arsenic may present certain hazards... Do not use treated wood under circumstances where the preservative may become a component of food."<sup>155, 156</sup> In the years to come, a number of field and laboratory studies discovered that all components of the CCA treatment were susceptible to high rates of leaching, especially in wet, acidic environments where organic chelating agents were in direct contact with the wood.<sup>137, 138, 141, 142, 157</sup> Even with low leach rates resulting in the release primarily of As(V) (acting as a bridge between Cr(III) dimers) to the environment, the sheer volume of CCA treated lumber in use across the United States made the continued use of the products

unacceptable.<sup>140, 156, 158</sup> For this reason, the lumber industry began a voluntary phase-out of CCA lumber production starting in February of 2002 with final sales of CCA to be completed by January 2004.<sup>140, 159</sup>

**Arsenic Speciation, Environmental Chemistry, and Toxicity.** To understand the transport and effects of arsenic on a given ecosystem, it is critical to discover, identify and quantify the forms and magnitude of arsenic species that may be present.<sup>87</sup> The discussion of arsenic speciation and environmental chemistry is probably best facilitated by first identifying major species in each environmental “compartment” and then engaging in a discussion of the relevant chemistry therein. It is important to note that the difficulties associated with arsenic analysis have led to quantities of “hidden” arsenic. That is, while a total arsenic analysis will reveal the concentration of all arsenic species, the structures of these species may not have been fully elucidated due to solubility and/or oxidation issues.<sup>74, 82</sup> Whenever applicable, the presence of an unknown arsenic species that has been detected in an environmental compartment will be noted. Once this chemistry has been reviewed, the related toxicology of the major arsenic species to organisms in that environment will be reviewed. A general discussion of arsenic biomethylation will follow as it pertains to most environmental compartments and owing to its importance, the toxicology of arsenic species in humans will be reviewed in a separate section.

Airborne arsenic originating from smelters, coal-fired power plants, and volcanoes is most often present as particulate  $As_2O_3$ .<sup>82, 83, 87</sup> The capture and analysis of volatile arsenicals is difficult, revealing only limited information on the species present in the air.<sup>82</sup> However, arsine gas ( $AsH_3$ ) and methylated arsines ( $MeAsH_2$ ,  $Me_2AsH$ , and  $Me_3As$ , see Figure 1.1) have been found as trace constituents, especially over areas of intense biological activity.<sup>82, 87</sup> Trimethylarsine, smaller amounts of the other methylated arsines and some ethylated arsines have also been detected in landfill biogases.<sup>82, 160</sup> Every year it is estimated that volcanoes, microbial activity, and fossil fuel combustion release 3,000, 20,000, and 80,000 metric tons of atmospheric arsenic, respectively.<sup>83</sup>

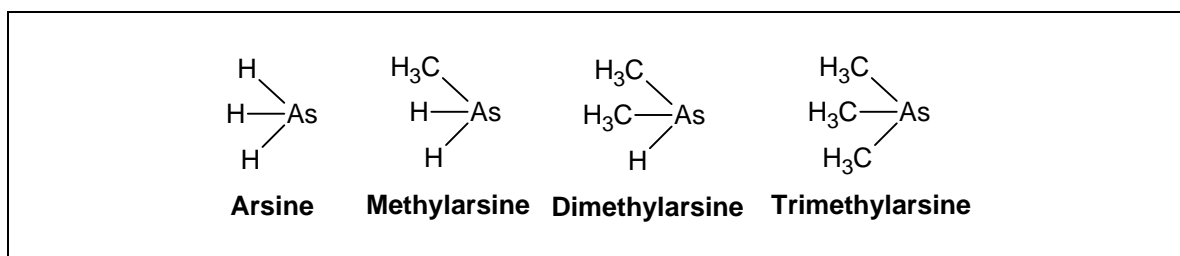


**Figure 1.1:** Major Arsine Species

In soils and sediments, arsenate, arsenite, methylarsonate and dimethylarsinate are commonly found.<sup>82</sup> The arsenic content of soils averages 5 - 6 ppm but ranges from 0.2 – 40 ppm.<sup>83</sup> Under oxic conditions, arsenate [As(V)] will predominate over the more toxic arsenite [As(III)].<sup>82, 87, 91, 94, 115</sup> Arsenic mobility in the environment is generally dominated by the formation of thermodynamically stable inner-sphere complexes with heavy metal oxides.<sup>91, 93, 161-164</sup> Adsorption affinities are strongly tied to the redox potential and pH in which the arsenic and metal oxides are found.<sup>91</sup>

Arsenate can exist in several pH-dependent forms from the fully protonated arsenic acid,  $\text{H}_3\text{AsO}_4$  to the fully deprotonated  $\text{AsO}_4^{-3}$  though in most environmental systems the charged  $\text{H}_2\text{AsO}_4^-$  and  $\text{HAsO}_4^{-2}$  species dominate. Following conventional practice, the term “arsenate” shall be used to refer to arsenic acid and all of its deprotonated ionic forms. The  $\text{pK}_a$  values for arsenate 2.20, 6.97, and 11.53 are remarkably similar to the values for phosphoric acid at 2.12, 7.20, 12.40.<sup>87, 165</sup> Due to the similarities in both structure and charge,<sup>94</sup> competition between phosphate and arsenate for soil sorption sites has been the focus of several studies. As(V) will form strong bonds with aluminum, manganese, iron (oxy)hydroxides and clays although the exact mineralogy of the sorbents varied from study to study, significant suppression of As adsorption becomes apparent when phosphate is added first.<sup>83, 91, 92, 94, 96, 166-170</sup> Due to the smaller size of the anion, phosphate binds more strongly to mineral surfaces than arsenate to the point of causing sorbed arsenate to be displaced from soils when concentrations of both were low, but comparable.<sup>110, 165, 171</sup> However, at high arsenate and low phosphate concentrations, a reversal in this trend is observed due to the mass action effect. For this reason, Lambkin (2003) took the stance that input of As to soil could mobilize phosphate

to the point of affecting crop yield, although the effects of As toxicity and phosphate deficiency are impossible to distinguish from one another by visual inspection alone.<sup>83, 165</sup>

In contrast to the charged arsenate species, arsenite  $pK_a$  values (9.22, 12.13, 13.40) reveal that the uncharged arsenous acid  $H_3AsO_3$  form will be the most prevalent under anaerobic conditions in environmental systems.<sup>87, 94, 172</sup> Following conventional practice, the term “arsenite” shall be used to refer to arsenous acid and all of its deprotonated ionic forms. Like carbonic acid, arsenous acid has never been isolated from solution or otherwise.<sup>5</sup> The differences in charge between arsenate and arsenite may be largely responsible for the differences observed in mobility and biological uptake.<sup>87</sup> This is especially true when considering that clay minerals and metal oxide surfaces present in soils often carry a permanent surface charge, the magnitude of which is also pH dependent.<sup>172, 173</sup> Confirmation of this proposed trend was observed by Pierce in 1982 when it was noted that amorphous hydroxides of Fe and Al with their loose, highly hydrated structures and high isoelectronic points were able to sorb As(V) to a greater extent than As(III).<sup>166</sup> Optimal As(III) adsorption was observed at pH 7 when the mineral surface was likely to be negative and arsenite neutral while optimal As(V) sorption was observed at pH 4 when the surface was more likely to be neutral or positively charged and arsenate was present as the uninegative species.<sup>166</sup>

To summarize, adsorption affinities for As(V) tend to be more favorable at low pH while As(III) adsorption affinities are higher at higher pH values.<sup>174</sup> As(III) forms much weaker bonds with manganese and iron (oxy)hydroxides than does As(V), making it more soluble and more mobile.<sup>91, 94</sup> General arsenic mobility in an aerated environment tends to increase with decreasing pH due to mineral dissolution, proton competition for surface binding sites, and increased surface potential. An increase in the pH can also promote arsenic release by destabilizing the metal oxide complexes. A change to a more reducing environment can initiate reductive dissolution of mineral phases complexed with arsenic, causing arsenic release to the environment.<sup>91, 164, 166, 174</sup>

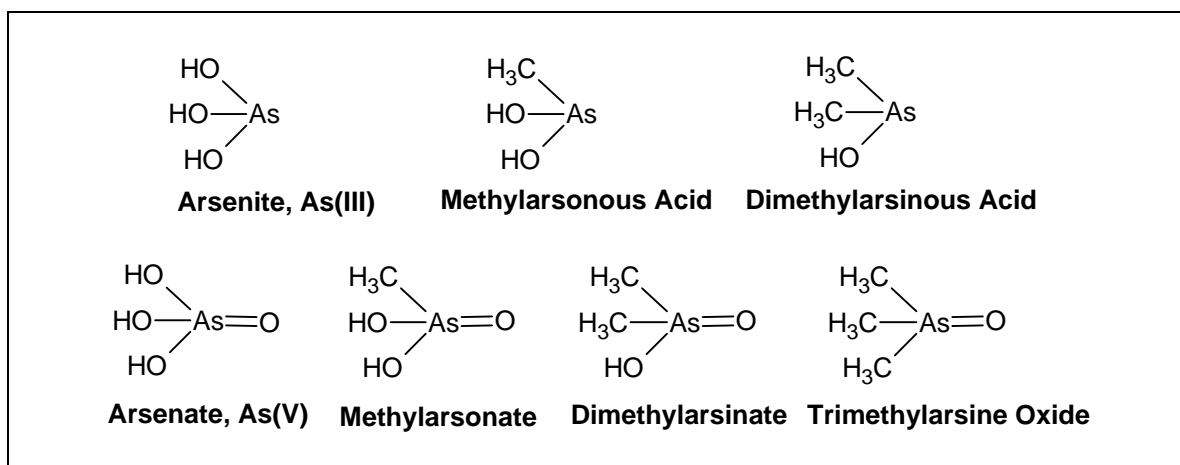


**Figure 1.2:** Arsenic Species Commonly Found in Soils, Sediments and Water

The average concentration of arsenic in the world's oceans is  $0.5 - 3.0 \mu\text{g As}\cdot\text{L}^{-1}$  and present mainly as arsenate.<sup>82, 87, 175</sup> Arsenite, methylarsonate and dimethylarsinate can also be present as a consequence of biotransformations of arsenate involving reduction and methylation by phytoplankton and bacteria.<sup>82</sup> Beyond the photic zone, methylarsonate and dimethylarsinate levels decrease sharply and arsenate levels rise owing to the poor stability of methylated arsenicals in seawater.<sup>82</sup> Methylarsonate and dimethylarsinate are common metabolites that often occur together in many environmental compartments with dimethylarsinate often found in greater concentrations than methylarsonate.<sup>82</sup> Furthermore, trimethylarsine oxide is produced by the same pathway as methylarsonate and dimethylarsinate, but is often reported as being absent from environmental samples due to poor detection limits for the analysis of this arsenical.<sup>82</sup>

In marine algae, sixteen arsenosugars have been identified, but only four are found in large amounts.<sup>82</sup> Arsenite, arsenate, methylarsonate, and dimethylarsinate are all proposed intermediates in the biogenesis of arsenosugars in a mechanism proposed by Challenger in 1945 which will be discussed shortly.<sup>82, 87</sup> Marine algae have also been found to contain up to 50% of lipid-soluble arsenic identified on only one occasion as a phospholipid derivative of an arsenosugar.<sup>82, 87</sup> Though the occurrence of arsenic compounds in marine algae have been the subject of multiple studies, the same does not hold true for marine plants which do not appear to contain arsenosugars.<sup>82</sup>

Marine animals contain a plethora of arsenic compounds with arsenobetaine most often present as the major arsenical (> 80%) in the muscle tissues of fish, crustaceans, and mollusks.<sup>82, 83, 87</sup> Bivalve mollusks can also harbor large quantities of tetramethylarsonium ion while scallops have been documented with high levels of arsenosugars, presumably due to their algae diet.<sup>82, 87</sup> Marine mammals tend to exhibit only low levels of arsenic in their tissues with arsenobetaine as the most prevalent form.<sup>87</sup> Several novel, lipid-soluble arsenic compounds have been found in lobster and shark tissue that contain arsenocholine, arsenosugars, and dimethylated arsenic moieties.<sup>82</sup> Arsenocholine will rapidly biotransform into arsenobetaine and may serve as a precursor.<sup>82</sup> Although the presence of arsenobetaine in a wide variety of organisms suggests a common biogenetic pathway, the origin of arsenobetaine remains unknown.<sup>82</sup>

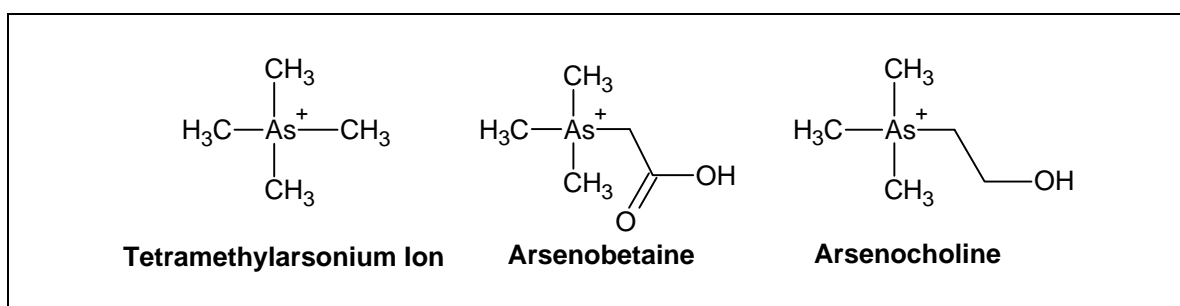


**Figure 1.3:** Arsenic Species Common to Marine Animals and Terrestrial Fungi

A much wider variation of arsenic concentrations is present in fresh waters. Depending upon the geological drainage area, total arsenic concentrations of 0.1 – 80 ppb are not uncommon but water sources in close contact with arsenic-bearing minerals can easily reach concentrations as high as 2,500 ppb (Taiwanese well) as inorganic As(III) and As(V).<sup>87, 175</sup> Arsenic contaminated aquifers have been reported worldwide in Argentina, Bangladesh, Cambodia, Chile, China, Ghana, Hungary, Inner Mongolia, Mexico, Nepal, New Zealand, Philippines, Taiwan, and the United States.<sup>83</sup> The most poignant example of the ramifications of arsenic contaminated aquifers is portrayed by the story of Bangladesh. In the 1960's, surface water containing water-borne pathogens was leading to high infant mortality rates.<sup>83</sup> In an effort to drive down the mortality rates, international agencies installed over 4 million tube wells beginning in 1971 and finishing



in the early 1990s.<sup>83</sup> Tube wells are two-inch diameter pipes drilled 50 m deep to reach pathogen-free water in the aquifer.<sup>83</sup> However, pumping the water to the surface spurred the dissolution of arsenic minerals, resulting in the largest mass poisoning in history as 20,000 Bangladeshis die every year due to arsenic-related complications.<sup>83</sup>

Methylarsonous acid and dimethylarsinous acid have been reported in lake water although their precise chemical structures have not been demonstrated owing to the lack of a solvent extraction step to separate As(III) and As(V) species prior to analysis for total As.<sup>82</sup> Freshwater algae have not been studied as much as their marine counterparts but seem to have a similar disposition of arsenic compounds except for arsenite which has not been detected.<sup>82</sup> Freshwater plants present a different picture as they often contain arsenite and arsenate as the major forms of arsenic in addition to an unspecified lipid-soluble arsenic species.<sup>82, 87</sup> Arsenosugars are only occasionally detected and methylarsonate, dimethylarsinate and tetramethylarsonium ion are present in low to trace quantities.<sup>82</sup> Data for arsenic in fresh water animals is similarly lacking although arsenobetaine is generally the major arsenical in what few studies have been conducted.<sup>82</sup>

Of the terrestrial organisms, it must be said that fungi contain the most interesting array of arsenic compounds, often in high ( $> 2000 \mu\text{g}\cdot\text{g}^{-1}$ ) concentrations.<sup>82</sup> Fungi are the only organisms known to contain methylarsonate and all fungi species examined thus far contain dimethylarsinate.<sup>82</sup> Other common arsenic species in fungi include arsenate, arsenite, arsenobetaine and sometimes arsenocholine and tetramethylarsonium ion; the latter three species were traditionally considered marine animal metabolites prior to their discovery in fungi.<sup>82</sup> Indeed, the ability of fungi to methylate arsenic through a series of reactions involving reduction, methylation and ultimately adenosylation is what led Challenger to develop his famous method for arsenite methylation.<sup>82, 87</sup>

Unlike fungi, lichens contain arsenosugars which is not entirely surprising considering their fungi-algae symbiotic relationship.<sup>82</sup> Lichens have been found to contain other organoarsenic compounds, but their arsenic chemistry is dominated by inorganic arsenite and arsenate.<sup>82</sup> Like the lichens, the arsenate and arsenite are the main arsenicals found in terrestrial plants with methylarsonate, dimethylarsinate, and trimethylarsine oxide present in minor amounts.<sup>82</sup>

The effects of arsenic on terrestrial plants have garnered much research due earlier uses of arsenicals in agriculture.<sup>87</sup> Uncontaminated plants typically contain ~0.2 ppm arsenic with vegetables containing up to 0.4 ppm arsenic, depending on where they are grown.<sup>83, 87</sup> The hyper-accumulation of arsenic at levels up to 1% arsenic by dry mass of the plant have been documented. Even though arsenite is more phytotoxic than arsenate, hyper-accumulating ferns in particular tend to store the arsenic as arsenite in their fronds.<sup>82, 94</sup> Furthermore, pine seedlings, the Douglas fir, corn, melon, pea and tomato plants tend to accumulate arsenic.<sup>87</sup> The presence of arsenic in Douglas firs up to 1,000 ppm arsenic have been documented when the trees were located within 200 feet of mineralized arsenic and gold deposits, again pointing to arsenic as a “pathfinder” element for gold deposits.<sup>87</sup>

The biomethylation of arsenic can occur in geogenic as well as anthropogenic systems.<sup>74</sup> Arsenic methylation was originally studied as the result of poisonings from the fungal transformations of arsenic in paints releasing poisonous arsine gas.<sup>73, 101</sup> Since then, a number of bacteria and algae have been found to use arsenic for cellular energy production and growth.<sup>176-183</sup> In fact, the phenomenon of arsenic biomethylation is widespread but not universal. In addition to microorganisms and fungi, the process has been documented in algae, plants, certain animals, and in humans but not in several monkeys, or guinea pigs, for example.<sup>101</sup>

Biomethylation of inorganic arsenic occurs through a series of strictly alternating reductions and oxidative methylations as depicted in Figure 1.4, a variation of the 1945 mechanism proposed by Challenger.<sup>74, 184</sup> Arsenic methylation proceeds with the reduction of the As(V) species to the corresponding As(III) species using glutathione, cysteine, dithiothreitol, or lipoic acid (6,8-dithiooctanoic acid) as the reductants and is catalyzed enzymatically by reductases.<sup>74, 101, 175, 184, 185</sup> After reduction, the oxidative addition of a methyl group occurs with biogenic sources such as methylcobalamine, methyltetrahydrofolate, methyl-coenzyme M, and *S*-adenosyl methionine and anthropogenic sources such as tetramethyllead, tetramethyltin, polydimethylsiloxane from polluted sites providing the methyl group.<sup>74, 101, 175</sup> While biomethylation may serve as a detoxification mechanism, the hydrophobic nature of methylated products causes them to accumulate in the food chain though not to the extent of mercury.<sup>74, 75, 101, 129</sup>

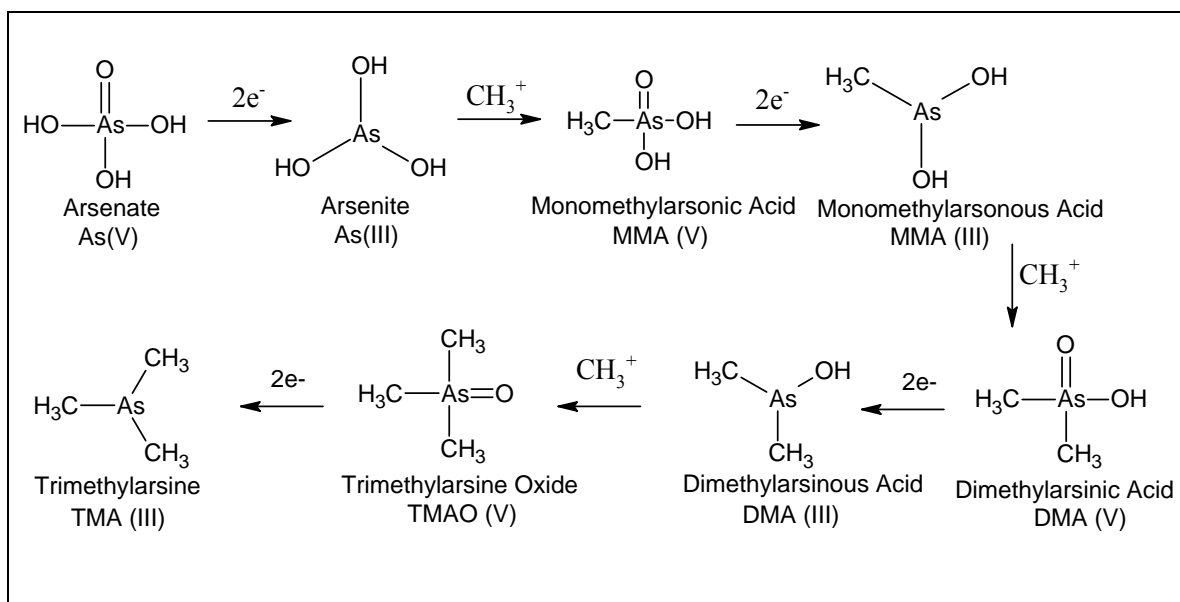


**Figure 1.4:** Basic Sketch of the Challenger Mechanism<sup>75, 87, 101, 184</sup>

**Arsenic and Human Health.** Arsenic has poisoned and killed more people than any other toxin known to man.<sup>93</sup> Worldwide production of arsenic trioxide increased from less than 5,000 tons per year in 1850 to over 60,000 tons per year in 1950 at the peak of production.<sup>93</sup> During this time, human beings were exposed to untold amounts of arsenic in their medicine, food, water, and environmental surroundings due to the dissipative nature in which over 80% of the arsenic produced was applied as herbicides, insecticides, desiccants, feed additives, wood treatments, and warfare agents.<sup>93</sup> Currently, public concern about the health effects of arsenic have driven worldwide production down to less than 20,000 tons per year.<sup>93</sup>

Perhaps the largest threat to human health from arsenic stems from the ingestion of fresh water and food with a high inorganic arsenic burden, accounting for 99% of the total human intake of arsenic.<sup>83, 175</sup> Worldwide an estimated 150 million people are consuming water with greater than  $50 \mu\text{g}\cdot\text{L}^{-1}$  arsenic; 50 million of these people are located in Bangladesh and 6 million people in China.<sup>90, 91, 93</sup> Absorption of soluble arsenic species is believed to reach 60 - 90% through the gastrointestinal tract with >90% of inorganic clearing from the blood in 1 - 2 h and 40 - 70% clearing the body in 48 h.<sup>83, 175</sup> Arsenic does not significantly bioaccumulate in the body.<sup>83</sup>

The extent of arsenic metabolism and excretion depends on the form ingested.<sup>175</sup> Arsenic ingested by humans from uncontaminated food sources is primarily excreted in the urine as arsenite, arsenate, and the metabolites methylarsonate, and dimethylarsinate.<sup>75, 82, 87</sup> The liver is the primary site of arsenic metabolism in mammals and proceeds via a method similar to the Challenger mechanism described in Figure 1.4.<sup>83, 175</sup> Minor routes of arsenic elimination from the body are through the feces, sweat, and incorporation into hair and nails.<sup>83, 101</sup> Human subjects fed a diet rich in arsenic-containing marine organisms also excrete a large amount of undetectable (non-hydride forming) organoarsenicals, or “fish arsenic,” indicating that these species (most likely arsenobetaine and arsenocholine) are not readily metabolized by humans and therefore should pose no health risk.<sup>83, 87, 101, 175</sup> Smelter workers exposed to high levels of airborne  $As_2O_3$  eliminate the arsenic primarily as the dimethylated form.<sup>87</sup>

Arsenic is not essential to any function in mammals.<sup>176-183</sup> Arsenic exposure at the cellular level causes inhibition of oxidative phosphorylation in cell energy production by arsenate, a phosphate molecular analog, and broad toxicity due to the arsenite binding to protein sulfhydryl groups and disrupting enzymatic activity.<sup>83, 176</sup> Arsenic binding to sulfhydryl groups can disrupt cellular glucose uptake, gluconeogenesis, fatty acid oxidation, and glutathione production.<sup>83, 129</sup> Arsenate compounds substituting for phosphate compounds can disrupt many processes.<sup>83</sup> For example, arsenocholine has been implicated in the replacement of choline in lecithin synthesis in the body.<sup>87</sup> Although it holds counter to conventional wisdom, studies published in 2000-2001 have evidence that suggests that trivalent methylated arsenic species may actually be more toxic than inorganic arsenic though this remains debatable.<sup>74, 140, 186-188</sup>

Chronic exposure to arsenic in drinking water is thought to contribute to a broad spectrum of very significant illnesses including, cancer of the skin,<sup>93, 175, 189-195</sup> bladder,<sup>93, 175, 189-192, 196</sup> lungs,<sup>93, 175, 189-192, 197</sup> kidneys,<sup>93, 191, 192, 197</sup> liver,<sup>189, 191, 198</sup> colon,<sup>191</sup> prostate and sinus passages. The element has also been implicated in damage to the cardiovascular,<sup>191, 192, 199-204</sup> pulmonary,<sup>192</sup> immunological, neurological,<sup>191, 192, 205, 206</sup> endocrine,<sup>101, 191, 192, 204, 207-212</sup> and reproductive systems.<sup>93</sup> Arsenic poisoning has even been implicated in “Black Foot” disease, a peripheral vascular disorder that results in gangrene of the feet and sometimes the hands.<sup>87</sup> Moderate exposures to arsenic (< 10

ppb) during pregnancy cause reductions in birth weight similar to that observed for exposure to other environmental contaminants such as tobacco smoke and benzene.<sup>93, 213</sup> Newborn infants had similar arsenic levels to that found in the urine<sup>214</sup> of the mother and strong correlations between cord blood and maternal arsenic levels were found.<sup>215</sup> Arsenic exposure has also been linked to congenital birth defects and spontaneous abortion.<sup>93</sup> Citing the increased evidence for arsenic genotoxicity, mutagenicity, and teratogenicity, the Environmental Protection Agency, the National Research Council and World Health Organization have set the maximum contaminant level (MCL) for arsenic at 10 ppb ( $0.01 \text{ mg}\cdot\text{L}^{-1}$ ).<sup>83, 88, 93, 175, 216</sup>

**Arsenic Remediation.** Citing the fact that the major source of arsenic poisoning in humans occurs from the consumption of drinking water and in light of the lowered permissible arsenic limits, arsenic remediation from water sources represents a critical and necessary research target.<sup>217, 218</sup> The most common methods of removing arsenic from water involve filtration of particulate arsenic and adsorption or chemical precipitation of aqueous arsenic followed by filtration.<sup>217</sup> There are currently no technologies, besides expensive membrane filtration techniques, that can achieve the low arsenic level mandated by the different governing bodies. Of the two inorganic species, arsenite is the more toxic, more highly mobile, and historically most difficult form of arsenic to remove from water.<sup>129, 218-220</sup> A discussion of the strengths and weaknesses of current arsenic remediation methods from drinking water will be covered in Chapter 3.

## **PREFERENTIAL SULFUR BINDING: A TEMPLATE FOR PERMANENT REMEDIATION**

**Mercury and Arsenic Binding Affinities.** Mercury and arsenic are widespread contaminants in aqueous environments throughout the world. Both elements have significant negative health impacts on humans due to the fact that they are cumulative toxins that bind to the sulfhydryl groups in proteins, disrupting many biological functions. The elements arise from multiple sources including coal-burning power plants for mercury and wells placed in natural geological deposits of arsenic-containing minerals. There are currently no robust techniques for removing either mercury or arsenic from aqueous sources to the levels mandated by governing bodies. We propose that a superior removal method exists that exploits the similar reactions of both elements with

sulfur despite the fact that mercury and arsenic have very different chemical properties otherwise.

A review of mercury's binding affinities points to sulfur as the logical functional group for irreversibly precipitating mercury from contaminated industrial and environmental water sources. Recall that HgS (cinnabar) constitutes the only significant mercury ore.<sup>5, 6</sup> Soils serve as a net sink for environmental mercury through the formation of the complexes as Hg(OH)<sub>2</sub>, HgCl<sub>2</sub>, HgOH<sup>+</sup>, HgS and Hg(0) in aerated soils and HgSH<sup>+</sup>, HgOHSH and HgClSH in reducing environments.<sup>4, 50, 56</sup> In these complexes, mercury sorbs strongest to soil organic matter followed by amorphous FeS and the amorphous oxides, hydroxides, and oxyhydroxides of iron, manganese and aluminum followed at last by sorption to clay minerals.<sup>2, 50, 56</sup>

In natural waters, Hg(II) is present as chloride complexes (HgCl<sup>+</sup>, HgCl<sub>2</sub>, HgCl<sub>3</sub><sup>-</sup>, and HgCl<sub>4</sub><sup>-</sup>) and hydroxide complexes (Hg(OH)<sup>+</sup>, Hg(OH)<sub>2</sub>, Hg(OH)<sub>3</sub><sup>-</sup>, and HgClOH) with up to 95% of these species found sorbed strongly to sulfur and sorbed weakly to oxygen functional groups in dissolved organic matter.<sup>2, 45, 48, 56, 60-62</sup> Dissolved organic matter sulfur often competes with inorganic sulfur in natural waters for binding to mercury, especially in anaerobic environments.<sup>45, 56, 60</sup> In fact, the formation of highly insoluble HgS<sub>(s)</sub> is the oft-cited process for removal of Hg(II) from the water column and incorporation into sediments.<sup>2, 45, 48, 60, 64</sup> Along the same mercury-removal theme, mercury sorption to particles in coal-fired power plants occurs primarily due to active sites on fly ash surfaces that allow for the formation of HgCl<sub>2</sub>, HgO, HgSO<sub>4</sub>, and HgS.<sup>30, 33, 36</sup> Solid HgS or HgS sorbed to fly ash that can be captured by particulate control devices can be created through the injection of sodium sulfide, sodium hydrogen sulfide, or activated carbons impregnated with iodine or sulfur.<sup>29, 33, 36, 39</sup>

Even inside the body, mercury (especially methylmercury) shows such a preference for sulfur that it is bound almost exclusively to the thiol groups found in amino acids, metallothionein, glutathione, and cysteine.<sup>60, 76, 81</sup> Chelation therapies using British Anti-Lewisite (BAL), penicillamine, dimercaptopropansulphonic acid, *N*-acetylcysteine, and thiol resins to capture mercury all bind to mercury through sulfur groups.<sup>3, 6, 16</sup> Mercury has a demonstrated affinity for thiolates that is so important that

preferential binding between different species in competition occurs and should be exploited in any developing remediation strategy.<sup>2, 221</sup>

The environmental interactions of arsenic, particularly as arsenite, are similar to those of mercury. For instance, the principal arsenic ores include  $\text{As}_4\text{S}_4$ ,  $\text{As}_2\text{S}_3$ ,  $\text{FeAsS}$ , and  $\text{Cu}_{12}\text{As}_4\text{S}_{13}$ ,  $\text{As}_4\text{S}_3$ ,  $\text{CoAsS}$ ,  $\text{Cu}_3\text{AsS}_4$ ,  $\text{Ag}_3\text{AsS}_3$ .<sup>5, 82</sup> Arsenic is stable in soils and water as the As(III) species  $\text{H}_3\text{AsO}_3$ ,  $\text{H}_2\text{AsO}_3^{-1}$ ,  $\text{HAsO}_3^{-2}$ ,  $\text{AsO}_3^{-3}$  and as As(V) species  $\text{H}_3\text{AsO}_4$ ,  $\text{H}_2\text{AsO}_4^{-1}$ ,  $\text{HAsO}_4^{-2}$ ,  $\text{AsO}_4^{-3}$  depending on the reduction potential and pH of the surrounding environment.<sup>87, 94, 165, 172</sup> The main sink for arsenite in the environment is iron sulfides.<sup>96</sup> Furthermore, arsenite has a demonstrated affinity for binding to free sulfhydryl groups as evidenced by this process occurring in humans and disrupting enzymatic function.<sup>129</sup> Unfortunately, the affinity of arsenic for sulfur has not been utilized to any great extent in current remediation practices.

**Use of B9 to Explore Preferential Binding.** B9, N,N'-Bis(2-mercaptoethyl)isophthalamide, has been characterized extensively under the previous trade names MetX, BDETH<sub>2</sub> and BDTH<sub>2</sub>. Unlike most thiol compounds, "B9" is unusually stable in that the free sulfur groups do not form disulfide linkages that are unavailable for the formation of new covalent bonds, making it an ideal compound for binding mercury and arsenic under a wide range of environmental conditions.<sup>221</sup> This is a feature unique to B9 by comparison to other common sulfur compounds, including the amino acid, cysteine. B9 has a demonstrated affinity for binding "soft" heavy metals such as lead, cadmium, and mercury from matrices as diverse as gold mining effluent, lead battery recycling effluent, acid mine drainage, contaminated soil, and coal refuse.<sup>222-228</sup> However, previous research has focused solely on remediation of the divalent forms of the metal salts in batch remediation situations using an ethanolic solution of dissolved B9 or the sodium- or potassium-salts of B9 to increase the water solubility of the compound.

## **GOALS OF THE CURRENT WORK**

The primary goal of the dissertation research is to explore the distinct binding modes of mercury and arsenic with a model compound, B9, which contains two sulfur equivalents as terminal thiol groups. Although both elements are thiophilic, differences in covalent bonding are expected due to the unique and contrasting chemistries displayed by

arsenic, a main-group metalloid, and mercury, a transition metal whose behavior is strongly influenced by relativistic effects. Knowledge gained from the execution of this research will be applied to remediation scenarios whereby mercury and arsenic shall be completely and irreversibly removed from aqueous phase sources using the model compound. “Complete” removal will be loosely defined as removal of the contaminant to well below typical maximum contaminant levels (5 ppb for Hg, 10 ppb for As) while “irreversible” removal shall refer to the stable covalent bond formation between the contaminant and compound *in situ* until such time as the contaminant-compound product is removed from service. Specific applications that will be addressed include the removal of mercury from coal-burning power plant scrubber solutions, with coal burning being one of the primary sources of environmental mercury contamination, and arsenic from drinking water sources in West Bengal, India and the western United States.

The goals of the current work can be assigned to three broad areas, including the general extension of the ligand’s utility, the exploration of ligand-mercury and ligand-arsenic compound stability, and the desire to develop a more robust, permanent, and inexpensive means of remediation for mercury and arsenic from contaminated waters.

**Extension of Ligand Utility.** Application of dissolved or metallated B9 in batch remediation scenarios limits the ultimate applicability of the compound. Batch treatment of contaminated waters may prove useful in municipal water treatment systems, but the desire to have a portable, lightweight column for use in homes and the arsenic-affected villages of West Bengal and India demands exploration of alternative ligand application methods. Problems also arise when the ligand must first be dissolved in ethanol or metallated prior to application. Use of an ethanolic B9 solution would carry inordinate risks in high-temperature environments such as the FGD tanks in coal-fired power plants. Injection of the flammable ethanolic slurry into a FGD tank would expose the mixture to hot flue gases, risking ignition of the mixture. Alternatively, the ligand could be applied as the sodium or potassium B9 salt, but this method requires the solubilized ligand to be applied quickly after formation of the metallated B9 to avoid decomposition to the unreactive, cyclized B9-disulfide product.

Batch precipitation of heavy metals often requires coagulation, flocculation, and a final filtration step to remove the hazardous solids formed. By immobilizing the B9



ligand in a filtration column, these subsequent treatment steps can potentially be eliminated. Ideally, the ligand would be covalently bound to a surface to reduce the possibility of the ligand washing out of the column. For the first “proof of concept” studies, however, simply mixing the solid ligand with a physical support should suffice. The ligand must be dispersed in an inert support material because the hydrophobicity of the compound will prevent the flow of water through the system if used alone. If the reaction between the solid ligand and the aqueous mercury and arsenic proves to occur quickly enough, further research can then proceed in order to covalently attach and immobilize the ligand to a surface.

B9 has proven successful in the batch remediation of the soft, divalent metals Pb(II), Cd(II), Cu(II), Mn(II), Zn(II), Fe(II) and Hg(II) from ground water, coal refuse, gold ore, lead battery recycling plant wastewater and contaminated soils.<sup>229-240</sup> Arsenic presents a slightly different challenge in that it most commonly exists in nature as the oxyanions arsenate,  $\text{AsO}_4^{-3}$ , and arsenite,  $\text{AsO}_3^{-3}$ , where arsenic is in the (V) and (III) oxidation states, respectively. Arsenic treatment is further complicated by the fact that the oxyanions are found in multiprotic acids that form equilibrium mixtures containing a variety of As(III) and As(V) species depending on the pH and redox potential of the water. For this reason, not only must one consider treatment of the element in two different oxidation states, but must also be able to appropriately address binding of the differently-protonated species  $\text{AsO}_4^{-3}$ ,  $\text{HAsO}_4^{-2}$ ,  $\text{H}_2\text{AsO}_4^{-1}$ ,  $\text{H}_3\text{AsO}_4$ ,  $\text{AsO}_3^{-3}$ ,  $\text{HAsO}_3^{-2}$ ,  $\text{H}_2\text{AsO}_3^{-1}$ , and  $\text{H}_3\text{AsO}_3$ .<sup>218-220, 241</sup> However, the thiophilic nature of arsenic should allow for binding with B9 and therefore be retained by the ligand long enough remove it from drinking water sources.

**Explore Ligand Stability with the Thiophilic Species Mercury and Arsenic in Aqueous Media.** The final phase of the dissertation work will focus on the stability of the B9-mercury and B9-arsenic compounds synthesized. Following the characterization of the compounds, the products will be leached over a pH range from 1-13, under oxidizing conditions, and under reducing conditions. The goals for this work are two-fold: (1) determine optimal storage conditions for the spent column media, and (2) attempt to discover a method of “releasing” the mercury and arsenic without destroying the B9 compound in hopes of regenerating the B9 for re-use. The leaching studies will

also serve to highlight the differences between mercury and arsenite binding to B9, the model sulfur compound.

**Develop a More Robust, Permanent and Inexpensive Means of Remediation.**

The complete dissertation work and related work should result in no less than eleven publications and three patents for technology that will be immediately applicable to solving two of the world's most ubiquitous environmental problems: aqueous mercury and arsenic contamination. While methods exist for handling both of these problematic species, all have deficiencies that can be overcome using B9 to effect permanent removal of mercury and arsenic from solution.

## CHAPTER TWO: REMEDIATION OF Hg(II) USING A B9 COLUMN

### INTRODUCTION

**Key Deployment Targets for Improved Remediation Technology.** The implementation of successful remediation techniques at a few key mercury emission sources would lend the greatest impact on global mercury pollution reduction. These key deployment targets should include coal-fired power plants, waste effluents from industry and medical sources, water bodies already carrying a high mercury burden, and abandoned mines and their associated tailings. While Hg(0) that is potentially generated from these sources is generally unreactive, the divalent mercury salts and methylmercury associated with such targets have the potential to be irreversibly and covalently bound to solid B9 under flow conditions using a remediation column.

To date, “no single best technology with broad application has been identified for controlling mercury emissions from coal-fired plants” even though coal-fired power plants in the United States release an estimated 40% of the controllable mercury emissions and represent a key target.<sup>29, 38, 44</sup> The estimated speciation of mercury emissions from coal-fired power plants in the United States is 3% Hg-p, 43% Hg(II), and 54% Hg(0), meaning that nearly half of the mercury emitted could be captured using the appropriate technology targeting the divalent species.<sup>38</sup> Processing the scrubber solution to prevent the reduction of Hg(II) and subsequent reemission as Hg(0) presents itself as a prime opportunity.<sup>29</sup> Furthermore, cleaning the excess Hg out of the coal combustion byproducts (CCBs), fly ash and FGD scrubber sludge will avoid the possible volatilization of mercury from commercial products and waste.

Waste effluents from industrial, medical and mining sources and bodies of water characterized as carrying a high mercury burden due to past anthropogenic discharges represent other key deployment targets. B9 remediation column treatment prior to discharge for chloralkali plants and manufacturing processes using mercury catalysts has the potential to avoid another Minamata Bay catastrophe. Due to past mercury discharges, advisories limiting the consumption of fish have been issued for 52,000 lakes and more than 238,000 miles of river within the United States.<sup>29</sup> Bodies of water overlying sediments overburdened with mercury compounds present another problem as

these sediments become a source of methylmercury production in the water column.<sup>2</sup> The selective treatment of these mercury “hot spots” could permanently remove mercury from the environmental cycle.

**Competing Mercury Remediation Technology.** It is difficult to separate the remediation of Hg(II) from Hg(0) when discussing mercury remediation technology as the ultimate goal is to decrease the amount of elemental mercury in the environment, often by oxidizing it to divalent mercury as a critical pre-treatment step. For this reason, the discussion of contemporary, competing mercury remediation technologies will incorporate intermittent references to Hg(0) in addition to focusing on Hg(II) technologies as the two strategies tend to go hand-in-hand. The three main categories of mercury remediation technologies include redox manipulation, sorbent capture, and mercury complexation or precipitation coupled with filtration.

Much of the relevant redox manipulation of mercury was previously discussed in the context of remediation of Hg(0) from coal-fired power plants in Chapter 1. Several methods of enhancing mercury oxidation through chemical addition or catalytic means are under investigation since Hg(II) is easier to remove from flue gas than the unreactive and water-insoluble Hg(0).<sup>35, 40</sup> For instance, in addition to choosing high chlorine coals to push the equilibrium of Hg(0) to the water soluble Hg(II) species,<sup>29, 30, 33, 38, 242, 243</sup> the use of additional chlorine,<sup>34, 40, 244-252</sup> bromine,<sup>250, 253, 254</sup> iodine,<sup>244, 250, 255</sup> fluorine,<sup>250</sup> and lime<sup>33, 34</sup> to enhance mercury oxidation and capture have been examined. The electro-catalytic oxidation (ECO) process, a multi-pollutant control device designed specifically for the removal of SO<sub>2</sub>, NO<sub>x</sub> and fine particulate emissions also holds promise in mercury removal through enhanced wet FGD capture of oxidized mercury, a by-product of the oxidation process.<sup>29, 34, 36</sup> Through reaction with either the catalyst or the ammonia reagent used in selective catalytic reduction (SCR) for removal of NO<sub>x</sub>, a portion of elemental mercury can be oxidized to Hg(II) and Hg-p as a side benefit, but this process is difficult to optimize for both efficient NO<sub>x</sub> and mercury removal.<sup>29, 36, 39, 40, 256</sup>

Photochemical oxidation of Hg(0) to Hg(II) using UV light provides another avenue for elevated capture rates using particulate control devices or FGD systems.<sup>34</sup> In the presence of 253.7 nm radiation, water, Hg(0) and TiO<sub>2</sub> react to form a TiO<sub>2</sub>·HgO complex capable of removing 99% of Hg(0) at low temperatures.<sup>40, 257</sup> Unfortunately, Hg

desorption from the  $\text{TiO}_2$  surface retards this method of capture at temperatures of only  $110^\circ\text{C}$ , much lower than is applicable to the coal-fired power plant scenario for which it was developed.<sup>40</sup> Other sorbents, including zeolites, iron oxides ( $\alpha\text{-Fe}_2\text{O}_3$ ,  $\alpha\text{-FeOOH}$ ,  $\gamma\text{-Fe}_2\text{O}_3$ ,  $\alpha\text{-Fe}_2\text{O}_3/\text{MnFe}_2\text{O}_4$ ,  $\text{Fe}_3\text{O}_4$ ), aluminosilicates, and titania pillared interlayered clays have been tested both with and without UV irradiation to gauge the effectiveness of mercury capture.<sup>34, 35, 252, 257</sup> In addition to  $\text{TiO}_2$  and titania pillared interlayered clays, zeolites and Trans Oxide Brown, the iron oxide containing hematite,  $\alpha\text{-Fe}_2\text{O}_3$  and the manganese complex, were found to have some photocatalytic ability enabling mercury capture.<sup>257</sup> Alternatively, it has been proposed that ultraviolet (UV) light in the presence of mercury enhances ozone formation through “sensitized oxidation” which can, in turn, react with mercury to form solid mercuric oxide with a net decrease in gaseous mercury contamination.<sup>258-260</sup> Regardless of the exact mechanism for photocatalytic mercury removal, this process is optimal at temperatures below  $300^\circ\text{F}$  and could be applied in a manner similar to the UV irradiation already used in some water treatment plants.<sup>259, 260</sup>

Conversely, some researchers feel that the reduction of mercury to  $\text{Hg}(0)$  holds greater promise for capture and removal of mercury from the environment. For instance, photoreduction of solid wastes from a chlor-alkali plant allowed for the selective precipitation of  $\text{Hg}(0)$  and  $\text{Hg}_2\text{Cl}_2$  on the surface of a  $\text{TiO}_2$  surface though it was unclear how the  $\text{Hg}(0)$  was handled once separated from the surface using a mixed acid rinse.<sup>261</sup> Another reductive technique processes wastewater using  $\text{Hg}(\text{II})$ -reducing microorganisms in bioreactors engineered to capture the resulting water-insoluble  $\text{Hg}(0)$  vapor.<sup>26, 262, 263</sup> As previously discussed, some organisms are able to reduce  $\text{Hg}(\text{II})$  to  $\text{Hg}(0)$  as a detoxification mechanism.<sup>71</sup> These microorganisms are contained in the reactor to avoid introduction into the natural food chain and to prevent the potential for bioaccumulation of mercury in higher organisms. Two major drawbacks to this method include the need to carefully monitor the mercury concentration of the influent water to avoid killing the microorganisms and handling of the  $\text{Hg}(0)$  vapor once it has been generated, especially considering the general unreactivity of this species.<sup>26, 262</sup> Pilot scale studies have relied on activated carbon to trap the  $\text{Hg}(0)$  generated which is an undesirable entrapment method as will be discussed shortly.<sup>262, 263</sup>

Besides redox manipulation of mercury, sorbent injection for the remediation of mercury from coal-fired power plants has garnered wide spread attention in recent years. Sorbent injection has been touted as one of the most promising technologies as virtually all coal-fired power plants use either ESPs or baghouses to capture particulate materials from flue gases.<sup>264</sup> Dry sorbents in particular have the singular ability to remove both elemental and oxidized forms of mercury.<sup>35, 264</sup> Sorbents act to remediate mercury through the processes of amalgamation, physical adsorption, chemical adsorption, and chemical reaction.<sup>35</sup> Sorbents are injected as either a dry powder or a wet slurry prior to particulate control devices to bind the mercury, allowing the products to be captured in ESPs or bag houses.<sup>33, 44</sup>

Adsorption results in a thin film of mercury accumulating on the adsorbate surface. When only weak electrostatic attractions due to induced dipole moments or van der Waals forces results between mercury and the adsorbate, the process is physical adsorption or “physisorption.” Stronger interactions between mercury and the adsorbate resulting in the formation of covalent or ionic chemical bonds is termed “chemical adsorption” or “chemisorption.” Amalgamation and physisorption are low-temperature processes (< 300 °F) while chemisorption tends to occur at higher temperatures due to the larger enthalpies and activation energies associated with bond formation.<sup>35, 265</sup> The exact mechanisms by which sorbents remove mercury remain unknown.<sup>35</sup> Mercury adsorbates can be carbonaceous in nature, noble metals, or composed of various sulfur- and oxygen-based inorganic compounds.

In particular, injection of carbonaceous products including unburned carbon from fly ash, char (mildly activated carbon), and activated carbon injection (ACI) have all experienced measured degrees of successful application for the removal of Hg(0) and Hg(II) through physisorption.<sup>34, 40, 44, 264, 266-268</sup> Originally, ACI was applied to incinerators with great success.<sup>267, 269</sup> Since ACI application has been tested in coal-fired power plants capture rates of up to 95% have been reported although removal efficiencies reported in other tests have often fallen short of these generous results.<sup>44, 264, 268</sup> This may be due to the wide differences in flue gas environments and temperatures examined as each coal-fired power plant is singularly unique in design, operation, and coal used, making reproducible results across different power plants difficult. In fact, incinerator flue gases

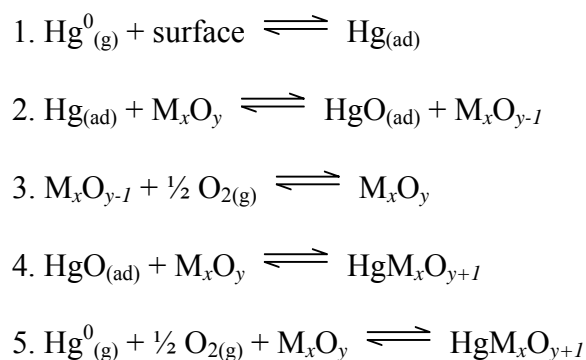
are often much richer in chlorine and mercury compared to coal-derived flue gases, with both factors contributing to the higher reported mercury capture rates.<sup>264, 267</sup>

AC capture of Hg works over a limited temperature range, generally below 300 °F since physisorption is the initial mechanism for mercury capture.<sup>35, 252, 267, 269</sup> Sorbent capture of mercury can be optimized by lowering the temperature of the flue gas or by chemically “promoting” ACI with sulfur, iodine, chlorine or nitric acid or hydrochloric acid treatment.<sup>34, 38, 244, 270-272</sup> In addition to physisorption, promoted ACI chemically reacts with the mercury, oxidizing the element to form the corresponding mercury sulfide, iodide, etc. and allowing for slight increases in mercury capture in laboratory tests using synthetic flue gas or pure nitrogen.<sup>35, 244, 268, 270, 272, 273</sup> Alternatively, AC can be doped with chelating agents such as  $\beta$ -aminoanthraquinone or 2-(aminomethyl)pyridine to effect greater capture, but both of these additives demonstrated poor performance at elevated temperatures.<sup>271</sup> While the move to a chemisorptive process is desirable, the additional treatment of AC prior to application often comes with increased time and capital costs without a substantial increase in mercury capture capacity.

While activated carbon has been touted as the gold standard for mercury sorption from vapor, AC is highly inefficient for removing aqueous mercury due to its function as a general adsorbent.<sup>262</sup> In coal-fired power plants, most components of flue gas will adsorb to AC, some even in direct competition to mercury such as the very abundant SO<sub>2</sub> gas and NO.<sup>26, 35, 40, 269, 274</sup> AC is expensive, translating into annual operating costs of approximately one million dollars for a typical 500-MW coal-burning power plant.<sup>264, 267</sup> In fact, the US Department of Energy estimates that a 90% mercury capture efficiency using ACI would cost \$25,000 to \$70,000 per lb Hg removed.<sup>271</sup> Contributing to these costs are the facts that AC can only be regenerated a few times and has a low capacity for mercury capture requiring high carbon-to-mercury ratios to be effective.<sup>35, 264, 267, 269, 271,</sup><sup>275</sup> The long-term stability of mercury captured by AC is questionable as the mercury is only physisorbed in un-promoted ACI and therefore labile to volatilization and complicating disposal options.<sup>26, 35, 264</sup> An early DOE estimate for disposal of fly ash containing carbonaceous sorbents is approximately \$3 billion annually.<sup>264</sup> Furthermore, the long-term effects of sorbent injection on coal-fired power plant facilities and on the properties of the saleable ash byproducts such as cement and wallboard have yet to be

determined; questions linger about the evolution of mercury from these products.<sup>34</sup> The adsorption of oxygen by AC in fly ash has already been shown to affect the quality of Portland cement in concrete.<sup>264</sup> While quite promising, ACI has yet to be used commercially.<sup>44</sup>

One inorganic alternative to carbonaceous mercury sorbents are partial oxidation oxide catalysts such as manganese dioxide, vanadium pentoxide, and molybdenum trioxide.<sup>35, 40, 268</sup> These metal oxides function as mercury oxidants to form the corresponding mercury manganates, vanadates, and molybdates according to the following Mars-Maessen mechanism adapted from Granite, et al. (2000)<sup>35</sup>:



**Scheme 2.1:** Mechanism of Mercury Capture Using Metal Oxide Catalysts<sup>35</sup>

Mercury is first adsorbed to the surface in step (1) where it then reacts with the metal oxide,  $\text{M}_x\text{O}_y$ , resulting in mercuric oxide and the reduced form of the sorbent surface in step (2). The surface is quickly oxidized as shown in step (3) in the flue gas environment. In step (4), mercuric oxide reacts with the re-oxidized sorbent surface to form the binary mercury oxide,  $\text{HgM}_x\text{O}_{y+1}$ . The overall mechanism is summarized in step (5). The surface area of the metal oxide catalysts can be increased by using alumina ( $\text{Al}_2\text{O}_3$ ) or celkate ( $\text{MgSiO}_3$ ) as solid supports which have themselves proven inert to mercury capture.<sup>35, 268</sup> The chemisorption demonstrated by these partial oxidation oxides is superior to physisorption but may be compromised by sulfate formation on the catalyst surface prior to reaction with mercury as sulfur dioxide is many orders of magnitude more abundant in flue gas than mercury.



Metal sulfides, including  $\text{Na}_2\text{S}$ ,  $\text{Na}_2\text{S}_4$ , and  $\text{MoS}_2$ , have been shown to first physisorb elemental mercury and later chemisorb it as mercury sulfide on the sorbent surface.<sup>33, 35, 264, 271</sup> While molybdenum disulfide has a high adsorption capacity for mercury, it decomposes at high temperatures and is relatively expensive.<sup>35, 271</sup> Injection of sodium sulfides results in the formation of finely divided  $\text{HgS}$  particles that are difficult to capture with ESPs.<sup>33, 264</sup> Mercury capture by metal oxides and metal sulfides both depend on the occurrence of physisorption as the rate-limiting step, which is only favored at low temperatures. For this reason, high temperature application of metal oxides and sulfides is unlikely to result in mercury capture as physisorption is disfavored.<sup>265</sup>

The noble metals are often used for mercury sampling and analysis. Mercury is collected by amalgamation on gold, for example, thermally desorbed, and vented to a UV detector for measurement in combustion gold amalgamation atomic absorption (C-GA-AA). Palladium, platinum, iridium, rhodium, and gold have all been utilized as modifiers for graphite tube atomic absorption (GTAA) spectroscopy.<sup>265</sup> Palladium in particular effectively adsorbs and retains the semivolatile elements Hg, As, Se, and Cd at elevated temperatures during the drying and pyrolysis stages of GTAA, possibly through alloy formation.<sup>265</sup> Citing the success of these noble metal sorbents in the analytical world, a logical extension involved testing copper, gold, silver, palladium, platinum, iridium and others for mercury remediation in coal-fired power plants.<sup>35, 40</sup> While palladium, platinum, and iridium function well in this regard, it is highly unlikely to become useful for more than an academic exercise in gas-phase mercury capture due to costs though some have argued the cost to be minimal when the metals are used on a solid support.<sup>40, 265</sup> Less costly, the reduction of  $\text{Hg(II)}$  and amalgamation of the resulting  $\text{Hg(0)}$  using mossy tin has been demonstrated as a remediation method.<sup>26, 276</sup> Both mossy tin and copper shavings have been found to capture  $\text{Hg(II)}$  through this process in aqueous applications.<sup>276, 277</sup> Regardless, amalgamation will most likely not supplant other methods of remediation due not only to cost, applicability only at low temperatures, and problems with ash buildup on the metals surfaces but also due to the undesirable ability of mercury to be volatilized via deamalgamation from the noble metals.<sup>40</sup> Recall that this property was central to the use of mercury in amalgamation mining techniques for gold described in

Chapter 1 and was responsible for significant mercury vapor release to the atmosphere.<sup>35,</sup>  
265

The third major category of current mercury remediation technology involves the use of precipitation agents coupled with filtration or chelating resins to remove mercury from the gas or aqueous phases. Direct chemical reaction of mercury with a precipitation or chelation agent has a distinct advantage over sorbent capture in that the capacity of the agents is often much greater than demonstrated for sorbent technology which relies on physisorption for the initial reaction step.<sup>275</sup> Many reagents exist that precipitate mercury from aqueous solutions including sodium dimethyldithiocarbamate (DMDTC), sodium thiocarbamate (STC), and trisodium 2,4,6-trimercatotriazine (TMT).<sup>26, 236, 262, 278-280</sup> Unfortunately, metal binding is not discriminatory, a secondary filtration step is required and the long-term stability of metal precipitating ligands remains questionable as toxic decomposition products including thiram, cinnabar, and free mercury itself have been documented.<sup>26, 230, 236, 262</sup> Even if decomposition does not occur, binding to these reagents tends to be reversible under acidic and alkaline pH ranges.<sup>230</sup> For example, TMT metal compounds (M = Cd, Pb, Zn) have been found to exhibit significantly higher solubility than the corresponding metal sulfides or hydroxides at pH 3.<sup>279</sup> Several varieties of Hg-TMT exist, many of which are unstable in both water and air, leading to significant mercury releases post-treatment.<sup>280</sup>

Similarly, complexing surfactants can be added to a solution to change the solubility of mercury and other toxic metals so that they can be extracted in organic solvents and removed.<sup>26, 275</sup> Complexing mercury in a surfactant has the advantage of not requiring flocculation and filtration; rather a liquid-liquid extraction is performed to remove the complexed metal(s).<sup>275, 281</sup> However, this method generates what may arguably be a worse secondary waste: metal-contaminated organic solvents. Furthermore, the general non-selectivity of complexing surfactants presents a problem as mercury is in direct competition for binding sites with other heavy metal contaminants including Cd, Cr, Cu, Ni, Pb, and Zn.<sup>275</sup> For the complexing surfactants reviewed, a mixture of phenolic, pyridine, an amine binding sites were used in mercury bonding rather than free thiol groups which represent a far superior choice for mercury retention.<sup>275</sup>

Chelating resins are considered to be one of the most effective separation techniques.<sup>261</sup> Chelates most often act on the ionized form of a metal by forming covalent bonds through two or more donor groups to the metal to form one or more rings.<sup>271</sup> Ideally, additional charged groups in the ring are available for electron donation to the metal to lend additional stability.<sup>271</sup> Several functional groups have been examined for this application including pyridines, imines, amines, and sulfur-functionalized surfaces.<sup>221, 271, 281-286</sup>

Nitrogen groups are not expected to be specific for mercury chelation. Nitrogen is a soft ligand that will complex with soft metal ions besides Hg(II) including Cd(II), Pb(II), Zn(II) and possibly borderline soft metal ions such as Cu(II) and Fe(II).<sup>283</sup> Add to this sub-optimal situation the competition for mercury binding to species in the mother liquor, whether it be chloride, humic acid or any number of naturally-occurring ligands in the solution being treated and the performance of a nitrogen-containing chelating agent will certainly suffer.<sup>282</sup>

Ion exchange resins, minerals, and mineral-like surfaces functionalized with polysulfonates and various thiol ligands have been used as filters for the capture of mercury.<sup>26, 221, 262, 271, 281, 285, 286</sup> In order to function effectively, ion exchange resins need to be able to bind all of the different free complexes of mercury that may be present. Mercury species in water, for example, can range from the cationic  $\text{Hg}^{+2}$  or  $\text{HgCl}^+$  to neutral  $\text{HgCl}_2^0_{(\text{aq})}$  or anionic species including  $\text{HgCl}_3^-$  or  $\text{HgCl}_4^{-2}$  depending on the chloride concentration.<sup>275</sup> In the case of one sulfonate ion exchange resin, the pH had to be adjusted to the acidic range and even then only the cationic mercury species was retained; HCl treatment generated the  $\text{HgCl}_4^{-2}$  complex which was rejected by the resin.<sup>281</sup> A separate study using thiol groups on commercial resins required oxidation, filtration and dechlorination prior to application of the resin to achieve desirable results.<sup>221</sup> Another difficulty with these materials lies in the synthesis of functionalized surfaces which can often require multiple steps, some of which result in undesirable secondary reactions and put the thiol group at risk for oxidation.<sup>221, 271</sup>

Despite these shortcomings, thiol-functionalized materials have offered one of the better options for mercury binding as thiols linked to a high surface area for application are ideal.<sup>285</sup> Reports of thioalkylated montmorillonite clay and thioalkylated mesoporous

silica have shown mercury capture rates of  $65 \text{ mg Hg}\cdot\text{g}^{-1}$  and  $505 \text{ mg Hg}\cdot\text{g}^{-1}$  as opposed to rates of  $1 \text{ mg Hg}\cdot\text{g}^{-1}$  for AC.<sup>286</sup> A styrene-divinylbenzene copolymer with pendant aryl thiol groups from Rohm and Haas called TMR for “total mercury removal” still one of the best mercury resins with a binding rate of nearly  $0.7 \text{ g Hg}\cdot\text{g}^{-1}$  of resin.<sup>221, 262</sup> Binding of sulfur to mercury is often 2:1 with mercury in either a linear, two-fold coordination or in a tetrahedral configuration bridging sulfur centers in a polymeric product.<sup>271, 285</sup> The shortcomings of difficult syntheses and elaborate pre-treatment steps prior to application need to be eliminated to make this an ideal solution, however.

### **B9: Intelligent Ligand Design to Exploit Preferential Mercury-Sulfur**

**Binding.** The B9 dithiol ligand was designed to mimic the metalloregulatory protein MerP binding site which has two cysteine residues available for bidentate mercury bonding.<sup>233, 262, 287</sup> As a mercury chelating ligand, B9 is ideal as it offers two thiol groups that can chelate mercury in an nearly linear fashion, the preferred geometry for Hg(II) complexes.<sup>288</sup> The thiol groups function as soft bases and will have a propensity to chelate soft metals Hg(II), Pb(II), Cd(II), and Zn(II).<sup>229, 230, 236, 262</sup> In mixed metal solutions, even though B9 is not mercury specific, it is optimized such that Hg binds in preference to all other competing soft metals.<sup>237</sup>

B9 has demonstrated potential to work effectively even at low pH without pre-treatment of the solutions. For example, up to 99.4% of Pb(II) was removed from pH 1.5 lead battery recycling wastewaters.<sup>232</sup> Similarly, > 90% of problematic metals were removed from acid mine drainage (AMD) without prior manipulation of the AMD samples.<sup>229</sup> B9-metal complexes are also remarkably stable. Mercury-sulfide decomposition products have never been detected in long-term stability studies.<sup>236</sup> These properties make B9 an ideal candidate for “proof of concept” column remediation tests using  $\text{HgCl}_2$  to demonstrate that covalent bond formation occurs quickly enough to remove mercury from water.

**Goals of the Current Work.** The current work will combine solid B9 with an inert support material to remediate  $\text{Hg(II)}_{(\text{aq})}$  under a variety of flow rates to determine if this alternative application method is a viable solution in addition to previously described batch application techniques. The products formed from this remediation method will be characterized and leached under a wide range of pH and redox conditions to explore the

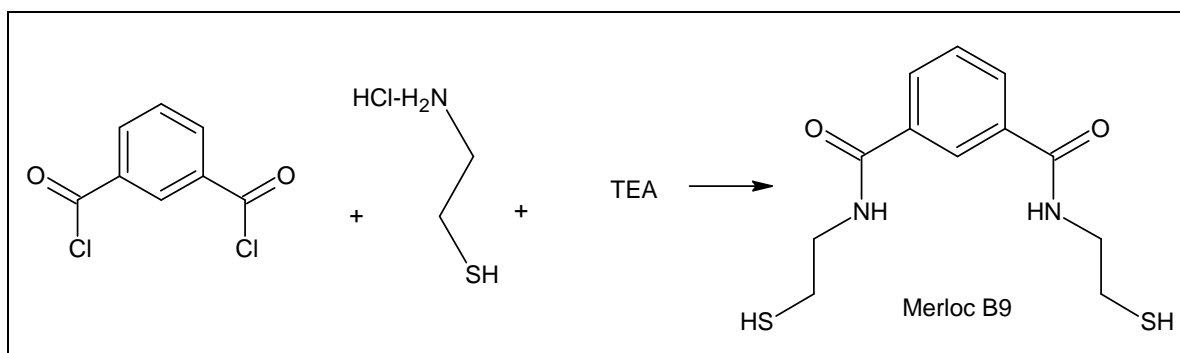
stability of the expected mercury covalent bond to the model dithiol compound B9. Should the column remediation of  $\text{Hg(II)}_{(\text{aq})}$  prove successful, this will offer a fast, efficient, portable, and permanent means of removing mercury from waste water effluent and natural bodies of water carrying a high mercury burden.

## EXPERIMENTAL

**B9 Synthesis and Characterization.** The synthesis of B9 has been previously published under the trade names “MetX,” “BDETH<sub>2</sub> and “BDTH<sub>2</sub>,”<sup>230, 234, 237</sup> The synthesis reported here represents a slightly modified method. All glassware and stir bars were rinsed once with acetone (Fisher) and twice with chloroform (Roan Industries, Inc.) prior to the synthesis. Cysteamine hydrochloride (34.08 g, 30 mmol, Bricchem (Haikou) Co. Ltd.) was added to a 500 mL round-bottom flask with chloroform (approx. 200 mL) and allowed to stir with nitrogen streaming into the open mouth of the reaction vessel. Isophthaloyl chloride (20.30 g, 10 mmol Gow Chemical Corp. Ltd.) was dissolved with stirring in a separate beaker of chloroform (approx 100 mL). Triethylamine (TEA, 60.71 g, 60 mmol, Acros Organics) was weighed out into a capped glass bottle. TEA (approx. 40 mL) was slowly added to the reaction flask followed by the gradual addition of half of the isophthaloyl solution. These additions were repeated until all portions of TEA and dissolved isophthaloyl chloride had been added to the reaction flask. The resulting clear liquid was a pale violet in color and unlike past synthetic techniques heat was not generated during the additions of TEA and isophthaloyl to the reaction vessel. The round-bottom flask was purged with nitrogen, sealed, and allowed to stir overnight. The basic synthesis is depicted in Scheme 2.2.

A 10% HCl solution (900 mL deionized water to 100 mL conc. Omnitrace HCl, EM Science) was prepared. The reaction mixture and approximately 500 mL of the acid solution was transferred to a 2-L separatory funnel and agitated vigorously with occasional venting. The layers quickly separated and the chloroform layer was collected while the aqueous layer was discarded. The chloroform mixture and another portion of the acid solution were added back to the separatory funnel and the process repeated. During the extraction procedure, the B9 compound began precipitating out of solution as a crystalline white solid. The chloroform and solid was transferred to an Erlenmeyer flask

with a continuous air stream blowing across the mouth to evaporate the solvent until only 50 mL of the solvent was left. The solvent-solid mixture was filtered with vacuum filtration and rinsed with diethyl ether to dry it. The remaining solid product was allowed to dry open to air until such time as it could be ground into a free-flowing, white, crystalline powder for characterization. Yield was 76% as calculated from the mass of the final, dried product divided by the theoretical yield. The B9 solid was characterized by melting point, infrared spectroscopy (IR),  $^1\text{H}$  NMR,  $^{13}\text{C}$  NMR, and elemental analysis. The characterization data agreed well with previous findings. Melting point:  $126^\circ\text{C}$ . IR(KBr): 3242s (vNH), 3070m[vC-H(arom)], 2936m[vC-H(methylene)], 2557w (vSH), 1640ss (vCO), 1542ss( $\delta\text{NH}$ ), 1431m(vC=C), 1319m(in plane bending C-H), 1085m(vC-S), 802m(out of plane bending C-H), 697m(out of plane bending C-H)  $\text{cm}^{-1}$ .  $^1\text{H}$  NMR ( $\text{CDCl}_3$ , 400 MHz)  $\delta$ : 1.44 (t, SH, 2H), 2.90 (m,  $\text{CH}_2\text{SH}$ , 4H), 3.71 (m,  $-\text{NHCH}_2$ , 4H), 6.58 (s,  $-\text{CONH}$ , 2H), 7.56 (t, ArH, 1H), 7.98 (d, ArH, 2H), 8.21 (s, ArH, 1H).  $^{13}\text{C}$  NMR ( $\text{CDCl}_3$ , 200 MHz)  $\delta$ : 169.1 (CO), 136.1, 131.2, 129.8, 127.2 (ArC), 45.1 ( $\text{NHCH}_2$ ), 24.7 ( $\text{CH}_2\text{S}$ ). Anal. Calcd. for  $\text{C}_{12}\text{H}_{16}\text{N}_2\text{O}_2\text{S}_2$ : C, 50.68; H, 5.67; N, 9.85; O, 11.25; S, 22.55. Found: C, 50.6; H, 5.9; N, 9.9; S, 22.7.



**Scheme 2.2:** Synthesis of B9.

**B9 Supported by Activated Carbon.** B9 (3.003 g) was physically mixed with activated carbon (AC) pellets (3.0045 g, Norit 0.8, Sigma-Aldrich) and poured into a glass column (0.7 ID x 50 cm, Kontes). One liter of 200 ppm Hg(II) solution was freshly prepared (0.2721g, Baker) using 18 M $\Omega$  deionized (DI) water at ambient pH, approximately pH 5.5. The Hg(II) solution was poured slowly into the column reservoir

and allowed to flow without added pressure. Three portions of the effluent were collected, capped, and stored overnight. After sitting, all three effluent samples displayed an obvious precipitate. The second sample had to be discarded due to contamination with the influent solution but the remaining two samples were filtered with 0.2  $\mu\text{m}$  syringe filters (Environmental Express) prior to acidification and digestion.

**B9 Supported by White Quartz Sand.** B9 (3.0017 g) was physically mixed with white quartz sand (15.16 g, -50 +70 mesh, Sigma-Aldrich) and poured into a glass column (0.7 ID x 50 cm). The same 200 ppm Hg(II) solution prepared previously was poured into the column and allowed to flow without added pressure. Unlike the B9-AC column samples, each 20-mL effluent sample was clear prior to filtration, acidification and digestion.

A second column of B9 (3.0059 g) physically mixed with white quartz sand (20.0449 g) was prepared to examine the effects of varying flow rates on the magnitude of remediation. A 20 ppm Hg(II) stock solution (0.0364 g in 1 L DI) was freshly prepared. A blank sample of DI water was run through the column prior to adding the 20 ppm Hg(II) with varying amounts of air pressure. As each 20-mL sample was collected the time to reach the prescribed volume was recorded with a stopwatch.

A third column containing only sand (20.0384 g) was constructed to evaluate the extent of potential Hg sorption. Similar to the last column, a DI water blank sample was collected followed by nine more effluent samples. The 20 ppm Hg(II) solution was allowed to flow without the addition of external pressure.

**Characterization and Stability of B9-Hg.** B9 (4.2659 g, 15 mmol) was dissolved in 95 % ethanol (200 mL, Acros) with gentle heating. The ethanolic B9 solution was added to HgCl<sub>2</sub> (3.9854 g, 15 mmol) dissolved in DI water (100 mL). A white precipitate formed immediately, but the solution was allowed to stir overnight before being subjected to vacuum filtration. The white solid was triple rinsed with DI water (50 mL x 3) and 95% ethanol (50 mL x 3) and allowed to dry open to air. Yield of the solid B9-Hg precipitate was 93% of the theoretical yield and the purity of the compound was checked by melting point (mp), infrared (IR) analyses, and mass spectral analyses and agreed well with previous findings.<sup>239</sup> Melting point: 156 °C. IR (KBr, cm<sup>-1</sup>): 3283s (secondary -N-H), 3024m (aromatic C-H's), 2920m (methylene C-H's), 1638ss

(-CO), 1533<sub>ss</sub> (-NH), 698 (C-S)]. EI-MS: [Hg-(SC<sub>2</sub>H<sub>4</sub>NHCO)<sub>2</sub> (406), Hg-(SC<sub>2</sub>H<sub>4</sub>NH)<sub>2</sub> (350), C<sub>6</sub>H<sub>4</sub>(CO)<sub>2</sub>NHC<sub>2</sub>H<sub>4</sub> (174), C<sub>6</sub>H<sub>4</sub> (75)]. Anal. Calcd. for C<sub>12</sub>H<sub>15</sub>HgN<sub>2</sub>O<sub>3</sub>S<sub>2</sub>: C, 29.84; H, 5.67; N, 9.85; O, 11.25; S, 22.55. Found: C, 18.26; H, 5.76; N, 3.31; O, 63.26; S, 8.77.

Due to the unique challenges associated with handling mercury, Teflon digestion tubes (Environmental Express) and disposable PTFE stir bars (Fisher) were used for the leaching study. In addition to the B9-Hg samples being leached, blank samples were maintained to evaluate the magnitude of contamination introduced through acid and base addition and from ambient mercury levels in the lab diffusing into the samples. The study leached 20.0 mg portions of B9-Hg in 20.0 mL of pH adjusted (pH 1, 3, 5, 7, 9, 11, 13) DI water for one week, one month, and two months with separate samples being prepared for each time period to minimize the possibility of contamination. The oxidative leaching study utilized 20.0 mL portions of NaOCl (Fisher) as a source of 13% active chlorine. The reductive leaching study combined approximately 20 mg of B9-Hg with 100 mg of Zn(0) in 20.0 mL of pH neutral deionized water. At the end of each leaching period, the mixtures were subjected to 0.20 μm Teflon syringe filter filtration (Environmental Express) and stored in 50-mL glass volumetric flasks with Teflon caps (Cole Parmer).

**Analytical Procedures.** Melting points were recorded using a Mel-Temp melting point apparatus from Laboratory Devices. Infrared spectra were obtained using KBr disks on a Thermo Nicolet Avatar 360 FTIR spectrometer. NMR spectra were taken in CDCl<sub>3</sub> using a Varian 200 MHz Gemini and 400 MHz INOVA instruments in the University of Kentucky Nuclear Magnetic Resonance Facility. Elemental analyses were performed on a LECO CHN-2000 analyzer at the University of Kentucky Center for Applied Energy Research. Mass spectra were obtained at the University of Kentucky Mass Spectrometry Facility using direct probe insertion (DIP) with EI<sup>+</sup> ionization.

All column effluent samples were prepared for analysis by adding enough concentrated nitric acid to bring the sample to 10% acidity, digesting for a minimum of two hours at 100 °C, cooling, and diluting to volume with 1% nitric acid. Just prior to analysis, each leaching study sample was treated with BrCl (250 μL, Environmental Express) in accordance with EPA Method 1631e to oxidize the mercury present as well as desorb it from the walls of the glass container.<sup>289</sup> Samples were mixed well, diluted to



50 mL, and allowed to stand 24 hours before transfer to 50 mL digestion tubes and heating to 100 °C for two hours. The samples were allowed to cool, brought to 50 mL with DI water, and stored at 4 °C until analysis.

Low-level aqueous B9-Hg leaching samples were analyzed using Combustion Gold Amalgamation Atomic Absorption (C-GA-AA) techniques on a Nippon MA-2000 Direct Mercury Analyzer (DMA). Those leaching study samples found to be incompatible with the DMA were re-analyzed using Cold Vapor Atomic Absorption (CVAA) on a Cetac M-6000-A dedicated mercury analyzer. All column effluent samples were also analyzed by CVAA. Unless otherwise noted, reported results are the means and standard deviations of instrumental measurements.

High-concentration leaching study samples, Hg stock solutions, and the sand-only filtration column effluent samples were analyzed using a Varian Vista Pro Inductively Coupled Plasma Optical Emission Spectrometer (ICP-OES) run at 1.2 kW with 4.0 s replicate read times at 253.652 nm for the leaching study and 194.164 nm for all other samples. An extended 120 s, 5% HCl/10% HNO<sub>3</sub> rinse was used between samples; all other instrumental settings were used as pre-set by the manufacturer without modification. To correct for matrix effects, the concentration of a 1.0 ppm continuous feed Y internal standard was monitored at 371.029 nm. Method blanks were included between every sample with concentrations  $\leq 2.0$  ppm to estimate the limit of quantitation and for determination of an appropriate blank subtraction for each run to eliminate the effects of Hg carryover between samples.

For all spectroscopic methods employed, curve verifiers (CVs), laboratory control samples (LCSs), duplicate samples, and spiked samples were included at both high and low concentrations every tenth sample and for every unique sample matrix. CV and LCS recovery was  $\geq 95\%$  while spiked sample recovery typically ranged from 75% (ICP) to 90% (CVAA and DMA) and relative standard deviation (RSD) was kept well below 5%.

## RESULTS AND DISCUSSION

**B9 Filtration Columns.** When B9 is supported by AC in a column, the combination was able to decrease a 200 mg·L<sup>-1</sup> (ppm) Hg(II) solution to  $< 0.5$  µg·L<sup>-1</sup> (ppb) Hg, the lowest standard used to calibrate the CVAA. To insure this remediation

was due to the B9 and not the AC, a duplicate column was tested using B9 supported by white quartz sand instead of AC. Sorption of Hg(II) by the AC is an undesirable side effect that could result in Hg release during continued use of the column for remediation.

The possibility of Hg loss due to absorption to the sand in the column was evaluated first by running a 20 ppm Hg stock solution through a volume of sand similar to that used in the B9-sand mixture column without pressure. Table 2.1 lists the samples collected for this sand-only column, their respective mercury concentrations, the calculated mercury loss and the feed solution in use at the time the sample was collected.. Hg-sand-01 was a DI water method blank. Hg-sand-02 was the first sample collected during introduction of the 20 ppm Hg stock solution and is clearly affected by mixing of the DI water as the concentration is suppressed by 29.2%. Presumably Hg-sand-03 is also be affected by mixing with the last dregs of the DI water flushing from the column because by sample Hg-sand-04, suppression of the stock Hg concentration becomes negligible as the Hg loss due to adsorption to the sand and glass column walls remains < 1.5%. By sample Hg-sand-10, the mercury concentration of the effluent solution is statistically no different than that of the influent solution. Therefore, all of the observed mercury remediation in the B9 sand columns are attributable solely to the reaction of B9 with the Hg(II) as it flows through the column and not to mercury absorption to the sand.

Sample	Hg (ppm)	% Loss	Feed Solution
Hg-sand-01	< 0.50	N/A	DI water
Hg-sand-02	13.48 ± 0.11	N/A	Hg stock
Hg-sand-03	18.58 ± 0.14	2.41%	Hg stock
Hg-sand-04	18.88 ± 0.12	0.87%	Hg stock
Hg-sand-05	18.89 ± 0.18	0.81%	Hg stock
Hg-sand-06	18.94 ± 0.15	0.54%	Hg stock
Hg-sand-07	18.93 ± 0.17	0.59%	Hg stock
Hg-sand-08	18.97 ± 0.26	0.38%	Hg stock
Hg-sand-09	18.76 ± 0.16	1.49%	Hg stock
Hg-sand-10	18.99 ± 0.27	0.28%	Hg stock
Hg stock	19.04 ± 0.13	N/A	N/A

**Table 2.1:** Results for the Sand-Only Filtration Column with 20 ppm Hg

While the effective remediation under a flow scenario is in itself a positive outcome, we also wished to simultaneously examine the effects of varying flow rate on the magnitude of remediation that could be achieved. Therefore, a  $19.91 \pm 0.13$  ppm Hg(II) solution was run through a column containing 3 g B9 and 20 g quartz sand at varying flow rates. Results of the CVAA analysis of the effluent samples, in parts-per-trillion (pptr or  $\text{ng}\cdot\text{L}^{-1}$ ), are listed in Table 2.2 and graphed in Figure 2.1. For this analysis, the detection limit of  $10 \text{ ng}\cdot\text{L}^{-1}$  is representative of the lowest concentration CVAA standard used. Flow rates were determined by measuring the time required for each 20 mL sample to elute from the column. Flow rates were manipulated by adding air pressure to samples Hg-B9/sand-05 through Hg-B9/sand-10. Sample Hg-B9/sand-01 was a method blank consisting of DI water run through the column.

Sample	Effluent Hg (pptr)	Flow (mL·min <sup>-1</sup> )	Percent Removal
Hg-B9/sand-01	< 10	N/A	>99.99995%
Hg-B9/sand-02	< 10	0.726	>99.99995%
Hg-B9/sand-03	< 10	0.688	>99.99995%
Hg-B9/sand-04	< 10	0.469	>99.99995%
Hg-B9/sand-05	24.5 ± 0.9	1.471	99.99987%
Hg-B9/sand-06	23.8 ± 1.4	1.622	99.99988%
Hg-B9/sand-07	19.0 ± 1.0	2.449	99.99990%
Hg-B9/sand-08	529.6 ± 0.8	3.704	99.99734%
Hg-B9/sand-09	197.2 ± 1.6	3.261	99.99901%
Hg-B9/sand-10	825.6 ± 0.9	2.934	99.99585%

**Table 2.2:** Results for 20 ppm Hg passed through a B9 Supported by Sand Remediation Column

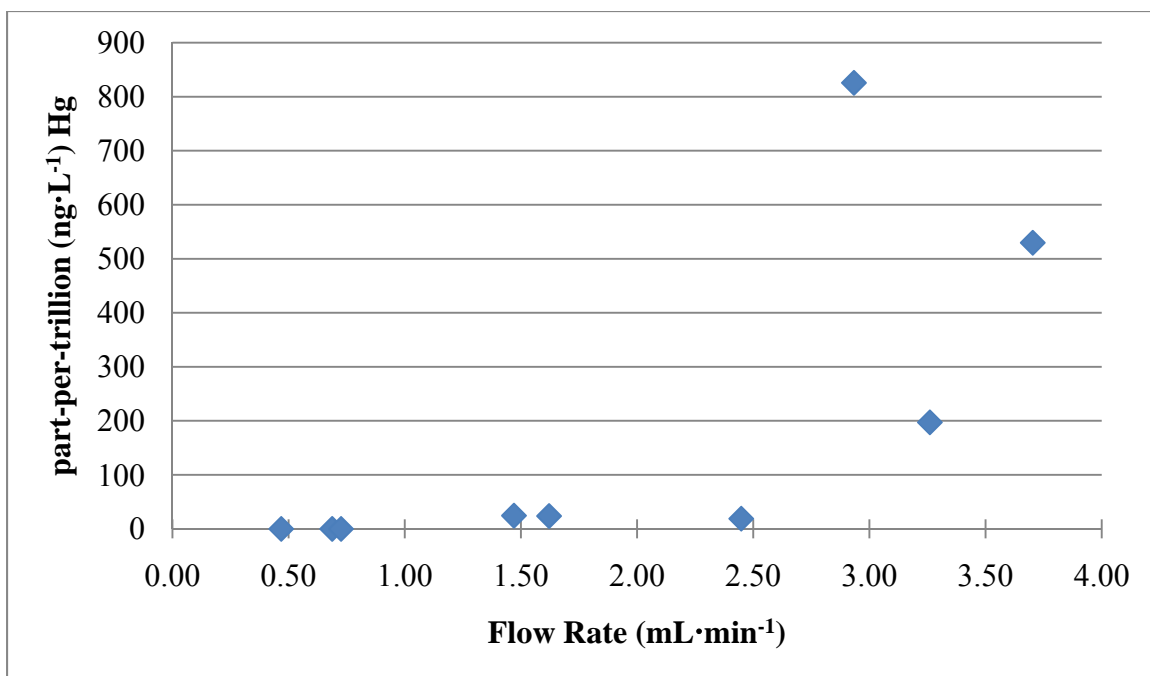


**Figure 2.1:** Hg Concentration vs. Flow Rate for the B9 Supported in Sand Remediation Column

The results for the B9 remediation column were excellent, proving that the reaction between  $\text{Hg(II)}_{(\text{aq})}$  and solid B9 occurs quickly enough in low flow situations to indicate that the column remediation of aqueous  $\text{Hg(II)}$  is a viable solution. Although the instrumental accuracy of Hg measurements does not allow the calculation of a seven-digit percent removal value, taking liberties with the results and calculating to five decimal places of accuracy demonstrates that  $> 99.99\%$  of the Hg is captured by the B9 irrespective of flow rates with only minor variations. For example, even under higher flow conditions, the final mercury concentration of  $825.6 \pm 0.9$  pptr in the column effluent represents a 99.99585% decrease in  $\text{Hg(II)}$  contamination. Under median flow conditions (average of  $1.54 \text{ mL}\cdot\text{min}^{-1}$  for samples Hg-B9/sand-05 through Hg-B9/sand-07), the average  $\text{Hg(II)}$  concentration of  $22.43 \text{ ng}\cdot\text{L}^{-1}$  represents a 99.99989% rate of  $\text{Hg(II)}$  removal, well below the US EPA standard of 5 ppb (or 5,000 pptr) in drinking water. Low flow conditions ( $< 1 \text{ mL}\cdot\text{min}^{-1}$ ) provided the highest level of remediation with mercury concentrations below  $10 \mu\text{g}\cdot\text{L}^{-1}$  or greater than 99.99995% removal. The lack of a clear trend of final Hg effluent concentration dependence on flow rate is further emphasized by the plot in Figure 2.1. While these results are adequate for this proof of

concept study, the flows dictated by common household use and industrial water treatment would require much higher flow rates, a problem that needs to be addressed in future work.

**B9-Hg Characterization and Stability.** Characterization of the B9-Hg product(s) agreed well with previous findings for mercury binding to thiol groups.<sup>239, 285</sup> Infrared spectra confirmed the S-H stretch ( $\nu_{\text{SH}}$ ) present in B9 at  $2556\text{ cm}^{-1}$  was absent in the white precipitate formed from the addition of  $\text{HgCl}_2$  and B9 dissolved in EtOH. The insolubility of the B9-Hg product in typical NMR solvents precluded analysis by that method. Fragments identified by mass spectrometry included  $\text{Hg}-(\text{SC}_2\text{H}_4\text{NHCO})_2$ , mercury bound to one cysteamine “arm” and a pendant carbonyl from B9,  $\text{Hg}-(\text{SC}_2\text{H}_4\text{NH})_2$ , mercury bound to two cysteamines,  $\text{C}_6\text{H}_4(\text{CO})_2\text{NHC}_2\text{H}_4$ , the bulk of the B9 molecule save for the missing thiol groups, and  $\text{C}_6\text{H}_4$ , the aromatic ring that serves as the “backbone” for the B9 molecule. Previous work using XAFS and XANES spectroscopy to characterize the nature of the B9-Hg product arrived at the final structure shown in Figure 2.1.<sup>239</sup>

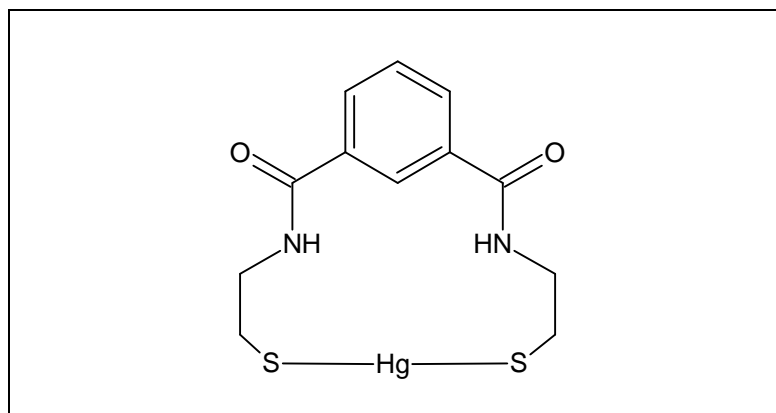


**Figure 2.2:** Proposed Structure of the B9-Hg(II) Product

Organic sulfhydryl groups (RSH) can exist at redox potentials higher than sulfide sulfur but lower than sulfate sulfur due to the stability added by bonding to an organic residue.<sup>2</sup> The mercury bound to organic thiols is in the +2 state, requiring the participation of two  $-\text{SH}$  groups to satisfy the mercury octet as demonstrated by the proposed structure in Figure 2.1.<sup>2</sup> This can be accomplished through bidentate binding of

a single ligand or monodentate binding of two separate thiol-containing ligands. For this reason, the B9-Hg products can exist as discrete molecular products and as an infinite array of polymeric solids where Hg(II) serves as the bridging unit between individual B9 molecules, giving rise to a wide range of molecular weights for individual units.

Concerning the molecular geometry of the proposed product, the rather large Hg(II) ion commonly adopts a tetrahedral geometry with the octahedral geometry being even less prevalent.<sup>5</sup> When the octahedral geometry does occur it is usually highly distorted with two short and four long bonds.<sup>5</sup> At its extreme, this distortion results in the two-coordinate linear stereochemistry characteristic of Hg(II).<sup>5</sup> This stereochemistry is typical of the large Hg(II) ion because as two ligands approach from opposite ends of the z-axis, the resulting  $d^{10}$  electron deformation increases the electron density in the xy-plane, discouraging the approach of other ligands.<sup>5</sup>

The aqueous stability of the B9-Hg compound(s) formed was examined across the pH range 1 to 13, under pH-neutral reducing conditions using Zn(0) as the reductant, and under aggressively oxidizing conditions using NaOCl as a source of active chlorine. Results were calculated as the unitless mass-by-mass ratios in parts-per-thousand (ppth = mg Hg in solution divided by mg B9-Hg leached  $\times 10^3$ ) or parts-per-million (mg Hg in solution divided by mg B9-Hg leached  $\times 10^6$ ) as appropriate to normalize Hg concentrations to the original mass leached. Results for the low pH and reducing conditions (Table 2.3) and for the high pH and oxidizing conditions (Table 2.4) studies are treated separately.

Under low to neutral pH conditions, very little Hg is released as shown by the ppm (m/m) results in Table 2.3 and the graphical data in Figure 2.3. The highest amount of Hg released to solution occurred in wk 1 for the pH 1 sample (1086 ppm, m/m), but this release decreases with the wk 4 sample and continues to decrease through wk 8 until the concentration was less than that for the corresponding blank solution. The B9-Hg compound stability is excellent for the pH range 3 to 7, the pH range most likely to be encountered under environmental conditions, with leaching remaining below 250 ppm (m/m) for all samples.

Conditions	1 week (ppm or m/m x 10 <sup>6</sup> )	4 weeks (ppm or m/m x 10 <sup>6</sup> )	8 weeks (ppm or m/m x 10 <sup>6</sup> )
pH 1	1086	93	BDL
pH 3	114	215	126
pH 5	208	85	231
pH 7	112	220	144
Reducing	769	2767	988

**Table 2.3:** Results for Low pH and Reductive Leaching Study of B9-Hg

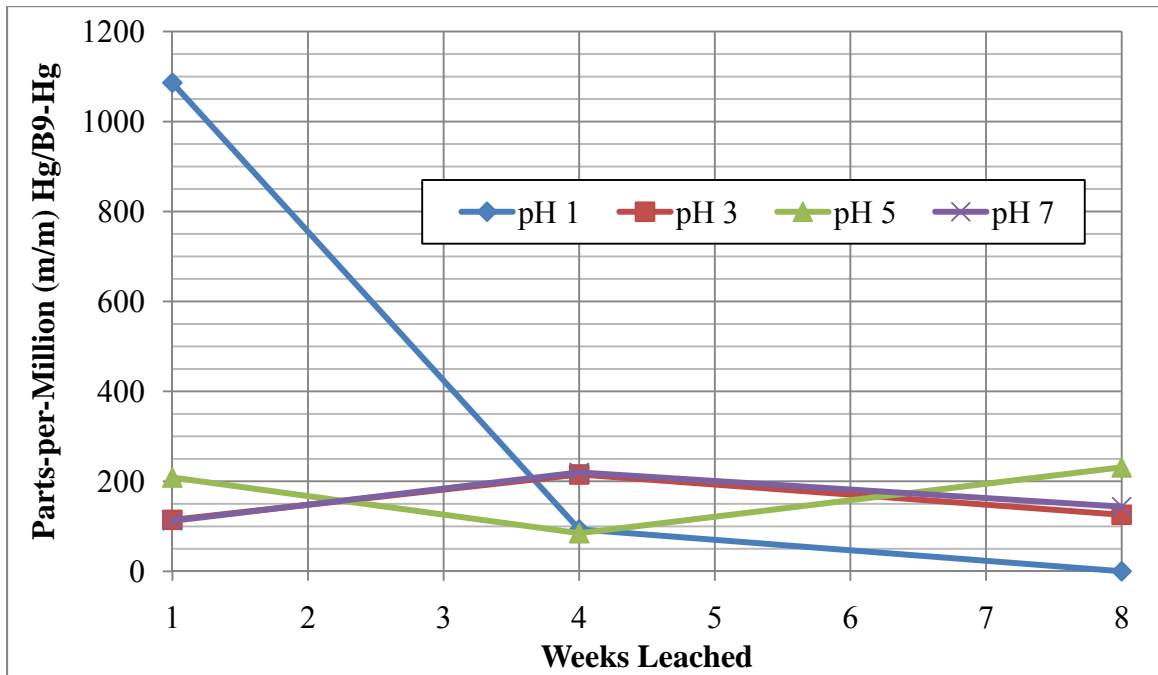


**Figure 2.3:** Low pH B9-Hg Leaching Results

Results for the pH-neutral reducing conditions are listed in Table 2.3 but not graphed in Figure 2.3 because the Hg released was significantly higher overall and did not demonstrate any clear trends due to a probable outlier at the 4 wk sampling. The 1 wk reducing sample released 769 ppm (m/m) Hg which increased to 988 ppm (m/m) Hg by the 8 wk sample. The 4 wk sample with 2767 ppm (m/m) Hg is nearly three times the



concentration of the 8 wk sample making sample contamination likely. In any event, this increased fraction of Hg released from the B9-Hg compound(s) leached warrants further investigation should spent column materials be subjected to potential reducing conditions during storage.

Analysis of the high pH samples proved to be more challenging as the high salt content from the NaOH additions during pH adjustments caused physical interferences during the ICP analysis that subsequently required large corrections using the yttrium internal standard. Results for the pH 9 and pH 13 studies showed low (0.1 – 3.1 ppth, m/m) mercury concentrations that generally increased with time and pH, but the pH 11 study had significantly higher levels with 9.33 ppth Hg at wk 1, 12.61 ppth at wk 4, and 2.66 ppth Hg by wk 8. If the Hg released to solution is expected to generally increase with increasing pH, the entire pH 11 study could be considered anomalous rather than attributing the high leaching to any remarkable leaching mechanism at this isolated pH value. For this reason, the pH 9, 11, and 13 studies were repeated. Sample names from the first study are appended with an “A” and samples from the repeat study are appended with the letter “B.” The numerical results for the high pH leaching study are detailed in Table 2.4 and graphed in Figure 2.4.

Conditions	1 week (ppth or m/m x 10 <sup>3</sup> )	4 weeks (ppth or m/m x 10 <sup>3</sup> )	8 weeks (ppth or m/m x 10 <sup>3</sup> )
pH 9A	0.31	0.14	2.89
pH 9B	4.09	18.19	0.88
pH 11A	9.33	12.61	2.66
pH 11B	4.10	1.49	1.27
pH 13A	0.16	1.10	3.13
pH 13B	7.99	7.44	5.02
Oxidizing	248	257	244

**Table 2.4:** Results for High pH and Oxidative Leaching Study of B9-Hg

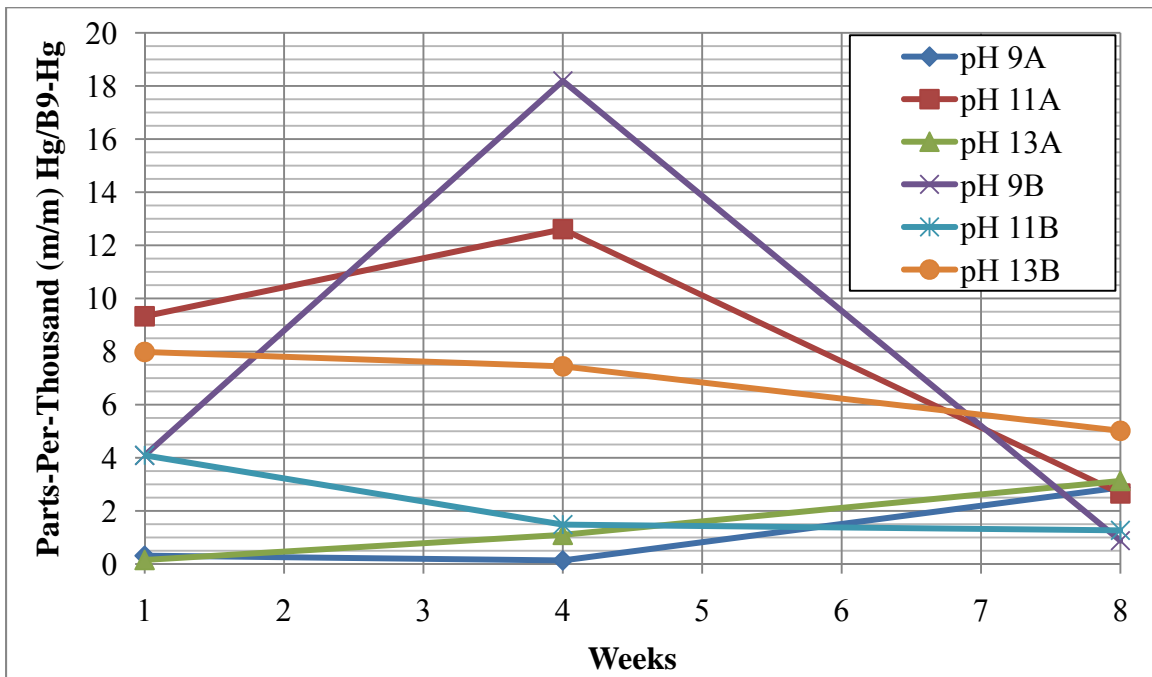


**Figure 2.4:** All High pH B9-Hg Leaching Results

In order to ease the comparison between the first and second trials for each high pH study, Figure 2.4 is broken into three separate graphs of the same scale with Figure

2.5 corresponding to the pH 9 work, Figure 2.6 giving the details for pH 11, and Figure 2.7 representing the pH 13 data. In these individual graphs, the original study is drawn with blue lines and data points while the repeat study is denoted by red lines and data points. Unfortunately, no reproducibility was apparent between the first and second trials at any of the higher pH values tested. This is especially true for the pH 9B study which displays the same anomalous peak at wk 4 (Figure 2.5, red line) that the original pH 11A study displayed (Figure 2.6, blue line). The pH 9B study displays much more Hg in solution that decreases from wk 1 to wk 8 while the original pH 9A study is lower in concentration and displays a gentle increase in Hg(II)(aq) from wk 1 to wk 8.

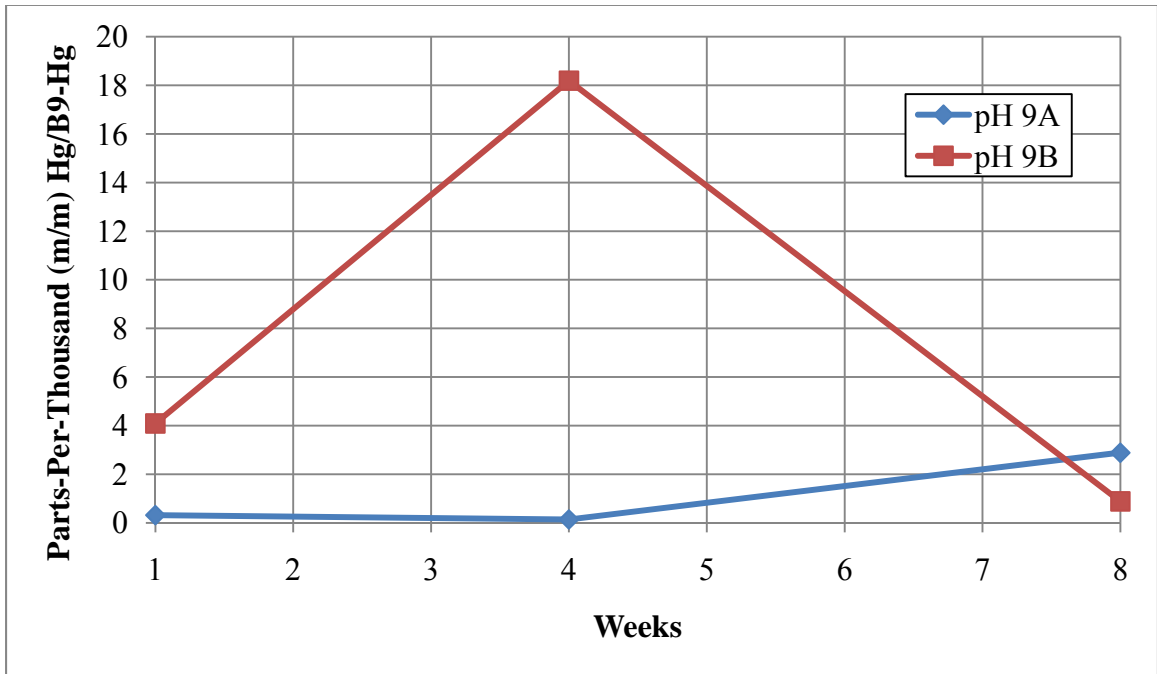


**Figure 2.5:** B9-Hg Leaching Results at pH 9

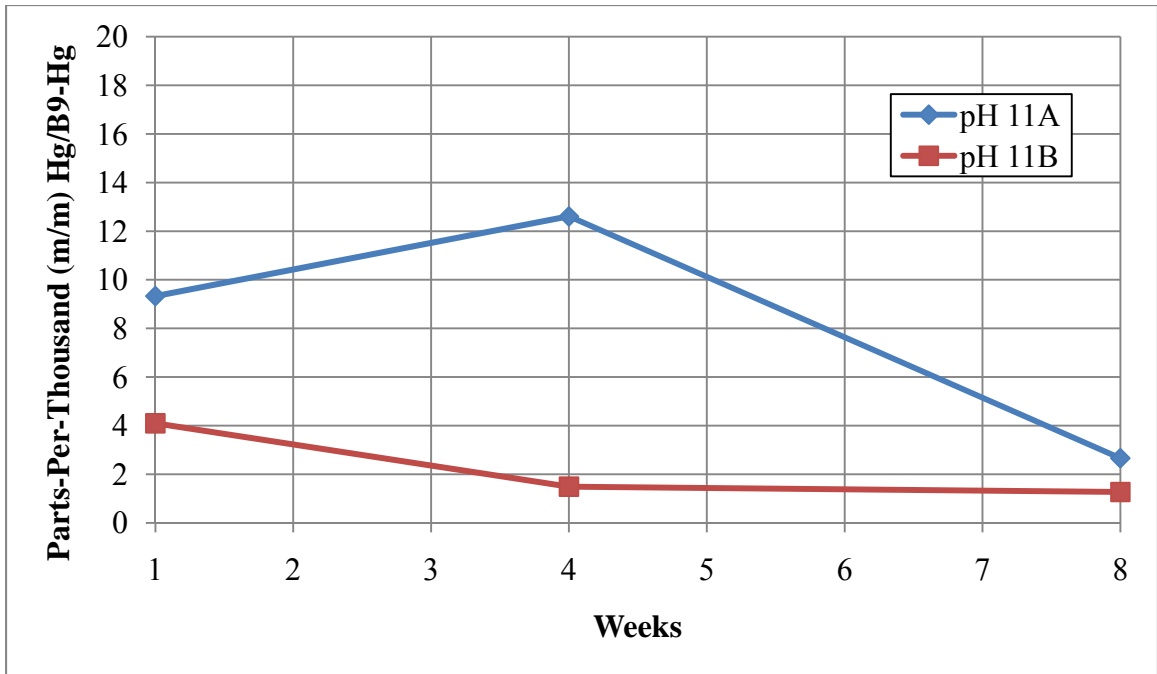


**Figure 2.6:** B9-Hg Leaching Results at pH 11

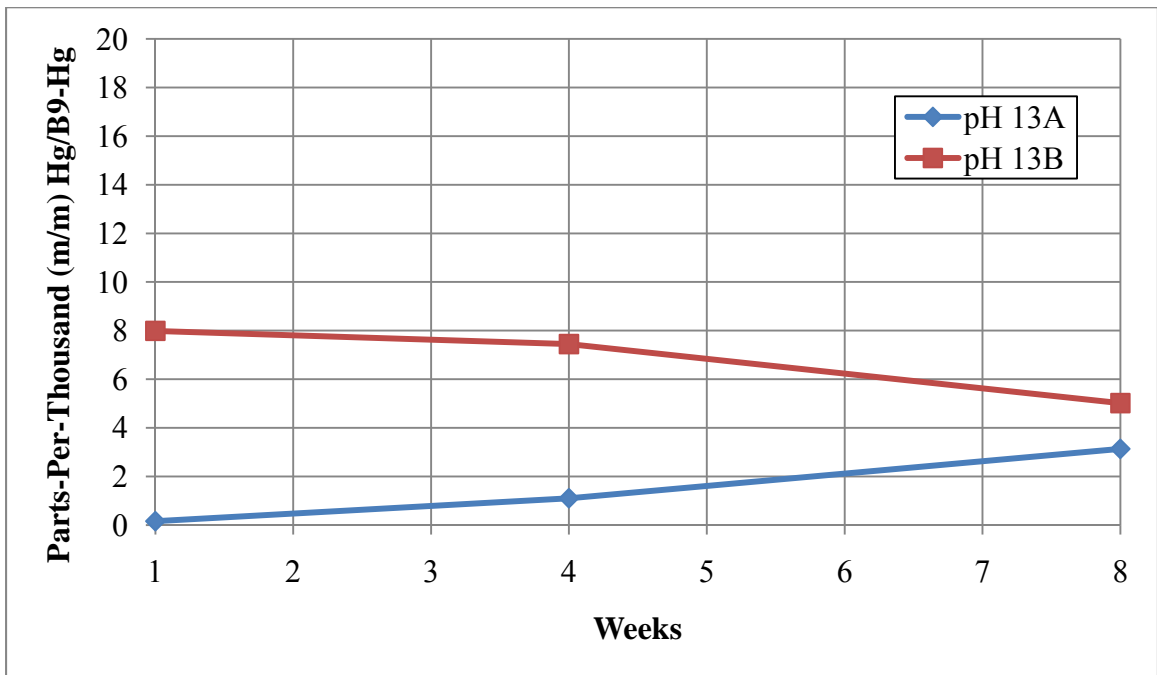


**Figure 2.7:** B9-Hg Leaching Results at pH 13

The original data set for pH 9 and pH 13 did not seem suspect, but was repeated nonetheless on the off chance that the NaOH used in pH adjustments could be a source of mercury contamination. As mentioned in Chapter 1, the chlor-alkali process used in countries outside of the U.S. to manufacture NaOH still utilizes mercury cell technology, allowing the potential for Hg contamination of the final product. The NaOH used for our experiments was typical ACS grade reagent as the availability of a trace-metal grade hydroxide product seemed highly unlikely. However, blank subtractions were used to correct for this possible contamination, ruling this option out internal to each individual study as the same pH adjusted solution was used for all samples at a particular pH. Mercury-contaminated NaOH would still manifest as the same curve shape from one study to another but with one important difference. If one study was compromised with mercury, the curve would be offset to either higher or lower concentrations relative to the other study in question. This phenomenon was not observed for any of the higher pH studies unless the wk 4 outlier is removed from the original pH 11A study. In that case, both pH 11 studies show generally decreasing mercury trends with the original study offset from the baseline by 2.66 ppth and the pH 11B study offset by 1.27 ppth as noted by the lowest concentration (8 wk) samples. The difference of these lowest values could point to a mercury contamination of 1.39 ppth (m/m) relative to the mass of the B9-Hg compound leached.

While this logic may prove satisfactory to explain the pH 11 results, at least in part, the general trend of decreasing mercury concentrations exhibited by the pH 13B study are in direct opposition to the earlier pH 13A results. The pH 13 B results are shifted significantly upward by 5.02 ppth (m/m) as noted by the lowest sample concentration. Subtraction of this upward shift gives 2.97, 2.42, and 0 ppth (m/m) for the 1 wk, 4 wk, and 8 wk pH 13B samples while following the same procedure for the pH 13A study (subtraction of the lowest sample value from all samples) gives 0, 0.94, and 2.97 ppth (m/m) for the 1 wk, 4 wk, and 8 wk samples respectively. In any event, a mercury release to the solution of 2.97 ppth is guaranteed at pH 13 but the question remains as to what sort of time frame this release occurs. Nevertheless, a pH of 11 or greater represents an extremely basic environment that the B9-Hg compound is not likely

to see under natural circumstances should the spent column material be disposed of in a landfill.

It would be ideal to run a third and fourth set of higher pH B9-Hg leaching studies with slightly modified conditions. The elimination of the NaOH and replacement with the appropriate buffer for the pH of interest would be the first major improvement. Switching to a non-chelating buffer system would eliminate the question of possible Hg-contaminated hydroxide skewing the results. Furthermore, the addition of dilute HCl to balance excess hydroxide during the pH adjustment process lends free chloride to the system that could stabilize any Hg(II) released into solution as any number of Hg(II) chloride complexes and leading to an increased solubility for B9-Hg. However, like the issue of Hg-contaminated hydroxide, this should result in a similar curve shape with a pronounced shift to either higher or lower concentrations. This was not observed and the data for the pH 9 and pH 13 studies are in fact directly conflicting, eliminating this as a possibility.

The possibility exists that a high pH B9-Hg leaching study may not be possible using current practices. Given the large amount of mercury work dealing with both Hg(0) and Hg(II) in the lab where the leaching study was prepared, the possibility exists that Hg(0) or Hg-p deposition to the individual leaching study samples may be contributing to the random nature of final sample concentrations. Conversely, the reduction of Hg(II) in solution to Hg(0) followed by volatilization could also explain the random nature of aberrant data points. Reduction is unlikely given the oxic conditions, but cannot be completely ruled out unless careful monitoring of the leaching sample headspace was performed.

A final point to consider involves the effect that B9-Hg structure may play in the release of Hg(II) under basic conditions. The structure proposed in Figure 2.1 is just one of many possible products as Hg(II) capture does not necessarily occur in a 1:1 ratio. Indeed, Hg(II) could serve as a bridge between an infinite number of linked B9 molecules and the variable polymeric nature could contribute to the observed random leaching since each 20 mg sample is not any one pure B9-Hg compound. The fact that this randomness is not manifested in the low pH leaching samples points to differences in the B9-Hg release mechanism between acidic and basic conditions.

Under acidic conditions, proton attack is most likely on the amide and thiolate portions of the B9-Hg compound, resulting in R-Hg(II) release with R denoting an associated organic fragment from the parent compound. Basic conditions favor hydroxide attack on atoms displaying a partial positive charge including the carbonyl carbon and mercury as the bonding between mercury and the more electronegative sulfurs is likely to withdraw electron density from the metal center. Hydroxide attack on the carbonyl carbon is likely to produce Hg in solution associated with organic residues, but the case for hydroxide attack on the metal center may lead to the formation of unique products. For instance, under mildly basic conditions, hydroxide attack on a 1:1 B9-Hg molecule could lead to a B9-Hg-OH product with the bond between mercury and one thiolate center broken. The free sulfide resulting from this broken bond could then bond with the other B9 thiolate, causing the release of free Hg(OH)<sub>2</sub> and production of the cyclized B9 disulfide. In the case of a more polymeric material where mercury is bound to at least two B9 molecules, the sulfide attack on the remaining thiolate bound to Hg may be limited due to steric constraints, leaving the mercury bound to the B9 molecule as B9-Hg-OH without Hg(OH)<sub>2</sub> release to the solution occurring. The variable nature of the B9-Hg product may lead to a lesser or greater amount of the polymeric B9-Hg material from one sample to the next which only becomes apparent in light of the basic degradation mechanism leading to two different product categories (one with free Hg, the other without) unlike the case for acidic degradation where only one product category is likely to manifest. This theory is supported by the significantly greater concentrations of free Hg(II) found in solution in basic solutions. The discrepancies between repeated trials and the lack of recurring trends can be attributed to the variable nature of the B9-Hg compounds used in the leaching studies.

Finally, the results for the oxidative leaching study can be found at the bottom of Table 2.4. Similar to the reducing study, these results were not depicted graphically as the amount of mercury leached into solution did not demonstrate any time-dependent trends and was almost certainly completed in a very short period of time during the initial hours of the leaching study. The amount of mercury leached from the B9-Hg compound under oxidizing conditions was the highest of all of the conditions studied with a range from 244 – 257 ppb (m/m). The large Hg release was most likely due to oxidation of the sulfur

groups to  $\text{SO}_3^{-2}$ . This is a common and not unexpected occurrence for thiols in the presence of strong oxidants such as  $\text{NaOCl}$  and  $\text{H}_2\text{O}_2$ . Post-oxidation, the  $\text{SO}_3^{-2}$  group becomes harder, causing a bonding mismatch with the softer mercury atom and resulting in the release of  $\text{Hg(II)}$  to solution.

While knowledge of the stability of the B9-Hg compound is important for storage considerations, conditions that demonstrate high mercury leaching without oxidation of the ligand may offer a means of B9 regeneration should this prove to be of interest.

## CONCLUSIONS

The effective column remediation of  $\text{Hg(II)}$  using solid B9 dispersed in a quartz sand solid support was demonstrated under varying flow conditions. The most important outcome of this work was the discovery that the reaction between aqueous  $\text{Hg(II)}$  and solid B9 occurs fast enough to effect remediation of high mercury concentrations to below levels deemed acceptable for drinking water. B9 has the potential to be superior to other mercury remediation technologies currently in use because of the permanent, irreversible, and preferential binding of mercury to the ligand under a moderate range of pH values in the presence of competing ligands such as chloride.

This was an excellent early test of the ligand's capabilities, but before this process is applied in a commercially-available remediation column, it would be ideal to have a solid-supported ligand. Tethering the ligand to a surface is desirable to prevent the release of B9 or the B9-Hg complex formed to the environment as is possible with using only a loosely packed solid compound. A surface studded with the ligand would also prove beneficial by maximizing the surface area of the thiol binding sites and allowing for higher-flow scenarios than is achievable with a simpler column with B9 solid dispersed in quartz sand. Work is currently underway to functionalize the cysteine "arms" of B9 with groups that would enable the attachment of the ligand to a silica or polystyrene surface.



## CHAPTER 3: REMEDIATION OF As(III) USING A SIMPLE B9 FILTRATION COLUMN

### INTRODUCTION

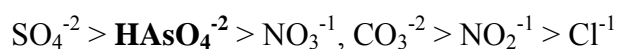
**Competing Groundwater Arsenic Remediation Technology.** Despite exposure to anthropogenic arsenic from the application of herbicides, insecticides, desiccants, feed additives, wood treatments, and warfare agents to the environment, the largest threat to human health from arsenic stems from the ingestion of water with a high inorganic arsenic burden of geogenic origins, accounting for 99% of the total human intake of arsenic.<sup>83, 93, 175</sup> This knowledge, coupled with the fact that the Environmental Protection Agency, the National Research Council and the World Health Organization have set the maximum contaminant level for arsenic at 10 ppb ( $0.01 \text{ mg}\cdot\text{L}^{-1}$ ) provides for an interesting challenge in the area of arsenic remediation from drinking water.<sup>83, 88, 93, 175, 216</sup> To date, the challenge has been addressed by a variety of methods involving arsenic sorption or chemical precipitation and filtration, all of which rely heavily on the pre-oxidation of arsenite to arsenate for their success.<sup>216, 217</sup> This critical arsenic treatment step is accomplished through the addition of the strong oxidants chlorine, permanganate, and ozone (pH range 6.3 – 8.3) but not through the use of common, weaker water treatment oxidants such as chlorine dioxide, monochloramine, or UV light.<sup>216, 290</sup> Emerging arsenic remediation technologies include bioremediation (through biosorption and biomethylation), phytoremediation, and electrocoagulation, to name a few, and will not be discussed due to their lack of widespread use.<sup>94, 217</sup>

Several chemicals can be added directly to water to cause the precipitation or coprecipitation of oxidized arsenic and its removal through flocculation/coagulation and filtration. Lime softening is used to reduce hardness by precipitating calcium and magnesium. The process can be manipulated to remove arsenate by adding lime until the pH exceeds 10.5 at which time magnesium hydroxide precipitates and As(V) coprecipitates.<sup>129, 216, 290</sup> Aluminum and ferric salts are also typically used in water treatment processes to aid in coagulation, flocculation and eventual clarification and filtration of the water.<sup>217, 290</sup> The aluminum and iron salts hydrolyze in water to form hydroxides that will sorb arsenate.<sup>129, 217</sup> Ferric sulfate and ferric chloride generally perform better than

aluminum due to the poor stability of aluminum hydroxides in the pH range of 5.5 to 8.5.<sup>216</sup> However, arsenate sorption to iron hydroxides can be compromised by high levels of natural organic matter, phosphates, and silicates which compete for sorption sites.<sup>216</sup>

A number of materials, including ion exchange resins, activated alumina, silicate clays, and iron-based sorbents will adsorb arsenic.<sup>129, 217</sup> For example, strong-base anion exchange resins are effective at removing arsenate in the pH range of 6.5 to 9.0 but can be strongly compromised by pH effects and the presence of competing anions.<sup>216, 217</sup>

Arsenite is unaffected in this range as it remains in the uncharged  $\text{H}_3\text{AsO}_3$  form with  $\text{H}_2\text{AsO}_3^{-1}$  becoming a prevalent near pH 9 while arsenate is present as  $\text{H}_2\text{AsO}_4^{-1}$  or  $\text{HAsO}_4^{-2}$  and even as significant amounts of  $\text{AsO}_4^{-3}$  near pH 9. Due to this reliance on charge to effect remediation, anions such as  $\text{SO}_4^{-2}$  and  $\text{NO}_3^{-1}$  compete strongly with  $\text{HAsO}_4^{-2}$  for sites on the exchange resin in the following order:<sup>216, 290</sup>



This preferential sorption can lead to chromatographic peaking, a case in which arsenate and nitrate concentrations in the effluent exceed concentrations in the influent as sulfate replaces these ions on the resin. The performance of ion exchange resins is further hindered by high total dissolved solids (TDS) and fouling of the resin surface clogging available sorption sites.<sup>216</sup>

Activated alumina is another ion exchange media that has been shown to remove arsenic with the following selectivity:  $\text{OH}^{-1} > \mathbf{H}_2\text{AsO}_4^{-1} > \text{Si}(\text{OH})_3\text{O}^{-1} > \text{F}^{-1} > \text{HSeO}_3^{-1} > \text{TOC} > \text{SO}_4^{-2} > \text{H}_3\text{AsO}_3$ .<sup>216, 217</sup> Alumina filtration is optimal for the pH range 5.5 – 6.0, a range which offers poor selectivity for uncharged arsenite, but allows the alumina to last 5 – 20 times longer than using alumina under natural pH conditions (pH 6 – 9).<sup>216</sup> To increase their effectiveness, several sulfur- and iron-modified activated aluminas are currently under investigation.<sup>216</sup> This presents itself as a sensible solution in light of the fact that the main sink for arsenate in the environment is iron hydroxides while the main sink for arsenite is iron sulfides.<sup>96, 129, 217</sup>

A wide array of iron based sorbents have demonstrated stronger arsenic affinities than activated alumina under natural pH conditions although optimal operating conditions are at low pH as well.<sup>216</sup> As noted previously, phosphate will compete aggressively with arsenate for iron sorption sites due to the similar charge and shape. For every 0.5 ppm

increase in phosphate above 0.2 ppm, the adsorption capacity for arsenate is reduced by 30%.<sup>216</sup> Iron based sorbents include amorphous iron hydroxide, granular ferric hydroxide, ferric oxide, zerovalent iron (ZVI), and iron filings mixed with sand and iron oxide coated sand.<sup>216, 217, 290</sup>

Nanofiltration and reverse osmosis (RO) are membrane filtration techniques that remove dissolved solutes from water based on particle size, dielectric characteristics, and hydrophilicity/hydrophobicity.<sup>216, 290</sup> As such, organic carbon, calcium, magnesium, silica, sulfate, chloride, carbonate, arsenic, and color can be removed without noticeable pH effects.<sup>216</sup> The processes are pressure-driven, water recover is generally 60 – 80% for RO, and the ions removed can cause scaling of the membrane with reduced rejection of arsenic.<sup>216, 290</sup> For this reason, oxidation of arsenic and pre-filtration through sand or activated carbon is recommended. Furthermore, the removal of alkalinity could result in decreased corrosion control in water distribution systems.

This brief review of current remediation practices exposes two major flaws in the current methods for dealing with arsenic-contaminated drinking water. First and foremost, no satisfactory technique exists to deal with As(III) directly. All methods reviewed rely upon the pre-oxidation of arsenite to arsenate species that will typically sorb to different materials due to the negative charge carried under natural pH conditions. The second major flaw is that all of the processes rely on sorption of arsenic to different surface groups rather than on covalent bond formation. Much like the problems with anion exchange resins, all of the sorbents reviewed will be subject to competitive sorption that could lead to the preferential desorption of arsenic should a higher concentration of a competing sorbate be present. For these reasons, a method of removing As(III) from water through covalent bond formation is highly desirable.

**Goals of the Current Work.** Unlike the previous chapter dealing with aqueous mercury remediation, much more work lies ahead to demonstrate that B9 is an effective remediation agent for arsenic. Past work with the B9 ligand has focused on dissolving the compound and applying it to a batch remediation scenario. This work will omit the ligand dissolution step and instead apply the powdered ligand directly to solutions of arsenic. Should this prove successful, using the solid ligand in a column remediation scenario will be explored.

Unlike mercury which exists as Hg(0) and Hg(II) associated with hydroxyl and chloride groups in water, arsenic displays a much more interesting array of species under normal environmental conditions. Common oxidation states of arsenic include -3 (arsine), 0 (arsenic metal), +3 (arsenite), and +5 (arsenate). Arsenate, the more common form of arsenic under oxic conditions, is a triprotic oxyanion with pK<sub>a</sub> values of 2.2, 6.97, and 11.53. Under reducing conditions, arsenic adopts the trivalent oxidation state with arsenite pK<sub>a</sub> values of 9.22, 12.13, and 13.40 for the triprotic oxyanion.<sup>87, 165</sup> A pH range of 3 - 9 will be tested as this range is expected to fully evaluate the pH values of typical groundwater this column is designed to treat. Selection of this pH range means that arsenite will exist primarily as the uncharged H<sub>3</sub>AsO<sub>3</sub> species while arsenate will be present as a mixture of H<sub>2</sub>AsO<sub>4</sub><sup>-1</sup> and HAsO<sub>4</sub><sup>-2</sup> ions.<sup>87, 94, 172</sup> The charge exhibited by arsenate has traditionally made it more susceptible to remediation through adsorptive techniques; the partial positive surface charge adopted by clays and metal hydroxides at low to neutral pH values attracts arsenate, forming complexes readily. The lack of charge on arsenite has had the opposite effect, making it the more mobile and difficult to capture species. However, arsenite arsenic is a softer Lewis acid with its +3 charge compared to the +5 charge on arsenate arsenic. This should allow for the preferential metathesis reaction that will essentially swap the hydroxyl groups on the arsenous acid for the B9 thiol groups on the arsenic center. While metal sulfides are extremely insoluble, it will be interesting to observe if the metalloid sulfides produced from this reaction are insoluble enough to effect long-term remediation of arsenic from water.<sup>73</sup>

Oxidation of the arsenic during testing is a concern that will be addressed by conducting arsenite tests open to air as well as under nitrogen. Arsenite oxidation does not occur quickly without microbial assistance, but working under nitrogen will insure that oxidation does not occur during the time scale of the experiments and lead to possibly misinterpretation of the results. Tests of the column packing materials will also be conducted in batch tests (quartz sand) and simple one-component remediation columns (zerovalent iron) to insure that the silicon hydroxide groups on the quartz sand and the zerovalent iron do not oxidize (sand) or reduce (iron) the arsenic species in the time scales expected to complete our experiments. The bulk of the arsenic should be captured as the B9-arsenite complex since arsenite is the predominant species in freshly

pumped groundwater (which itself is usually anoxic). Much research has been conducted in the area of using iron for an arsenate remediation tool and since B9 is not predicted to affect arsenate, iron was included in column testing to address this minor shortcoming.

The effects of competing ions in solution on column performance were deemed worthy of further exploration since analogs exist in nature that mimic arsenite (nitrate) and arsenate (phosphate) due to similar geometries, charges, and in the case of arsenate and phosphate, similar  $pK_a$  values. Rather than explore the effects of these ions individually in the lab, the opportunity to construct and test a prototype treatment column for deployment in West Bengal presented itself at a very opportune time during the course of the research. Groundwater is the ultimate remediation target for this technology, making it the obvious next step in column testing. Success in this phase of the project would satisfy the goal of constructing a lightweight, affordable, and reliable arsenic remediation column should it prove successful.

An attempt to characterize any B9-arsenic products formed during the course of experimentation will be conducted. Knowledge gained from this characterization coupled with two-month leaching studies under a range of pH values, oxidative, and reducing conditions will shed light on the stability of the B9-arsenic compound(s) formed. Should the arsenic covalent thiolate bonding prove reversible, this could allow for the regeneration of spent remediation columns. Regardless, this information will be used to compare the similarities and differences in the bonding of arsenic and mercury to a model thiol compound despite having very different elemental properties.

## **EXPERIMENTAL**

**Batch Testing of Column Packing Materials.** B9 was synthesized as previously described and used as prepared. Four 2-L beakers were filled with deionized water through which nitrogen was bubbled and adjusted to pH 3, 5, 7 and 9 using dilute  $HNO_3$  (EM Science) or dilute NaOH (Mallinckrodt) as appropriate. From these pH adjusted solutions, 1-L portions of 150 ppb As(III) were made using sodium metaarsenite ( $NaAsO_2$ , Aldrich) and subsequently treated with 0.5 g of solid B9 each. One set of solutions was placed back under nitrogen and covered to suppress oxidation to As(V) while the other set was allowed to remain open to air. Although a white precipitate was

immediately evident, solutions were stirred 24 hours before samples were collected. Likewise, four 1-L solutions of As(V) were prepared using sodium hydrogenarsenate heptahydrate ( $\text{Na}_2\text{HAsO}_4 \cdot 7 \text{H}_2\text{O}$ , Aldrich) at pH 3, 5, 7, and 9, treated with 0.5-g B9, and allowed to stir open to air for 24 hours.

Two each of separate 150 ppb As(III) and As(V) 1-L solutions were treated with activated carbon (AC) pellets (3 g, Norit 0.8, Sigma-Aldrich) and left to stir either open to air or under nitrogen for 24 hrs. Similarly, 24 hr batch tests of white quartz sand (15 g, -50 +70 mesh, Sigma-Aldrich) with 150 ppb As(III) solutions open to air and under nitrogen and a single 150 ppb As(V) solution open to the air were conducted.

**Column Testing Using Standard Arsenic Solutions.** Simple two-component columns were designed to separately address the issues of As(III) and As(V) remediation in flow scenarios. The first column consisted of B9 (3 g) mixed with sand (20 g) supported in a glass column (0.7 I.D. x 50 cm, Kontes). The column was tested by applying 250 ppb As(III) under ambient flow and pressurized flow conditions and collecting the effluent. The quartz sand was not found to sorb arsenic to an appreciable extent.

A second set of columns was tested using 100 ppm As(V) allowed to flow freely through varying depths of zerovalent iron filings, ZVI (~40 mesh, Fisher) supported by Whatman filter paper and a small plug of glass wool in plastic syringes with the plungers removed (BD, 20 mL, Fisher). Syringes were filled with ZVI roughly to the 5cc, 10cc, and 20 cc graduations and topped with another layer of filter paper to the specifications outlined in Table 3.1. A single, 0 cc control column without any ZVI was included. The effluents were analyzed by ICP for As.

Column	ZVI Depth (cm)	ZVI Volume (mL)	As(V) (ppm)
0 cc	0.0	0.0	101.6 ± 1.5
5 cc	1.7	4.4	14.7 ± 0.3
10 cc	3.2	8.4	< 5.00
20 cc	6.9	18.0	< 5.00

**Table 3.1:** Column Dimensions and Treatment Results for the ZVI Only As(V) Study Columns

**Field Column Construction.** Two 20-mL Luer Lock syringes (Fisher) with the plungers removed and attached end-to-end post-packing served as the body of the field study column. B9 (25 cc, used as synthesized) was mixed with white quartz sand (15cc, -50+70 mesh, Sigma-Aldrich, used as received) and was used throughout the column packing process. The field study column was constructed, from top to bottom, using Whatman filter paper cut to size, sand, a B9/sand mixture, sand, ZVI, sand, filter paper, ZVI, sand, pre-mixed B9/sand, sand, AC, sand and a final filter paper layer (exact dimensions are outlined in Table 3.2). The flanges of the two syringes were hot-glued together to give a final column measuring approximately 20 cm in length with an I.D. of 1.895 cm. To increase the stability of this union, holes were drilled in each of the syringes' flanges through which plastic security ties were threaded and closed. The entire perimeter of the flanges was then sealed with more hot glue and allowed to cool. To complete the column, two short lengths of beverage-grade tubing were attached, top and bottom, such that the top tube could be affixed to a water collection device and the bottom tube could be directed into a small sample vessel. This arrangement also allowed for collection of a water sample in another syringe which could be attached to the tubing and used to force the sample through the column should this prove to be the easier sampling method in the field.

<b>Material</b>	<b>Layer Depth (cm)</b>	<b>Layer Volume (mL)</b>
Filter Paper	0.00	0.00
Sand	1.40	3.95
B9/Sand Mixture	4.03	11.35
Sand	0.88	2.47
ZVI	1.40	3.95
Sand	1.56	4.41
Filter Paper	0.00	0.00
ZVI	2.26	6.38
Sand	1.05	2.96
B9/Sand Mixture	3.50	9.87
Sand	0.35	0.99
Activated Carbon	1.75	4.94
Sand	0.35	0.99
Filter Paper	0.00	0.00

**Table 3.2:** Dimensions for the B9 ZVI Field Study Column

**Sampling Area and Procedures.** Thirty-nine groundwater samples were collected from 2” to 4” diameter wells attached with hand operated pumps in severely arsenic affected villages of the Indian state of West Bengal as denoted in Figure 3.1. These wells are frequently pumped throughout the day and supply drinking water to multiple villages within the study area. The groundwater samples were collected according to standard drinking water sampling practices. An in-line flow cell was connected to the well head such that the pumped water had minimal contact with the atmosphere. Wells were purged to eliminate standing water in the pipes and obtain representative aquifer water. After pumping was initiated,  $E_H$ , pH and temperature of the



water passing through the flow cell were noted at regular intervals until they had stabilized, typically 15-30 min., and these end values were recorded. The B9-ZVI column was then connected to the sampling outlet and was flushed 2-3 times prior to sampling to flush residues from previous sampling sites. Both unfiltered and filtered samples were collected in 15-mL white HDPE tubes (Environmental Express) and immediately acidified with ~ 0.2 mL 6N HNO<sub>3</sub> to approximately pH 2.

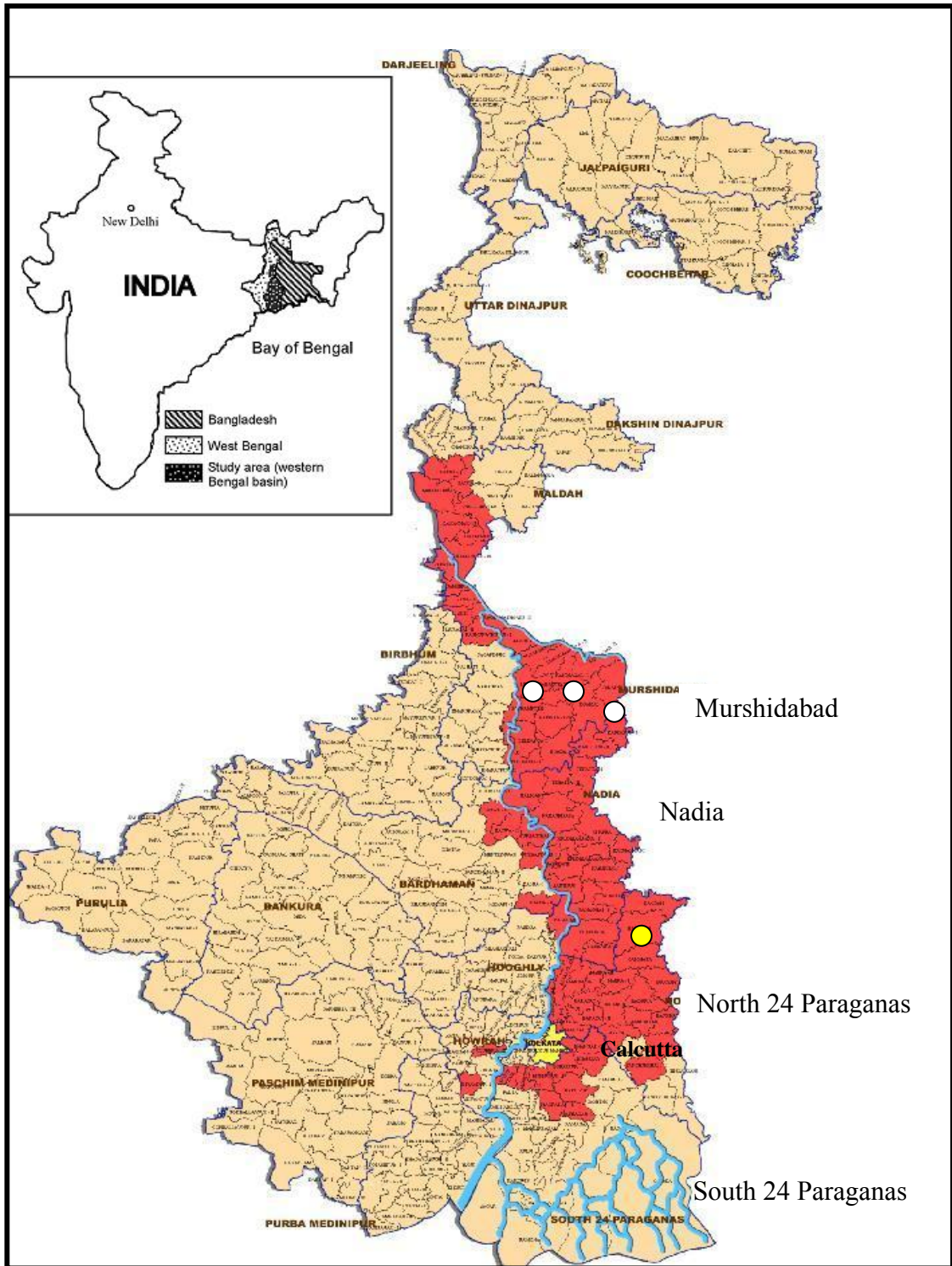


**Figure 3.1:** Map of West Bengal showing the arsenic-affected areas (red) and sampling areas (2007-2008) for the arsenic remediation project (white circles).

**Characterization and Stability of B9-As(III).** B9-As(III) was synthesized on a larger scale by adding B9 (2.13 g, 7.5 mmol) dissolved in 95% ethanol (25 mL) to a solution of NaAsO<sub>2</sub> (1.0 g, 7.5 mmol) at ambient pH and stirring for 24 hours under nitrogen. The white precipitate was filtered under vacuum and washed with deionized water (50 mL x 3), washed with 95% ethanol (50 mL x 3) and allowed to dry open to air. Yield was 50.4%. Product was characterized by MP, IR, and MS. Melting point: 270 °C. IR (KBr, cm<sup>-1</sup>): 3413s (-NH), 3004m [-CH (aromatic)], 2908m [-CH (methylene)], 1715ss (-CO), 1630 (-NH), 702 (C-S)]. EI-MS: [As-(SC<sub>2</sub>H<sub>4</sub>NHCO)<sub>2</sub>C<sub>6</sub>H<sub>4</sub> (356), As-(SC<sub>2</sub>H<sub>4</sub>NHCO)<sub>2</sub> (281), As-(SC<sub>2</sub>H<sub>4</sub>NH)<sub>2</sub> (227), C<sub>6</sub>H<sub>4</sub>(CO)<sub>2</sub>NHC<sub>2</sub>H<sub>4</sub> (174), C<sub>6</sub>H<sub>4</sub> (75)]. Anal. Calcd. for C<sub>12</sub>H<sub>15</sub>AsN<sub>2</sub>O<sub>3</sub>S<sub>2</sub>: C, 38.51; H, 4.04; N, 7.48; O, 12.82; S, 17.13. Found: C, 40.75; H, 4.68; N, 7.83; O, 24.83; S, 20.00.

Six sets of nine glass snap-cap digestion tubes (Environmental Express) were prepared for the study. One tube from each set was allocated for leaching with 20.0 mL deionized water pH-adjusted to pH 1, 3, 5, 7, 9, 11, and 13 using dilute HCl (VWR) or KOH (EMD). The eighth tube was used for a reductive leaching study using granular Zn(0) (~100 mg, 20-30 mesh, Sigma Aldrich) in pH 7 deionized water (20.0 mL) and the ninth tube constituted the oxidative leaching study using NaOCl (20.0 mL, Fisher) as a source of 13% active chlorine. For each leaching period, a set of tubes with 10 mg B9-As(III) added and a control set without compound was prepared. Samples were tightly capped and stirred continuously with using disposable PTFE stir bars (Fisher) during the 1 wk, 4 wk, and 8 wk leaching periods.

At the end of the prescribed leaching periods, the final pH was noted, samples were syringe filtered using 0.20 µm PTFE syringe filters (Environmental Express), the original leaching tube and syringe filter were rinsed twice with DI water and the rinse was added to the original sample for a final volume of approximately 25 mL. NaOCl samples were treated with 10 drops of a 10% (m/v) solution of sodium thiosulfate (EM Science) prior to filtration. All samples were acidified with 3 mL of concentrated nitric acid and digested at 100° C for two hours. Samples were allowed to cool and diluted to a final volume of 50 mL.

**Analytical Procedures.** Melting points were recorded using a Mel-Temp melting point apparatus from Laboratory Devices. Infrared spectra were obtained using KBr disks

on a Thermo Nicolet Avatar 360 FTIR spectrometer. Elemental analyses were performed on a LECO CHN-2000 analyzer at the University of Kentucky Center for Applied Energy Research. Mass spectra were obtained at the University of Kentucky Mass Spectrometry Facility using direct probe insertion (DIP) with EI<sup>+</sup> ionization.

Portions of the untreated As solutions were analyzed for every batch and column study conducted. Treated As samples were syringe filtered to 0.45- $\mu\text{m}$  (Environmental Express). All samples were brought to 10% HNO<sub>3</sub> acidity unless otherwise noted and digested at 100°C for two hours prior to ICP or GFAAS analysis.

A Varian Vista Pro CCD Simultaneous Inductively Coupled Plasma Optical Emission Spectrometer (ICP-OES) was used to analyze for Fe at 254.940 nm and As at 234.984 nm at 1.20 kW power, 4.0 second replicate read times and default values for all other parameters for the field study column and B9-As(III) leaching study samples. The ZVI column As effluent was analyzed at 228.812 nm, 1.00 kW power, and 1.00 second replicate read times. A 1.0 ppm yttrium internal standard was used (371.029 nm) to evaluate and/or correct for matrix effects during all analyses. Quality control included duplicate and spiked samples every tenth sample followed by a laboratory control sample (LCS) to match the concentration of the corresponding spiked sample.

Arsenic was analyzed at 193.7 nm using a Varian SpectrAA 880Z Zeeman graphite furnace atomic absorption spectrometer (GFAAS). Samples were combined with a 1% Pd modifier, ashed for 8.0 s at 1400 °C and atomized at 2600 °C for 2.6 s during analysis. Every tenth sample, duplicate samples were added and every twentieth sample, a spike and LCS was included for quality control. To evaluate data spread, all samples and standards were fired four times. Whenever possible, the samples were also diluted to minimize noise in the background signal. Unless otherwise noted, reported results are the means and standard deviations of instrumental measurements.

## **RESULTS AND DISCUSSION**

**Batch Testing of Column Packing Materials.** B9 treatment of an As(III) solution at pH 5 or 7 under either air or nitrogen effected a drop in the As(III) to < 5.00 ppb, essentially a 100% removal (see Table 3.3). At pH 9, B9 was able to remove 96.7% and ~100% of the As(III) under nitrogen and open to air, respectively. The pH 9

treatment under nitrogen left approximately 5.4 ppb of arsenic, which represents a measurement only 0.4 ppb above the detection limit of the instrument. Uncertainties in the arsenic measurement in this range make it difficult to justify calling the 0.4 ppb of arsenic above the detection limit anything other than essentially 100% remediation as well. Both pH 9 results are still below the 10 ppb maximum contaminant level for arsenic and for this reason the remediation under pH 5 – 9 conditions are all judged successful. The products characterized suggest a mixture of B9-As-OH and B<sub>9</sub>As<sub>2</sub> as depicted in Figure 3.2 with detailed characterization data in the Appendix. Thioarsenic structures similar to the ones proposed here with increasing replacement of As-O bonds for As-S bonds have been previously documented.<sup>291</sup>

As	Material Tested	pH	Under Nitrogen			Open to Air		
			Initial	Treated	Removal	Initial	Treated	Removal
III	B9	3	126.4 ± 1.8	97.5 ± 3.2	22.9%	135.8 ± 1.9	88.9 ± 0.8	34.5%
III	B9	5	121.4 ± 2.3	< 5.0	~100%	148.0 ± 1.3	< 5.0	~100%
III	B9	7	121.4 ± 3.0	< 5.0	~100%	130.0 ± 0.4	< 5.0	~100%
III	B9	9	161.0 ± 2.1	5.4 ± 0.1	96.7%	160.6 ± 5.3	< 5.0	~100%
III	AC	N/A	152.0 ± 6.5	43.4 ± 0.5	71.4%	151.6 ± 3.8	28.7 ± 0.6	81.1%
V	AC	N/A	152.0 ± 5.6	15.2 ± 0.4	90.0%	134.0 ± 1.7	22.9 ± 0.8	82.9%

**Table 3.3:** Results for B9 and AC Batch Tests. As in Parts-Per-Billion (ppb or  $\mu\text{g L}^{-1}$ ).

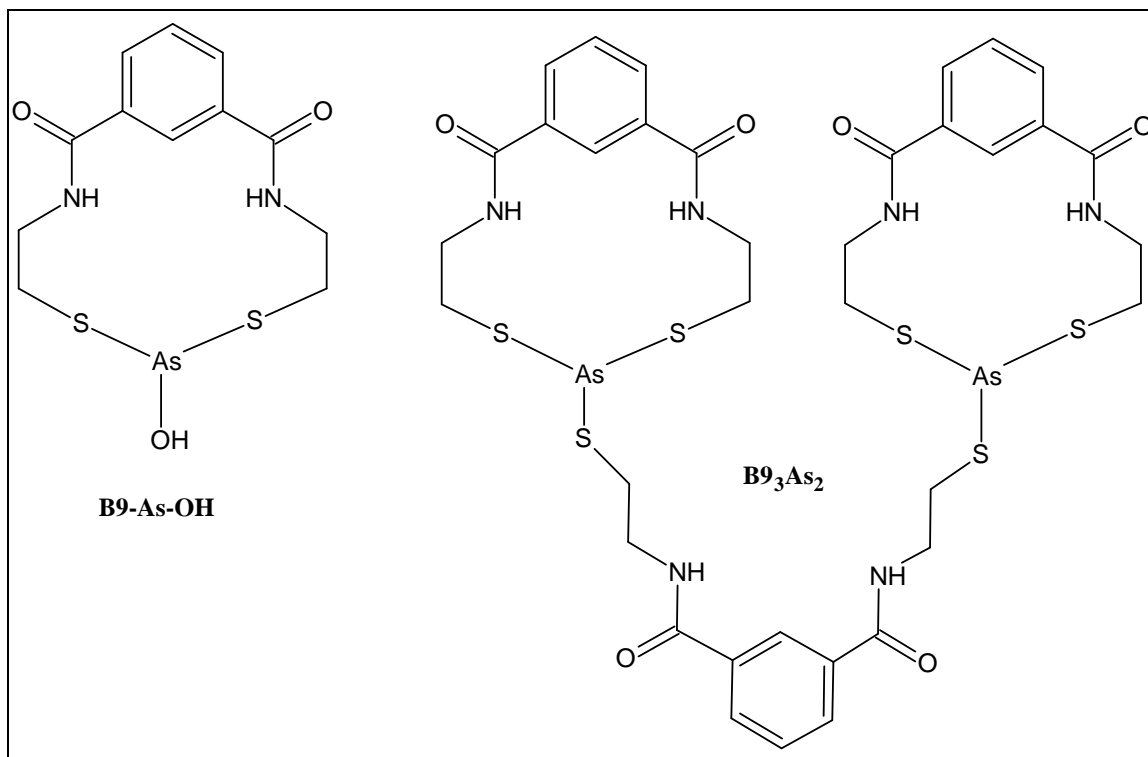


**Figure 3.2:** Proposed Structures of the B9-As(III) Insoluble Products

The batch treatment of As(III) at pH 3 failed to demonstrate efficient covalent bond formation to B9. The removal of As(III) at pH 3 was minimal: only a 22.9% decrease under nitrogen and a 34.5% decrease in total arsenic concentrations for samples open to air was observed. To explain this observation, a series of equations were derived using the arsenite  $pK_a$  values and a total arsenic concentration,  $C_T$ , of 150 ppb (or  $2.00 \times 10^{-6}$  M) to approximate the experiment as shown below:

$$[H_3AsO_3] = \frac{C_T}{1 + \frac{ka_1}{[H^+]} + \frac{ka_1ka_2}{[H^+]^2} + \frac{ka_1ka_2ka_3}{[H^+]^3}}$$

$$[H_2AsO_3^-] = \frac{C_T}{\frac{[H^+]}{ka_1} + 1 + \frac{ka_2}{[H^+]} + \frac{ka_2ka_3}{[H^+]^2}}$$

$$[HAsO_3^{2-}] = \frac{C_T}{\frac{[H^+]^2}{ka_1ka_2} + \frac{[H^+]}{ka_2} + 1 + \frac{ka_3}{[H^+]}}$$

$$[AsO_3^{3-}] = \frac{C_T}{\frac{[H^+]^3}{ka_1ka_2ka_3} + \frac{[H^+]^2}{ka_2ka_3} + \frac{[H^+]}{ka_3} + 1}$$

A plot of the log of the molar concentrations of the major arsenite species for a given pH was constructed using these equations as shown in Figure 3.3. Hydronium and hydroxide ion concentrations were included for clarity. Dark vertical bars are imposed over the arsenite speciation plot to indicate the pH values evaluated in the batch testing of solid B9 with arsenite.

Examination of the plot reveals that the uncharged species  $H_3AsO_3$  is essentially the only arsenite species present from pH 0 to pH 5 when  $H_2AsO_3^{-1}$  makes the first appearance at a very dilute  $10^{-10}M$  concentration. The concentration of  $H_2AsO_3^{-1}$  increases until equal amounts of  $H_2AsO_3^{-1}$  and  $H_3AsO_3$  are present at pH 9.22. Arsenite remediation was shown to be effective for the range pH 5 – 9 where  $H_3AsO_3$  constitutes the majority of the arsenite species present. The question that begs an answer at this point is this: what is different enough about a pH 3 solution to prevent covalent bond formation between arsenous acid and B9?



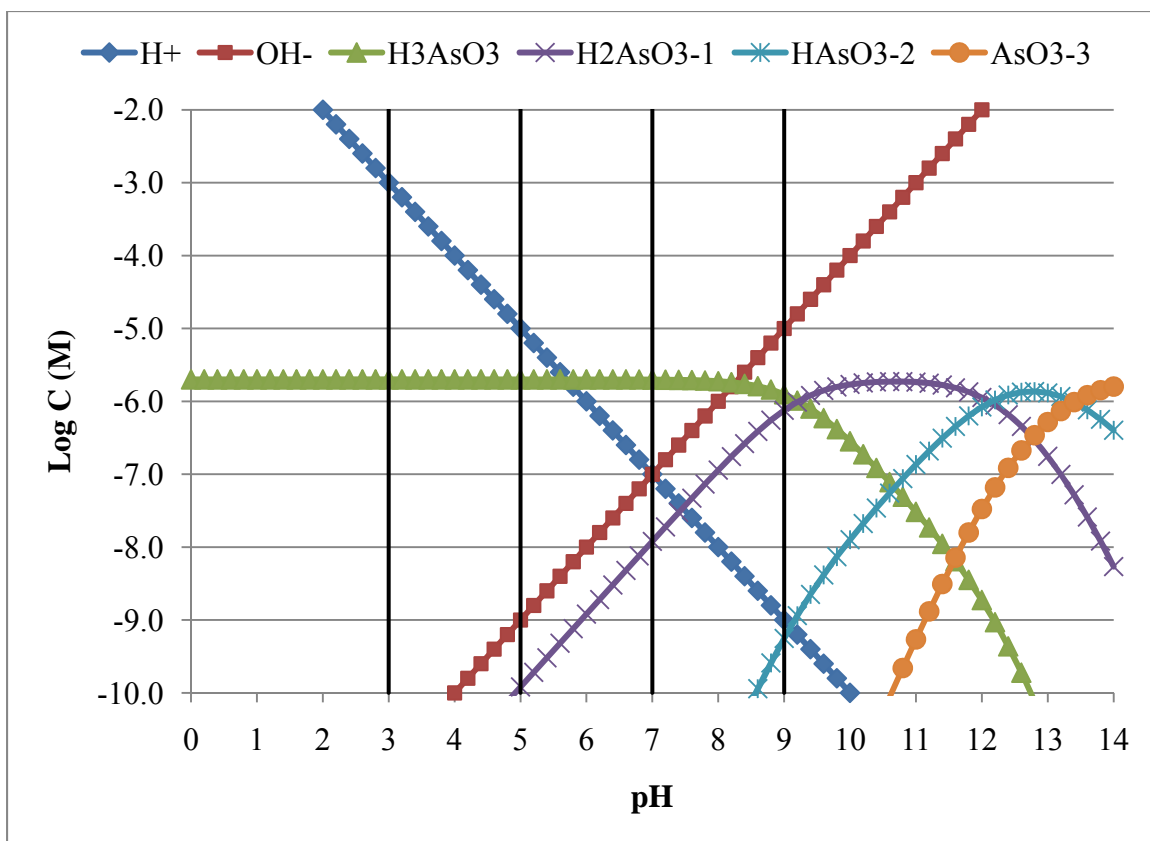


**Figure 3.3:** Speciation of Arsenite under pH 0 – 14 Conditions

Previous work with acid mine drainage was performed at low pH and remediation of a multitude of divalent metals was found to be effective. However, the species in question here is not a divalent metal salt but rather a covalent compound. Another key difference between the acid mine drainage work and the current body of work is that B9 was pre-dissolved, most often as  $\text{Na}_2\text{BDET}$  or  $\text{K}_2\text{BDET}$ , before contacting the aqueous metal solution, thus facilitating a quick reaction as both thiol protons had already been removed. In the current situation, the thiol groups (themselves soft Lewis bases) of B9 could become protonated in the low pH water, causing at least one of the lone pairs of electrons on the sulfur to be unavailable for attach of the As(III) center to drive the B9-As(III) reaction to completion. Unfortunately, the  $\text{pK}_a$  values for the thiol protons on B9 have never been measured or this hypothesis could be modeled to gauge the accuracy of this explanation. Alternatively, protonation of the arsenic center itself could be preventing the reaction in acidic pH solutions.

B9 batch treatment of As(V) did not decrease the arsenate concentrations to any significant degree so this data has been omitted from Table 3.3. This outcome is not surprising since arsenate has never been shown to react with sulfhydryl groups.<sup>129</sup> This is most likely due to the arsenate center acting as a harder Lewis acid which will not form bonds with thiol groups due to their soft Lewis base character. Similar to the exercise for the arsenite results, equations were derived using the arsenate  $pK_a$  values and a plot of the log of the molar concentrations of the major arsenate species for a given pH was constructed as shown in Figure 3.4. Total arsenate was again set to 150 ppb and the dark vertical bars are indicative of the pH values at which batch tested was performed.

The last set of batch tests examined the effects of adding quartz sand and activated carbon to the arsenic concentrations of arsenite and arsenate solutions. The quartz sand did not sorb arsenic to a measurable extent but the activated carbon was able to reduce arsenic concentrations significantly as shown in Table 3.3. As(III) removal rates were 71% and 81% under nitrogen and open to air while 90% and 83% rates were observed for arsenate. Final arsenic concentrations were still 15 – 23 ppb for arsenate and 29 – 43 ppb for arsenite, still well above the 10 ppb acceptable limit for As in drinking water. While the sorption of arsenic by AC is a positive outcome, it would be unwise to rely on AC sorption alone to treat drinking water since removal depends solely on physisorption of arsenic to the carbon surface rather than removal by covalent bond formation.

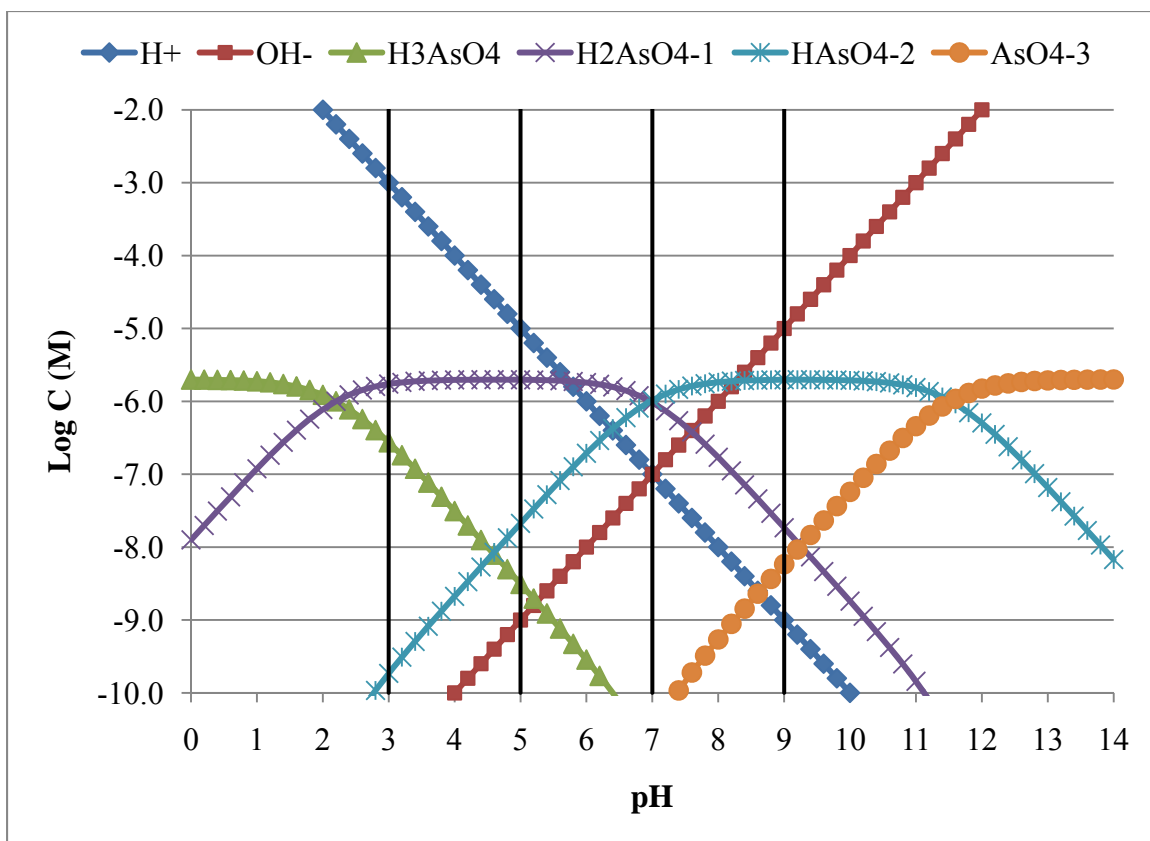


**Figure 3.4:** Speciation of Arsenate under pH 0 – 14 Conditions

**Column Testing Using Standard Arsenic Solutions.** Separate columns were constructed to evaluate the magnitude of arsenite remediation with B9 and arsenate adsorption using zerovalent iron. The first column was a simple mixture of B9 dispersed in quartz sand. A stock solution of  $250.74 \pm 12.04$  ppb As (III) was applied with an average flow rate of  $0.50 \pm 0.06$  mL $\cdot$ min $^{-1}$ , resulting in As(III) concentrations all below the 5.00 ppb detection limit for three samples. Increasing the flow rate to  $1.71 \pm 0.19$  mL $\cdot$ min $^{-1}$  by applying air pressure to the column’s headspace caused the As(III) concentration in the effluent to rise to  $6.56 \pm 0.37$  for three samples which is still below the 10 ppb permissible limit for drinking water.

A series of ZVI columns was constructed to evaluate the depth of iron filings needed to cause a significant drop in the arsenic concentration of a  $101.6 \pm 1.5$  ppm arsenate solution. A “5 cc” ZVI column reduced the arsenate level to  $14.7 \pm 0.3$  ppm while the “10 cc” and “20 cc” columns reduced the arsenic concentration to below 5 ppm,

the As detection limit for the ICP. Arsenic concentrations in the part-per-million range were chosen as an extreme example with the hopes that the changes would be correspondingly large and observable. It is unlikely that 100 ppm As would be observed in drinking water sources but the possibility exists that such high As concentrations may be present in industrial wastes and acid mine drainage. Information gathered from this experiment was used to add an adequate amount of ZVI to the field column to address the unlikely event that arsenate would be present in the wells surveyed. Keep in mind that while the results were favorable for As(V) adsorption, As(III) forms much weaker bonds with iron (oxy)hydroxides than does As(V), making it more soluble and more mobile.<sup>91, 94</sup>

**Field Study Column.** Of the 39 groundwater samples collected, eleven had total arsenic levels less than the 5.00 ppb detection limit of the GFAAS. The remaining 28 samples had arsenic ranging from  $8.82 \pm 0.19$  ppb to  $220.47 \pm 4.85$  ppb (mean  $55.35 \pm 1.61$  ppb, median  $36.44 \pm 1.22$  ppb). Post-filtration, none of the 28 samples contained detectable arsenic. Pre-treatment iron levels ranged from  $0.36 \pm 0.00$  ppm to  $8.65 \pm 0.24$  ppm (mean  $3.05 \pm 0.04$  ppm, median  $2.89 \pm 0.02$  ppm) while post-filtration iron was elevated in 27 of the 28 samples, ranging from  $2.23 \pm 0.00$  ppm to  $95.09 \pm 16.96$  ppm (mean  $19.47 \pm 0.74$  ppm, median  $18.01 \pm 0.10$  ppm). Full sample details can be found in Table 3.4.

The field study column was quite successful in the removal of arsenic. Samples were pushed through using a syringe, causing flow rates to be greater than expected for a gravity filtration, and yet arsenic was completely removed. Furthermore, other species in the groundwater were not found to affect the function of the B9 ligand in removing arsenic. Unfortunately, groundwater quality data was not available from the collaborative party at the time of this writing.

The only disappointment in the field column work is the high level of iron returned to the effluent water in the majority of the arsenic-bearing samples. While iron is an essential nutrient, it also tends to color the water an orange, “rusty” hue at high concentrations, leading to taste and odor issues. Furthermore, the possibility that iron could form small amounts of soluble arsenate complexes that could be carried out of the column was of some concern.<sup>216</sup> Activated carbon has been used to remove organics and metal ions from water and while the capacity of AC is 0.020 grams As(V) per gram of

AC, As(III) is not effectively removed by AC.<sup>216, 290</sup> However, since AC acts as a general sorbent, it was hoped that inclusion of a significant AC zone in the field column would ameliorate any high iron effluent levels but this was not found to be the case. Any soluble arsenic-iron complexes should have been captured by the AC.

Future iterations of treatment columns would do well to either omit the ZVI altogether and focus solely on As(III) removal or to use an alternative arsenate sorbent should arsenate and arsenite remediation need to be addressed by a single column.

Sample ID	Pre-Filtration		Post-Filtration	
	As (ppb)	Fe (ppm)	As (ppb)	Fe (ppm)
3	83.58 ± 1.84	2.93 ± 0.03	BDL < 5.00	29.19 ± 0.11
4	63.30 ± 2.72	2.30 ± 0.01	BDL < 5.00	16.34 ± 0.65
5	57.68 ± 3.40	2.10 ± 0.03	BDL < 5.00	21.63 ± 0.09
6	58.05 ± 2.67	2.46 ± 0.03	BDL < 5.00	16.00 ± 0.04
7	8.82 ± 0.19	0.36 ± 0.00	BDL < 5.00	4.25 ± 0.02
8	9.80 ± 0.47	6.08 ± 0.00	BDL < 5.00	18.48 ± 0.20
9	60.37 ± 3.14	4.18 ± 0.02	BDL < 5.00	23.34 ± 0.10
10	38.30 ± 0.54	3.56 ± 0.04	BDL < 5.00	20.73 ± 0.22
11	17.29 ± 0.38	3.01 ± 0.02	BDL < 5.00	16.50 ± 0.05
12	36.08 ± 1.77	3.17 ± 0.02	BDL < 5.00	24.86 ± 0.17
14	20.36 ± 0.49	8.65 ± 0.13	BDL < 5.00	95.09 ± 16.96
15	29.77 ± 1.28	4.31 ± 0.02	BDL < 5.00	31.19 ± 0.16
16	10.86 ± 0.40	3.08 ± 0.03	BDL < 5.00	31.66 ± 0.14
17	39.84 ± 1.95	4.94 ± 0.04	BDL < 5.00	29.05 ± 0.19
18	45.78 ± 1.14	2.95 ± 0.04	BDL < 5.00	24.77 ± 0.14
19	13.91 ± 0.29	1.92 ± 0.01	BDL < 5.00	13.91 ± 0.78
20	183.84 ± 3.86	6.60 ± 0.02	BDL < 5.00	20.29 ± 0.09
21	31.79 ± 0.67	3.42 ± 0.01	BDL < 5.00	18.87 ± 0.12
23	141.60 ± 4.25	1.63 ± 0.12	BDL < 5.00	18.68 ± 0.05
24	220.47 ± 4.85	1.37 ± 0.24	BDL < 5.00	15.68 ± 0.12
25	31.74 ± 0.60	5.75 ± 0.02	BDL < 5.00	15.28 ± 0.06
26	33.06 ± 1.09	0.99 ± 0.01	BDL < 5.00	17.54 ± 0.11
41	148.78 ± 1.79	1.57 ± 0.08	BDL < 5.00	6.46 ± 0.03
42	32.11 ± 1.41	2.84 ± 0.02	BDL < 5.00	2.37 ± 0.01
43	40.30 ± 0.73	0.86 ± 0.00	BDL < 5.00	3.07 ± 0.02
45	36.80 ± 0.63	2.15 ± 0.21	BDL < 5.00	4.65 ± 0.03
46	33.15 ± 1.16	1.63 ± 0.01	BDL < 5.00	3.08 ± 0.02
47	22.28 ± 1.31	0.71 ± 0.01	BDL < 5.00	2.23 ± 0.00
<b>High</b>	220.47 ± 4.85	8.65 ± 0.24	< 5.00	95.09 ± 16.96
<b>Mean</b>	55.35 ± 1.61	3.05 ± 0.04	< 5.00	19.47 ± 0.74
<b>Median</b>	36.44 ± 1.22	2.89 ± 0.02	< 5.00	18.01 ± 0.10
<b>Low</b>	8.82 ± 0.19	0.36 ± 0.00	< 5.00	2.23 ± 0.00

**Table 3.4:** Results of the Field Study Column Test for Samples with Detectable Pre-Treatment Arsenic

**Stability of B9-As(III) Products and Potential for Regeneration.** The leaching study demonstrated that leaching of As from the solid B9-As(III) products is relatively low (up to 0.77%) over the course of eight weeks over the range of pH 3-9 and under reducing conditions (high of 0.70%). The higher (~10%) leaching observed for pH 13, most likely due to the oxidation of As(III) to As(V) and its subsequent release from the B9-As complex, may offer a means of free B9 regeneration. Results are summarized in Table 3.5 and graphed in Figure 3.5.

Condition	mg As/g B9-As		
	1 week	4 weeks	8 weeks
pH 1	0.045 ± 0.002	16.172 ± 0.467	10.292 ± 0.113
pH 3	1.078 ± 0.031	2.708 ± 0.003	2.389 ± 0.081
pH 5	0.377 ± 0.007	1.857 ± 0.002	4.120 ± 0.082
pH 7	< 0.025	4.178 ± 0.004	6.753 ± 0.128
pH 9	0.157 ± 0.004	0.219 ± 0.002	7.700 ± 0.025
pH 11	50.558 ± 0.477	83.104 ± 1.428	91.159 ± 2.421
pH 13	82.093 ± 0.285	123.590 ± 4.114	105.819 ± 1.128
Reducing	2.257 ± 0.242	7.010 ± 0.001	0.256 ± 0.008
Oxidizing	74.155 ± 3.455	19.858 ± 0.005	13.546 ± 0.637

**Table 3.5:** Arsenic Leached from the B9-As Products over Time

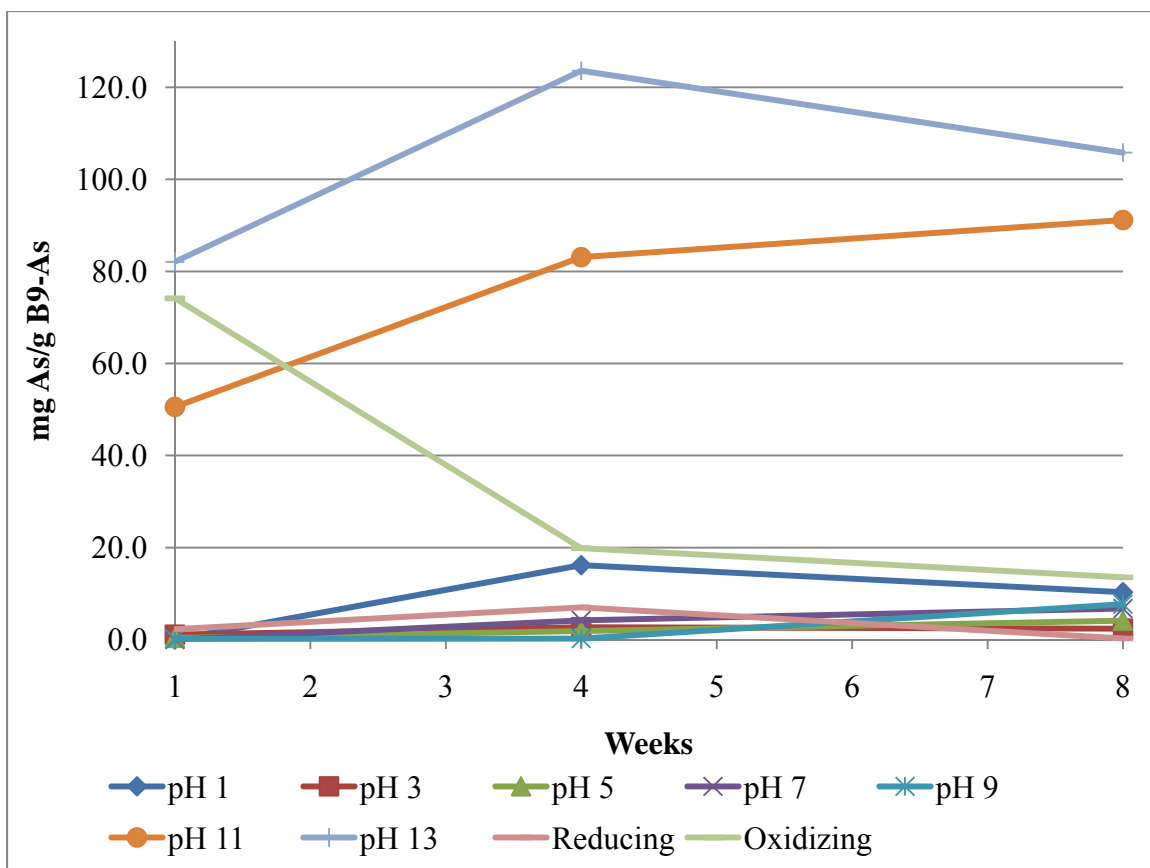


**Figure 3.5:** Arsenic Leached from the B9-As Products versus Time

## CONCLUSIONS

To evaluate the ability of B9 to bind arsenate and arsenite, a series of batch tests using solid B9 and  $150 \mu\text{g L}^{-1}$  arsenic solutions at pH 3, 5, 7, and 9 were conducted. It was determined that B9 binds arsenite at pH 5, 7, and 9, a range typical for drinking water, to levels below  $5 \mu\text{g L}^{-1}$  (part-per-billion) arsenic. As expected, the arsenate (As(V)) was not bound by B9. This is easily remedied as technologies exist, such as the use of zerovalent iron, that effect the preferential adsorption of the less toxic arsenate anion from water.<sup>292-295</sup> A system for the complete remediation of arsenic from water will be developed and optimized that will employ the use of solid-supported B9 for As(III) and an appropriate sorbent for As(V), providing a column that can address remediation of both oxidation states of arsenic at pH values relevant to water remediation.

The goals of the current work were well satisfied using B9 to remove arsenite from water in the pH range 5 – 9. The general utility of the ligand was improved by



applying the ligand as a solid for remediation rather than pre-dissolving it. This allowed for the successful batch and column remediation of 150 ppb arsenite solutions to < 5.00 ppb As post-treatment. Unlike previous work, this application of B9 to a main group element is the first time covalent bond formation was demonstrated between B9 and a species other than a divalent metal salt. This is especially interesting in light of the fact that arsenite is present as an oxyanion in water.

## CHAPTER 4: CONCLUSIONS

### GENERAL CONCLUSIONS

Three broadly-defined goals were proposed for the current work. First, a general extension of the B9 ligand's utility, both in how it is applied and to what species it was applied was necessary to expand knowledge of the compounds capabilities and to allow for a greater variation in application methods for problematic environmental species. Second, application of B9, a model dithiol compound with excellent chemical properties, to explore the similarities in mercury-thiol and arsenic-thiol bonding despite widely differing elemental properties was designed to satisfy basic scientific curiosity. Should B9 prove to be effective in the first two goals, the third goal of developing a more robust, permanent, and inexpensive remediation column superior to conventional technological approaches was ultimately the most desirable end product. Each of these three goals was satisfied to a certain extent.

Previous work using the B9 ligand under the trade names MetX, BDET, and BDETH<sub>2</sub> demonstrated successful batch remediation of the soft, divalent metals Pb(II), Cd(II), Cu(II), Mn(II), Zn(II), Fe(II) and Hg(II) from ground water, coal refuse, gold ore, lead battery recycling plant wastewater and contaminated soils.<sup>229-240</sup> However, divalent metals are not the only thiophilic species and the effective remediation of arsenic using this compound was judged a possibility. Beginning with batch tests with water adjusted to nominal environmental pH values, it was found that arsenite formed covalent bonds to the ligand while arsenate did not. This was completely expected considering that iron sulfides provide a sink for arsenite in natural systems while in contrast, arsenate is preferentially physisorbed to iron oxyhydroxides and has never been shown to bind to sulfhydryl groups. The covalent bond formation between arsenite and B9 was especially pleasing considering that at the pH range most commonly encountered in natural waters, arsenite is present as the uncharged species H<sub>3</sub>AsO<sub>3</sub>, making it more difficult to engage in chemical reactions compared to the ionic arsenate species H<sub>2</sub>AsO<sub>4</sub><sup>-1</sup> and HAsO<sub>4</sub><sup>-2</sup> which will participate in sorption reactions at the very least. This was also a major milestone in drinking water treatment considering that As(III) is also the more toxic form of arsenic and its elimination from waters was the most desirable goal to achieve.

Earlier studies using B9 applied the compound to aqueous solutions either as the sodium or potassium metallated salt through reaction with NaOH or KOH or by dissolving the compound in ethanol prior to treatment. This was effective in situations warranting batch remediation followed by filtration, primarily for industrial effluents and environmental waters with a high burden of dissolved metals. However, for the ligand to find usefulness as a drinking water treatment tool, suspending B9 in a column proved to be a more sensible solution if covalent bond formation between the solid ligand and the species of interest could be effected quickly enough in a flow scenario. Given the crude construction of the columns in this work, the flows examined and the amount of mercury and arsenic removed, the column remediation method using B9 was certainly successful enough for a “proof of concept” test.

Future iterations of the column will need to address the combined issues of improved flow rates and attaching the B9 to a solid support. Work is currently in progress to functionalize the thiol “arms” of B9 to allow for covalent bonding to different surface functional groups such as polystyrene and silica. Covalently attaching the ligand to a surface will inherently increase the surface area of the thiol groups available for binding, making greater treatment possible with a minimal amount of ligand used. Higher flow rates should also be possible as the compression issues induced from adding pressure to the B9-sand and B9-AC mixtures could be avoided by using appropriately sized, ligand functionalized beads in future columns. Finally, it is highly appropriate to tether the ligand to a solid support to avoid potentially eluting the B9, B9-Hg or B9-As(III) products from the columns and creating another environmental problem. While the solid B9 columns presented in this work do not represent the final answer to a better remediation method quite yet, they are certainly a step in the right direction.

The demonstration of arsenate remediation using the B9 columns was not one of the goals clearly defined for this work but was worth exploring. Historically, many treatment methods for dealing with arsenate in drinking water have been demonstrated while arsenite removal was most often the Holy Grail that was sought but rarely found. B9 was extremely effective for arsenite removal from pH 5 to 9, making it the perfect solution for arsenic removal from anoxic groundwater. The fact remains that zerovalent

iron is not the most desirable solution to the arsenate problem in water sources as treatment is not effected through covalent bond formation.

Two options exist to address the issue of arsenate remediation using B9 column technology. The first, and most obvious choice, is to simply omit the zerovalent iron from the columns altogether. The B9 columns were designed to address arsenite removal, the major form of arsenic in groundwater. Arsenate is more likely to be present in oxic surface waters that will require a different and more rigorous treatment regimen as surface waters will also need processing to address sanitation issues. Given that over four million tube wells are affected by arsenic in the Indian subcontinent, the B9 columns seem to be an adequate solution for the problem at hand.

Omission of an appropriate method for dealing with arsenate removal necessarily limits the applicability of B9 columns to other remediation scenarios, most notably the processing of acid mine drainage in which arsenate may be present. Drinking water treatment is certainly the larger and more pressing issue, but modifications could be made to generalize the application of B9 treatment columns. Similar to the field column deployed in West Bengal, a column with an initial B9 zone followed by another material for the selective reduction of arsenate to arsenite and subsequent capture in another B9 zone downstream would solve this problem. Zerovalent zinc metal filings could effect this reduction, but would add Zn(II) to the metals needing to be captured by B9, which could easily be managed. Excess zinc in drinking water is not acceptable, however, so this set of treatment columns would be limited to mining and industrial applications.

Truly, the extension of the ligand's physical application methods as the solid ligand instead of dissolving it prior to use and by using B9 in columns rather than batch remediation scenarios represent two major steps forward in the area of environmental research into the remediation of problematic species. While these results are interesting from more of an engineering perspective, the third goal of this work, to study the preferential sulfur binding of mercury and arsenic to a model dithiol compound, satisfies a basic curiosity involving the chemistry of these two very different elements.

## COVALENT THIOLATE BONDING TO PROBLEMATIC SPECIES

A quick comparison of the elemental properties of mercury and arsenic would tend to leave one thinking that the two share nothing in common. Mercury is a d-block metal with electronic relativistic effects due to a filled 4f shell, making it act much differently than its lighter mass analogues zinc and cadmium. At room temperature, mercury is a liquid with an appreciable vapor pressure ( $1.9 \times 10^{-3}$  mm Hg or 0.25 Pa at 25°C), an exceptionally high electrical resistivity for a metal ( $95.8 \mu\text{ohm}^{-1}\cdot\text{cm}^{-1}$  at 20°C), and is relatively inert and unreactive to non-oxidizing acids.<sup>5</sup> Mercury is the only element besides the noble gases to exist almost entirely in the monatomic state as a vapor.<sup>5</sup> The d electrons of mercury are tightly bound to the nucleus; metallic bonding is considerably weakened and due to the outer s electrons only.<sup>5</sup> For this reason, the only oxidation states common to mercury are 0, +1, and +2 with the +1 oxidation state exhibited by the curious dimer  $\text{Hg}_2^{+2}$ .

In contrast, arsenic is a main group metalloid element that follows the expected periodic trends for a pnictogenic element. Like phosphorus, the arsenic oxides tend to hydrate readily, forming acidic species in water. Arsenic displays the oxidation states -3, 0, +3, and +5; As(0) metal is a solid at room temperature. All in all, the chemistry of arsenic is much less remarkable in comparison to mercury.

Although the elements seem quite dissimilar, mercury and arsenic are found primarily as sulfidic ores. In fact, the synonym “mercaptan” for the thiol functional group (RSH) plays off of the demonstrated affinity mercury has for sulfur, even when in competition with different species.<sup>2, 60, 221</sup> In particular, the toxic effects of Hg(II) and As(III) as  $\text{H}_3\text{AsO}_3$  on the body highlight their similar chemical interactions with thiol groups. The free sulfhydryl groups (-SH) found in proteins provide an especially attractive source of free sulfur in living organisms through incorporation of the amino acid cysteine [ $\text{H}_2\text{NCH}(\text{COOH})\text{CH}_2\text{SH}$ ].<sup>2</sup> The Gibbs free energy of formation between Hg(II) and cysteine is  $\Delta G(25^\circ\text{C}) = -55$  and  $-59 \text{ kcal}\cdot\text{mol}^{-1}$  depending on the pH of the system and explains the toxicity of mercury since the result is a compromise in enzymatic function.<sup>2, 60</sup> Mercury binding to the thiol-containing moieties of metallothionein, glutathione, and cysteine occur in the body.<sup>1, 3, 6, 7, 10, 16, 271</sup> Similarly, As(III) has been found to form covalent bonds to cysteine, glutathione, dithiothreitol, and 2-

mercaptoethanol.<sup>129, 296-298</sup> In light of this information, it only made sense to capitalize off of this preferential binding to thiol compounds in order to remove two very toxic species from water using the B9 dithiol ligand.

Previous work using B9 focused solely on the remediation of divalent metals for which Hg(II) seemed to fit well into this category whereas the covalently-bonded metalloid oxyanion  $\text{H}_3\text{AsO}_3$  did not. B9 had been shown to form covalent bonds with ionic species in solution, so how could it possibly engage a neutrally charged metalloid in a metathesis reaction? Wouldn't there be some barrier to this reaction occurring? It seemed highly likely that a reaction between B9 and arsenite would not be spontaneous, but the reaction was practically instantaneous as long as the pH was only slightly acidic, neutral, or mildly basic. With a little more research, Hg(II) was found to be even more similar to As(III) than to the divalent metals examined in past research since  $\text{HgCl}_2$  actually forms *molecular* rather than ionic crystals.<sup>299</sup> This is surprising considering the electronegativity differences between mercury and chloride, (1.9 for mercury vs. a 3.0 for chloride) which seems to dictate an ionic interaction.<sup>300</sup>

Regarding electronegativity considerations, arsenic is close to mercury with an electronegativity of 2.0.<sup>300</sup> Oxygen, a harder Lewis base, rates at a 3.5 while sulfur, a softer Lewis base, is closer to mercury and arsenic with an electronegativity of only 2.5.<sup>300</sup> Hg-S bonds for  $\text{Hg}(\text{SR})_2$  complexes range from 2.32 to 2.36 Å which is slightly longer than 2.25 Å for Hg-Cl.<sup>299, 301</sup> The As-S bond distances for thioarsenites are slightly shorter than Hg-S bonds at 2.15 to 2.31 Å while the As-O bonds in thioarsenites are much shorter at 1.77 to 1.82 Å.<sup>291, 299</sup> Mercury will establish two bonds to the thiol groups of one or more B9 molecules while maintaining the preferred linear geometry around the metal center.<sup>285, 288</sup> Conversely, arsenic can either form two bonds to a single B9 molecule, forming the B9-As-OH product, or all of the arsenite hydroxyl groups can be replaced by B9 thiol groups in forming either discrete or polymeric  $\text{B9}_3\text{As}_2$  products while maintaining a trigonal geometry around the metalloid center.

The pH of a solution to which solid B9 is to be applied may also be useful to highlight another potential difference between mercury and arsenic. Previous batch remediation of acid mine drainage was able to effectively chelate Hg(II) and other divalent species under low pH conditions. The effect of pH on the remediation of Hg(II)

from solution was not evaluated in this work for this reason. However, the acidic nature of As(III) necessitated the examination of pH effects in the current work. Unfortunately, efficient covalent bond formation between arsenic and B9 was not observed at low pH. This could be due either to protonation of the thiol groups of B9 or to protonation of the arsenic center at low pH blocking the reaction from proceeding. Unfortunately, the  $pK_a$  of B9 thiol groups has never been measured so without further investigation it is difficult to discern which explanation is the correct one. This phenomenon would not have been observed in the acid mine drainage work since B9 was applied as the dipotassium or disodium salt of the ligand.

The stability of the B9-Hg and B9-As products exemplifies the final difference between these surprisingly similar thiophilic species. The release of mercury and arsenic from the solid remediation products is clearly lower for acidic pH ranges and reducing conditions. However, the leaching of arsenic is much higher than that observed for mercury overall, thus reinforcing the appropriateness of the title “mercaptan” for the thiol functional group. This may be due in part to the oxidation of As(III) to As(V), resulting in the release of As from the B9-As complex. Although the high pH leaching study results were less straightforward to interpret for mercury than they were for arsenic, gentle treatment of the ligand with a basic solution may offer a means of regenerating the ligand should this be deemed a worthy goal.

## CHAPTER 5: DIRECTIONS FOR FUTURE RESEARCH

### INTRODUCTION

The body of this work served mainly to demonstrate the “proof of concept” concerning the efficacy of solid B9 to remediate problematic, thiophilic species using column filtration techniques. Success in this preliminary work has opened multiple avenues for application to a variety of related species in scenarios demonstrating great need of metal(loid) remediation to prevent harm to human health and the environment. The most extensive investigations to related species have already begun exploring the interaction of solid B9 with elemental mercury liquid and gas phase elemental mercury, especially as they pertain to capture in coal-fired power plants. Success has also been realized in the remediation of aqueous selenite, a species that mirrors the chemistry explored between arsenite, arsenate, and solid B9 (unpublished work by Preece, Blue, et al.). However, the main obstacle to overcome at this point involves optimization of ligand application methods with the development of support-bound ligands as the ultimate goal. What follows is a brief exploration of the research that should continue as an extension of this work as well as preliminary results from selected exploratory studies.

### APPLICATION TO RELATED SPECIES

**Methylmercury.** Given the success of B9 to irreversibly bind Hg(II), MeHg should also prove amenable to remediation via this route. The chemistry of the two species is quite similar since MeHg acts much like a substituted salt of Hg(II). In fact, MeHg shows affinity for the common ligands in water in the order:  $RS^- > SH^- > OH^- > Cl^-$ , but unlike Hg(II), MeHg is limited in its ability to bind to multiple ligands.<sup>2, 56, 76</sup> MeHg has a strong tendency toward linear coordination with sulfhydryl ligands given its soft Lewis acid character.<sup>2, 76</sup>

**Aqueous Selenium.** Batch tests revealed that 150 ppb arsenite As(III) in the pH range of pH 5-9 could be successfully remediated to below 5 ppb using B9 while 150 ppb arsenate As(V) remained unaffected regardless of pH. As these results proved quite interesting and other elements are also known to form such oxyanions, the application of B9 to selenite and selenate solutions was explored.



Selenium is a toxic yet essential element for proper human nutrition that is found in natural waters as selenite ( $\text{SeO}_3^{-2}$ ) and selenate ( $\text{SeO}_4^{-2}$ ).<sup>302</sup> Unlike arsenic, selenium exists in higher oxidation states with selenite in the +4 and selenate in the +6 oxidation state. Similar to arsenic, the lower oxidation state of selenium forms a trigonal planar structure while Se(VI) adopts a tetrahedral geometry mirroring that of As(V). Given these similarities between arsenic and selenium, selenite is expected to bind with B9 while selenate is predicted to be unreactive. Structures of the arsenic and selenium oxoanions are presented for comparison in Figure 5.1.

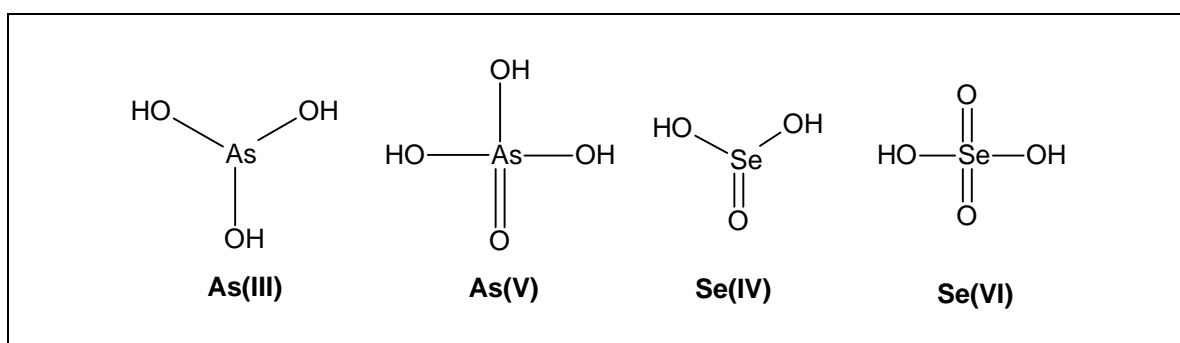


**Figure 5.1:** Comparison of Arsenic and Selenium Oxyanion Structures

Batch tests using solid B9 and solutions of Se(IV) and Se(VI) were examined to determine if this extension of ligand utility to another oxyanion in a higher oxidation state for the purpose of remediation could be achieved. Sodium selenite (1.105 g, 6.389 mmol, Alfa Aesar) and sodium selenate (1.195 g, 6.324 mmol, Alfa Aesar) were used to prepare 1000 ppm stock solutions. From these solutions, 500 mL of 20 ppm solutions were prepared at ambient pH (approximately 5.5) and allowed to stir continuously open to air. One gram of solid B9 was added to each solution; within one minute a light brown precipitate was observed in the B9-selenite mixture while the B9-selenate mixture remained unchanged. At time periods of 0.5, 1, 2, and 24 hrs, 50 mL samples were extracted and syringe filtered to 0.2  $\mu\text{m}$  (Environmental Express). The batch remediation samples were acidified with concentrated nitric acid and digested at 100°C for approximately two hours before being brought back to volume with 1%  $\text{HNO}_3$ . Samples were analyzed on a Varian Vista Pro ICP-OES at 196.026 nm, 1.2 kW power, and with 4

s replicate read times. Spike recoveries and laboratory control samples demonstrated 90.2 % and 93.1% recoveries, respectively. Results are listed in Table 5.1.

Time (hrs)	Selenite		Selenate	
	Concentration	% Remediation	Concentration	% Remediation
0.0	18.178	N/A	17.778	N/A
0.5	6.233 ± 0.052	65.7 %	17.796 ± 0.130	0 %
1.0	2.103 ± 0.022	88.4 %	17.834 ± 0.084	0 %
2.0	0.844 ± 0.012	95.4 %	17.380 ± 0.111	2.2 %
24	0.824 ± 0.004	95.5 %	18.356 ± 0.113	0 %

**Table 5.1:** Selenium Concentrations for the B9 Batch Remediation Experiment

B9 was found to precipitate selenite with up to 95% removal within the 2 hrs while selenate remained unreactive towards the ligand. A comparison of the predicted precipitation products between B9 with As(III) and B9 with Se(IV) is illustrated in Figure 5.2. As(III) has been found to bind in a 1:1 and a 3:2 ligand-to-arsenic ratio. Selenite is not expected to adopt anything but the 1:1 configuration due to the presence of the doubly-bonded oxygen group on the metal center.

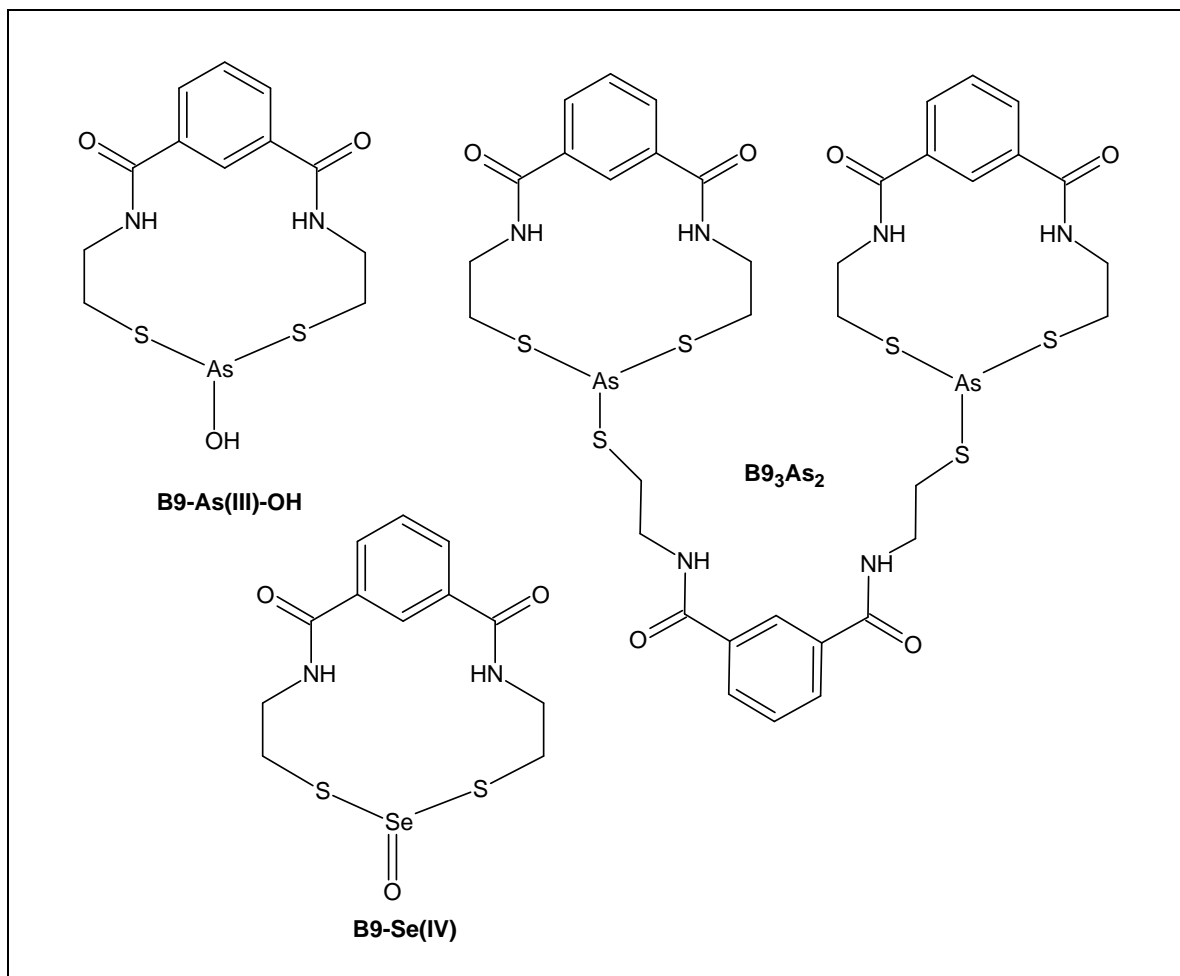


**Figure 5.2:** Comparison of Potential B9-As(III) and B9-Se(IV) Precipitates Formed

Work is in progress to characterize the B9-Se(IV) compound using melting point, IR, mass spectral analysis, crystal structure determination, and leaching studies to determine compound stability under pH extremes, oxidative and reducing conditions. In the future, the effects of pH on the formation of the B9-Se(IV) compound also needs to be explored in batch remediation scenarios.

**Elemental Mercury Liquid.** Elemental mercury remediation is a lofty and oft-pursued goal as it represents the main avenue for global mercury transport and widespread environmental contamination. Given the stability and general unreactive nature of the element, Hg(0) remediation remains elusive. The bulk behavior of elemental mercury liquid with solid B9 is of principal interest as this could provide insight into potential gas phase elemental mercury reactions. For this reason, the behavior of

elemental mercury with solid B9 was examined at both ambient and elevated temperatures.

$\text{Hg}^0_{(l)}$  (20.1418 g, 100.41 mmol, Strem) and B9 (16.4316 g, 57.78 mmol) were combined in a 1.74:1 molar ratio in a Teflon digestion tube (Environmental Express) with a PTFE stir bar (Fisher), sealed, and allowed to stir at room temperature for 1 wk with intermittent shaking by hand and a final 10 min vortexing to eliminate all visible elemental mercury sheen. Solid particles of B9 physically affected the  $\text{Hg}(0)_{(l)}$  at room temperature by forcing the Hg into smaller and smaller droplets and preventing their re-agglomeration upon contact with one another. The resulting powder was uniformly gray with a few isolated white clumps of solid B9. A melting point of 127°C was recorded, indicating that Hg capture was not due to covalent bonding. The product was rinsed with 95% EtOH (100 mL, Fisher) under vacuum filtration during which time visible beads of elemental mercury formed and began agglomerating as the B9 dissolved. Further rinsing caused copious amounts of  $\text{Hg}^0_{(l)}$  to be released from the gray powder and re-combine into a single, large pool of  $\text{Hg}_{(l)}$ .

The large excess of Hg (1.74:1 ratio) compared to the ligand may have facilitated the release of free Hg with the ethanol rinse if the ideal ligand-metal bonding occurs in a 1:1 ratio. To test this possibility,  $\text{Hg}^0_{(l)}$  and B9 were combined in a 2:1 ratio (3.3827 g, 16.86 mmol Hg; 9.6430 g, 33.91 mmol B9) and a 1:1 ratio (1.0491 g, 5.23 mmol Hg; 1.5471 g, 5.44 mmol B9) in separate Teflon centrifuge tubes (Thermo Fisher Scientific) and vortexed for approximately 5 minutes until  $\text{Hg}^0_{(l)}$  was no longer visible. Samples were centrifuged at 7,818 G (10,000 rpm, SS34 rotor, Sorvall RC-5B centrifuge) for 10 min, revealing a substantial pool of  $\text{Hg}^0_{(l)}$  in both samples and lending even more support to the idea that physisorption was responsible for the “disappearance” of  $\text{Hg}_{(l)}$  when mixed with  $\text{B9}_{(s)}$ . An adsorptive process with chemical bond formation is called “chemisorption” while the process that occurs through van der Waals contacts is called “physisorption.” Ideally, the means to push the physisorption event to one of chemisorption needs to be found to insure the successful remediation of mercury.

Physisorbed  $\text{Hg}_{(l)}$  should also be easily displaced by vacuum and/or heating, assuming the heat used is not enough to overcome the activation energy for forming covalent B9-Hg bonds. To examine this possibility, triplicate samples of 2:1 B9: $\text{Hg}^0_{(l)}$

samples were prepared in Teflon centrifuge tubes with vortexing until visible  $\text{Hg}_{(l)}^0$  was absent. Samples were deposited in a round bottom flask, subjected to vacuum ( $10^{-3}$  Torr), and heated to 50°C, 100°C or 200°C. The three temperatures chosen represent the lowest temperature slowly begin driving off  $\text{Hg}_{(l)}$ , but probably not high enough to force covalent bond formation, 100°C, and 200 °C, a temperature at which bond formation may occur. The flasks were vented to a pre-weighed receiving flask under liquid nitrogen (-196°C) to condense any  $\text{Hg}_{(g)}$  extracted from the mixture. After 8 hr, the receiving flask was reweighed and no mass changes were found. The products in the round-bottom flask were slurried with EtOH and centrifuged to facilitate separation of solid B9-Hg products from unreacted mercury and dissolved B9. Mercury quantification of portions of the solids collected during the EtOH washing process was completed by ICP (see Appendix for details) and the results are recorded in Table 5.1.

Sample (°C)	mg Hg/g B9
50	85.40 ± 2.10
100	105.74 ± 3.80
200	224.10 ± 13.41
Theoretical (1:1 Binding)	705.31

**Table 5.2:** Liquid Phase Hg Capture under Vacuum at Elevated Temperatures

The presence of ethanol insoluble solids containing mercury was indicative of the formation of B9-Hg<sub>(s)</sub> product. However, the theoretical capture assuming a 1:1 B9:Hg ratio and 100% efficiency would have resulted in over 700 mg Hg captured per g of B9 analyzed. Based upon this comparison, a sizable amount of the elemental mercury was participating in physisorption with the B9 solid rather than covalent bond formation. This finding still represents an overall improvement in handling the disposal of elemental mercury waste as solid B9 provides an efficient mechanism for sorbing mercury long enough to dispose of it properly.

**Gas Phase Elemental Mercury Flask-to-Flask Study.** Finely dispersed droplets of gas phase elemental mercury may allow for quicker progression from a physisorption event to irreversible mercury capture through covalent bond formation with B9. To test this possibility, the behavior of gas phase elemental mercury brought in contact with solid and liquid B9 in a simple “flask-to-flask” study was examined.  $\text{Hg}^0_{(l)}$  (50.0 g, 0.249 mol, Strem) was placed into a side-arm flask nestled in a heating mantle kept at 356°C, the boiling point of  $\text{Hg}_{(l)}$ , creating a molten mercury generator. Once the second side-arm flask containing B9 (1.0 g, 3.52 mmol) was pre-heated to the target temperature, the stopcocks to both flasks were opened to allow the flow of heated, gaseous Hg to both vessels via a short section of rubber tubing connecting the two flasks. Reactions were run with B9 at 26°C, 100°C, 150°C and 200°C for 1 hr and 3 hr runs; additional 4 hr runs were conducted at 100°C and 200°C and a single 5 hr run was conducted at 150°C (see Table 5.2). Spent B9 samples were analyzed by ICP for total Hg content (see Appendix for details) and the results were compiled in Table 5.2.

<b>B9 Temp. (°C)</b>	<b>Time (hr)</b>	<b>Hg Content (ppm)</b>
26°C	1	104.9
	3	70.8
50°C	1	110.6
	3	78.7
100°C	1	113.4
	3	115.0
	4	91.5
150°C	1	Insuff. Sample
	3	114.5
	5	128.9
200°C	1	351.3
	3	716.1
	4	Insuff. Sample

**Table 5.3:** Hg Content of B9 from Gas Phase Flask-to-Flask Hg Capture

The flask-to-flask study effectively demonstrated the “capture” of  $\text{Hg}_{(g)}^0$  at high part-per-million levels regardless of time or temperature (Table 5.2). The temperatures chosen were representative of several key ranges for B9 stability and Hg remediation: room temperature (26°C, 78.8°F), the normal operating temperature on the “cold side” of a coal-fired power plant bag house (50°C, 122°F), the highest temperature expected in a wet scrubber system and just below the melting point of B9 (100°C, 212°F), above the melting point of B9 (150°C, 302°F), and above the decomposition temperature of B9-Hg<sub>(s)</sub> (200°C, 392°F) synthesized from the combination of ethanolic B9 and mercuric chloride.<sup>239</sup>

In the lowest temperature range studied (26 – 50°C) greater Hg capture is observed for 1 hr than for 3 hr, most probably due to the physisorption of Hg to the solid B9 rather than covalent bond formation. If saturation is occurring within the first hour, the additional run time is only serving to drive the excess Hg off as an equilibrium between physisorbed  $B9_{(s)} \cdots Hg^0_{(g)}$  and  $Hg^0_{(g)}$  is achieved. At 100°C, this decrease is not observed until a 4 hr run time and then the decrease is not nearly as dramatic (19.9% decrease compared to 32.5% and 28.8% for 26 °C and 50°C, respectively). The loss is not observed for the  $B9_{(l)}$  Hg capture at 150 °C; rather, the 3 hr capture is comparable to the 1 hr capture at lower temperatures and the 5 hr run demonstrates a slight increase in Hg capture.

At 200°C, the Hg capture rate increases dramatically, signaling the change from a physisorption event, whereby the Hg is held weakly in multilayer coverage to the B9 by intermolecular (van der Waals) interactions, to an occurrence of chemisorption, which is characterized by monolayer adsorption due to covalent bond formation between the adsorbate and the substrate. Chemisorption has a high activation energy which may be overcome by heating both the B9 and the Hg to 200 °C to yield either chemisorbed  $B9H_2-Hg_{(s)}$  or  $B9-Hg_{(s)}$  and  $H_{2(g)}$ .

**Gas Phase Elemental Mercury Filter Frit Studies.** A more refined approach to studying the effects of solid B9 on gas phase elemental mercury capture involved moving away from the static flask-to-flask system to a dynamic system with controllable gas flows. This was accomplished by suspending the solid ligand on a gas permeable filter frit above the molten mercury generator through which a gas flow could be added. Using this system, the effects of B9 particle size, mercury exposure time on ligand performance, and elevated ligand temperature on mercury capture efficiency were explored.

The effect of solid B9 particle size at ambient temperature was tested first. B9 (5.00 g, 17.58 mmol) was sieved to 250 – 500  $\mu\text{m}$  or 125 – 250  $\mu\text{m}$  (Fisherbrand U.S. Standard Brass Test Sieves) and added to a glass filter frit suspended 6.50 cm from the bottom of a glass tube 3.20 cm in diameter creating a layer of B9 approximately 1.65 cm deep. This glass tube was connected to a molten Hg generator and a stream of  $N_2$  was passed through the Hg generator-filter frit system at  $100 \text{ mL} \cdot \text{min}^{-1}$  before venting to a series of 3-100 mL traps containing 0.3 M  $KMnO_4$  (JT Baker) in 1%  $H_2SO_4$  (EM



Science). Triplicate runs were conducted for 3 hr on each particle size of B9. Subsequently, triplicate runs were conducted for 200, 220, and 240 min using B9 sieved to 125 – 250  $\mu\text{m}$  and venting to 0.03 M KOH (Mallinckrodt) traps adjusted to pH 8 using dilute Omnitrace HCl (EM Science) to determine if Hg saturation in the B9 would occur during these timeframes. At the end of every run, the spent B9 and permanganate or KOH/HCl traps were analyzed by ICP for total Hg (see Appendix for details). Mercury capture results for the varied particle-size filter frit study are compiled in Table 5.4 while the time-dependent filter frit study results are compiled in Table 5.5.

B9 Particle Size ( $\mu\text{m}$ )	Hg Content				Total Hg (mg)	% Bound
	B9 (mg/kg)	B9 (mg)	Trap 1 (mg)	Trap 2 (mg)		
250 – 500	110.4 $\pm$ 7.4	0.552 $\pm$ 0.037	0.091 $\pm$ 0.001	0.189 $\pm$ 0.002	0.873 $\pm$ 0.037	63
	95.4 $\pm$ 12.5	0.479 $\pm$ 0.063	0.110 $\pm$ 0.0002	0.098 $\pm$ 0.002	0.687 $\pm$ 0.063	70
	186.4 $\pm$ 20.8	0.936 $\pm$ 0.105	0.127 $\pm$ 0.005	0.154 $\pm$ 0.001	1.283 $\pm$ 0.105	73
125 – 250	114.8 $\pm$ 13.1	0.574 $\pm$ 0.066	BDL	BDL	0.574 $\pm$ 0.066	100
	90.3 $\pm$ 8.9	0.455 $\pm$ 0.045	0.021 $\pm$ 0.004	BDL	0.476 $\pm$ 0.045	96
	67.8 $\pm$ 7.7	0.341 $\pm$ 0.039	0.020 $\pm$ 0.011	BDL	0.361 $\pm$ 0.040	95

**Table 5.4:** Hg Capture by Various Particle Sizes of B9 Suspended on a Filter Frit at Ambient Temperatures

Time (min)	Hg Content						Total Hg (mg)	% Bound
	B9 (mg/kg)	B9 (mg)	Trap 1 (mg)	Trap 2 (mg)	Trap 3 (mg)			
200	48.0 ± 1.6	0.240 ± 0.008	0.011 ± 0.001	0.006 ± 0.001	0.003 ± 0.000	0.260 ± 0.008	92	
	60.0 ± 1.8	0.300 ± 0.009	0.011 ± 0.001	0.005 ± 0.001	0.011 ± 0.000	0.327 ± 0.009	92	
	92.4 ± 1.5	0.462 ± 0.008	0.008 ± 0.000	0.007 ± 0.000	BDL, < 0.003	0.477 ± 0.008	97	
220	64.8 ± 0.0	0.324 ± 0.000	0.017 ± 0.001	0.008 ± 0.001	BDL, < 0.002	0.349 ± 0.000	93	
	104.6 ± 1.6	0.523 ± 0.008	0.004 ± 0.001	0.011 ± 0.001	BDL, < 0.003	0.537 ± 0.008	97	
	42.5 ± 1.1	0.212 ± 0.005	0.003 ± 0.001	BDL, < 0.002	BDL, < 0.002	0.215 ± 0.005	99	
240	48.0 ± 0.6	0.240 ± 0.003	0.011 ± 0.000	0.006 ± 0.000	BDL, < 0.002	0.257 ± 0.000	93	
	113.2 ± 1.8	0.566 ± 0.009	0.005 ± 0.000	0.005 ± 0.001	BDL, < 0.002	0.576 ± 0.009	98	
	106.3 ± 1.3	0.532 ± 0.006	0.004 ± 0.000	0.005 ± 0.000	BDL, < 0.002	0.540 ± 0.006	98	

**Table 5.5:** Hg Capture Capacity by 125 – 250 µm Filter Frit B9 at Ambient Frit Temperature at Varying Time Lengths

When B9<sub>(s)</sub> is suspended on a glass filter frit at ambient temperature, B9 is capable of removing Hg<sup>0</sup><sub>(g)</sub> with greater capture efficiencies (95 – 100%) observed for the smaller particle size versus an efficiency of 63 – 73% for the larger particle size during 3 hr trials (Table 5.4). Even with increasing time, Hg<sup>0</sup><sub>(g)</sub> capture remains high at 93 – 98% for the 125 – 250 μm B9 particle size at 240 min (Table 5.5). The concentrations of Hg<sup>0</sup><sub>(g)</sub> studied in this system (60–100 ppm) greatly exceed what would be observed in actual coal-fired power plant applications. However, use of this high-level Hg<sup>0</sup><sub>(g)</sub> contaminant stream is essential in testing the absolute performance limits of the ligand.

A thermal study of B9 was conducted to determine the stability of the ligand at relevant temperatures for gas phase Hg binding studies. B9 melts at 126°C and remains a liquid until 298°C before losing color. Solids heated to 245°C and 298°C contained a mixture of intact and decomposed B9 as evidenced by infrared and mass spectral analyses. Therefore, the effect of heated B9 on mercury capture in the filter frit system was examined next. B9 (3.00 g, 10.55 mmol) was sieved to ≤ 125 μm under low humidity conditions and added to the previously-described system. The temperature of the B9 on the filter frit was maintained at 32°C (ambient operating temperature), 60°C and 100°C for single 12 hr runs. Temperatures were monitored continuously throughout each run using a thermocouple (VWR) inserted directly into the B9. A continuous air flow of 100 mL·min<sup>-1</sup> was maintained for the 32°C and 60°C runs; air flow for the 100°C run had to be increased to 190 mL·min<sup>-1</sup> to effect active bubbling in the liquid traps following the filter frit due to the increased viscosity of B9<sub>(l)</sub> versus the free-flowing B9<sub>(s)</sub> powder. While the B9 in the center of the frit was at 100 °C, B9 near the glass walls of the frit was heated past the boiling point (126°C) during the experiment and began to decompose as evidenced by the formation of a yellow, sticky solid along the walls of the filter frit tube.

Upon termination of each run, the solid was rinsed out of the filter frit with EtOH (Aaper), centrifuged at 7,818 G for 10 min and inspected for a visible Hg<sup>0</sup><sub>(l)</sub> pellet. After vacuum pumping the product to dryness, two portions of the “pre-washed” B9 were weighed and digested for total Hg analysis by ICP. The rest of the spent B9 was then washed with EtOH (~400 mL) under vacuum filtration, yielding a cloudy white filtrate.

The remaining “post-wash” sample was weighed and digested for ICP analysis (see Appendix for details) with final mercury concentrations listed in Table 5.6.

Run Temp. (°C)	Pre-Wash (mg Hg/g B9)		Avg. Pre-Wash (mg Hg/g B9)	Post Wash (mg Hg/g B9)
	Sample 1	Sample 2		
32	0.4433 ± 0.0050	0.6120 ± 0.0106	0.5276 ± 0.0117	5.4217 ± 0.0783
60	45.7208 ± 0.3283	67.2904 ± 0.9536	56.5056 ± 1.0085	23.3100 ± 0.2531
100	N/A	N/A	N/A	34.5638 ± 0.2870

**Table 5.6:** Gas Phase Hg Capture at Elevated Frit Temperatures

The filter frit runs of gas phase Hg(0) with solid B9 at elevated temperatures demonstrated the presence of covalently bound B9-Hg as evidenced by the appearance of an ethanol-insoluble product in contrast to unreacted B9 which dissolves readily in ethanol. The ambient temperature (32°C) run had observable Hg pellets at the bottom of the centrifuge tubes. Although the Hg was not recoverable, most of the B9 was dissolved by the ethanol washing, leaving only a small amount of B9-Hg<sub>(s)</sub>. The solid from the 60°C run had to be ground using a mortar and pestle prior to washing with ethanol. The 100°C run was quite interesting as 2.6g of Hg(0) was recovered from the yellow B9 decomposition product along the much hotter sides of the frit. Extraction in EtOH left 0.5 g of insoluble material. The results of the ICP analyses are compiled in Table 5.6. The 60°C run demonstrated the highest Hg capture of all three runs.

Overall, B9 was shown to capture elemental Hg in both the liquid and gas phases. This could take place through a combination of absorption (where the mercury is trapped within the material), adsorption or covalent bond formation. Further characterization is required to determine the amount of physisorption vs. chemisorption and whether the balance can be tipped in favor of covalent bond formation between solid B9 and Hg(0). The filter frit studies were able to demonstrate that decreased B9 particle size and higher ligand temperatures favor greater Hg(0) capture. Exposure time to Hg(0) did not significantly affect relative mercury capture with the ligand compared to Hg traps which

may be due to an equilibrium between adsorptive and desorptive processes maintaining a steady-state mercury concentration. Further examination in a more elegant system will be needed to elucidate further information into the nature of the  $\text{Hg}(0)_{(g)}$  binding to solid B9.

## **FEASIBILITY OF APPLICATION IN COAL FIRED POWER PLANTS**

**Questions to Consider.** While the filter frit system previously described was adequate for probing certain aspects of  $\text{Hg}(0)$  with solid B9, a more robust system with greater flexibility is needed to answer many pertinent questions prior to testing in a full-scale coal-fired power plant. For instance, the behavior of B9 in a mixture of heated gases representative of true flue gas conditions is a prerequisite to examine the stability of B9 under normal operating conditions. It would also be interesting to discover if pre-reduction of  $\text{Hg}(0)$  to  $\text{Hg}(\text{II})$  in the flue gas would facilitate greater chemisorption rather than physisorption in a time scale to make B9 remediation applicable. If this was the case, the pre-reductive measures to convert gas phase arsenic and selenium to the appropriate valence states would allow for their remediation from coal-fired power plant flue gases as well. Questions regarding the chemistry of the flue gas and its effects on B9 are quite relevant, but unable to be answered at the present time.

The exact methods for application of the ligand present perhaps the largest arena of uncertainty. While solid B9 was used in this work for “proof of concept,” many other modes of using the ligand may yield greater remediation efficiency in coal-fired power plants. Much like activated carbon and solid sodium sulfide, B9 could be applied using direct injection with capture of the resulting B9-Hg particulates using downstream fabric filters or electrostatic precipitators. B9 could also be applied to wet scrubber systems where flue gas desulfurization is already used without any incurring any great expenses for adding this mercury-specific technology. Modifying B9 so that it is applied as a support-bound ligand would also open many other avenues. For instance, a fabric filter material woven from filaments covalently studded with B9, for example PS-AB9, a polystyrene B9 material that is currently in preparation, could prove the best alternative for capturing  $\text{Hg}(0)_{(g)}$  as it diffuses through the fabric.

**The Prototype Gas Phase Flow Reactor.** Before large sums of capital are expended to test the efficacy of different application methods in actual coal-fired power

plants, it is highly desirable to employ a bench-scale model with which to gauge the success of our different remediation permutations on gas phase Hg(0) using real-time monitoring techniques. Constant tracking of the remediation dynamics would provide key information to several questions, especially concerning how fast the ligand capture efficiency is likely to decrease. A bench scale model with the capabilities of using single gases to gauge each flue gas component's action on the ligand as well as the ability to examine gas mixtures is critical since much of the flue gas chemistry concerning mercury and potential remediating agents is difficult to predict. The key component of a bench scale flow reactor would be the reaction bed, ideally an interchangeable component that could be used to simulate key areas where the ligand is likely to be applied. This could range from the area upstream of an electrostatic precipitator where the ligand could be applied by direct injection to a wet scrubber system where B9 could be added to the slurry currently used to reduce sulfur gases in the FGD process. Development of a satisfactory support-bound ligand could result in bag-houses using fabric filters that incorporate the ligand into the weave of the material, a scenario that should be tested on the small scale prior to retrofitting an actual bag house with such a material whose performance has not yet been optimized. Towards that end, a prototype gas phase flow reactor was constructed to explore the feasibility of manufacturing an adequate model for ligand testing with real-time monitoring capabilities. The schematic of the basic flow reactor is shown in Figure 5.3.

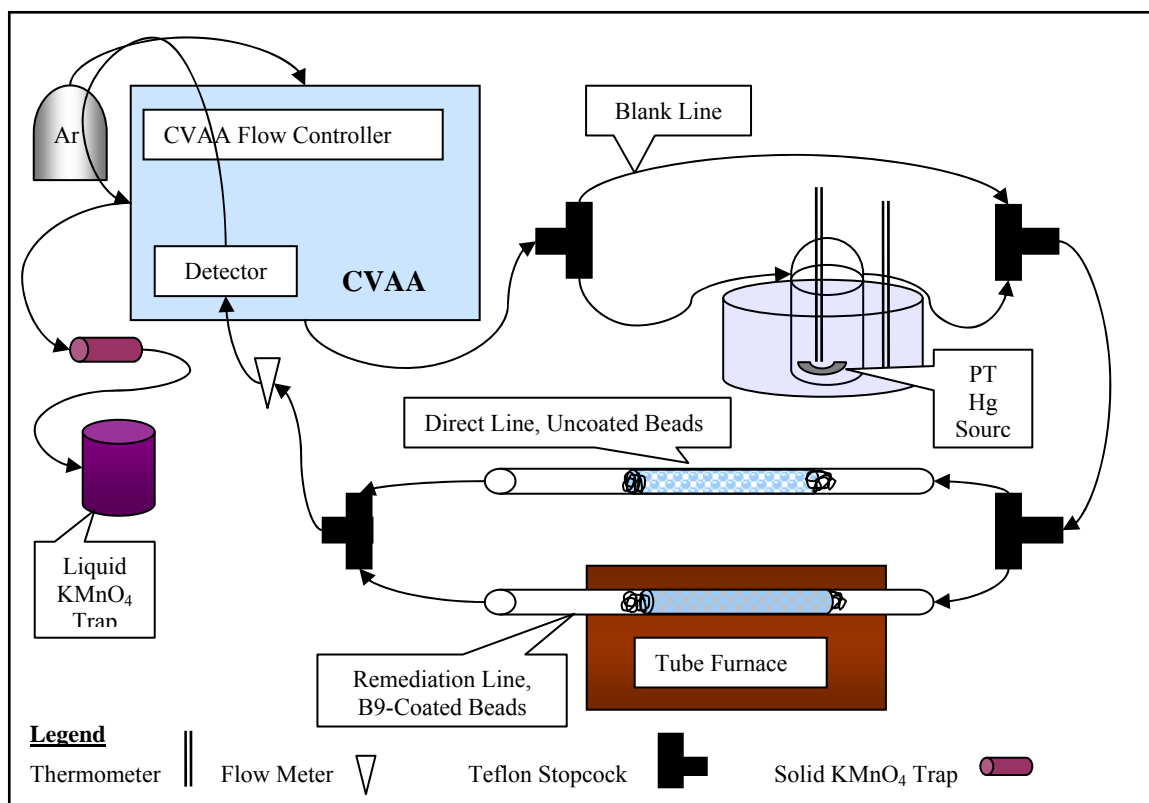


**Figure 5.3:** Prototype Gas Phase Flow Reactor Schematic

Beginning at the argon cylinder, the gas flow was connected directly to the reference cell of a Cetac M-600A Cold Vapor Atomic Absorption Spectrometer (CVAA), bypassing the instrument's flow controller. Teflon reducing connectors (Cole Parmer) were used to tie the instrument into the gas phase system. Cleaned, fluoroethylene polymer-lined (FEP) tubing (Environmental Express) designed specifically for low-level mercury analysis and denoted by the thin black lines in Figure 5.3 served to connect the system components. The reference cell outlet was routed to the first of four Teflon three-way stopcocks (Plasmatech) used to direct gas flows throughout the system. From the first stopcock, the gas flow into two paths. The first path was simply a length of tubing running to the next stopcock and served as a path for making baseline, mercury-free measurements. The other path connected the stopcock to a specially-designed glass permeation tube vessel (PTV).

Unlike a typical round-bottom flask, the PTV was made in a general bottle shape with a wider base to ensure the majority of the Dynacal Permeation Device (8.0 cm, VICI



Metronics) would remain below the level of the warming bath at all times. When heated to 60°C, the permeation tube (PT) was certified to release Hg(0) at a rate of 191 ng·min<sup>-1</sup>. Temperature was monitored using a thermometer inserted through a PTFE thermometer adapter (Cole Parmer) in the top port of the PTV. Temperature was maintained using a Branson 3510 sonicator water bath shrouded in aluminum foil for insulation.

Flow from the PTV was directed to the second stopcock where it joined with the blank line. The second stopcock was connected to a third stopcock that allowed gas to be shunted to a “direct” line, thus avoiding the ligand being tested and flowing to the next system junction, or through the remediation line where the ligand in question would be supported on glass beads (3 mm, Fisher; see the Appendix for the bead coating procedure using B9) in the hopes of diminishing continual flow rate issues experienced using the solid powdered ligand, especially as treatment bed lengths were increased. Glass beads were also included in the direct line to provide comparable flow rates through both lines and to eliminate the need for a baseline correction factor to absorbance readings made during real-time gas phase monitoring experiments. While providing a larger binding surface, the ligand-coated beads had the added benefit of reducing the amount of compound required to create a remediation bed of substantial length. The remediation line was routed through a tube furnace to control the temperature of the remediation bed for future elevated temperature experiments. The direct and remediation lines were rejoined in the fourth three-way stopcock leading to a low-flow meter (Bel-Art) before entering the CVAA detector. Inclusion of the appropriately sized flow meter allowed for accurate gas flow measurement and calculation of the gas phase Hg contamination rate could be calculated for comparison to the microabsorbance readings from the CVAA detector.

Due to the rigid nature of the tubing and the inner FEP lining’s tendency to delaminate and wrinkle, connections between the tubing, the glass tubes and the flow meter proved to be troublesome. To simplify the glass tube replacements, a 1/4 inch brass hose barb (Watts) inserted into the Teflon tubing was screwed into a 3/8 inch barb (Watts) that lie just inside the remediation tubes. The hose barb was be secured to the glass tube by means of a short Tygon sleeve covering both the glass tube and the FEP tubing with clamps added to hold the apparatus in place. To join the flow meter securely

to the FEP tubing, the factory-installed plastic hose barbs had to be replaced with smaller, single-piece brass hose barbs (1/4" barb with 1/8" NPT threads).

After leaving the CVAA detector, the gas phase mercury flow was vented to a fresh solid  $\text{KMnO}_4$  (EM Science) trap. The solid trap's exhaust was then plumbed to the nearest fume hood where it was connected to a saturated liquid  $\text{KMnO}_4$  bubbler with a flared outlet to prevent solid permanganate precipitation from possibly blocking the exhaust. The liquid trap was added as a precautionary measure since relatively high levels of continuous mercury were being used for experimentation.

One successful gas-phase experiment was conducted on the prototype gas flow reactor. The low gas flow selected ( $155 \text{ mL}\cdot\text{min}^{-1}$ ) required that the permeation tube be maintained at  $26^\circ\text{C}$  rather than heating to the full  $60^\circ\text{C}$ , the temperature at which the mercury emission rate is certified. This was done to suppress the mercury emissions to a range well within that of the CVAA detector's limits. The remediation line was loaded with glass wool (0.1012 g), B9-coated glass beads (35.29 g), and another glass wool plug (0.1050 g) to hold the beads in place. The direct line was loaded with glass wool (0.1094 g), uncoated glass beads (30.0117g), and glass wool (0.1176 g). Fine-tuning the flow rates between the remediation and direct lines required the addition of approximately 0.0500 g of glass wool in the direct line to match the flow rates perfectly.

The baseline was set using the blank line and remediation line pathway. The path was switched to the direct line, then the PTV line, and flow was increased briefly to purge excess Hg from the system. The flow was reset to  $155 \text{ mL}\cdot\text{min}^{-1}$  and the mercury ceiling was established at 50,000 microabsorbance units as depicted by the red line in Figure 5.4. Switching to the remediation line caused readings to dip to 2,000 units for 7 s before returning swiftly to 14,000 units 3 min into the experiment. From 14,000 units, the Hg levels climbed in a steady, linear fashion to 35,000 units for another 2 min before the rate of increase declined. By the end of 15 min, Hg concentrations through the remediation line were back up to the initial 50,000 units and the run was terminated. While these results are very encouraging, the need to continue optimizing the gas-phase capture system is still apparent from the difficulties that keep appearing.

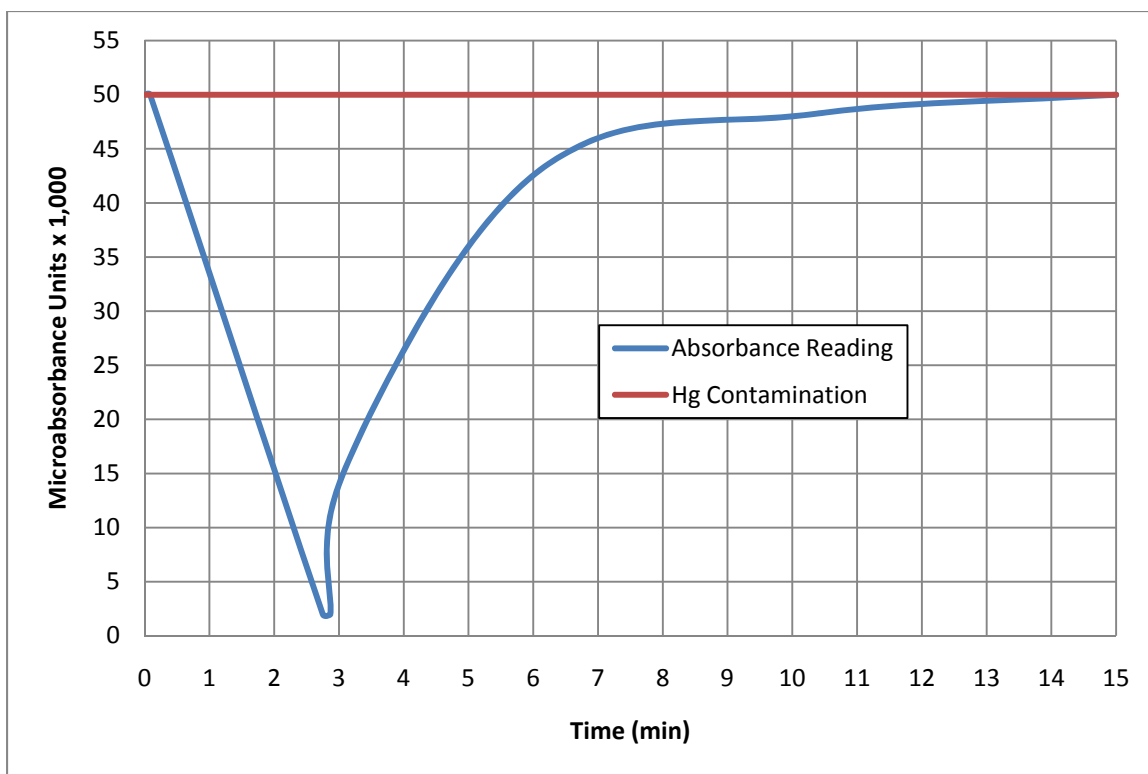


**Figure 5.4:** Real-Time Results for the Prototype Gas Phase Flow Reactor

Perhaps the largest drawback to the prototype gas phase flow reactor was the continual loss of mercury from the system. Total mercury capture was attempted with the system at four different flow rates with very low overall mercury capture compared to calculated amounts of mercury released from the PT. This problem may have been aggravated by the general instability of the system as the FEP tubing was constantly being moved during manipulation of the system to adjust flows, PT heating, and change-outs of the direct and remediation lines. All of this movement was sure to contribute to multiple leaks that were all very time-consuming to discover and repair.

**Plans for the All-Steel Gas Phase Flow Reactor.** Several key improvements over the prototype gas phase flow reactor will need to be implemented during the final planning and construction of an all-steel gas phase flow reactor. To begin, rather than utilizing a single gas source, a bank of cylinders with mass flow controllers for varying the relative contributions of each gas to the system and a means of adequately pre-heating these gases prior to reaching the reaction bed will be required. A series of permeation

tubes that emit over a range of mercury concentrations typical of those encountered in combustion sources would also prove useful. Construction of the entire system out of stainless steel components affixed to a wall-mounted system will provide the stability needed to prevent movement of individual pieces and the possibility incurring leaks. While the majority of components will be permanently fixed, the sections of the flow reactor that will ultimately be attached to potential remediation beds needs to have some flexibility such that remediation beds modeling direct injection into the flue gas, flows through wet and dry scrubbers systems, and the passage of gas phase mercury through a bag house can be simulated. Placement of the remediation bed in a vertical rather than a horizontal position would also be desirable in order to mimic solid phase B9 testing in the earlier filter frit studies.

A means of more accurately monitoring the gas phase flow reactor experiments also deserves careful consideration before finalizing the all-steel system plans. Reproducibility between experiments was difficult to achieve with the prototype model but this problem can be remedied through the application of several different improvements. To be sure, the presence of undetected leaks and flow issues hampered successful data collection. This problem is easily alleviated by adding accurate means to control flows from the source(s) and the addition of flow meters on both the front and back ends of the system. Discrepancies between flows measured at the beginning of the system and just prior to mercury measurement would signal corruption of the system. Furthermore, a better method of gas phase mercury entrainment in the system's exhaust would further alleviate flow issues encountered in previous prototypes while providing added value by enabling mass balance studies for mercury capture experiments should they become a priority in conjunction with real-time monitoring data. Finally, incorporation of a gas phase mercury instrument that could be calibrated to give absolute mercury concentrations directly rather than results in relative concentrations would prove invaluable.

## **CONCLUSIONS**

B9 has proven useful in the remediation of a variety of species ranging from divalent metals to the metalloid oxyanions As(III) and Se(IV). Exploration into the utility

of the ligand in remediating related species such as liquid and gas phase elemental mercury with direct relevance to application in the coal-fired power plant industry holds very promising. The exact application method that would prove most useful, including any manipulation of flue gas chemistry to shift the reaction of mercury with solid B9 from physisorption to true covalent bond formation, needs to be explored using an all-steel gas phase flow reactor before incurring the expenses associate with ligand testing in real-world situations.

## APPENDIX

**Analytical Procedures for the Determination of Hg by ICP in Liquid and Gas Phase Elemental Mercury Experiments.** Solid B9-Hg samples slurried in EtOH were digested for ICP analysis using a modified EPA 3050B<sup>303</sup> procedure as follows: 10 mL 50% nitric acid, reflux 10 min; add 5 mL concentrated nitric acid, reflux for 30 min, repeat until digestion complete; evaporate to 5 mL, cool; add 5 mL of 2:3 DI water-30 % peroxide mixture (Fisher); add 1 mL 30% H<sub>2</sub>O<sub>2</sub> and repeat until bubbling subsides; reduce volume to 5 mL; add 10 mL concentrated HCl, cover, reflux 15 min; dilute to volume and filter with a 0.45 µm plunge filter (Environmental Express).

High-concentration aqueous and solid Hg samples were analyzed using a Varian Vista Pro Inductively Coupled Plasma Optical Emission Spectrometer (ICP-OES) run at 1.2 kW with 4.0 s replicate read times at 253.652 nm. An extended 120 s, 5% HCl/10% HNO<sub>3</sub> rinse was used between samples; all other instrumental settings were used as pre-set by the manufacturer without modification. To correct for matrix effects, the concentration of a 1.0 ppm continuous feed yttrium internal standard was monitored at 371.029 nm. Curve verifiers (CVs), laboratory control samples (LCSs), duplicate samples, and spiked samples were included at both high and low concentrations every 10 samples and for every unique sample matrix. CV and LCS recovery was  $\geq 95\%$ ; spiked sample recovery typically ranged from 75 – 90%. Method blanks were included between every sample with concentrations  $\leq 2.0$  ppm to estimate the limit of quantitation and for determination of an appropriate blank subtraction for each run to eliminate the effects of Hg carryover between samples.

**Procedure for Coating Glass Beads with B9.** Solid Pyrex glass beads (3 mm, Fisher) were coated with B9 using the following procedure. All glassware and other equipment were washed with base, then acid, and finally with copious amounts of water before being oven-dried for at least one hour. Storage containers used were certified metals-free plastic containers with caps to prevent any contamination with adventitious mercury. Glass beads (92 g) were weighed and stored in a drying oven at least one hour prior to use. A comparison of the mass of the beads weighed directly as received versus the mass of the same beads heated in the oven revealed that the masses were the same.

Thus, there is very little water on or in the glass beads, even at room temperature. Still, heating will prevent water from accumulating on the surface of the beads, thereby improving the ability of the B9 to stick to the surface. Two grams of B9 were dissolved in 100 mL of ethanol and brought to reflux in a three-necked flask connected to a vacuum line until the solution became clear (30 min). The solution was brought to reflux under nitrogen as a precaution to prevent any disulfide forming through oxidation although this has never been observed with B9. The three-necked flask was equipped with a mechanical stirrer. The stirring blade was rounded to prevent any of the glass beads from sticking to the bottom of the flask. Once the B9 solution became clear, the pre-weighed, hot glass beads were poured into the three-necked flask. Mechanical stirring was started and the flask was put under vacuum ( $10^{-2}$  Torr). The flask was evacuated to dryness with continual stirring until the flask reached room temperature. The dried glass beads were poured onto a 2 mm sieve and rolled gently until no more free powder was associated with the beads.

## REFERENCES

1. Florea, A. M.; Busselberg, D., Occurrence, use and potential toxic effects of metals and metal compounds. *Biometals* **2006**, *19* (4), 419-427.
2. Gavis, J.; Ferguson, J. F., The cycling of mercury through the environment. *Water Research* **1972**, *6* (9), 989-1008.
3. Tchounwou, P. B.; Ayensu, W. K.; Ninashvili, N.; Sutton, D., Environmental exposure to mercury and its toxicopathologic implications for public health. *Environmental Toxicology* **2003**, *18* (3), 149-175.
4. Schroeder, W. H.; Munthe, J. In *Atmospheric mercury - An overview*, 1998; pp 809-822.
5. Greenwood, N. N.; Earnshaw, A., *Chemistry of the elements*. 2 ed.; Reed Educational and Professional Publishing, Ltd.: Oxford, Great Britain, **2001**.
6. Clarkson, T. W., The three modern faces of mercury. *Environ. Health Perspec.* **2002**, *110*, 11-23.
7. Langford, N. J.; Ferner, R. E., Toxicity of mercury. *Journal of Human Hypertension* **1999**, *13* (10), 651-656.
8. ATSDR, Toxicological profile for mercury: TP-93/10. Centers for Disease Control: Atlanta, Georgia, **1999**.
9. Baughman, T. A., Elemental mercury spills. *Environmental Health Perspectives* **2006**, *114* (2), 147-152.
10. Clarkson, T. W.; Magos, L., The toxicology of mercury and its chemical compounds. *Crit. Rev. Toxicol.* **2006**, *36*, 609-662.
11. Camargo, J. A., Contribution of Spanish-American silver mines (1570-1820) to the present high mercury concentrations in the global environment: a review. *Chemosphere* **2002**, *48* (1), 51-57.
12. Malm, O., Gold mining as a source of mercury exposure in the Brazilian Amazon. *Environmental Research* **1998**, *77* (2), 73-78.
13. Ventura, H. O.; Mehra, M. R.; Young, J. B., Treatment of heart failure according to William Stokes: the enchanted mercury. *J. Cardiac Failure* **2001**, *7* (3), 277-282.
14. Dale, R. A.; Sanderson, P. H., The mode of action of a mercurial diuretic in man. *J. Clin. Invest.* **1954**, *33* (7), 1008-1014.
15. Hewitson, L.; Houser, L. A.; Stott, C.; Sackett, G.; Tomko, J. L.; Atwood, D. A.; Blue, L. Y.; White, E. R., Delayed acquisition of neonatal reflexes in newborn primates



receiving a thimerosal-containing Hepatitis B vaccine: influence of gestational age and birth weight. **2009**, *in press*.

16. Magos, L.; Clarkson, T. W., Overview of the clinical toxicity of mercury. *Annals of Clinical Biochemistry* **2006**, *43*, 257-268.
17. Bakir, F.; Damluji, S. F.; Aminzaki, L.; Murtadha, M.; Khalidi, A.; Alrawi, N. Y.; Tikriti, S.; Dhahir, H. I.; Clarkson, T. W.; Smith, J. C.; Doherty, R. A., Methylmercury poisoning in Iraq - interuniversity report. *Science* **1973**, *181* (4096), 230-241.
18. Goldman, L. R.; Shannon, M. W., Technical report: Mercury in the environment: Implications for pediatricians. *Pediatrics* **2001**, *108* (1), 197-205.
19. Ditri, F. M., Mercury contamination - what we have learned since Minamata. *Environ. Monit. Assess.* **1991**, *19*, 165-182.
20. Morita, M.; Yoshinaga, J.; Edmonds, J. S., The determination of mercury species in environmental and biological samples (Technical report). *Pure Appl. Chem.* **1998**, *70* (8), 1585-1615.
21. Pacyna, E. G.; Pacyna, J. M.; Steenhuisen, F.; Wilson, S., Global anthropogenic mercury emission inventory for 2000. *Atmospheric Environment* **2006**, *40* (22), 4048-4063.
22. Lacerda, L. D., Global mercury emissions from gold and silver mining. *Water Air and Soil Pollution* **1997**, *97* (3-4), 209-221.
23. Nriagu, J. O., Legacy of mercury pollution. *Nature* **1993**, *363* (6430), 589-589.
24. Schuster, P. F.; Krabbenhoft, D. P.; Naftz, D. L.; Cecil, L. D.; Olson, M. L.; Dewild, J. F.; Susong, D. D.; Green, J. R.; Abbott, M. L., Atmospheric mercury deposition during the last 270 years: A glacial ice core record of natural and anthropogenic sources. *Environ. Sci. Technol.* **2002**, *36* (11), 2303-2310.
25. Nriagu, J. O.; Pfeiffer, W. C.; Malm, O.; Desouza, C. M. M.; Mierle, G., Mercury pollution in Brazil. *Nature* **1992**, *356* (6368), 389-389.
26. Hutchison, A. R.; Atwood, D. A., Mercury pollution and remediation: the chemist's response to a global crisis. *J. Chem. Crystallogr.* **2003**, *33* (8), 631-645.
27. Johnson, N. C.; Manchester, S.; Sarin, L.; Gao, Y.; Kulaots, I.; Hurt, R. H., Mercury vapor release from broken compact fluorescent lamps and in situ capture by new nanomaterial sorbents. *Environ. Sci. Technol.* **2008**, *42* (15), 5772-5778.
28. Nriagu, J. O.; Pacyna, J. M., Quantitative assessment of worldwide contamination of air, water and soils by trace-metals. *Nature* **1988**, *333* (6169), 134-139.

29. Sondreal, E. A.; Benson, S. A.; Pavlish, J. H.; Ralston, N. V. C., An overview of air quality III: mercury, trace elements, and particulate matter. *Fuel Process. Technol.* **2004**, *85*, 425-440.
30. Galbreath, K. C.; Zygarlicke, C. J., Mercury transformations in coal combustion flue gas. *Fuel Process. Technol.* **2000**, *65-66*, 289-310.
31. Hall, B.; Lindqvist, O.; Ljungstrom, E., Mercury chemistry in simulated flue-gases related to waste incineration conditions. *Environ. Sci. Technol.* **1990**, *24* (1), 108-111.
32. Park, K. S.; Seo, Y. C.; Lee, S. J.; Lee, J. H., Emission and speciation of mercury from various combustion sources. *Powder Technol.* **2008**, *180*, 151-156.
33. Carpi, A., Mercury from combustion sources: a review of the chemical species emitted and their transport in the atmosphere. *Water, Air, Soil Pollut.* **1997**, *98*, 241-254.
34. Feeley, T. J.; Murphy, J. T.; Hoffmann, J. W.; Granite, E. J.; Renninger, S. A., DOE/NETL's mercury control technology research program for coal-fired power plants. *J. Environ. Manag.* **2003**, 16-23.
35. Granite, E. J.; Pennline, H. W.; Hargis, R. A., Novel sorbents for mercury removal from flue gas. *Ind. Eng. Chem. Res.* **2000**, *39* (4), 1020-1029.
36. Yudovich, Y. E.; Ketris, M. P., Mercury in coal: a review, Part 2. Coal use and environmental problems. *Int J. Coal Geol* **2005**, *62*, 135-165.
37. Hall, B.; Schager, P.; Lindqvist, O., Chemical-reactions of mercury in combustion flue-gases. *Water, Air, Soil Pollut.* **1991**, *56*, 3-14.
38. Milford, J. B.; Pienciak, A., After the Clean Air Mercury Rule: prospects for reducing mercury emissions from coal-fired power plants. *Environ. Sci. Technol.* **2009**, *43* (8), 2669-2673.
39. Srivastava, R. K.; Hutson, N.; Martin, B.; Princiotta, F.; Staudt, J., Control of Mercury Emissions from Coal-Fired Electric Utility Boilers. *Environ. Sci. Technol.* **2006**, 1385-1393.
40. Presto, A. A.; Granite, E. J., Survey of catalysts for oxidation of mercury in flue gas. *Environ. Sci. Technol.* **2006**.
41. Shock, S. S.; Noggle, J. J.; Bloom, N.; Yost, L. J., Evaluation of potential for mercury volatilization from natural and FGD gypsum products using flux-chamber tests. *Environ. Sci. Technol.* **2009**, *43* (7), 2282-2287.
42. Nieschmidt, A. K.; Kim, N. D., Effects of mercury release from amalgam dental restorations during cremation on soil mercury levels of three New Zealand crematoria. *Bull. Environ. Contam. Toxicol.* **1997**, *58* (5), 744-751.

43. Ghorishi, S. B.; Lee, C. W.; Jozewicz, W. S.; Kilgroe, J. D., Effects of fly ash transition metal content and flue gas HCl/SO<sub>2</sub> ratio on mercury speciation in waste combustion. *Environ. Eng. Sci.* **2005**, *22* (2), 221-231.
44. Streets, D. G.; Zhang, Q., Projections of global mercury emissions in 2050. *Environ. Sci. Technol.* **2009**, *43* (8), 2983-2988.
45. Fitzgerald, W. F.; Lamborg, C. H.; Hammerschmidt, C. R., Marine biogeochemical cycling of mercury. *Chem. Rev.* **2007**, *107* (2), 641-662.
46. Lin, C. J.; Pehkonen, S. O., The chemistry of atmospheric mercury: a review. *Atmospheric Environment* **1999**, *33* (13), 2067-2079.
47. Nriagu, J. O., A global assessment of natural sources of atmospheric trace-metals. *Nature* **1989**, *338* (6210), 47-49.
48. Morel, F. M. M.; Kraepiel, A. M. L.; Amyot, M., The chemical cycle and bioaccumulation of mercury. *Annu. Rev. Ecol. Syst.* **1998**, *29*, 543-566.
49. Pirrone, N.; Keeler, G. J.; Nriagu, J. O., Regional differences in worldwide emissions of mercury to the atmosphere. *Atmospheric Environment* **1996**, *30* (17), 2981-2987.
50. Schluter, K., Review: evaporation of mercury from soils. An integration and synthesis of current knowledge. *Environmental Geology* **2000**, *39* (3-4), 249-271.
51. Boening, D. W., Ecological effects, transport, and fate of mercury: a general review. *Chemosphere* **2000**, *40* (12), 1335-1351.
52. Mason, R. P.; Fitzgerald, W. F.; Morel, F. M. M., The biogeochemical cycling of elemental mercury: anthropogenic influences. *Geochim. Cosmochim. Acta* **1994**, *58* (15), 3191-3198.
53. Lyman, S. N.; Gustin, M. S.; Prestbo, E. M.; Kilner, P. I.; Edgerton, E.; Hartsell, B., Testing and application of surrogate surfaces for understanding potential gaseous oxidized mercury dry deposition. *Environ. Sci. Technol.* **2009**, *43* (16), 6235-6241.
54. Seigneur, C.; Wrobel, J.; Constantinou, E., A chemical kinetic mechanism for atmospheric inorganic mercury. *Environ. Sci. Technol.* **1994**, *28* (9), 1589-1597.
55. Kim, J. P., Methylmercury in rainbow-trout (*Oncorhynchus-mykiss*) from Lakes Okareka, Okaro, Rotomahana, Rotorua and Tarawera, North-Island, New-Zealand. *Sci. Tot. Environ.* **1995**, *164* (3), 209-219.
56. Gabriel, M. C.; Williamson, D. G., Principal biogeochemical factors affecting the speciation and transport of mercury through the terrestrial environment. *Environmental Geochemistry and Health* **2004**, *26* (4), 421-434.

57. Schroeder, W. H.; Munthe, J.; Lindqvist, O., Cycling of mercury between water, air, and soil compartments of the environment. *Water Air and Soil Pollution* **1989**, *48* (3-4), 337-347.
58. Celso, V.; Lean, D. R. S.; Scott, S. L., Abiotic methylation of mercury in the aquatic environment. *Sci. Total Environ.* **2006**, *368*, 126-137.
59. Sunderland, E. M.; Krabbenhoft, D. P.; Moreau, J. W.; Strode, S. A.; Landing, W. M., Mercury sources, distribution, and bioavailability in the North Pacific Ocean: insights from data and models. *Glob. Biogeochem. Cycles* **2009**, *23*, 1-14.
60. Ravichandran, M., Interactions between mercury and dissolved organic matter - a review. *Chemosphere* **2004**, *55* (3), 319-331.
61. Wolfenden, S.; Charnock, J. M.; Hilton, J.; Livens, F. R.; Vaughan, D. J., Sulfide species as a sink for mercury in lake sediments. *Environ. Sci. Technol.* **2005**, *39* (17), 6644-6648.
62. Liu, G.; Cai, Y.; Mao, Y.; Scheidt, D.; Kalla, P.; Richards, J.; Scinto, L. J.; Tachiev, G.; Roelant, D.; Appleby, C., Spatial variability in mercury cycling and relevant biogeochemical controls in the Florida Everglades. *Environ. Sci. Technol.* **2009**, *Articles ASAP*.
63. Brigham, M. E.; Wentz, D. A.; Aiken, G. R.; Krabbenhoft, D. P., Mercury cycling in stream ecosystems. 1. Water column chemistry and transport. *Environ. Sci. Technol.* **2009**, *43* (8), 2720-2725.
64. Fabbri, D.; Locatelli, C.; Snape, C. E.; Tarabusi, S., Sulfur speciation in mercury-contaminated sediments of a coastal lagoon: the role of elemental sulfur. *J. Environ. Monit.* **2001**, *3*, 483-486.
65. Wiatrowski, H. A.; Das, S.; Kukkadapu, R.; Ilton, E. S.; Barkay, T.; Yee, N., Reduction of Hg(II) to Hg(0) by magnetite. *Environ. Sci. Technol.* **2009**, *ASAP*.
66. Mason, R. P.; Fitzgerald, W. F., Mercury speciation in open ocean waters. *Water Air and Soil Pollution* **1991**, *56*, 779-789.
67. Black, F. J.; Conaway, C. H.; Flegal, A. R., Stability of dimethyl mercury in seawater and its conversion to monomethyl mercury. *Environ. Sci. Technol.* **2009**, *ASAP*.
68. Barkay, T.; Wagner-Dobler, I., Microbial transformations of mercury: Potentials, challenges, and achievements in controlling mercury toxicity in the environment. In *Advances in Applied Microbiology*, Vol 57, 2005; Vol. 57, pp 1-52.
69. Bruins, M. R.; Kapil, S.; Oehme, F. W., Microbial resistance to metals in the environment. *Ecotoxicology and Environmental Safety* **2000**, *45* (3), 198-207.

70. Osborn, A. M.; Bruce, K. D.; Strike, P.; Ritchie, D. A., Distribution, diversity and evolution of the bacterial mercury resistance (mer) operon. *Fems Microbiology Reviews* **1997**, *19* (4), 239-262.
71. Lovley, D. R., Dissimilatory metal reduction. *Annual Review of Microbiology* **1993**, *47*, 263-290.
72. Bruce, K. D., Analysis of mer gene subclasses within bacterial communities in soils and sediments resolved by Fluorescent-PCR-restriction fragment length polymorphism profiling. *Applied and Environmental Microbiology* **1997**, *63* (12), 4914-4919.
73. Ford, T.; Ryan, D., Toxic Metals in Aquatic Ecosystems - a microbiological perspective. *Environ. Health Perspect.* **1995**, *103*, 25-28.
74. Dopp, E.; Hartmann, L. M.; Florea, A.-M.; Rettenmeier, A. W.; Hirner, A. V., Environmental distribution, analysis, and toxicity of organometal(loid) compounds. *Crit. Rev. Toxicol.* **2004**, *34* (3), 301-333.
75. Fatoki, O. S., Biomethylation in the natural environment: A review. *South African Journal of Science* **1997**, *93* (8), 366-370.
76. Rabenstein, D. L., Aqueous-solution chemistry of methylmercury and its complexes. *Accounts of Chem. Res.* **1978**, *11* (3), 100-107.
77. Hylander, L. D.; Goodsite, M. E., Environmental costs of mercury pollution. *Sci. Tot. Environ.* **2006**, *368*, 352-370.
78. Siegler, R. W.; Nierenberg, D. W.; Hickey, W. F., Fatal poisoning from liquid dimethylmercury: A neuropathologic study. *Human Pathology* **1999**, *30* (6), 720-723.
79. Nierenberg, D. W.; Nordgren, R. E.; Chang, M. B.; Siegler, R. W.; Blayney, M. B.; Hochberg, F.; Toribara, T. Y.; Cernichiari, E.; Clarkson, T., Delayed cerebellar disease and death after accidental exposure to dimethylmercury. *New England Journal of Medicine* **1998**, *338* (23), 1672-1676.
80. Zahir, F.; Rizwi, S. J.; Haq, S. K.; Khan, R. H., Low dose mercury toxicity and human health. *Environmental Toxicology and Pharmacology* **2005**, *20* (2), 351-360.
81. Virtanen, J. K.; Rissanen, T. H.; Voutilainen, S.; Tuomainen, T. P., Mercury as a risk factor for cardiovascular diseases. *Journal of Nutritional Biochemistry* **2007**, *18* (2), 75-85.
82. Francesconi, K. A.; Kuehnelt, D., Arsenic compounds in the environment. In *Environmental Chemistry of Arsenic*, 1st ed.; Frankenberger, W. T., Jr., Ed. CRC Press: Boca Raton, FL, **2001**; pp 51-94.
83. Jones, F. T., A broad view of arsenic. *Poult. Sci.* **2006**, *86*, 2-14.

84. Goessler, W.; Kuehnelt, D., Analytical methods for the determination of arsenic and arsenic compounds in the environment. In *Environmental Chemistry of Arsenic*, 1st ed.; Frankenberger, W. T., Jr., Ed. CRC Press: Boca Raton, FL, **2001**; pp 27-50.
85. Ruiz-Chanco, M. J.; Lopez-Sanchez, J. F.; Rubio, R., Analytical speciation as a tool to assess arsenic behaviour in soils polluted by mining. *Anal. Bioanal. Chem.* **2007**, *387*, 627-635.
86. Jackson, B. P.; Miller, W. P., Soluble arsenic and selenium species in fly ash/organic waste-amended soils using ion chromatography-inductively coupled plasma mass spectrometry. *Environ. Sci. Technol.* **1999**, *33*, 270-275.
87. Cullen, W. R.; Reimer, K. J., Arsenic speciation in the environment. *Chem. Rev.* **1989**, *89*, 713-764.
88. Bissen, M.; Frimmel, F. H., Arsenic - a review. Part I: occurrence, toxicity, speciation, mobility. *Acta Hydrochim. Hydrobiol.* **2003**, *31* (1), 9-18.
89. Dousova, B.; Kolousek, D.; Kovanda, F.; Machovic, V.; Novotna, M., Removal of As(V) species from extremely contaminated mining water. *Appl. Clay Sci.* **2005**, *28*, 31-42.
90. Smedley, P. L.; Kinniburgh, D. G., A review of the source, behaviour and distribution of arsenic in natural waters. *Appl. Geochem.* **2002**, *17*, 517-568.
91. Al-Abed, S. R.; Jegadeesan, G.; Purandare, J.; Allen, D., Arsenic release from iron rich mineral processing waste: influence of pH and redox potential. *Chemosphere* **2007**, *66*, 775-782.
92. Reith, F.; McPhail, D. C., Mobility and microbially mediated mobilization of gold and arsenic in soils from two gold mines in semi-arid and tropical Australia. *Geochim. Cosmochim. Acta* **2007**, *71*, 1183-1196.
93. Nriagu, J. O., Arsenic poisoning through the ages. In *Environmental Chemistry of Arsenic*, 1st ed.; Frankenberger, W. T., Jr., Ed. CRC Press: Boca Raton, FL, **2001**; pp 1-26.
94. Carbonell-Barrachina, A. A.; Rocamora, A.; Garcia-Gomis, C.; Martinez-Sanchez, F.; Burlo, F., Arsenic and zinc biogeochemistry in pyrite mine waste from the Aznalcollar environmental disaster. *Geoderma* **2004**, *122*, 195-203.
95. Impellitteri, C. A., Effects of pH and phosphate on metal distribution with emphasis on As speciation and mobilization in soils from a lead smelting site. *Sci. Total Environ.* **2005**, *345*, 175-190.
96. Yudovich, Y. E.; Ketris, M. P., Arsenic in coal: a review. *Int. J. Coal Geol.* **2005**, *61*, 141-196.

97. Urban, D. R.; Wilcox, J., A theoretical study of properties and reactions involving arsenic and selenium compounds present in coal combustion flue gases. *J. Phys. Chem. A* **2006**, *110* (17), 5847-5852.
98. Al-Abed, S. R.; Jegadeesan, G.; Scheckel, K. G.; Tolaymat, T., Speciation, characterization, and mobility of As, Se, and Hg in flue gas desulphurization residues. *Environ. Sci. Technol.* **2008**, *42* (5), 1693-1698.
99. Wang, T.; Wang, J.; Tang, Y.; Shi, H.; Ladwig, K., Leaching characteristics of arsenic and selenium from coal fly ash: role of calcium. *Energy Fuels* **2009**, *23*, 2959-2966.
100. Jackson, B. P.; Miller, W. P., Arsenic and selenium speciation in coal fly ash extracts by ion chromatography-inductively coupled plasma mass spectrometry. *J. Anal. At. Spectrom.* **1998**, *13*, 1107-1112.
101. Mandal, B. K.; Suzuki, K. T., Arsenic round the world: a review. *Talanta* **2002**, *58*, 201-235.
102. Antman, K. H., Introduction: the history of arsenic trioxide in cancer therapy. *The Oncologist* **2001**, *6* (suppl2), 1-2.
103. Lloyd, N. C.; Morgan, H. W.; Nicholson, B. K.; Ronimus, R. S., The composition of Ehrlich's Salvarsan: resolution of a century-old debate. *Angew. Chem. Int. Ed.* **2005**, *44*, 941-944.
104. Bednar, A. J.; Garbarino, J. R.; Ferrer, I.; Rutherford, D. W.; Wershaw, R. L.; Ranville, J. F.; Wildeman, T. R., Photodegradation of roxarsone in poultry litter leachates. *Sci. Total Environ.* **2003**, *302*, 237-245.
105. Han, F. X.; Kingery, W. L.; Selim, H. M.; Gerard, P. D.; Cox, M. S.; Oldham, J. L., Arsenic solubility and distribution in poultry waste and long-term amended soil. *Sci. Total Environ.* **2004**, *320*, 51-61.
106. Chapman, H. D.; Johnson, Z. B., Use of antibiotics and roxarsone in broiler chickens in the USA: analysis for the years 1995 to 2000. *Poultry Sci.* **2002**, *81*, 356-364.
107. Jackson, B. P.; Seaman, J. C.; Bertsch, P. M., Fate of arsenic compounds in poultry litter upon land application. *Chemosphere* **2006**, *65*, 2028-2034.
108. Rutherford, D. W.; Bednar, A. J.; Garbarino, J. R.; Needham, R.; Staver, K. W.; Wershaw, R. L., Environmental fate of roxarsone in poultry litter. Part II. Mobility of arsenic in soils amended with poultry litter. *Environ. Sci. Technol.* **2003**, *37*, 1515-1520.
109. Muir, L. A., Safety of 3-nitro to humans and the environment. Alpharma: Fort Lee, N.J.

110. Woolson, E. A., The persistence and chemical distribution of arsanilic acid in three soils. *J. Agr. Food Chem.* **1975**, *23* (4), 677-681.
111. Anderson, B. K.; Chamblee, T. N., The effect of dietary 3-nitro-4-hydroxyphenylarsonic acid (roxarsone) on the total arsenic level in broiler excreta and broiler litter. *J. Appl. Poult. Res.* **2001**, *10*, 323-328.
112. Rosal, C. G.; Momplaisir, G.; Heithmar, E. M., Roxarsone and transformation products in chicken manure: determination by capillary electrophoresis-inductively coupled plasma-mass spectrometry. *Electrophoresis* **2005**, *26*, 1606-1614.
113. Jackson, B. P.; Bertsch, P. M.; Cabrera, M. L.; Camberato, J. J.; Seaman, J. C.; Wood, C. W., Trace element speciation in poultry litter. *J. Environ. Qual.* **2003**, *32*, 535-540.
114. Kpombrekou-A, K.; Ankumah, R. O.; Ajwa, H. A., Trace and nontrace element contents of broiler litter. *Commun. Soil Sci. Plant Anal.* **2002**, *33* (11&12), 1799-1811.
115. Lasky, T.; Sun, W.; Kadry, A.; Hoffman, M. K., Mean total arsenic concentrations in chicken 1989-2000 and estimated exposures for consumers of chicken. *Environ. Health Perspect.* **2004**, *112* (1), 18-21.
116. Cortinas, I.; Field, J. A.; Kopplin, M.; Garbarino, J. R.; Gandolfi, A. J.; Sierra-Alvarez, R., Anaerobic biotransformation of roxarsone and related N-substituted phenylarsonic acids. *Environ. Sci. Technol.* **2006**, *40*, 2951-2957.
117. Moody, J. P.; Williams, F. D., The metabolism of 4-hydroxy-3-nitrophenylarsonic acid in hens. *Food Cosmet. Toxicol.* **1964**, *2*, 707-715.
118. Morrison, J. L., Distribution of arsenic from poultry litter in broiler chickens, soil and crops. *J. Agr. Food Chem.* **1969**, *17* (6), 1288-1290.
119. Wershaw, R. L.; Rutherford, D. W.; Rostad, C. E.; Garbarino, J. R.; Ferrer, I.; Kennedy, K. R.; Momplaisir, G.; Grange, A., Mass spectrometric identification of an azobenzene derivative produced by smectite-catalyzed conversion of 3-amino-4-hydroxyphenylarsonic acid. *Talanta* **2003**, *59*, 1219-1226.
120. Staats, K. E.; Arai, Y.; Sparks, D. L., Alum amendment effects on phosphorus release and distribution in poultry litter-amended sandy soils. *J. Environ. Qual.* **2004**, *33*, 1904-1911.
121. Kelley, T. R.; Pancorbo, O. C.; Merka, W. C.; Thompson, S. A.; Cabrera, M. L.; Barnhart, H. M., Accumulation of elements in fractionated broiler litter during re-utilization. *J. Appl. Poultry Res.* **1998**, *7*, 27-34.
122. Gupta, G.; Charles, S., Trace elements in soils fertilized with poultry litter. *Poult. Sci.* **1999**, *78*, 1695-1698.



123. NASS, Poultry - production and value 2006 summary. Agriculture, U. S. D. o., Ed. Agricultural Statistics Board: **2007**.
124. Jackson, B. P.; Bertsch, P. M., Determination of arsenic speciation in poultry wastes by IC-ICP-MS. *Environ. Sci. Technol.* **2001**, *35*, 4868-4873.
125. Garbarino, J. R.; Bednar, A. J.; Rutherford, D. W.; Beyer, R. S.; Wershaw, R. L., Environmental fate of roxarsone in poultry litter. I. Degradation of roxarsone during composting. *Environ. Sci. Technol.* **2003**, *37*, 1509-1514.
126. Stolz, J. F.; Basu, P.; Santini, J. M.; Oremland, R. S., Arsenic and selenium in microbial metabolism. *Annu. Rev. Microbiol.* **2006**, *60*, 107-130.
127. Stolz, J. F.; Perera, E.; Kilonzo, B.; Kail, B.; Crable, B.; Fisher, E.; Ranganathan, M.; Wormer, L.; Basu, P., Biotransformation of 3-nitro-4-hydroxybenzene arsonic acid (roxarsone) and release of inorganic arsenic by *Clostridium* species. *Environ. Sci. Technol.* **2007**, *41*, 818-823.
128. Arai, Y.; Lanzirrotti, A.; Sutton, S.; Davis, J. A.; Sparks, D. L., Arsenic speciation and reactivity in poultry litter. *Environ. Sci. Technol.* **2003**, *37*, 4083-4090.
129. Ferguson, J. F.; Gavis, J., A review of the arsenic cycle in natural waters. *Water Res.* **1972**, *6*, 1259-1274.
130. Tomkins, B. A.; Segal, G. A.; Ho, C.-H., Determination of Lewisite oxide in soil using solid-phase microextraction followed by gas chromatography with flame photometric or mass spectrometric detection. *J. Chromatogr. A* **2001**, *909*, 13-28.
131. Kinoshita, K.; Shida, Y.; Sakuma, C.; Ishizaki, M.; Kiso, K.; Shikino, O.; Ito, H.; Morita, M.; Ochi, T.; Kaise, T., Determination of diphenylarsinic acid and phenylarsonic acid, the degradation products of organoarsenic chemical warfare agents, in well water by HPLC-ICP-MS. *Appl. Organomet. Chem.* **2005**, *19*, 287-293.
132. Hanaoka, S.; Nomura, K.; Kudo, S., Identification and quantitative determination of diphenylarsenic compounds in abandoned toxic smoke canisters. *J. Chromatogr. A* **2005**, *1085*, 213-223.
133. Dich, J.; Zahm, S. H.; Hanberg, A.; Adami, H.-O., Pesticides and cancer. *Cancer Causes and Control* **1997**, *8*, 420-443.
134. Wolz, S.; Fenske, R. A.; Simcox, N. J.; Palcisko, G.; Kissel, J. C., Residential arsenic and lead levels in an agricultural community with a history of lead arsenate use. *Environ. Res.* **2003**, *93*, 293-300.
135. Bednar, A. J.; Garbarino, J. R.; Ranville, J. F.; Wildeman, T. R., Presence of organoarsenicals used in cotton production in agricultural water and soil of the southern United States. *J. Agric. Food Chem.* **2002**, *50*, 7340-7344.

136. Killelea, D. R.; Aldstadt, J. H. I., Identification of dimethylchloroarsine near a former herbicide factory by headspace solid-phase microextraction gas chromatography-mass spectrometry. *Chemosphere* **2002**, *48*, 1003-1008.
137. Warner, J. E.; Solomon, K. R., Acidity as a factor in leaching of copper, chromium and arsenic from CCA-treated dimension lumber. *Environ. Toxicol. Chem.* **1990**, *9*, 1331-1337.
138. Comfort, M., Environmental and occupational health aspects of using CCA treated timber for walking track construction in the Tasmanian Wilderness World Heritage area. Hobart, Tasmania, **1993**; Vol. Scientific Report 93/1.
139. Bhattacharya, P.; Mukherjee, A. B.; Jacks, G.; Nordqvist, S., Metal contamination at a wood preservation site: characterisation and experimental studies on remediation. *Sci. Tot. Environ.* **2002**, *290*, 165-180.
140. Khan, B. I.; Solo-Gabriele, H. M.; Townsend, T. G.; Cai, Y., Release of arsenic to the environment from CCA-treated wood. 1. Leaching and speciation during service. *Environ. Sci. Technol.* **2006**, *40* (3), 988-993.
141. Stillwell, D. E.; Gorny, K. D., Contamination of soil with copper, chromium, and arsenic under decks built from pressure treated wood. *Bull. Environ. Contam. Toxicol.* **1997**, *58*, 22-29.
142. Zagury, G. J.; Samson, R.; Deschenes, L., Occurrence of metals in soil and ground water near chromated copper arsenate-treated utility poles. *J. Environ. Qual.* **2003**, *32*, 507-514.
143. Micklewright, J. T., Wood Preservation Statistics, 1990. Association, A. W. P. s., Ed. Woodstock, MD, **1992**.
144. Lebow, S. **1993**.
145. Dahlgren, S. E.; Harford, W. H., Kinetics and mechanism of fixation of Cu-Cr-As wood preservatives. Part I. *Holzforschung* **1972**, *26*, 62-69.
146. Dahlgren, S. E., The course of the fixation of Cu-Cr-As wood preservatives. In *Record Annual Convention British Wood Preserver's Association*, **1972**; pp 109-128.
147. Dahlgren, S. E., Kinetics and mechanism of fixation of preservatives. Part V. Effect of wood species and preservative composition on leaching during storage. *Holzforschung* **1975**, *29*, 84-95.
148. Van den Broeck, K.; Helsen, L.; Vandecasteele, C.; Van den Bulck, E., *Analyst* **1997**, *122*, 695-700.
149. Cooper, P. A.; T., U. In *Moderate temperature fixation of CCA-C.*, Stockholm, Sweden, International Research Group: Stockholm, Sweden, **1989**.

150. McNamara, W. S. In *CCA fixation experiments--Part I*, Stockholm, Sweden, International Research Group: Stockholm, Sweden, **1989**.
151. Pizzi, A., The chemistry and kinetic behavior of Cu/Cr-As/B wood preservatives. I. Fixation of chromium to wood. *J. Polymer Sci.* **1981**, *19*, 3093-3121.
152. Pizzi, A., The chemistry and kinetic behavior of Cu/Cr-As/B wood preservatives. II. Fixation of the Cu/Cr system on wood. *J. Polymer Sci.* **1982**, *20*, 707-724.
153. Pizzi, A., The chemistry and kinetic behavior of Cu/Cr-As/B wood preservatives. III. Fixation of a Cr/As system on wood. *J. Polymer Sci.* **1982**, *20*, 725-738.
154. Pizzi, A., The chemistry and kinetic behavior of Cu/Cr-As/B wood preservatives. IV. Fixation of CCA to wood. *J. Polymer Sci.* **1982**, *20*, 739-764.
155. Rist, C., Arsenic and old wood. *This Old House* **1998**.
156. Nico, P. S.; Fendorf, S. E.; Lowney, Y. W.; Holm, S. E.; Ruby, M. V., Chemical structure of arsenic and chromium in CCA-treated wood: implications of environmental weathering. *Environ. Sci. Technol.* **2004**, *38* (19), 5253-5260.
157. Blue, L. Y. An evaluation of the loss of copper, chromium, and arsenic preservatives from pressure-treated lumber. Missouri State University, Springfield, MO, **2002**.
158. Khan, B. I.; Jambeck, J.; Solo-Gabriele, H. M.; Townsend, T. G.; Cai, Y., Release of arsenic to the environment from CCA-treated wood. 2. Leaching and speciation during disposal. *Environ. Sci. Technol.* **2006**, *40* (3), 994-999.
159. EPA Manufacturers to use new wood preservatives, replacing most residential uses of CCA. [http://yosemite.epa.gov/pesticides/citizens/cca\\_transition.htm](http://yosemite.epa.gov/pesticides/citizens/cca_transition.htm) (accessed February).
160. Pinel-Raffaitin, P.; Le Hecho, I.; Amouroux, D.; Potin-Gautier, M., Distribution and fate of inorganic and organic arsenic species in landfill leachates and biogases. *Environ. Sci. Technol.* **2007**, *41* (13), 4536-4541.
161. Fendorf, S.; Eick, M. J.; Grossl, P.; Sparks, D. L., Arsenate and chromate retention mechanisms on goethite. 1. Surface structure. *Environ. Sci. Technol.* **1997**, *31* (2), 315-320.
162. Manning, B. A.; Goldberg, S., Arsenic(III) and arsenic(V) adsorption on three California soils. *Soil Sci.* **1997**, *162* (12), 886-895.
163. Manning, B. A.; Fendorf, S. E.; Goldberg, S., Surface structures and stability of arsenic(III) on goethite: spectroscopic evidence for inner-sphere complexes. *Environ. Sci. Technol.* **1998**, *32* (16), 2383-2388.

164. Raven, K. P.; Jain, A.; Loeppert, R. H., Arsenite and arsenate adsorption on ferrihydrite: kinetics, equilibrium, and adsorption envelopes. *Environ. Sci. Technol.* **1998**, *32* (3), 344-349.
165. Lambkin, D. C.; Alloway, B. J., Arsenate-induced phosphate release from soils and its effect on plant phosphorus. *Water, Air, Soil Pollut.* **2003**, *144*, 41-56.
166. Pierce, M. L.; Moore, C. B., Adsorption of arsenite and arsenate on amorphous iron hydroxide. *Water Res.* **1982**, *16*, 1247-1253.
167. Smith, E.; Naidu, R.; Alston, A. M., Chemistry of inorganic arsenic in soils: II. Effect of phosphorus, sodium, and calcium on arsenic sorption. *J. Environ. Qual.* **2002**, *31*, 557-563.
168. Livesey, N. T.; Huang, P. M., Adsorption of arsenate by soils and its relation to selected chemical properties and anions. *Soil Sci.* **1981**, *131* (2), 88-94.
169. Goldberg, S., Chemical modeling of arsenate adsorption on aluminum and iron oxide minerals. *Soil Sci. Soc. Am. J.* **1986**, *50*, 1154-1157.
170. Melamed, R.; Jurinak, J. J.; Dudley, L. M., Effect of adsorbed phosphate on transport of arsenate through an Oxisol. *Soil Sci. Soc. Am. J.* **1995**, *59*, 1289-1294.
171. Sadiq, M., Arsenic chemistry in soils: an overview of thermodynamic predictions and field observations. *Water Air Soil Pollut.* **1997**, *93*, 117-136.
172. Bowell, R. J., Sorption of arsenic by iron oxides and oxyhydroxides in soils. *Appl. Geochem.* **1994**, *9*, 279-286.
173. Sparks, D. L., *Environmental soil chemistry*. 2nd ed.; Elsevier Science: New York, **2003**.
174. Masscheleyn, P. H.; Delaune, R. D.; Patrick, W. H., Effect of redox potential and pH on arsenic speciation and solubility in a contaminated soil. *Environ. Sci. Technol.* **1991**, *25* (8), 1414-1419.
175. Le, X. C., Arsenic speciation in the environment and humans. In *Environmental Chemistry of Arsenic*, 1st ed.; Frankenberger, W. T., Jr., Ed. CRC Press: Boca Raton, FL, **2001**; pp 95-116.
176. Oremland, R. S.; Stolz, J. F., The ecology of arsenic. *Science* **2003**, *300*, 939-944.
177. Kulp, T. R.; Hoefl, S. E.; Asao, M.; Madigan, M. T.; Hollibaugh, J. T.; Fisher, J. C.; Stolz, J. F.; Culbertson, C. W.; Miller, L. G.; Oremland, R. S., Arsenic(III) fuels anoxygenic photosynthesis in hot spring biofilms from Mono Lake, California. *Science* **2008**, *321*, 967-970.

178. Hoefft, S. E.; Blum, J. S.; Stolz, J. F.; Tabita, F. R.; Witte, B.; King, G. M.; Santini, J. M.; Oremland, R. S., *Alkalilimnicola ehrlichii* sp. nov., a novel, arsenite-oxidizing haloalkaliphilic gammaproteobacterium capable of chemoautotrophic or heterotrophic growth with nitrate or oxygen as the electron acceptor. *Int. J. Syst. Evol. Microbiol.* **2007**, *57*, 504-512.
179. Santini, J. M.; Sly, L. I.; Schnagl, R. D.; Macy, J. M., A new chemolithoautotrophic arsenite-oxidizing bacterium isolated from a gold mine: phylogenetic, physiological, and preliminary biochemical studies. *Appl. Environ. Microbiol.* **2000**, *66* (1), 92-97.
180. Kulp, T. R.; Hoefft, S. E.; Oremland, R. S., Redox transformations of arsenic oxyanions in periphyton communities. *Appl. Environ. Microbiol.* **2004**, *70* (11), 6428-6434.
181. Oremland, R. S.; Kulp, T. R.; Blum, J. S.; Hoefft, S. E.; Baesman, S.; Miller, L. G.; Stolz, J. F., A microbial arsenic cycle in a salt-saturated, extreme environment. *Science* **2005**, *308*, 1305-1308.
182. Saltikov, C. W.; Wildman, R. A.; Newman, D. K., Expression dynamics of arsenic respiration and detoxification in *Shewanella* sp. strain ANA-3. *J. Bacteriol.* **2005**, *187* (21), 7390-7396.
183. Yamamura, S.; Yamashita, M.; Fujimoto, N.; Kuroda, M.; Kashiwa, M.; Sei, K.; Fujita, M.; Ike, M., *Bacillus selenatarsenatis* sp. nov., a selenate- and arsenate-reducing bacterium isolated from the effluent drain of a glass-manufacturing plant. *Int. J. Syst. Evol. Microbiol.* **2007**, *57*, 1060-1064.
184. Challenger, F., Biological Methylation. *Chem. Rev.* **1945**, *36* (3), 315-361.
185. Styblo, M.; Delnomdedieu, M.; Thomas, D. J., Mono- and dimethylation of arsenic in rat liver cytosol in vitro. *Chemico-Biological Interactions* **1996**, *99* (1-3), 147-164.
186. Petrick, J. S.; Ayala-Fierro, F.; Cullen, W. R.; Carter, D. E.; Aposhian, H. V., Monomethylarsonous acid (MMA(III)) is more toxic than arsenite in Chang human hepatocytes. *Toxicology and Applied Pharmacology* **2000**, *163* (2), 203-207.
187. Vega, L.; Styblo, M.; Patterson, R.; Cullen, W.; Wang, C. Q.; Germolec, D., Differential effects of trivalent and pentavalent arsenicals on cell proliferation and cytokine secretion in normal human epidermal keratinocytes. *Toxicology and Applied Pharmacology* **2001**, *172* (3), 225-232.
188. Styblo, M.; Del Razo, L. M.; Vega, L.; Germolec, D. R.; LeCluyse, E. L.; Hamilton, G. A.; Reed, W.; Wang, C.; Cullen, W. R.; Thomas, D. J., Comparative toxicity of trivalent and pentavalent inorganic and methylated arsenicals in rat and human cells. *Archives of Toxicology* **2000**, *74* (6), 289-299.

189. Tapio, S.; Grosche, B., Arsenic in the aetiology of cancer. *Mutat. Res.* **2006**, *612*, 215-246.
190. Basu, A.; Mahata, J.; Gupta, S.; Giri, A. K., Genetic toxicity of a paradoxical human carcinogen, arsenic: a review. *Mutat. Res.* **2001**, *488*, 171-194.
191. Tchounwou, P. B.; Patlolla, A. K.; Centeno, J. A., Carcinogenic and systemic health effects associated with arsenic exposure - a critical review. *Toxicol. Path.* **2003**, *131*, 575-588.
192. Cantor, K. P.; Lubin, J. H., Arsenic, internal cancers, and issues in inference from studies of low-level exposures in human populations. *Toxicol. Appl. Pharmacol.* **2007**, *222*, 252-257.
193. Rossman, T. G.; Uddin, A. N.; Burns, F. J., Evidence that arsenite acts as a cocarcinogen in skin cancer. *Toxicol. Appl. Pharmacol.* **2004**, *198*, 394-404.
194. Yu, H.-S.; Liao, W.-T.; Chai, C.-Y., Arsenic carcinogenesis in the skin. *J. Biomed. Sci.* **2006**, *13*, 657-666.
195. Patterson, T. J.; Rice, R. H., Arsenite and insulin exhibit opposing effects on epidermal growth factor receptor and keratinocyte proliferative potential. *Toxicol. Appl. Pharmacol.* **2007**, *221*, 119-128.
196. Pu, Y.-S.; Yang, S.-M.; Huang, Y.-K.; Chung, C.-J.; Huang, S. K.; Chiu, A. W.-H.; Yang, M.-H.; Chen, C.-J.; Hsueh, Y.-M., Urinary arsenic profile affects the risk of urothelial carcinoma even at low arsenic exposure. *Toxicol. Appl. Pharmacol.* **2007**, *218*, 99-106.
197. Hopenhayn-Rich, C.; Biggs, M. L.; Smith, A. E., Lung and kidney cancer mortality associated with arsenic in drinking water in Cordoba, Argentina. *Int. J. Epidemiol.* **1998**, *27*, 561-569.
198. Mazumder, D. N. G., Effect of chronic intake of arsenic-contaminated water on liver. *Toxicol. Appl. Pharmacol.* **2005**, *206*, 169-175.
199. Sauvant, M.-P.; Pepin, D., Drinking water and cardiovascular disease. *Food Chem. Toxicol.* **2002**, *40*, 1311-1325.
200. Simeonova, P. P.; Luster, M. I., Arsenic and atherosclerosis. *Toxicol. Appl. Pharmacol.* **2004**, *198*, 444-449.
201. Bhatnagar, A., Environmental cardiology: studying mechanistic links between pollution and heart disease. *Circ. Res.* **2006**, *99*, 692-705.
202. Kwok, R. K., A review and rationale for studying the cardiovascular effects of drinking water arsenic in women of reproductive age. *Toxicol. Appl. Pharmacol.* **2007**, *222*, 344-350.

203. Straub, A. C.; Stolz, D. B.; Vin, H.; Ross, M. A.; Soucy, N. V.; Klei, L. R.; Barchowsky, A., Low level arsenic promotes progressive inflammatory angiogenesis and liver blood vessel remodeling in mice. *Toxicol. Appl. Pharmacol.* **2007**, *222*, 327-336.
204. Chen, C.-J.; Wang, S.-L.; Chiou, J.-M.; Tseng, C.-H.; Chiou, H.-Y.; Hsueh, Y.-M.; Chen, S.-Y.; Wu, M.-M.; Lai, M.-S., Arsenic and diabetes and hypertension in human populations: a review. *Toxicol. Appl. Pharmacol.* **2007**, *222*, 298-304.
205. Rodriguez, V. M.; Jimenez-Capdeville, M. E.; Giordano, M., The effects of arsenic exposure on the nervous system. *Toxicol. Lett.* **2003**, *145*, 1-18.
206. Vahidnia, A.; van der Voet, G. B.; de Wolff, F. A., Arsenic neurotoxicity - a review. *Hum. Exper. Toxicol.* **2007**, *26*, 823-832.
207. Walton, F. S.; Harmon, A. W.; Paul, D. S.; Drobna, Z.; Patel, Y. M.; Styblo, M., Inhibition of insulin-dependent glucose uptake by trivalent arsenicals: possible mechanism of arsenic-induced diabetes. *Toxicol. Appl. Pharmacol.* **2004**, *198*, 424-433.
208. Tseng, C.-H., The potential biological mechanisms of arsenic-induced diabetes mellitus. *Toxicol. Appl. Pharmacol.* **2004**, *197*, 67-83.
209. Diaz-Villasenor, A.; Sanchez-Soto, M. C.; Cebrian, M. E.; Ostrosky-Wegman, P.; Hiriart, M., Sodium arsenite impairs insulin secretion and transcription in pancreatic  $\beta$ -cells. *Toxicol. Appl. Pharmacol.* **2006**, *214*, 30-34.
210. Diaz-Villasenor, A.; Burns, A. L.; Hiriart, M.; Cebrian, M. E.; Ostrosky-Wegman, P., Arsenic-induced alteration in the expression of genes related to type 2 diabetes mellitus. *Toxicol. Appl. Pharmacol.* **2007**, *225*, 123-133.
211. Paul, D. S.; Hernandez-Zavala, A.; Walton, F. S.; Adair, B. M.; Dedina, J.; Matousek, T.; Styblo, M., Examination of the effects of arsenic on glucose homeostasis in cell culture and animal studies: development of a mouse model for arsenic-induced diabetes. *Toxicol. Appl. Pharmacol.* **2007**, *222*, 305-314.
212. Diaz-Villasenor, A.; Burns, A. L.; Salazar, A. M.; Sordo, M.; Hiriart, M.; Cebrian, M. E.; Ostrosky-Wegman, P., Arsenite reduces insulin secretion in rat pancreatic  $\beta$ -cells by decreasing the calcium-dependent calpain-10 proteolysis of SNAP-25. *Toxicol. Appl. Pharmacol.* **2008**, *231*, 291-299.
213. Hopenhayn, C.; Ferreccio, C.; Browning, S. R.; Huang, B.; Peralta, C.; Gibb, H.; Herz-Picciotto, I., Arsenic exposure from drinking water and birth weight. *Epidem.* **2003**, *14* (5), 593-602.
214. Hopenhayn, C.; Huang, B.; Christian, J.; Peralta, C.; Ferreccio, C.; Atallah, R., Profile of urinary arsenic metabolites during pregnancy. *Environ. Health Perspect.* **2003**, *111* (16), 1888-1891.

215. Hall, M.; Gamble, M.; Slavkovich, V.; Liu, X.; Levy, D.; Cheng, Z.; van Geen, A.; Yunus, M.; Rahman, M.; Pilsner, J. R.; Graziano, J., Determinants of arsenic metabolism: blood arsenic metabolites, plasma folate, cobalamin, and homocysteine concentrations in maternal-newborn pairs. *Environ. Health Perspect.* **2007**, *115* (10), 1503-1509.
216. EPA, Arsenic treatment technology evaluation handbook for small systems. Office of Water (4606M): **2003**.
217. Mahimairaja, S.; Bolan, N. S.; Adriano, D. C.; Robinson, B., Arsenic contamination and its risk management in complex environmental settings. *Adv. Agron.* **2005**, *86*, 1-82.
218. Bissen, M., Frimmel, F. H., Arsenic - a Review. Part I: Occurrence, Toxicity, Speciation, Mobility. *Acta Hydrochim. Hydrobiol.* **2003**, *31* (1), 9-18.
219. Smedley, P. L., Kinniburgh, D. G., A Review of the Source, Behaviour and Distribution of Arsenic in Natural Waters. *Appl. Geochem.* **2002**, *17*, 517-568.
220. Cullen, W. R., Reimer, K. J., Arsenic Speciation in the Environment. *Chem. Rev.* **1989**, *89*, 713-764.
221. Dujardin, M. C.; Caze, C.; Vroman, I., Ion-exchange resins bearing thiol groups to remove mercury. Part 1: synthesis and use of polymers prepared from thioester supported resin. *React. Funct. Polym.* **2000**, *43* (1-2), 123-132.
222. Matlock, M. M., Howerton, B. S., Van Aelstyn, M. A., Nordstrom, F. L., Atwood, D. A., Advanced Mercury Removal from Gold Leachate Solutions Prior to Gold and Silver Extraction: A Field Study from an Active Gold Mine in Peru. *Environ. Sci. Technol.* **2002**, *36*, 1636-1639.
223. Matlock, M. M., Howerton, B. S., Atwood, D. A., Chemical Precipitation of Lead from Lead Battery Recycling Plant Wastewater. *Ind. Eng. Chem. Res.* **2002**, *41*, 1579-1582.
224. Matlock, M. M., Howerton, B. S., Robertson, J. D., Atwood, D. A., Gold Ore Column Studies with a New Mercury Precipitant. *Ind. Eng. Chem. Res.* **2002**, *41*, 5278-5282.
225. Matlock, M. M., Howerton, B. S., Atwood, D. A., Chemical Precipitation of Heavy Metals from Acid Mine Drainage. *Wat. Res.* **2002**, *36*, 4757-4764.
226. Matlock, M. M., Howerton, B. S., Van Aelstyn, M., Henke, K. R., Atwood, D. A., Soft Metal Preferences of 1,3-Benzenediamidoethanethiol. *Wat. Res.* **2003**, *37*, 579-584.
227. Matlock, M. M., Howerton, B. S., Atwood, D. A., Irreversible Binding of Mercury from Contaminated Soil. *Adv. Environ. Res.* **2003**, *7*, 347-352.



228. Matlock, M. M., Howerton, B. S., Atwood, D. A. (University of Kentucky, Lexington, KY). Novel Multidentate Sulfur Containing Ligands. U.S. Patent No. 6,586,600, July 1, 2003.
229. Matlock, M. M.; Howerton, B. S.; Atwood, D. A., Chemical precipitation of heavy metals from acid mine drainage. *Water Res.* **2002**, *36*, 4757-4764.
230. Matlock, M. M.; Howerton, B. S.; Atwood, D. A., Irreversible precipitation of mercury and lead. *J. Hazard Mater.* **2001**, *B84*, 73-82.
231. Matlock, M. M.; Howerton, B. S.; Atwood, D. A. Novel multidentate sulfur containing ligands. U.S. Patent No. 6,586,600, July 1, 2003, **2002**.
232. Matlock, M. M.; Howerton, B. S.; Atwood, D. A., Chemical precipitation of lead from lead battery recycling plant wastewater. *Ind. Eng. Chem. Res.* **2002**, *41*, 1579-1582.
233. Matlock, M. M.; Howerton, B. S.; Atwood, D. A., Irreversible binding of mercury from contaminated soil. *Adv. Environ. Res.* **2003**, *7*, 347-352.
234. Matlock, M. M.; Howerton, B. S.; Robertson, J. D.; Atwood, D. A., Gold ore column studies with a new mercury precipitant. *Ind. Eng. Chem. Res.* **2002**, *41*, 5278-5282.
235. Matlock, M. M.; Howerton, B. S.; Van Aelstyn, M.; Henke, K. R.; Atwood, D. A., Soft metal preferences of 1,3-benzenediamidoethanethiol. *Water Res.* **2003**, *37*, 579-584.
236. Matlock, M. M.; Howerton, B. S.; Van Aelstyn, M. A.; Nordstrom, F. L.; Atwood, D. A., Advanced mercury removal from gold leachate solutions prior to gold and silver extraction: a field study from an active gold mine in Peru. *Environ. Sci. Technol.* **2002**, *36*, 1636-1639.
237. Matlock, M. M.; Howerton, B. S.; Van Aelstyn, M. A.; Henke, K. R.; Atwood, D. A., Soft metal preferences of 1,3-benzenediamidoethanethiol. *Water Res.* **2003**, *37*, 579-584.
238. Blue, L. Y.; Van Aelstyn, M. A.; Matlock, M.; Atwood, D. A., Low-level mercury removal from groundwater using a synthetic chelating ligand. *Water Res.* **2008**, *42* (8-9), 2025-2028.
239. Zaman, K. M.; Blue, L. Y.; Huggins, F. E.; Atwood, D. A., Cd, Hg, and Pb compounds of benzene-1,3-diamidoethanethiol (BDETH<sub>2</sub>). *Inorg. Chem.* **2007**, *46* (6), 1975-1980.
240. Zaman, K. M.; Chusuei, C.; Blue, L. Y.; Atwood, D. A., Prevention of sulfide mineral leaching through covalent coating. *Main Group Chemistry* **2007**, *6* (3), 169-184.

241. Ferguson, J. F., Gavis, J., A Review of the Arsenic Cycle in Natural Waters. *Water Res.* **1972**, *6*, 1259-1274.
242. Liu, K.; Gao, Y.; Riley, J. T.; Pan, W.; Mehta, A. K.; Ho, K. K.; Smith, S. R., An investigation of mercury emission from FBC systems fired with high-chlorine coals. *Energy & Fuels* **2001**, *15* (5), 1173-1180.
243. Wilcox, J.; Robles, J.; Marsden, D. C. J.; Blowers, P., Theoretically predicted rate constants for mercury oxidation by hydrogen chloride in coal combustion flue gases. *Environ. Sci. Technol.* **2003**, *37* (18), 4199-4204.
244. Huggins, F. E.; Huffman, G. P., XAFS examination of mercury sorption on three activated carbons. *Energy & Fuels* **1999**, *13*, 114-121.
245. Agarwal, H.; Romero, C. E.; Stenger, H. G., Comparing and interpreting laboratory results of Hg oxidation by a chlorine species. *Fuel Process. Technol.* **2007**, *88*, 723-730.
246. Li, L. C.; Deng, P.; Tian, A. M.; Xu, M. H.; Zheng, C. G.; Wong, N. B., A study on the reaction mechanism and kinetics of mercury oxidation by chlorine species. *J. Mol. Struct. (Theochem.)* **2003**, *625*, 277-281.
247. Sliger, R. N.; Kramlich, J. C.; Marinov, N. M., Towards the development of a chemical kinetic model for the homogeneous oxidation of mercury by chlorine species. *Fuel Process. Technol.* **2000**, *65-66*, 423-438.
248. Wilcox, J.; Marsden, D. C. J.; Blowers, P., Evaluation of basis sets and theoretical methods for estimating rate constants of mercury oxidation reactions involving chlorine. *Fuel Process. Technol.* **2004**, *85*, 391-400.
249. Zhao, Y.; Mann, M. D.; Pavlish, J. H.; Mibeck, B. A. F.; Dunham, G. E.; Olson, E. S., Application of gold catalyst for mercury oxidation by chlorine. *Environ. Sci. Technol.* **2006**, *40* (5), 1603-1608.
250. Cao, Y.; Gao, Z.; Zhu, J.; Wang, Q.; Huang, Y.; Chiu, C.; Parker, B.; Chu, P.; Pan, W. P., Impacts of halogen additions on mercury oxidation, in a slipstream selective catalyst reduction (SCR), reactor when burning sub-bituminous coal. *Environ. Sci. Technol.* **2008**, *42* (1), 256-261.
251. Wilcox, J., A kinetic investigation of high-temperature mercury oxidation by chlorine. *J. Phys. Chem A* **2009**, *113*, 6633-6639.
252. Charpentreau, C.; Seneviratne, R.; George, A.; Millan, M.; Dugwell, D. R.; Kandiyoti, R., Screening of low cost sorbents for arsenic and mercury capture in gasification systems. *Energy & Fuels* **2007**.

253. Liu, S.; Yan, N.; Liu, Z.; Qu, Z.; Wang, H. P.; Chang, S.; Miller, C., Using bromine gas to enhance mercury removal from flue gas of coal-fired power plants. *Environ. Sci. Technol.* **2007**, *41* (4), 1405-1412.
254. Cao, Y.; Wang, Q.; Chen, C.; Chen, B.; Cohron, M.; Tseng, Y.; Chiu, C.; Chu, P.; Pan, W., Investigation of mercury transformation by HBr addition in a slipstream facility with real flue gas atmospheres of bituminous coal and Powder River Basin coal. *Energy & Fuels* **2007**.
255. Ivanov, A. M.; Kalita, D. I.; Pereverzeva, Y. L., Kinetics of zinc and mercury oxidation by iodine in organic and aqueous-organic media. *Theor. Found. Chem. Eng.* **2003**, *37* (4), 407-411.
256. Cao, Y.; Chen, B.; Wu, J.; Cui, H.; Smith, J.; Chen, C.; Chu, P.; Pan, W., Study of mercury oxidation by a selective catalytic reduction catalyst in a pilot-scale slipstream reactor at a utility boiler burning bituminous coal. *Energy & Fuels* **2007**, *21*, 145-156.
257. Worathanakul, P.; Kongkachuichay, P.; Noel, J. D.; Suriyawong, A.; Giammar, D. E.; Biswas, P., Evaluation of nanostructured sorbents in differential bed reactors for elemental mercury capture. *Environ. Eng. Sci.* **2008**, *25* (7), 1061-1070.
258. Granite, E. J.; Pennline, H. W.; Hoffman, J. S., Effects of photochemical formation of mercuric oxide. *Ind. Eng. Chem. Res.* **1999**, *38* (12), 5034-5037.
259. Granite, E. J.; Pennline, H. W., Photochemical removal of mercury from flue gas. *Ind. Eng. Chem. Res.* **2002**, *41* (22), 5470-5476.
260. McLarnon, C. R.; Granite, E. J.; Pennline, H. W., The PCO process for photochemical removal of mercury from flue gas. *Fuel Process. Technol.* **2005**, *87*, 85-89.
261. Bussi, J.; Ohanian, M.; Vazquez, M.; Dalchiele, E. A., Photocatalytic removal of Hg from solid wastes of chlor-alkali plant. *J. Environ. Eng.-ASCE* **2002**, *128* (8), 733-739.
262. Atwood, D. A.; Zaman, K. M., Mercury removal from water. *Struct. Bonding (Berlin)* **2006**, *120*, 163-182.
263. Wagner-Dobler, I.; von Canstein, H.; Li, Y.; Timmis, K. N.; Deckwer, W. D., Removal of mercury from chemical wastewater by microorganisms in technical scale. *Environmental Science & Technology* **2000**, *34* (21), 4628-4634.
264. Lee, J.; Ju, Y.; Keener, T. C.; Varma, R. S., Development of cost-effective noncarbon sorbents for Hg<sup>0</sup> removal from coal-fired power plants. *Environ. Sci. Technol.* **2006**, *40* (8), 2714-2720.

265. Granite, E. J.; Myers, C. R.; King, W. P.; Stanko, D. C.; Pennline, H. W., Sorbents for mercury capture from fuel gas with application to gasification systems. *Ind. Eng. Chem. Res.* **2006**, *45* (13), 4844-4848.
266. Maroto-Valer, M. M.; Zhang, Y.; Granite, E. J.; Tang, Z.; Pennline, H. W., Effect of porous structure and surface functionality on the mercury capacity of a fly ash carbon and its activated sample. *Fuel* **2005**, *84*, 105-108.
267. Granite, E. J.; Freeman, M. C.; Hargis, R. A.; O'Dowd, W. J.; Pennline, H. W., The thief process for mercury removal from flue gas. *J. Environ. Manag.* **2006**.
268. O'Dowd, W. J.; Hargis, R. A.; Granite, E. J.; Pennline, H. W., Recent advances in mercury removal technology at the National Energy Technology Laboratory. *Fuel Process. Technol.* **2004**, *85*, 533-548.
269. O'Dowd, W. J.; Pennline, H. W.; Freeman, M. C.; Granite, E. J.; Hargis, R. A.; Lacher, C. J.; Karash, A., A technique to control mercury from flue gas: the Thief Process. *Fuel Process. Technol.* **2006**.
270. Yan, N.-Q.; Qu, Z.; Chi, Y.; Qiao, S.-H.; Dod, R. L.; Chang, S.-G.; Miller, C., Enhanced elemental mercury removal from coal-fired flue gas by sulfur-chlorine compounds. *Environ. Sci. Technol.* **2009**.
271. Abu-Daibes, M. A.; Pinto, N. G., Synthesis and characterization of a nano-structured sorbent for the direct removal of mercury vapor from flue gases by chelation. *Chem. Eng. Sci.* **2005**, *60*, 1901-1910.
272. Liu, W.; Vidic, R. D.; Brown, T. D., Impact of flue gas conditions on mercury uptake by sulfur-impregnated activated carbon. *Environ. Sci. Technol.* **2000**, *34* (1), 154-159.
273. Zeng, H.; Jin, F.; Guo, J., Removal of elemental mercury from coal combustion flue gas by chloride-impregnated activated carbon. *Fuel* **2004**, *83*, 143-146.
274. Ochiai, R.; Uddin, M. A.; Sasaoka, E.; Wu, S., Effects of HCl and SO<sub>2</sub> concentrations on mercury removal by activated carbon sorbents in coal-derived flue gas. *Energy Fuels* **2009**, *23*, 4734-4739.
275. Schwuger, M. J.; Subklew, G.; Woller, N., New alternatives for waste water remediation with complexing surfactants. *Colloid Surf. A-Physicochem. Eng. Asp.* **2001**, *186* (3), 229-242.
276. Biester, H.; Schuhmacher, P.; Muller, G., Effectiveness of mossy tin filters to remove mercury from aqueous solution by Hg(0) reduction and Hg(0) amalgamation. *Water Research* **2000**, *34* (7), 2031-2036.

277. Huttenloch, P.; Roehl, K. E.; Czurda, K., Use of copper shavings to remove mercury from contaminated groundwater or wastewater by amalgamation. *Environ. Sci. Technol.* **2003**, *37* (18), 4269-4273.
278. Matlock, M. M.; Henke, K. R.; Atwood, D. A., Effectiveness of commercial reagents for heavy metal removal from water with new insights for future chelate designs. *J. Hazard Mater.* **2002**, *B92*, 129-142.
279. Matlock, M. M.; Henke, K. R.; Atwood, D. A.; Robertson, D., Aqueous leaching properties and environmental implications of cadmium, lead, and zinc trimercaptotriazine (TMT) compounds. *Water Res.* **2001**, *35* (15), 3649-3655.
280. Henke, K. R.; Robertson, D.; Krepps, M. K.; Atwood, D. A., Chemistry and stability of precipitates from aqueous solutions of 2,4,6-trimercaptotriazine, trisodium salt, nonahydrate (TMT-55) and mercury(II) chloride. *Water Res.* **2000**, *34* (11), 3005-3013.
281. Monteagudo, J. M.; Ortiz, W. J., Removal of inorganic mercury from mine waste water by ion exchange. *J. Chem. Technol. Biotechnol.* **2000**, *75* (9), 767-772.
282. Wang, J.; Deng, B.; Chen, H.; Wang, X.; Zheng, J., Removal of Aqueous Hg(II) by Polyaniline: Sorption Characteristics and Mechanisms. *Environ. Sci. Technol.* **2009**, *43* (14), 5223-5228.
283. Bessbousse, H.; Rhallou, T.; Vercher, J.-F.; Lebrun, L., Novel metal-complexing membrane containing poly(4-vinylpyridine) for removal of Hg(II) from aqueous solution. *J. Phys. Chem. B* **2009**, *113* (25), 8588-8598.
284. Yantasee, W.; Warner, C. L.; Sangvanich, T.; Addleman, R. S.; Carter, T. G.; Wiacek, R. J.; Fryxell, G. E.; Timchalk, C.; Warner, M. G., Removal of heavy metals from aqueous systems with thiol functionalized superparamagnetic nanoparticles. *Environ. Sci. Technol.* **2007**, *41* (14), 5114-5119.
285. Billinge, S. J. L.; McKimmy, E. J.; Shatnawi, M.; Kim, H. J.; Petkov, V.; Wermeille, D.; Pinnavaia, T. J., Mercury binding sites in thiol-functionalized mesostructured silica. *Journal of the American Chemical Society* **2005**, *127* (23), 8492-8498.
286. Gash, A. E.; Spain, A. L.; Dysleski, L. M.; Flaschenriem, C. J.; Kalaveshi, A.; Dorhout, P. K.; Strauss, S. H., Efficient recovery of elemental mercury from Hg(II)-contaminated aqueous media using a redox-recyclable ion-exchange material. *Environ. Sci. Technol.* **1998**, *32* (7), 1007-1012.
287. Sahlman, L.; Skarfstad, E. G., Mercuric ion binding abilities of merP variants containing only one cysteine. *Biochem. Biophys. Res. Commun.* **1993**, *196* (2), 583-588.

288. Zaman, K. M.; Blue, L. Y.; Huggins, F. E.; Atwood, D. A., Cd, Hg, and Pb compounds of benzene-1,3-diamidoethanethiol (BDETH<sub>2</sub>). *Inorganic Chemistry* **2007**, *46* (6), 1975-1980.
289. Telliard, W. A.; Gomez-Taylor, M., Method 1631, Revision E: mercury in water by oxidation, purge and trap, and cold vapor atomic fluorescence spectrometry. United States Environmental Protection Agency, O. o. W., Ed. 2002.
290. Choong, T. S. Y.; Chuah, T. G.; Robiah, Y.; Koay, F. L. G.; Azni, I., Arsenic toxicity, health hazards and removal techniques from water: an overview. *Desalination* **2007**, *217*, 139-166.
291. Beak, D. G.; Wilkin, R. T.; Ford, R. G.; Kelly, S. D., Examination of arsenic speciation in sulfidic solutions using X-ray absorption spectroscopy. *Environ. Sci. Technol.* **2008**, *42* (5), 1643-1650.
292. Su, C., Puls, R. W., Arsenate and Arsenite Removal by Zerovalent Iron: Effects of Phosphate, Silicate, Carbonate, Borate, Sulfate, Chromate, Molybdate, and Nitrate, Relative to Chloride. *Environ. Sci. Technol.* **2001**, *35*, 4562-4568.
293. Manning, B. A., Hunt, M. L., Amrhein, C., Yarmoff, J. A., Arsenic(III) and Arsenic(V) Reactions with Zerovalent Iron Corrosion Products. *Environ. Sci. Technol.* **2002**, *36* (24), 5455-5461.
294. Su, C., Puls, R. W., Arsenate and Arsenite Removal by Zerovalent Iron: Kinetics, Redox Transformation, and Implications for in Situ Groundwater Remediation. *Environ. Sci. Technol.* **2001**, *35* (7), 1487-1492.
295. Su, C., Puls, R. W., In Situ Remediation of Arsenic in Simulated Groundwater Using Zerovalent Iron: Laboratory Column Tests on Combined Effects of Phosphate and Silicate. *Environ. Sci. Technol.* **2003**, *37* (11), 2582-2587.
296. Raab, A.; Meharg, A. A.; Jaspars, M.; Genney, D. R.; Feldmann, J., Arsenic-glutathione complexes--their stability in solution and during separation by different HPLC methods. *J. Anal. At. Spectrom.* **2004**, *19*, 183-190.
297. Jacobson, K. B.; Murphy, J. B.; Das Sarma, B., Reaction of cacodylic acid with organic thiols. *FEBS Lett.* **1972**, *22* (1), 80-82.
298. Rey, N. A.; Howarth, O. W.; Pereira-Maia, E. C., Equilibrium characterization of the As(III)-cysteine and the As(III)-glutathione systems in aqueous solution. *J. Inorg. Biochem.* **2004**, *98* (6), 1151-1159.
299. Cotton, F. A.; Wilkinson, G., *Advanced Inorganic Chemistry*. 5th ed.; John Wiley & Sons, Inc.: New York, **1988**.
300. Silberberg, M. S., *Chemistry: The Molecular Nature of Matter and Change*. 2nd ed.; McGraw-Hill: Boston, **2000**.

301. Manceau, A.; Nagy, K. L., Relationships between Hg(II)-S bond distance and Hg(II) coordination in thiolates. *Dalton Transactions* **2008**, (11), 1421-1425.
302. Yang, D. Y.; Chen, Y. W.; Gunn, J. M.; Belzile, N., Selenium and mercury in organisms: Interactions and mechanisms. *Environmental Reviews* **2008**, *16*, 71-92.
303. USEPA, Method 3050B: Acid digestion of sediments, sludges and soils **1996**.

## VITA

The author was born in Kirkwood, Missouri on April 16, 1975. She graduated from Pacific High School in 1993 and enrolled at Missouri State University in Springfield, Missouri. She earned a Bachelor of Science in Chemistry in 1998 while investigating the leaching and analysis of cadmium, cobalt, lead, and zinc in decals and glazes on greenware and bisque ceramics under the direction of Dr. Ralph Sheets. During this time, she was awarded the American Chemical Society Undergraduate Award in Analytical Chemistry (1995-6) and the Outstanding Environmental Chemistry Student Award (1997-8). The author returned to Missouri State to earn a Master of Science in Chemistry in 2002 by researching the loss of copper, chromium, and arsenic preservatives from pressure-treated lumber through their chelation with model organic compounds. This work was completed under the direction of Dr. Richard Biagioni.

During her time at Missouri State, the author was also employed as a cooperative education chemistry student at Kraft Foods, Inc. in 1996, the Dayco Factory Technical Laboratory in 1999, and the Blackman Water Treatment Laboratory from 1998 through 2000. She also worked as a teaching and research assistant at Missouri State, taught classes at Ozarks Technical Community College as an adjunct instructor, and worked as a tutor at Bellwether Learning Center. After completing her degrees at Missouri State, the author secured a position as a Basic Skills Instructor in the Speckman Academic Achievement Center at Ozarks Technical Community College while continuing to teach General Chemistry and Technical Mathematics as an adjunct instructor.

In 2003, the author elected to pursue a Ph.D. at the University of Kentucky under the guidance of Dr. David Atwood. While completing her coursework, the author initially served as Research Assistant and later as an Instructor in Analytical Chemistry. In addition to pursuing the research documented in this dissertation, the author undertook several additional projects related to the dissertation including zinc remediation using a thiol compound and the examination of a possible relationship between thimerosal in vaccines and occurrence of autism and gastrointestinal disorders in non-human infant primates.

While at UK, the author was awarded a Kentucky National Science Foundation Experimental Program to Stimulate Competitive Research (KY-NSF-EPSCoR) grant to investigate the link between mobile arsenic and poultry litter in amended agricultural soils. The author was also the recipient of the Research Challenge Trust Fund Fellowship (2003-2008), a University of Kentucky Chemistry Department Teaching Award (2004-2005), the Environmental Research and Training Laboratories Scholarship (2006-2008), and the Dissertation Year Fellowship (2008-2009) from the University of Kentucky.

Publications resulting from the dissertation and related research include:

Zaman, K. M., **Blue, L. Y.**, Huggins, F. E., Atwood, D. A. "Cd, Hg, and Pb compounds of benzene-1,3-diamidoethanethiol (BDETH<sub>2</sub>)," *Inorg. Chem.*, **2007**, *46*, 1975-1980.

Zaman, K.M.; Chusuei, C.; **Blue, L.Y.**; Atwood, D.A. "Prevention of sulfide mineral leaching," *Main Group Chem.*, **2007**, *6* (3-4), 169-184.



**Blue, L. Y.**; Van Aelstyn, M. A.; Matlock, M.; Atwood, D. A. “Low-level mercury removal from groundwater using a synthetic chelating ligand,” *Water Res.*, **2008**, *42*, 2025-2028.

Hewitson L.; Houser L.A.; Stott C.; Sackett G.; Tomko J.L.; Atwood D.; **Blue L.**; White E.R.; Wakefield A.J., “Delayed acquisition of neonatal reflexes in newborn primates receiving a thimerosal-containing Hepatitis B vaccine: influence of gestational age and birth weight,” *NeuroToxicol.*, **2009**, *in press*.

**Blue, L. Y.**; Jana, P.; Atwood, D. “Soft Metal Capture with the Synthetic Dithiolate, BDTH<sub>2</sub>,” *Fuel*, *in press*.

**Blue, L. Y.**; Bird, K. N.; Jana, P.; White, E. R.; Atwood, D. “Stability of a Synthetic Dithiolate of Cadmium Determined by Long Term Leaching,” *to be submitted to Main Group Chem.*

**Blue, L. Y.**; Bird, K. N.; Henson, G.; Beck, E. G.; Atwood, D.A. “Arsenic in Poultry Litter Amended Agricultural Soils, Part I: Investigation of a Karnak Silty Clay Soil from Western Kentucky,” *to be submitted to Environ. Sci. Technol.*

**Blue, L. Y.**; Bird, K. N.; Henson, G.; Beck, E. G.; Atwood, D. A. “Arsenic in Poultry Litter Amended Agricultural Soils, Part II: Investigation of a Belknap Silty Loam Soil from Western Kentucky,” *to be submitted to Environ. Sci. Technol.*

**Blue, L. Y.**; Bird, K. N.; Preece, C. A.; Henson, G.; Beck, E. G.; Atwood, D. A. “Arsenic in Poultry Litter Amended Agricultural Soils, Part III: Arsenic and Trace Metal Contaminants from Soil and Tile Drain Effluents,” *to be submitted to Environ. Sci. Technol.*

**Blue, L. Y.**; White, E. R.; Mukherjee, A. M.; Fryar, A.; Atwood, D. A. “Complete Remediation of Groundwater Arsenic Using a B9, Zerovalent Iron Filtration Column,” *to be submitted to Environ. Sci. Technol.*